CHAPTER 1

INTRODUCTION

Chapter 1

1.0. Introduction

1.1. General Introduction and scope of thesis

Cadmium (Cd) is ubiquitous in the environment and a serious industrial and environmental pollutant. It has no known essential biological function in cells. Cd has been referred to as a group 1 carcinogen (Merrill *et al*., 2001) and chronic and acute exposure to this metal has been reported to be carcinogenic to various organs in the body (Waalkes, 2000; Waisberg *et al*., 2003). The liver is one of the major target organs in acute and chronic cadmium exposure (Ohm and Lim, 2006). Cd is mainly a non-genotoxic metal but enhances the genotoxic effect of other compounds (Hartwig and Schwerdtle, 2002).

Cd has no known uniform mechanism of toxicity (Fotakis *et al*., 2005). It has been reported that one of the mechanisms by which Cd induces toxicity is by increasing the levels of reactive oxygen species within the cell (Hassoun and Stohs, 1996; Risso-de Faverney *et al* 2001; Galan *et al*., 2001). Another mechanism leads to an alteration in intracellular Ca^{2+} ions level (Berridge *et al*., 2000).

In this thesis, possible mechanisms of Cd toxicity are explored. The role of reactive oxygen species, glutathione (GSH) depletion and antioxidant enzymes activities levels are studied. The involvement of intracellular Ca^{2+} alteration via PLC-IP_3 pathway and the mitochondrial-cytochrome C dependent pathway are investigated and compared in three human cell lines in order to elucidate the mechanism(s) involves in Cd toxicity. This work also examines the role of Nrf2-Keap1-ARE pathway in the adaptive response of

human cell lines to Cd insult. The involvement of Protein kinase C (PKC) in this adaptive response is also investigated. In addition to this, my studies also examine the mechanisms involved in the protective effects of garlic extracts, in comparison with diallydisulfide (DADS) found in garlic, on Cd induced toxicity. Finally, my research examines the alterations in proteomic profiles in human cells exposed to Cd in order to identified protein markers for Cd toxicity.

1.2. Cadmium

Cd is a heavy metal belonging to Group IIb of the periodic table along with zinc and mercury and has filled 3d and 4d orbitals. It has two electrons in the outermost 5s orbital which are lost in the formation of Cd^{2+} ions.

1.2.1. Physico-Chemical Properties

Cd is a bluish-white, soft, ductile electropositive metal with high resistance to corrosion. It has an atomic number of 48 and relative atomic mass of 112.40. It is mostly found as ore in nature in combination with other metals such as zinc (Friberg and Elinder, 1983), copper and lead and in various rocks and soils as well as in water. It is not usually found in pure form. Cd corrosion is enhanced by the presence of moist ammonia and sulphur dioxide (Stokinger, 1981) and it is soluble in acids but insoluble in water (Stokinger, 1981).

Cd mostly forms inorganic salts. Organic Cd compounds do not occur in nature. The effects and mobility of Cd in the environment depend greatly on the nature of the salt formed by the metal. Cd has high relative vapour pressure and is therefore oxidized quickly in the air to produce Cd oxide.

The oxide in the presence of reactive gases or vapour such as hydrogen chloride, water, carbon dioxide, and sulphur dioxide and sulphur trioxide produces Cd chloride, hydroxide, carbonate, sulphate and sulphite respectively. The chloride, sulphate and nitrate forms of Cd are soluble but the oxide, sulphide, carbonate are insoluble (Table1.1) though can be made soluble by the reaction of oxygen and acids (IARC, 1993).

The presence of hydroxide ions results in the precipitation of Cd ions from solution to form an insoluble white hydrated compound with carbonates, phosphates arsenates, oxalates and ferrocyanides, all of which are soluble in ammonium hydroxide due to the formation of complex cations containing Cd and ammonia (Windholz *et al.*, 1976).

Table.1.1. Physical and Chemical Properties of Cd Compounds

Properties	Cadmium	Cadmium chloride	Cadmium acetate	Cadmium oxide	Cadmium hydroxide	Cadmium sulhide	Cadmium sulphate	Cadmium sulphite
Empirical formula	Cd	$CdCl_2$	$C_4H_6CdO_4$	CdO	$Cd(OH)_2$	CdS	$CdSO_4$	$CdSO_3$
Relative atomic or molecular mass	112.41	183.32	230.50	128.40	146.41	144.46	208.46	192.46
Relative density	8.64	4.05	2.34	6.95	4.79	4.82	4.69	
Melting point (ºC)	321	568	256	<1426	300 (decomposes)	1750	1000	Decomposes
Boiling point (ºC)	765	960	Decomposes	900-1000 (decomposes)				
Water solubility (µg/litre)	Insoluble	1400 (20ºC)	Very soluble	Insoluble	0.0026 (26ºC)	0.0013	755 (0ºC)	Slightly soluble

Source: WHO (1992)

1.2.2. Sources of Cd

There are various sources of Cd. The main sources of this metal in the environment include: natural, industrial and occupational sources

1.2.2.1. Natural Sources

Cd metal does not occur free in nature. The only mineral of Cd is greenockite (CdS), which is rarely found in nature but occurs as a coating on zinc sulphide ore, sphalerite. Natural sources of environmental Cd include volcanic eruption, forest burning and transport of soil particles by wind. An average concentration of Cd in the earth crust was reported to be about 0.1mg/kg and 0.1-0.4µg/kg on surface soil (Page *et al*., 1981). Cd finds its way into groundwater, and hence enters into plants and the food chain.

1.2.2.2. Uses, Industrial Sources and environmental release of Cd

About 50% of extracted Cd is mainly used in the electroplating of other metals especially steel, iron and copper. Cd alloys of copper, nickel, gold, silver, bismuth and aluminium are used as coating for other materials and have also found application in welding and soldering processes (Friberg and Elinder 1983; Sittig, 1985).

Apart from the above, Cd compounds have also found application in the production of pigments and dyes (Cd sulphide, Cd sulposelenide), in the production of nickel-Cd alkaline batteries and as stabilizer in plastic (Cd stearate).

Other uses of Cd include its use in printing, textiles, photography, lasers. Television phosphor, solar cells, scintillation counters, in jewellery, in

fluorescent lamp production, in paints and glass, as a neutron absorber in nuclear reactors, as pesticides etc. Cd is also a component of superphosphate fertilizers (Stokinger, 1981; Friberg and Elinder, 1983).

The main industrial sources of Cd include refinery, smelting of metals such as copper and zinc, combustion of fossil fuel, and nickel-cadmium (NiCd) battery manufacture and disposal. Phosphate fertilisers and contaminated sewage sludge are also important anthropogenic sources of release into the environment. An estimate of 30,000 t of Cd are released into the atmosphere each year due to the high usage of Cd worldwide, especially in the NiCd battery industry and out of these amounts, an estimate of 4000 to 13,000 t come from industrial activities (ATSDR, 2005). Contamination of groundwater can lead to a significant increase in Cd in crops.

1.2.2.3. Occupational and Other human Sources

The main occupational source is the smelting of non-ferrous metals, while the major non occupational source is cigarette smoke (WHO, 1992)
The total emission of Cd from human sources globally average in 1983 was 7570 tonnes (Nriagu and Pacyna, 1988).

1.2.3. Routes of Exposure and Acceptable daily intake (ADI)

The major routes of Cd exposure in the general population are mainly through ingestion of cadmium in certain foods and inhalation of cadmium from cigarette smoke. Negligible amounts of Cd exposure however occur through the skin (ATSDR, 1999).Incidental Inhalation of dust and fumes and ingestion of dust from contaminated hands, cigarettes, or food represent the major routes of occupational exposure (ATSDR, 1999). Food represents the

main source of human body exposure to Cd. Intake through drinking water and air contributes less to the daily intake (Van Assche, 1998). The average daily intake of Cd from food in non-smokers living in uncontaminated areas is estimated to be in the range 10 to 25μg of Cd (ATSDR, 1997). According to WHO, a tolerable weekly intake for Cd was estimated at 7 μg/kg of body weight and this corresponds to a daily tolerable intake level of 7 0μg of Cd for the average 70 kg man per day. It was estimated that a daily intake of 440 μg of Cd would be necessary for the western world population to reach the estimated critical concentrations of about 200 μg of Cd/g renal cortex (Friberg, 1979). It has been estimated that cigarette contains about 1-2μg of Cd and a smoker inhales about 10% of the Cd content when the cigarette is smoked (WHO 1992). Cd intakes from occupational exposures are reported to be generally below 5μg/m^3 (ATSDR 1997). Ambient air in rural areas has Cd concentration in the range of 0.001-0.005μg/m^3, 0.003-0.05μg/m^3 in urban area and up to 0.6μg/m^3 near Cd –emitting sources (Bernard and Lauwery, 1986).

1.2.4. Biological half life

Depending on the route of exposure, Cd has an estimated half-life between 20-40 years (Friberg *et al*., 1974)

1.3. Cd Toxicity

Cd induces both necrotic and apoptotic cell death (Galan *et al*., 2001). Although it has a multi-organ damaging effect, the risks and target organs depend mainly on the form of Cd and the route of exposure. Acute exposure by inhalation affects mostly the respiratory tract and lungs (WHO, 1992). While chronic exposure affects mainly the kidney and lung. Acute exposure

by ingestion affects mainly liver, kidney, cardiovascular and nervous system and intestine (WHO, 1992). While chronic ingestion affect mainly the kidney, liver and bone. Cd is classified as a human carcinogen (Category 1 Carcinogen). It is listed as one of the 126-priority pollutants by the US Environmental Protection Agency. It has been reported that the metal causes various types of cancer (lung, prostate, pancreas and kidney) (Waalkes and Rehn, 1994) and conditions such as anaemia, eosinophilia, renal tubular injury, anosmia, chronic rhinitis and osteoporosis (Waisberg *et al.,* 2003) in the body. Cd is mainly non-genotoxic but enhances the genotoxic effect of other genotoxic agents by inhibiting DNA repair process (Hartwig and Schwerdtle, 2002).

1.3.1. Mechanisms of Cd toxicity

There are several mechanisms by which Cd exerts its toxic effect and therefore no uniform mechanism has been proposed so far (Thevenod, 2009). Its mechanisms of action include induction of oxidative stress, inhibition of DNA repair, interference with signal transduction and gene expression, induction of apoptosis, inhibition of enzyme activities and inhibition of some biosynthetic pathways. The mechanism appears to depend on whether exposure is chronic (longer time exposure to low concentration) or acute (shorter time exposure to high concentration).

1.3.1.1. Induction of oxidative stress

Oxidative stress is the term given to the condition in which there is an imbalance between the oxidants and the antioxidants in favour of the former (Scheibmeir *et al.,* 2005). This may be due to more oxidants been produced or less availability of antioxidants. Oxidative stress is not synonymous with

oxidative damage since most cells have the machineries to detect changes in redox status and then adjust to cope with the stress. Oxidative damage occurs when there is severe imbalance that the cells can not cope with resulting in damage to macromolecules. Various studies have shown that Cd induces oxidative stress by depletion of intracellular GSH, enhancing the production of reactive oxygen species (ROS) and interference with the cellular antioxidant system.

1.3.1.1.1. Effects of oxidative stress and Chronic Cd exposure

Kidney, liver, lung, pancreas, testis, placenta, bone and blood are the most targeted organs in chronic Cd exposure (Fig.1.1; Thevenod, 2009). Chronic Cd exposure leads to renal dysfunction, anaemia, osteoporosis and bone fractures (Friberg *et al.,* 1986).The role of ROS in chronic Cd toxicity and carcinogenesis is controversial depending on experimental conditions (Liu *et al*., 2009). While ROS has been implicated in chronic Cd carcinogenesis (Waisberg *et al*.,2003), immunotoxicity (Ramirez and Gimenez, 2003) and nephrotoxicity (Shaikh *et al*., 1999), due to increased lipid peroxidation and DNA damage, exposure of animals to continual low dose of Cd for a year enhances hepatic and renal glutathione (GSH) levels without increasing tissue lipid peroxidation (Kamiyama *et al.,* 1995). The initial increase in lipid peroxidation and hepatic iron observed after 24hr single oral dose exposure to Cd diminishes after continuous repeated dose (Djukic-Cosic *et al*., 2008). Thijssen *et al* (2007) also observed that prolonged Cd exposure (100 ppm, 23 weeks) through drinking water does not affect cellular redox status and lipid peroxidation levels. However, increased ROS production has been observed under different experimental conditions following chronic exposure (Liu *et al*., 2009). For example, administration of Sprague-Dawley rats with oral

daily dose of 4.4 mg/kg Cd in drinking water increases lipid peroxidation in liver mitochondrial and microsomes after 15 days of administration reaching the peak between 60 and 75 days (Bagchi *et al*., 1997). Also an increase in hepatic and renal lipid peroxidation levels with increasing tissue GSH levels has been observed in chronic administration of 0.6mg/kg Cd (5days/week for 22week) in Sprague-Dawley rats (Shaikh *et al*., 1999). The reduced ROS production observed following chronic Cd exposure has been hypothesized to be as a result of an adaptive response which results in the elimination of oxidative stress (Liu *et al*., 2009). However, high level excess ROS production overwhelms antioxidant defences resulting in lipid peroxidation and oxidative damage.

1.3.1.1.2. Effects of oxidative stress and Acute Cd exposure

In acute exposure, the liver, lung, kidney and testes are the main target organs (Fig.1.1; Martelli *et al*., 2006). Exposure to acute dose of Cd by inhalation causes pulmonary edema and respiratory tract irritation in human (Friberg *et al*., 1986). Acute Cd toxicity is associated with GSH depletion and depletion of other protein- bound sulfhydryl groups thereby enhancing ROS production such as superoxide anion, hydrogen peroxide and hydroxyl radicals (Manca *et al*., 1994; Bagchi *et al*., 1997; Liu and Jan, 2000). The enhanced ROS production results in lipid peroxidation and DNA damage (Fig.1.1).

1.3.1.1.3. Effects of oxidative stress and Cd-induced malignant transformation

ROS have been reported to play a minimal role in the induction of malignant growth in rat liver cells exposed to Cd (Waalkes, 2003). Chronic exposure of

liver cells to 1 μM $CdCl_2$ for 28 weeks was reported to produce malignant transformation without ROS production (Qu *et al*., 2005). Using fluorescence probes such as dihydroethidium for superoxide anion and 2, 7′-dichlorofluorescein diacetate for hydrogen peroxide, Qu *et al* (2005) shows that ROS production was evident after acute exposure of rat liver cells to 10 and 50μM Cd, but cells exposed to chronic dose of Cd become malignant and are quite tolerant to a high Cd dose (50 μM) that induced ROS production. Exposure of human urothelial UROtsa cells to a chronic low dose (1.0μM) of Cd was also reported to produce malignant transformation which was not evident at higher lethal doses (5 μM or 9 μM) (Somji *et al*. 2006). The transformed UROtsa cells become more resistant to Cd toxicity, oxidative DNA damage and apoptosis (Somji *et al*. 2006). In another study using human prostate epithelial cells, chronic exposure to Cd resulted in malignant growth with increased resistance to apoptosis not only to Cd but to other anticancer agents such as etoposide and cisplatin (Achanzar *et al*., 2002). These series of studies show that exposure of rodent or human cells to low Cd concentrations at levels obtainable in the environment can induce malignant transformation without increasing ROS production, but showing a tolerance to oxidative stress and apoptosis (Achanzer *et al*., 2002, Qu *et al*., 2005; 2007; Somji *et al*., 2006). These show that Cd-induced malignant transformation involves induction of apoptotic resistance and tolerance to oxidative stress. The net effects are the avoidance of damage to DNA because of the repair and elimination machinery of the apoptotic process.

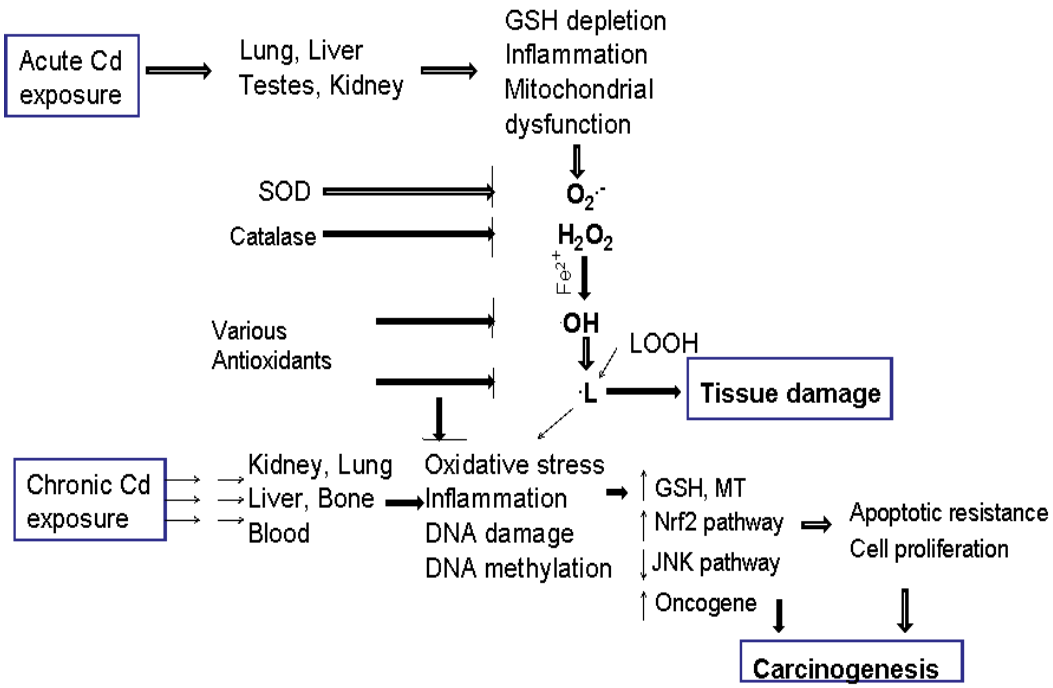

Source: Liu *et al.*, 2009.

Fig.1.1. Proposed pathways for the involvement of ROS in Cd toxicology and carcinogenesis following acute and chronic exposure. Effects of Cd depend mainly on the dose and duration of exposure. Long-term exposure to low dose of Cd induced adaptive response, increase GSH and decrease ROS leading to apoptotic resistance and malignant cells formation. Acute exposure leads to increase ROS production, GSH depletion and apoptosis.

1.3.1.2. Mechanisms of Increased ROS

Cd is a redox-stable metal; therefore the production of ROS by Cd is mediated by indirect mechanisms. These mechanisms include GSH depletion, Cd-induced inflammation and Fenton reaction driven with iron.

1.3.1.2.1. Depletion of intracellular GSH

Cd binds to intracellular sulfhydryl groups, thereby causing GSH depletion resulting in oxidative stress (Irano *et al*., 2001) (Fig.1.1). GSH is an endogenous non-enzymic antioxidant that scavenges intracellular ROS either directly or via the GSH redox cycle thereby preventing oxidative stress (Meister and Anderson, 1983). It is abundant in the liver and serves as the first line of defence against Cd hepatotoxicity as hepatic GSH depletion enhances Cd-induced hepatotoxicity (Dudley and Klaassen, 1984). Cd is known to have high affinity for thiol groups and the binding of Cd to GSH results in a decrease in the cellular level of glutathione which consequently enhances the susceptibility of the cells to free radical attack. Acute exposure to Cd results in GSH depletion (Dudley and Klassen, 1984; Liu *et al*., 1990) while chronic exposure often leads to enhanced GSH levels in tissue and cells (Kamaiyama *et al*., 1995; Shaikh *et al*., 1999; Waisberg *et al*., 2003) with the subsequent elimination of oxidative stress and this may account for the low levels of ROS observed in chronic Cd exposure.

1.3.1.2.2. Enhanced ROS production by inflammation and Fenton reaction

Cd toxicity and carcinogenicity has been reported to be mediated through the production of ROS that alter mitochondrial activity and trigger apoptosis (Shen *et al*., 2001; Pathak and Khandelwal, 2006). Cd has been reported to induce the production of superoxide anions, nitric oxide, hydrogen peroxide

(Galan *et al*., 2001 and Stohs *et al*., 2001) and hydroxyl radicals (O'Brien and Salacinski, 1998). The induction of inflammatory reactions has been reported to be an important mechanism by which Cd-induces ROS production in the liver (Yamano *et al*., 2000). It was shown that inhibiting Kuppffer cells function, the macrophages of the liver, by gadolinium chloride decreased Cd induced hepatotoxicity in rats (Sauer *et al*., 1997) and mice (Harstad and Klaassen, 2002) and this was due to decrease ROS production (Liu *et al*., 2009) resulting from absence of inflammatory cytokines such as IL-1β, TNF-α, IL-6 and IL-8 (Yamano *et al*., 2000). Cd displaces iron (Casalino *et al*., 1997) and copper from their intracellular sites thereby resulting in increased concentrations of these ions, which can undergo Fenton reactions to generate ROS (Fig.1.2; Waisberg *et al*., 2003)). In one study, the presence of desferal, an iron chelator, was shown to decrease ROS formation in the bile of rats exposed to Cd (Liu *et al*., 2009) indicating the involvement of Cd in ROS production by iron.

$$Fe^{2+} + H_2O_2 \xrightarrow{\text{Oxidised}} Fe^{3+} + .OH + OH^-$$

$$Fe^{3+} + H_2O_2 \xrightarrow{\text{Reduced}} Fe^{2+} + .OOH + H^+$$

Fig.1.2. Fenton reaction. Fe^{2+} is oxidised to Fe^{3+} in the presence of hydrogen peroxide to form hydroxyl radical (.OH) and hydroxyl anion (OH^-). The Fe^{3+} is further reduced back to Fe^{2+} to produce peroxide radical.

1.3.1.3. Interference with cellular antioxidant defence

Apart from depleting intracellular GSH level, Cd also alters the activities of various antioxidant enzymes involve in protection against free radical attack. The effects of Cd on these antioxidant enzymes are time and dose-

dependent. While Cd has been reported to decrease the activities of most of these enzymes in vitro and in vivo studies after short-term exposure, higher dose and longer exposure time increased activities (Waisberg *et al*., 2003). These increased activities may probably due to induction of protective genes as a result of adaptive response. Studies have shown that the activities of glutathione peroxidase (which catalyses the reduction of hydroperoxide with simultaneous oxidation of glutathione), superoxide dismutase (which catalyses the conversion of superoxide anion to molecular oxygen to hydrogen peroxide), and catalase (which catalyses the conversion of hydrogen peroxide to water and molecular oxygen) were decreased by the presence of Cd (Del Carmen *et al*., 2002, Tatrai *et al*., 2001, Ochi *et al*., 1987). Cd competes with copper and zinc in SOD, selenium in glutathione peroxidase and iron in catalase thereby reducing the activities of these antioxidant enzymes. In other studies, increased activities of SOD (Casalino *et al*., 1997), glutathione reductase and glutathione peroxidase were observed in various tissues of rodents exposed to Cd.

1.3.1.4. Inhibition of enzyme activities

Cd competes with some enzymes for their cofactors thereby inhibiting their activities. Cd depletes the body selenium resulting in inactivation of glutathione peroxidase activities (Ghosh and Bhattacharya, 1992). It competes with calcium for their binding sites on calcium dependent binding proteins such as calmodulin (Chao *et al*., 1984). Cd also competes with Zn and Cu for their binding sites on proteins. It also displaces Fe from its binding sites (Casalino *et al*., 1997) resulting in enhanced ROS production via Fenton reactions.

1.3.2. Apoptosis

Apoptosis is a programmed cell death by which cell gets rid of unwanted or worn-out cells. Apoptosis is characterized by cell shrinkage, nuclear, chromatin and cytoplasmic condensation, membrane blebbing, DNA fragmentation and protein fragmentation with the break down of the cells into smaller units called apoptotic bodies and consequent formation of necrotic cells (Thompson, 1995). In normal condition, apoptosis does not induce inflammatory responses. However, in an unregulated apoptosis cells become malignant. Apoptosis plays an important role in development, cancer, ageing and in neurological diseases such as Alzheimer and Parkinson's diseases (Thompson, 1995). Many of these neurological diseases share a common feature in that they are characterised by loss of neuronal cells and this is due largely to the uncontrolled activation of the apoptotic cell death. Two main pathways are involved in apoptosis; the **intrinsic pathways** which involve the activation of several procaspases and the release of apotogenic factors such as cytochrome c and apoptosis-inducing factor (AIF) from the mitochondrial into the cytoplasm and the **extrinsic pathways** which involve the activation of death receptors, Fas and tumour necrosis factor (TNF) receptors (Fig.1.3). Both pathways converge on the activation of the executioners of cell death, caspase 3 or caspase 7; however, non caspase dependent apoptosis has also been reported (Leist and Jaattela, 2001). Several families of protein such as caspases, Bcl-2 family proteins, Bax, Calpain, cathepsin and granyzme B interact under physiological and pathological conditions to drive the apoptotic process.

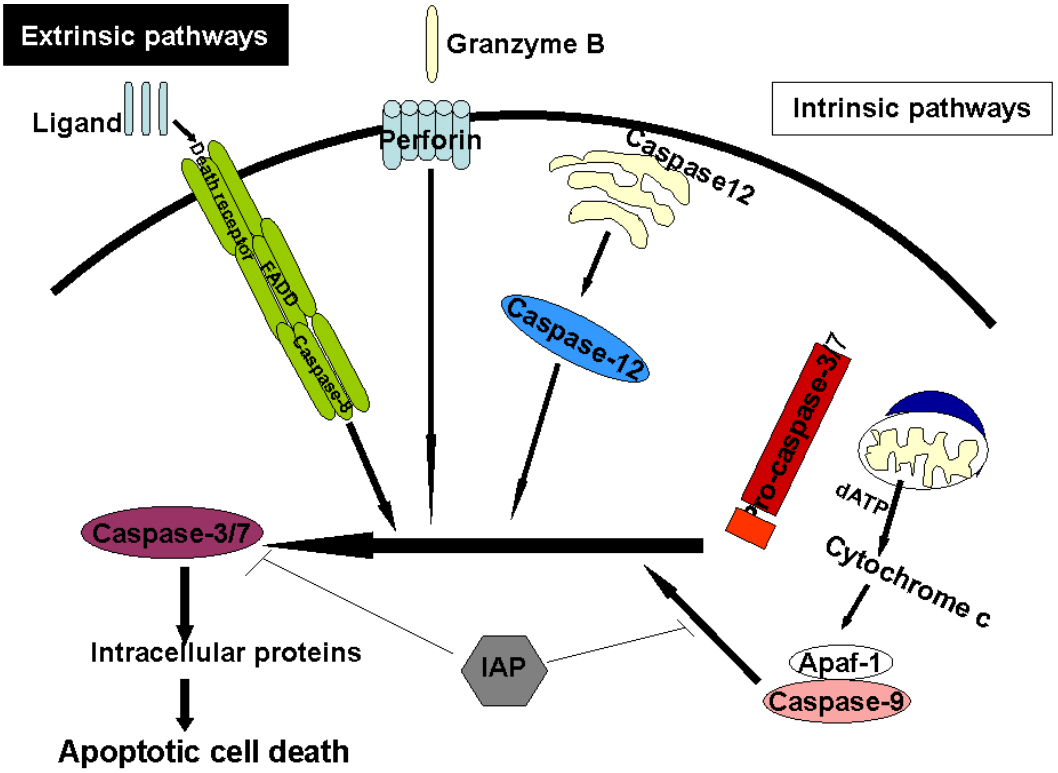

Fig.1.3 Schematic diagram of the major apoptotic signalling pathways The extrinsic pathway involves the activation of caspase-8 by the delivery of granzyme B through perforin to the cells as well as by activation of death receptor by ligand. The intrinsic pathways involve activation of caspase-9 by the interaction of cytochrome c released from the mitochondrial with Apaf1. Activation of caspase-12 can be induced by other forms of intracellular stress. Both the extrinsic and intrinsic pathways converge on the activation of caspase-3 or caspase-7. Inhibitor of apoptosis proteins (IAPs) can suppress these pathways either by blocking the activation of caspase-9 or by directly inhibiting the activity of caspase-3.

1.3.2.1. Mitochondrial-caspase dependent Apoptosis

The components of mitochondrial mediated apoptosis include;

Cytochrome c

Cytohrome c is a component of the electron transport chain in the mitochondrion and serves as an electron carrier in oxidative phosphorylation in the generation of ATP. The photon gradient generated across the inner mitochondrial membrane by the transfer of electrons from complex III to complex IV via cytochrome c (Mathew, 1985) helps in maintaining the membrane potential. Therefore, the release of cytochrome c from the electron transport chain, leads to a decrease in mitochondrial membrane potential and consequent generation of ROS as a result of incomplete reduction of oxygen and impaired ATP production (Tsujimoto, 1997). In the cytosol, cytochrome c interacts with Apaf-1 protein to activate DEVD-specific caspase (Yang *et al*., 1997) leading to apoptosis (Fig.1.3).

Caspases

Caspases are cysteine-dependent aspartate-specific proteases (Alnemri *et al*., 1996) that are expressed as inactive precursors (pro-enzymes) containing three domains: NH2 terminal, a large subunit (~20KDa) and a small subunit (~ 10KDa).

At least 14 different caspases have been identified in mammals to date but not all of them are involved in apoptosis (Cohen, 1997). However, most of them play distinct roles in apoptosis and/or inflammation (Philchenkov, 2004). The caspase family can be divided into three subgroups depending on factors such as substrate specificity, domain composition or the role in

apoptosis (Thornberry, 1997). These include initiator caspases such as caspase 2, 8, 9 and 10; executioner caspases such as caspase 3, 6 and 7 and caspases involved in cytokine activation such as caspase 1, 4, 5, 11, 12, 13 and 14. Both the initiator and executioner caspases play either a direct or indirect role in processing, propagation and amplification of apoptotic signals that eventually lead to cell destruction. The initiator caspases initiate the apoptotic cascade with the consequent activation of the executioner or effectors caspases. Stress-induced apoptotic cell death caused by β-amyloid toxicity and trophic factor deprivation are mediated by caspase-2 (Troy *et al*., 2000). A large protein complex with the death domain-containing protein PIDD and the adaptor protein RAIDD is involved in caspase-2 activation (Tinel and Tschopp, 2004). Caspase-9 and its adaptor Apaf-1 are involved in DNA damage, corticosteroid and staurosporine-induced cell death in thymocytes and embryonic fibroblasts (Hakeem *et al*., 1998). The caspase zymogen has an N-terminal prodomain followed by sequences comprising a large and a small subunit. Two cleavages are involved in the conversion of the zymogen into mature caspase; the cleavages involve the separation of the prodomain from the large subunit and the separation of the large and small subunits. The cleavage between the large and small subunits occurs before the cleavage of the prodomain. Two different mechanisms are involved in the activation of the initiator and executioner caspases. Initiators are activated by homoactivation such as the activation of caspase-8 that requires an adaptor protein for its activation and the activation of caspase-9 that requires formation of a complex with cytochrome c and Apaf-1 (Fig.1.3). Activation of executioner caspase is by heteroactivation i.e. it is dependent on the activation of the initiator caspases. The activated executioner caspases can in turn act on the inititiator zymogens to set up a cascade of activation

processes. Activated caspases then cleave specific target proteins to induce apoptosis. Caspase can also induce permeability transition pore in the mitochondrial with the consequent reduction in mitochondrial membrane potential leading to the release of apoptotic inducing factor and ROS production (Boise and Thompson, 1997).

Bax

The Bcl-2-associated X protein or Bax belongs to the Bcl-2 protein family and enhances apoptosis by competing with Bcl-2. Bax is a pro-apoptotic protein and the gene was the first identified pro-apoptotic member of the Bcl-2 protein family (Oltvai *et al*., 1993). Bax subfamily includes, Bax, Bak and Bok/Mtd all of which is pro-apoptotic channel-forming proteins and consist of BH1, BH2 and BH3 domains (Zhang *et al.,* 2004). In a normal healthy cell, Bax is found mainly in the cytosol, however, upon initiation of apoptosis signalling, Bax becomes anchored into the outer mitochondrial membrane. The migration and insertion of Bax is due to conformational change in the Bax protein (Wolter *et al.,* 1997). One of the mechanisms involved in the pro-apoptotic function of Bax is that it interacts with and induces the opening of the mitochondrial voltage-dependent anion channel (VDAC). Another proposed mechanism is that it forms oligomeric pore (MAC) with the outer mitochondrial membrane resulting in the release of cytochrome c and apoptotic inducing factor (AIF) from the mitochondria with the consequence of activation of caspases (Fig.1.3). p53, a transcription factor, enhanced the expression of Bax. The tumour suppressing function of p53 is reported to be mediated by Bax as observed in p53 null mutant experiments were Bax expression was suppressed in p53 null mutant mice with concomitant increase in tumour formation (Selimi *et al*., 2000).

1.3.2.2. Non-Caspase Proteases in Apoptosis

Calpain

Calpains are a group of ubiquitous or tissue-specific cysteine proteases located in the cytoplasm (Sorimachi *et al*., 1994; Croall and DeMartino, 1991).They are Ca^{2+}-activated proteases that have been implicated in apoptosis because they are activated during cell death and that apoptotic process is hindered by the presence of their inhibitors (Squier *et al*., 1994). Though several targeted proteins for calpain activity have been identified such as fodrin (Vanags *et al*., 1996), gelsolin (Wolf *et al*., 1999), $PKC_{\alpha/\beta/\gamma}$ (Kishimoto *et al*., 1989), p53 (Kubbutat and Vousden, 1997) and Bax (Wood *et al*., 1998), however, it is not currently known which of these substrates has the highest affinity for calpain and which is the most important for its proapoptotic action. Calpains has been reported to play a role in caspase activation (Thevenod, 2009). Inhibitor studies have shown that the presence of calpain inhibitor PD-150606 decreased caspase-3 activity and apoptosis after 24hr exposure (Lee *et al*., 2006). This suggested a link between calpain and caspase-dependent apoptotic pathways.

1.3.2.3. Induction of Apoptosis by Cd

The apoptotic pathways induced by Cd may depend on cell types and conditions of exposure. In some studies, the induction of apoptosis by Cd has been reported to be a mitochondria- dependent pathway through the activation of caspase-9 (Kondoh *et al*., 2002; Watjen *et al*., 2001). However, a non-caspase activated mitochondria-dependent pathway has also been reported in normal human lung cells (Shih *et al*., 2003). Cd decreases $Bcl\text{-}x_L$ and Bid expression significantly and also causes loss of mitochondrial membrane potential in human lymphoma U937 cells (Li *et al*., 2000). Cd

inactivates p53 protein and therefore promotes impaired induction of p53 in response to DNA damage. Cd also causes increase in reactive oxygen species at high concentrations (Waisberg *et al.,* 2003) resulting in oxidative stress and subsequent apoptosis (Hart *et al*., 1999). The picture of the role of cellular signalling pathways in Cd-induced apoptosis is not clear (Waisberg *et al.,* 2003). Cd has been reported to activate protein kinases ERK and p38-MAPK (Chao and Yang, 2001) and JNK (Chuang *et al*. 2003) in CL3 human lung cancer cells. The activation of ERK in CL3 human lung cancer cells enhances cell survival while p38-MAPK decreases survival. It was reported that only a fraction of cells become apoptotic after the induction of proto-oncogenes c-jun and c-myc and tumour suppressor gene p53 in normal human prostate cells exposed to Cd (Achanzar *et al*., 2000). This shows that induction of apoptosis by Cd does not necessary mean protection against malignant growth.

1.3.2.4. The Mitochondrion and Cd-induced toxicity

The toxicity of many metals including Cd is targeted toward the mitochondrion (Belyaeva *et al*., 2008).Cd has been reported to bind to protein thiols present at the mitochondrial membrane thereby altering mitochondrial permeability transition and inhibiting the respiratory chain reaction leading to ROS production (Dorta *et al.,*2003). Cd has also been reported to enhance the accumulation of semiubiquinones at the Q_O sites by inhibiting mitochondrial complex III. The unstable semiubiquinones enhanced superoxide production through the transfer of one electron to molecular oxygen (Wang *et al.,* 2004).

1.3.3. Interference with Signal Transduction pathways and Ca^{2+} Metabolism

1.3.3.1. Ca^{2+} and Apoptosis

An increase in intracellular calcium ion concentration leads to cell death or apoptosis and deregulation in the expression of genes due to its interaction with cAMP response element binding protein present at promoter regions of genes (Hardingham *et al*., 1997). The up regulation of Ca^{2+} can activate a number of proteases including calpain resulting in apoptosis and necrosis. Induction of apoptosis by calcium is reported to involve both a direct and indirect pathway. In the indirect pathway, Ca^{2+} activates calcineurin leading to the up regulation of CD95 (Fas, APO-1) ligand with the consequence of activation of death receptor and caspase (Fig.1.4). In the direct pathway, increased intracellular Ca^{2+} can trigger the apoptotic process by inducing permeability transition pore (Weis *et al*., 1994) in the mitochondrial with the consequent released of cytochrome c. The released cytochrome c induces formation of a caspase-activating complex (procaspase-9 bound to Apaf-1) in the presence of dATP (Li *et al*., 1997) with the subsequent activation of procaspase-3 and procaspase-7 (Pan *et al*., 1998).

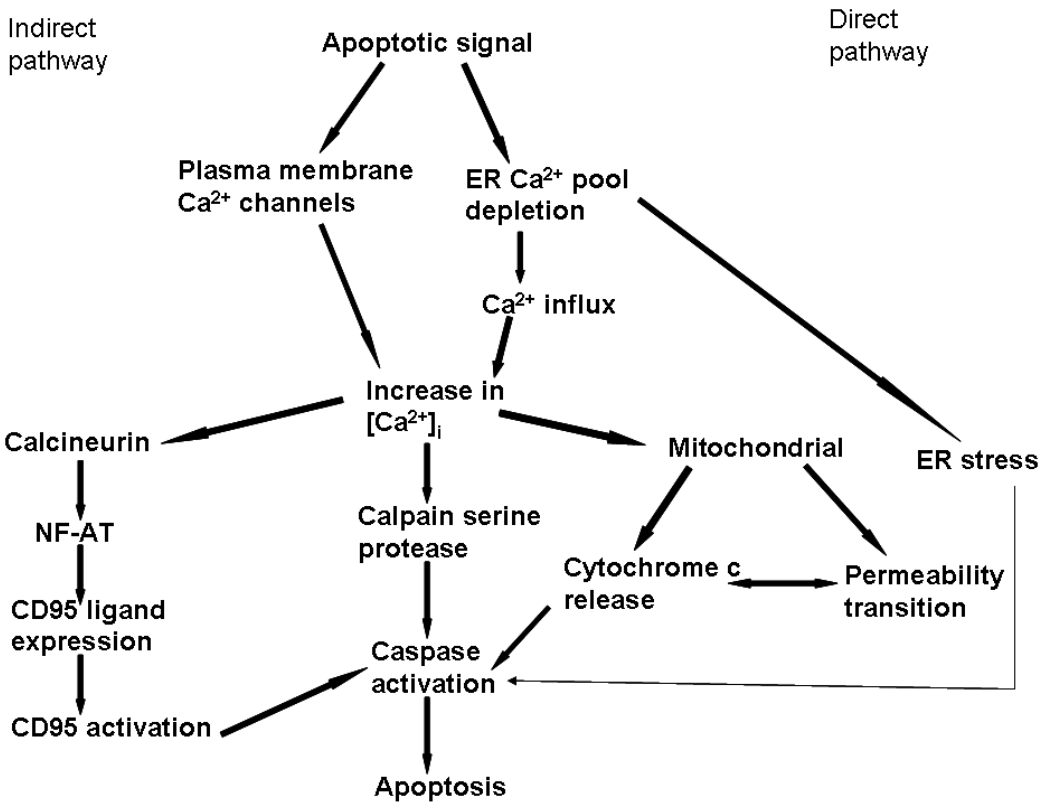

Adapted from Kass and Orrenius (1999)

Fig.1.4. Schematic representation of the proposed mechanisms of Ca^{2+} signals induced apoptosis. Changes in intracellular Ca^{2+} levels ($[Ca^{2+}]_i$) can induce apoptosis by two separate pathways; one that is indirect and requires activation of death receptor such as CD95 (Fas, APO-1) and a second pathway in which Ca^{2+} is the direct effector of apoptosis by targeting the mitochondrial and the endoplasmic reticulum (ER).

1.3.3.2. Cd^{2+} and Ca^{2+} signalling

Cd^{2+} has nearly the same ionic radii as Ca^{2+} (0.95 and 1.00 Å, respectively) and therefore mimics Ca^{2+} in most of its binding sites (Martelli et al., 2006). The concentration of calcium ions, an important intracellular signal messenger, in the cell can therefore be up regulated by Cd via the activation of phospholipase C_β (PLC_β) and inositol-1,4, 5-triphosphate (IP_3) production (Misra *et al*., 2002) (Fig.1.5). This activation is achieved by the binding of Cd to the surface Ca^{2+} sensing G-protein coupled metal binding receptor (Faurskov and Bjerregand, 2002) similar to the Ca^{2+} receptor (CaR) present in kidney, gut and parathyroid cells (Tfelt-Hansen and Brown, 2005). The involvement of PLC-IP_3 pathway in Cd-induced alteration in intracellular Ca^{2+} was investigated by Smith *et al* (1989) in human skin fibroblasts using U73122, a phospholipase C inhibitor, and neomycin, a CaR agonist and Fura-2 AM as Ca^{2+} probe. They found that the Cd^{2+}-evoked increase cytosolic Ca^{2+} was abolished in the presence U73122 and neomycin. The presence of TPEN, a cell permeable metal chelator, however, does not decrease cytosolic Ca^{2+} unlike the Ca^{2+} chelator BAPTA-AM showing the fura-2 specifically interacts with cytosolic Ca^{2+} and not Cd^{2+} (Smith *et al*., 1989).

Apart from the G-protein metal coupled receptor, acute Cd^{2+} can also bind to CaR to induce transient activation of Ca^{2+} dependent signal (Thevenod, 2009). Cd^{2+} can also enter the cells through various Ca^{2+} channels and transporters for essential metals (Dalton *et al.,* 2005).

The up regulation of intracellular Ca^{2+} makes Cd an alternative signalling molecule and consequently controls signal transduction pathways (Misra *et al*., 2002). Disruption of physiological signalling processes leading to

dysfunction in signalling is one of the mechanism by which Cd^{2+} exerts its toxicity in cells. Like other second messengers, Ca^{2+} transduced information by alteration in its cytosolic concentrations which rise by at least 10-fold from the low intracellular level of 0.1μM upon stimulation (Thevenod, 2009). However, unlike other second messengers, Ca^{2+} cannot be degraded by the cells; hence prolonged alteration in the cytosolic Ca^{2+} levels may be harmful to the cells and can induce unwanted cellular responses such as cell death. In order to maintain Ca^{2+} homeostasis, cells dispense much energy to keep the cytosolic Ca^{2+} level at its resting state. The mechanisms of compartmentalization, chelation and extrusion are used by cells to keep the cytosolic levels of Ca^{2+} as low as possible (Clapham, 2007). Highly specialised physiological functions of the cells such as exocytosis, excitability and motility may be due to the reversible alteration of targeted proteins by the binding of Ca^{2+} (Clapham, 2007).

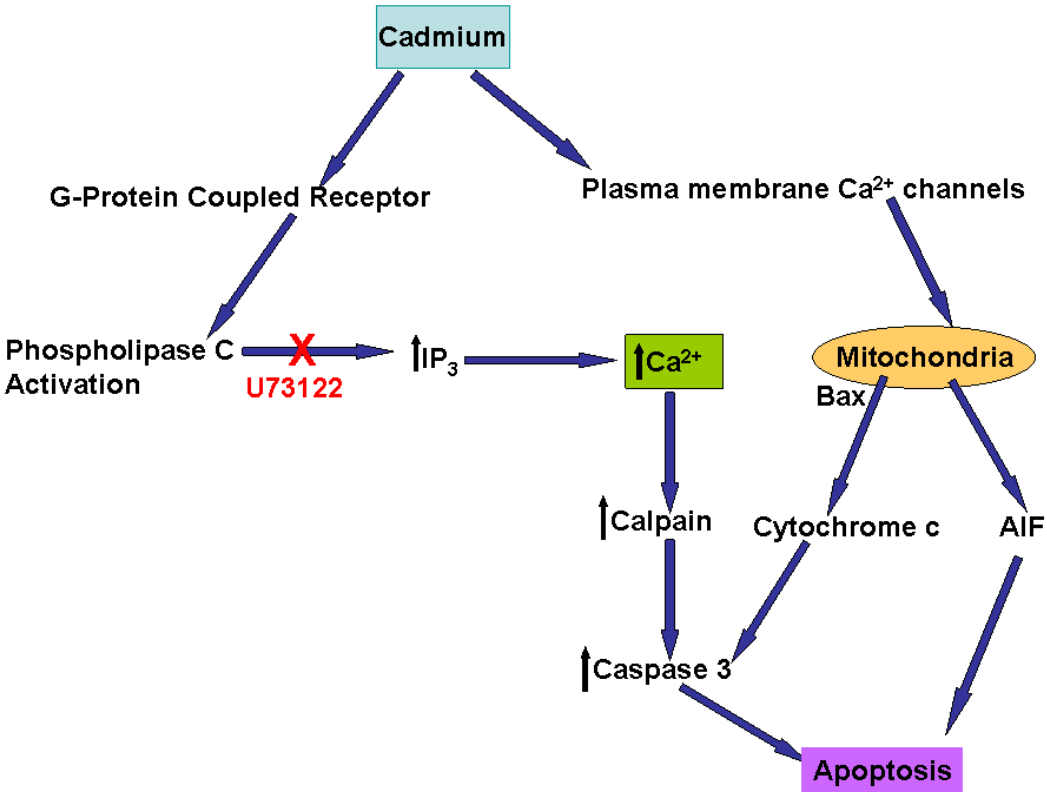

Fig.1.5. Proposed pathways of apoptosis induced by Cd. Cd can activate a G protein-metal coupled receptor on the cell surface resulting in the activation of phospholipase C (PLC$_\beta$).The activated PLC$_\beta$ can result in the release of Ca^{2+} from the intracellular store such as endoplasmic reticulum (ER) via the production of IP_3.The released Ca^{2+} can activate calpain which can further activate caspase-3. Cd^{2+} can also induce mitochondrial inner membrane permeability transition thereby creating pores resulting in loss of membrane potential. These pores can result in the release of cytochrome c and Apoptotic inducing factor (AIF) into the cytosol.

1.4. Adaptive Responses to Cd Exposure

An adaptive response is the ability of a cell, tissue or organism to cope or resist the damaging effect of xenobiotics and other toxic compounds at a low dose of exposure (Crawford and Davies, 1994). This response involves the induction of groups of genes encoding protective enzymes. Apart from toxic chemicals, exposure to antioxidants can also lead to the induction of cytoprotective genes thereby enhancing the protective machineries of the cells. The adaptive response confers on the cell the ability to resist the toxic effect of subsequent high dose of exposure to the toxic compounds (Crawford and Davies, 1994).

Exposure to low dose of Cd has been reported to activate a number of defensive mechanisms in the cells (Liu *et al*., 2009). Among these, the transcription factor Nrf2 plays a significant role in the regulation of the expression of large number of cytoprotective genes against Cd toxicity (Liu *et al*., 2009). In addition to Nrf2 activation, the oxidative stress caused by Cd as a result of increase ROS production is reported to trigger a variety of factors that are part of the protective response of the cells. These factors include induction of metallothionine, increased GSH levels activation of extracellular signal regulated kinases (ERK1/2) and protein kinases (Halliwell and Gutteridge, 2007) all of which enhance cell survival.

1.4.1. Nrf2-Keap1-ARE Transcription Pathway

The Nrf2-Keap1 pathway plays a very crucial role in cellular defence against oxidative stress and reactive electrophiles produced during food metabolism or in pathological conditions. This pathway constitutes a major regulatory system by which cells neutralise ROS elicited by toxic exposure and other

environmental insults and thus helps in maintaining the cellular redox homoeostasis (Venugopal and Jaiswal, 1996; Itoh *et al*. 1999). Arrays of genes that encode detoxifying and antioxidative stress enzymes and proteins are induced in a well coordinated process upon exposure to electrophiles and ROS by this pathway (Talalay *et al*., 2003).

Nrf2

Nuclear factor erythroid 2-related factor (Nrf2) is a basic region-leucine zipper (bZip)-type transcription factor (Moi *et al*., 1994; Itoh *et al*., 1995) identified as the major regulator of antioxidant responsive element (ARE)-mediated gene expression (Itoh *et al*., 1997) and is structurally related to the p45 subunit of NF-E2 (nuclear factor erythroid 2) (Fig.1.6). Originally identified as an erythroid-restricted DNA-binding activity that recognises the specific DNA sequence (A/G)TGA(G/C)TCAGCA (NF-E2 binding motif) containing a 12-O-tetradecanoylphorbol-13-acetate responsive element, NF-E2 was the second factor found among the transcription factors that have specificity for erythroid genes, the first being GATA-1, known initially as NF-E1. NF-E2 is a heterodimeric protein consisting of a large p45 and small p18 subunit (Ney *et al*., 1993). cDNA cloning has shown that the p45 contains a cap'n' collar (CNC) - type bZip domain (Andrews et al., 1993), which is highly conserved in the *Drosophila* transcription factor CNC (Mohler *et al*., 1991). The CNC-bZip domain of p45 subunit heterodimerized with p18 which was identified as MafK, one of the small Maf transcription factors that are cellular products of the Maf proto-oncogene family (Igarashi *et al*., 1994). The mouse p45 and MafK heterodimer confers DNA-binding activity to p45 while the p45 transactivation domain activates transcription (Igarashi *et al*., 1994). Five NF-E2-related proteins that have a common CNC-type bZip

domain have been cloned and characterised. These factors also heterodimerised with one of the small Mafs as requirement for binding to the NF-E2 motif (Kobayashi *et al*., 1999). Nrf1 (Caterina *et al*., 1994), Nrf2 (Moi *et al*., 1994) and Nrf3 (Kobayashi *et al.,* 1999) are expressed in large number of tissues. Bach1 (Oyake *et al*., 1996) is ubiquitously expressed especially in bone marrow and fetal liver (Igarashi *et al*., 1998) and Bach2 (Oyake *et al.,* 1996) is most abundant in the brain and B cell lineages (Muto *et al*., 1998). Endogenous products of oxidative stress or other stresses generated in the body such as 4-hydroxynonenal (Ishii *et al*., 2004), oxidised low-density lipoproteins (Anwar et al., 2005), heme (Nakaso *et al*., 2003) and nitric oxide (Buckley *et el*. , 2003) as well as keratinocyte growth factor (Braun *et al.,* 2002) and fibroblast growth factor (Vargas *et al.,* 2005) can activate Nrf2. Nrf2 targeted gene analysis has demonstrated that Nrf2 coordinates and regulates a battery of genes encoding drug-metabolizing enzymes and antioxidant proteins (Itoh *et al.,* 1997).

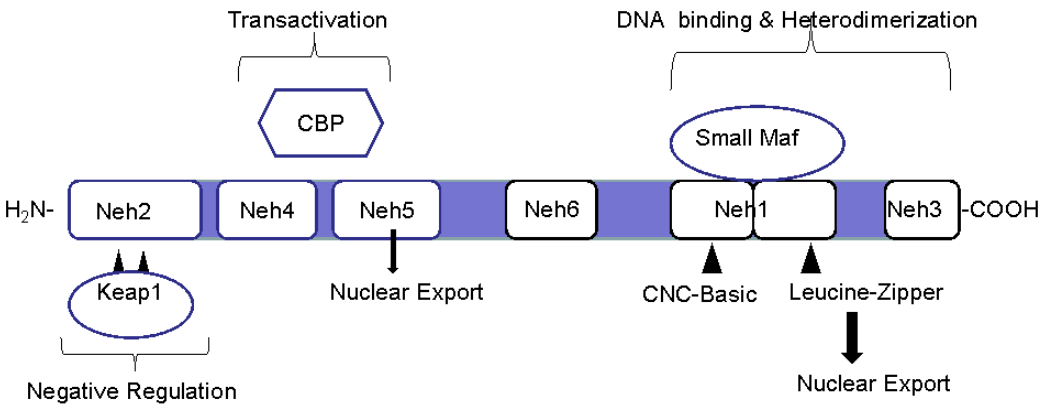

Fig.1.6. Nrf2 regulatory network Nrf2 has six domains that are highly conserved called Neh1 to Neh6. Neh2 is the most highly conserved domain among species located at the N-terminal and it is responsible for interaction with Keap1. At the C-terminus are the Neh1 and Neh3 and a basic leucine zipper structure and this region is involved in dimerization with small Mafs and binding to ARE. Interaction with co-activator CBP occurs at Neh4 and Neh5 domains during transcriptional activation in the nucleus.

Keap1

Detailed analysis of the structure and function of domains and regions homologous between human Nrf2 and chicken ECH (erythroid-derived CNC-homology factor) have identified six Neh (Nrf2-ECH) domains (Itoh *et al*., 1997) in Nrf2; namely, Neh1 to Neh6 (Fig.1.6). The deletion of the N-terminal Neh2 domain was found to enhance the transcriptional activity of Nrf2 (Itoh *et al*., 1999) suggesting that this domain may mobilise a negative regulator of Nrf2. This negative regulator was later identified in a yeast two-hybridization system as Keap1 (Kelch-like ECH associating protein 1) (Itoh *et al*., 1999) also known as inhibitor of Nrf2 (INrf2). Murine Keap1 primary structure analysis, based on Keap1 cDNA sequence, reveals that it consists of 624-amino-acids sequence with 95% homology between human and mouse (Itoh *et al*., 1999). Keap1 consists of five domains: the N-terminal region (NTR), the BTB (Bric-a-brac, tramtrack, broad-complex), the intervening region (IVR), the double glycine repeat (DGR) or Kelch domain, and the C-terminal region (CTR) (Fig.1.7). Protein homodimerization and heterodimerization and the making of homomeric and heteromeric multimers of Keap1 occur at the BTB domain (Yoshida *et al*., 1999). While the proteasome-dependent Nrf2 degradation activity of Keap1 occurs at both the BTB and IVR domains (Kobayashi *et al*., 2004).The DGR domain of Keap1 has six double glycine repeats and it is responsible for binding of Keap1 to the Neh2 of Nrf2 and to actin. This domain forms a six-bladed β-propeller which is tied firmly by hydrogen bonds and it is believed to be responsible for the formation of the complex structure of Keap1-Nrf2.

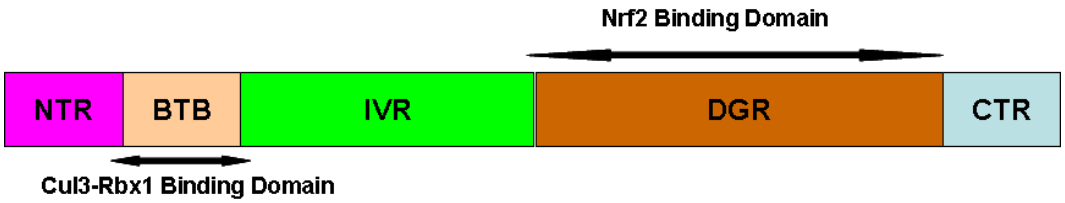

Fig.1.7. Schematic representation of Keap1. Keap1 has five domains; N-terminal region (NTR), bric-a-brac, tramack, broad complex (BTB), intervening region (IVR), double glycine repeat (DGR) or kelch and C-terminal region (CTR). The BTB and IVR are responsible for the proteasome dependent Nrf2 degradation activity of Keap1 and the DGR is the region for Keap1 binding to the Neh2 region of Nrf2.

Antioxidant Response Element

The Antioxidant Response Element (ARE) is a cis-acting enhancer sequence found in the promoter of the detoxification and antioxidant genes and regulates the expression of these genes in response to exposure to stimuli such as xenobiotics, metals, UV irradiation and antioxidants (Nguyen *et al*., 2003). Cotransfection-transactivation experiments show that Nrf1 and Nrf2 elevate ARE reporter expression (Venugopal and Jaiswal, 1996) and this coupled with Nrf2-null mutant mice experiments in which butylated hydroxyanisole (BHA) was found to induce four GST subunits (Ya1, Ya3, Yp and Yb) and NQO1 gene expression in the liver and intestine of the wild type mice but causes lower induction in the Nrf2-null mutant mice (Itoh *et al*., 1997), shows that the antioxidant and detoxification gene transcriptions occur by the interaction of the transcription factor Nrf2 with ARE. GTGACA***GC has been revealed by mutational analysis as the core sequence of the ARE (Copple *et al*., 2008). An ARE has been identified in the promoter regions of genes encoding NQO1 in rats and human (Favreau and Pickett, 1991; Li and Jaswal, 1992), GST-Ya in rat and mouse (Friling et al., 1990; Rushmore et al., 1990), GST-P in rat (Okuda *et al*., 1989), HO1 (Prestera *et al*., 1995), human γ-glutamylcysteine synthase (γGCSc) heavy subunit (Mulcahy and Gipp, 1995) and mouse GST-M1 and M3 (Reinhart and Pearson, 1993).

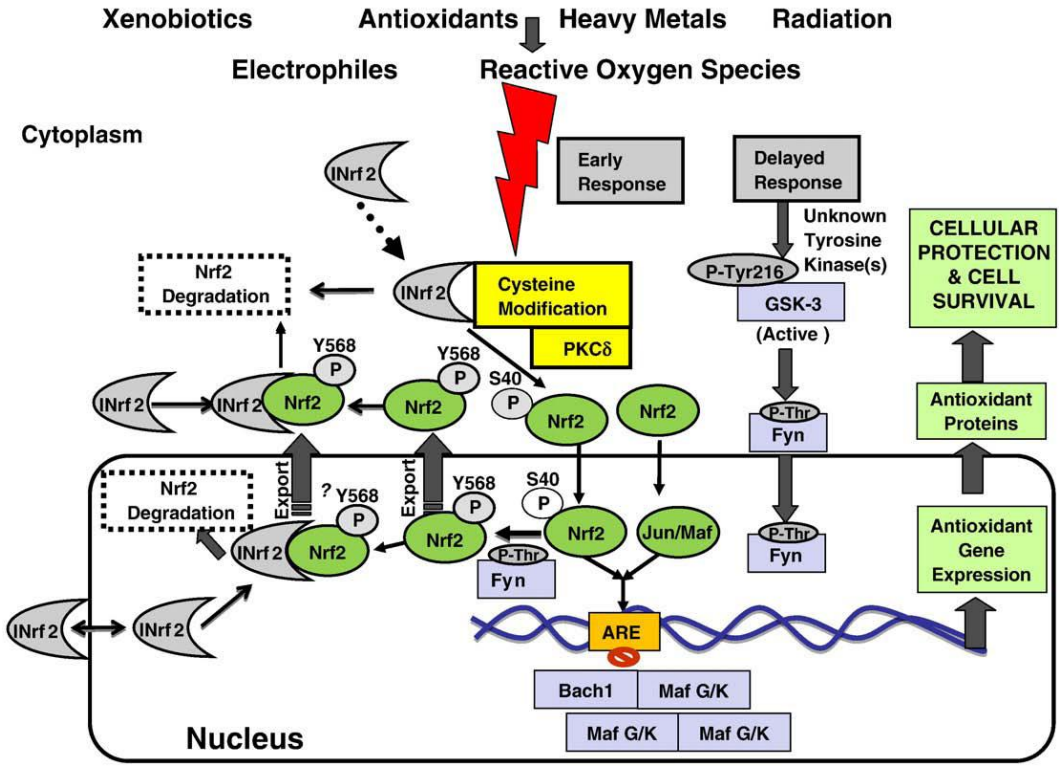

Source: Niture *et al.,* 2009

Fig.1.8. Oxidative/electrophilic stress and Nrf2:INrf2 signalling. S40 is serine 40 phosphorylation in Nrf2. Y568 is tyrosine phosphorylation in Nrf2.

1.4.2. Regulation of Nrf2 activation and degradation and mechanism of Nrf2-Keap1-ARE signal transduction

Nrf is a transcription factor whose expression and activity can be regulated at the transcription, degradation, translocation and post-translational levels (Purdom-Dickinson *et al.,* 2007).

1.4.2.1. Keap1-dependent and –independent degradation

Nrf2 controls the induction of all known ARE-regulated genes. Under unstressed conditions, Nrf2 is kept in the cytoplasm by the interaction with Keap1 (INrf2), but upon the addition of electrophiles, Nrf2 is released from Keap1 and translocates into the nucleus where it binds to ARE causing the transcriptional activation of protective genes (Itoh *et al*., 1999). The binding of Nrf2 to Keap1 enhances the ubiquitin-dependent degradation (**Keap1-dependent degradation**) of the former via the 26S proteasome and this association serves to regulate Nrf2 steady state levels in the cell (Nguyen *et al.,* 2003). Supporting this is the fact that Nrf2 with half time of less than 20 min (Itoh *et al*., 2003) or 10-40 min (Alam *et al*., 2003) after cycloheximide exposure is rapidly degraded in unstressed conditions but this degradation was inhibited by the presence of proteasome inhibitor (Itoh *et al*., 2003). In addition, Keap1 knocked down in 293T cells, was reported to lead to Nrf2 accumulation (Furukawa and Xiong, 2005). Several lines of evidence have also supported **Keap1-independent degradation** of Nrf2. Among these is the observation that the presence of proteasome inhibitor enhances the stability of Nrf2 even when Keap1 repressor is eliminated as in oxidative stress (Itoh *et al.,* 2003). Also the lack of Nrf2/Keap1 binding motif in Nrf2 mutants does not abolish Nrf2 degradation (McMahon *et al.,* 2003). In addition, Nrf2

degradation in Keap1 knocked down mice was observed to occur in a proteasomal-dependent manner (Itoh *et al*., 2004).

1.4.2.2. Inducers of Nrf2-Keap1-ARE pathway

The release of Nrf2 from Nrf2-Keap1 complex leading to alteration in the cytosolic and Nuclear Nrf2 protein levels and the consequent transcription of the protective genes may be as a result of the direct attack of the electrophiles or ROS or an indirect action such as phosporylation (post-translational modification)(Fig.1.8). ARE has been reported to respond to nine structurally dissimilar classes of inducers (Prestera *et al.,* 1993). Exposure to inducers has been reported to enhance transcription and inhibition of Nrf2 proteasomal degradation leading to increased nuclear translocation of Nrf2 and total cellular Nrf2 (Nguyen *et al*., 2003). For example, ARE-dependent gene expression was found to be activated in HepG2 cells treated with proteasome inhibitors (Sekhar *et al*., 2000).

1.4.2.2.1. Direct electrophilic attack on sensor molecules in Keap1

Inducers of protective genes have been reported to have the ability to modify sulfhydryl groups by alkylation, oxidation or reduction (Kobayashi and Yamamoto, 2006). These inducers react with highly reactive cysteine residues (sensor molecules) to initiate transcription of the cytoprotective genes (Prochaska *et al*., 1985)(Fig.1.8). Keap1, the repressor of Nrf2, contains 25 highly conserved cysteine residues in human and rat and some of these cysteine residues are said to be highly reactive as they are surrounded by basic amino acid residues (Snyder *et al.,* 1981). One or more cysteine residues in the IVR of Keap1 have been identified as probable target sites for electrophilic attack in vivo (Kobayashi and Yamamoto, 2005). In several

studies using cell culture systems, replacement of the cysteine residues of the Keap1 molecule by alanine or serine show that at least three cysteine residues; Cys151, Cys273 and Cys288 play a key role in Keap1 activity (Zhang and Hannink, 2003; Levonen *et a*l., 2004; Wakabayashi *et al*., 2004). In another study using bacteria, Dinkova-Kostova et al (2002) showed that Cys257 Cys273, Cys288 and Cys297 in the IVR are crucial to Keap1 activity. It was observed that the presence of inducers disrupts Keap1's interaction with Neh2 in a gel retardation assay (Dinkova-Kostova *et al*., 2002). The mutation studies show that replacement of either Cys273 or Cys288 disrupt the repressive action of Keap1 against Nrf2 leading to stability of the later. The modification of these two cysteines by electrophiles is therefore critical for the release of Nrf2 from Keap1.

1.4.2.2.2. Post-translational modification

Apart from the oxidative modification of cysteine residues in Keap1, several studies have shown that certain protein kinases such as extracellular signal regulated kinases (ERK1/2) (Buckley *et al*., 2003), protein kinase C (PKC) (Huang *et al*. 2002), MAPK and p38 MAP kinase (Yu *et al.,* 1999), PKR-like endoplasmic reticulum kinase (PERK) (Cullinan *et al*., 2003) and phosphoinositol-3-kinase (PI3K) may be involved in the modification of Nrf2 and hence activate its release from Keap1. Using a co-immunoprecipitation assay, it was observed that phosphorylation of Nrf2 at Ser40 by PKC enhances the disruption of Nrf2 from Keap1 in HepG2 cells and PKC (PKCδ) was the only signalling kinase found to directly phosphorylate Nrf2 in vitro and in vivo (Fig.1.8; Huang *et al.,* 2002). This observation was supported by the fact that Nrf2 phosphorylation was required for Nrf2 stabilization and accumulation in nucleus and the subsequent ARE-mediated NQO1

expression (Bloom and Jaiswal, 2003). This was further confirmed by a mutation study in which replacement of Ser40 by Alanine decreased the PKC-dependent dissociation of Nrf2 from Keap1 (Bloom and Jaiswal, 2003). The Nrf2 translocated into the nucleus heterodimerizes with small Maf and Jun and binds to the ARE leading to coordinate activation of gene expression (Fig.1.8; Kobayashi and Yamamoto, 2006; Copple *et al*., 2008). Atypical PKCs were identified in one study to be responsible for the phosphorylation of Nrf2 in human fibroblast WI-38 cells in response to 4-hydroxy-2, 3-nonenal and phorone (Numazawa *et al.,* 2003). Li *et al* (2004) observed that disruption of PKCδ in osteoblasts resulted in reduced Nrf2 accumulation after treatment with sodium arsenate. In another study, mutation of Ser104 of Keap1 was reported to disrupt the Keap1 dimer and enhanced release of Nrf2 (Zipper and Mulcahy, 2002). It was also observed that the phosphorylation of Tyrosine141 of Keap1 enhanced Nrf2-Keap1 stability (Jain *et al.,* 2008).

1.4.2.3. Negative regulation of Nrf2 activation

Nrf2 activation of gene expression is switched off by a delayed mechanism which involves GSK3β phosphorylation of Fyn at unknown threonine residue(s) with the consequent translocation of Fyn into the nucleus (Jain and Jaiswal, 2007). Fyn then induced the nuclear export and degradation of Nrf2 by enhancing the nuclear binding of Nrf2 with Keap1 (INrf2) through the phosphorylation of Nrf2 at tyrosine568 (Fig.1.8; Jain and Jaiswal, 2007). Bach 1 is another negative regulator of Nrf2 in the nucleus by competing with Nrf2 for binding to ARE thereby suppressing the expression of Nrf2 dependent genes (Fig.1.8; Dhakshinamoorthy *et al*., 2005).

1.4.3. Protein Kinase C (PKC)

Protein Kinase C (PKC) belongs to a family of serine/threonine protein kinases that play important roles in signal transduction and in the regulation of various cellular functions (Nishizuka, 1995). Eleven isoenzymes of PKC have been identified (Takai *et al.,* 1979) and are divided into 3 main groups based on their mode of activation and structure of their regulatory domains (Nishizuka, 1988; Demsey *et al.,* 2000). These include; the classical PKCs (cPKCs; α, ßi, ßii, ɣ) which require diacylglycerol (DAG) and calcium ion (Ca^{2+}) for maximal activity, the novel PKCs (nPKCs; δ, ϵ, ɳ , ø) which require DAG but not Ca^{2+} for activation, and the atypical PKCs (aPKCs; ɾ, ƛ/Ł) which are insensitive to either DAG or Ca^{2+}. PKCs are translocated to several cellular organelles in isoform and stimulation-specific manner when activated by various stimulations (Kashiwagi *et al*., 2002). After activation, PKCs recognise and phosphorylate their target substrates and cause the subsequent cellular responses (Ohimori *et al*., 2000). PKC maturation and phosphorylation at multiple serine/threonine sites in PKC is a requirement for the full activation of PKC in response to various stimulations (Newton 2003). Activation loop site, turn motif site and the hydrophobic motif site have been recognised as the three phosphorylation sites in cPKC and nPKC. However the threonine residue at the activation loop is the most essential phosphorylation site for the PKC kinase activity (Liu *et al*., 2002). 3-phosphoinositide-dependent protein kinase-1 (PDK1) has been recognised to phosphorylate this threonine residue (Dutil *et al.,* 1998; LeGood *et al*., 1998).

1.4.3.1. PKC and Cd toxicity

One mechanism by which Cd –induced up regulation of gene expression is by the activation of cellular PKC (Fig.1.9). Cd^{2+} can activate PKC directly by

replacing Ca^{2+} (Thevenod, 2009) or indirectly via Ca^{2+} and DAG formed from the PLC-IP_3 pathway (Fig.1.9; Thevenod, 2009). Activation of PKC by Cd results in enhanced phosphorylation of transcription factors with the consequent induction of targeted protective gene transcription (Waisberg *et al.,* 2003). Studies using inhibitors have shown that Cd activates protein kinase C (Watkin *et al.,* 2003).Cd was reported to induce PKC in lung epithelial cells resulting in apoptotic cell death, whereas the apoptosis induced by the metal in rat glioma cells was reported to be independent of PKC activation (Watkin *et al.,* 2003). In another study, PKCδ activation by Cd was found to mediate Cd-induced apoptosis in human promonocytic cells (U937) (Miguel *et al.,* 2004). In a different experiment, Cd did not activate PKC in rat mesangial cells (Wang and Templeton, 1998).

1.4.4. Nrf2-Keap1-ARE dependent cytoprotective enzymes

Several studies have shown that the Nrf2-Keap1-ARE pathway mediates the adaptive response in cells exposed to xenobiotics, electrophiles and even antioxidants through the induction of a array of defensive genes encoding detoxifying enzymes such as NAD(P)H:quinone oxidoreductase 1 (NQO1; Rushmore *et al.,* 1991), glutathione S-transferase (GST; Rushmore and Pickett, 1990), heme oxygenase 1 (HO-1; Alam *et al.,* 1995) and **γ**-glutamate cysteine ligase (**γ**-GCSc; Mulcahy *et al.,* 1997). The common feature among these genes is the presence of cis-acting element, antioxidant-response element (ARE; Rushmore *et al.,* 1991) or electrophile-responsive element (EpRE; Friling *et al.,* 1990), within their regulatory region. The induction of these genes was regulated by the binding of transcription factor, NF-E2-related protein 2 (Nrf2) to their ARE (Itoh *et al.,* 1997). This was confirmed by various studies in which the expressions and activities of these cytoprotective genes were

inhibited in Nrf2 knockdown cells (Ishii *et al*., 2000; Itoh *et al*., 2004; Keum *et al*., 2006), mice (Beyer *et al*., 2008), zebrafish and mammals (Kobayashi *et al*., 2002; Suzuki *et al*., 2005).

NQO1

NQO1 (NAD (P) H: quinone oxidoreductase 1) is a flavoprotein that catalyses two-electron reduction of quinines, quinone-imines, nitro and azo compounds. In addition the enzyme also helps in re-generating antioxidant forms of both vitamin E and ubiquinone after exposure to free radicals (Joseph and Jaiswal, 1994).The enzyme requires either NADH or NADPH for its activity. NQO1 functions as a homodimer with each monomer having one catalytic site and consisting of 273 amino acids. NQO1 is expressed in human epithelial and endothelial cells and occurs at high levels in many human solid tumours. NQO1 is a cytosolic enzyme but small amounts are found in the mitochondrial, endoplasmic reticulum and nucleus. Using Nrf2 knockdown cells, NQO1 gene transcription has been established to be regulated by Nrf2 transcription factor in human bladder urothelial cell line (UROtsa) exposed to arsenite and monomethylarsonos(Wang *et al*., 2007) and in mouse embryonic fibroblast (hepalc1c7 cells) exposed to Cd (He *et al*., 2008).

HO-1

Heme oxygenase (HO) is a rate limiting enzyme of heme catabolism (Bonkovsky and Elbirt, 2002) and catalyzes the conversion of heme to biliverdin, which is converted to bilirubin by the enzyme bilirubin reductase, with the production of iron and carbon monoxide (Tenhunen *et al*., 1969). HO exists in three isoforms: HO-1, which is highly inducible; HO-2 and HO-3,

which are primarily constitutive (Maines, 1988; McCoubrey *et a*l., 1997). HO-1 is highly expressed in spleen and kuppfer cells and its level in all tissues is enhanced by the presence of heme. The cytoprotectant, antioxidant, anti-inflammatory and immunomodulatory properties (Bonkovsky and Elbirt 2002; Lambrecht *et al*., 2005) of HO-1 have been attributed to its ability to convert harmful heme to less harmful iron and to the antioxidant properties of biliverdin and bilirubin formed (Bonkovsky and Elbirt, 2002). Many studies have shown that HO-1 could be up-regulated by variety of stress (UV radiations, irradiation, hyperthermia, inflammatory cytokines and heavy metals) including the presence of heme (Lincoln *et al*., 1988) and metalloporphyrins (Shan *et al*., 2000). These inductions primarily occur by increased gene transcription (Srivastava *et al.,* 1993). Many studies using Nrf2 null mutants have shown that the transcription of the HO-1 gene is regulated by Nrf2 (He *et al.,* 2008; Shan *et al*., 2006).

GST

Glutathione S-transferases (GSTs) are dimeric phase II detoxification enzymes found in the cytosol and catalyse the conjugation of reduced glutathione (GSH) via a sulhydryl group to electrophiles, aiding their removal (Tsuchida and Sato, 1992; Douglas, 1987). In addition to catalysing conjugation of electrophilic substrate with GSH, they also inhibit the Jun N-terminal kinase and are able to bind non-catalytically a wide range of endogenous and exogenous ligands (Sheehan *et al.,* 2001) They are found in the cytosol, mitochondrial and microsomes. Mammalian cytosolic GSTs, unlike the non-mammalian GSTs, are well characterised and are initially classified into Alpha, Mu, Pi and Theta (Sheehan *et al.,* 2001). Based on factors such as amino acid/nucleotide sequence, immunological, kinetic and

tertiary/quaternary structural properties, the GST family are classified into alpha (GSTA1, GSTA2, GSTA3, GSTA4 and GSTA5); kappa (GSTK1); mu (GSTM1, GSTM1L, GSTM2, GSTM3, GSTM4 and GSTM5); omega (GSTO1, GSTO2); pi (GSTP1); theta (GSTT1 and GSTT2); and microsomal (MGST1, MGST2 and MGST3).

The molecular forms of GST are divided into at least 2 groups each of which is made up of 2 subunits (Hayes, 1983; Mannervik and Jensson, 1982). These include the BL group such as Ligandin (YaYa), B (YaYc), AA (YcYc) and the AC group such as A (YbYb), C (YbYb') and D (Yb'Yb'). The Ya and Yc subunits have molecular weight of 22kDa and 25kDa respectively while Yb and Yb' subunits have similar molecular weight of 23.5kDa but Yb' is more acidic than Yb (Hayes, 1983; Mannervik and Jensson, 1982).

Studies have shown the presence of ARE in the promoter regions of genes encoding GST-Ya of rat and mouse (Friling *et al.,* 1990), GST-P of rat (Okuda *et al.,* 1989), and GST-M1 and M3 of mouse (Reinhart and Pearson, 1993). Using Nrf2 null mutant mice, it was observed that the level of inductions in the gene expression of four GST subunits (Ya1, Ya3, Yp; GST-P subunit, and Yb) were much lower in the null mice than in the wild-type after exposure to butylated hydroxyanisole (BHA; Itoh *et al*., 1997). Mutagenic study of the rat GST-Ya ARE reveals a high level of homology to the functional ARE sequence (Rushmore *et al*., 1991).

γ-GCSc

γ-glutamylcysteine synthase (**γ**-GCSc), also known as glutamate cysteine ligase (GCL), is the first and rate limiting enzyme in the glutathione

biosynthesis pathway and it catalyses the ATP-dependent condensation of cysteine to glutamate to form gamma-glutamylcysteine (Norgen, 2005). GLC is a heterodimeric enzyme that consists of two proteins: glutamate cysteine ligase catalytic subunit (GCLC, approximate molecular weight of 73kDa with catalytic properties); glutamate cysteine ligase modifier subunit (GCLM, approximate molecular weight of 31kDa) that enhances the catalytic efficiency of GCLC. These subunits are encoded by different genes and can be separated by reducing agents (Huang *et al*., 1993). GCL is regulated by GSH, which serves as a feedback competitive inhibitor, and by availability of cysteine (Kaplowitz *et al*., 1985).

Mulcahy and Gipp (1995) have reported the presence of ARE in the regulatory regions of heavy subunit of **γ**-GCSc and this discovery was supported by the Nrf2-null mutant experiment in which the expression of **γ**-GCSc heavy subunit was significantly reduced in the small intestine of null mice when compared to the wild-type after dietary intake of butylated hydroxyanisole (BHA) and etoxyquin (McMahon *et al*., 2001). In another study increased **γ**-GCSc expression was also found to correlate with increase nuclear Nrf2 and Nrf2-Keap1 in mice exposed to oxidative stress (Kensler *et al*., 2007).

1.4.5. Nrf2-Keap1-ARE pathway and Cd

One common feature of inducers of the Nrf2-dependent genes is that they are highly reactive with nucleophiles (Talalay *et al*., 1988) such as the sulfhydryl group of cysteine. The high affinity of Cd for sulfhydryl group does make it a candidate for the modification of the reactive cysteine residues in Keap1 with the consequent release of Nrf2 from the repressor (Fig.1.9). Cd has been

reported to induce the expression of Nrf2-dependent genes in kidney cell line, NRK-52E (He *et al*., 2007). In another study, He *et al* (2008) reported that Cd increased the basal and inducible expression of NQO1 and HO1 in mouse embryonic fibroblasts (MEF) but these enzymes were not induced in Nrf2 knock-out cells. They also observed that Nrf2 protein stabilization, increased Nrf2/Keap1 complex formation in the cytoplasm, increased translocation of these complex into the nucleus and increased disruption of the complex are the mechanisms by which Cd activates Nrf2. Sakurai *et al* (2004) reported that Cd –induced thioredoxin reductase (TrxR) gene expression in bovine arterial endothelial cells (BAEC) by activating Nrf2 transcription factor and its binding to ARE in TrxR1 gene promoter. Casalino *et al* (2007) also reported that acute Cd toxicity (24hrs exposure) induced Se-independent glutathione peroxidase activity of alpha-class GST and NQO1 in rat liver in the absence of transcription inhibitor, actinomycin D. These inductions were observed to be Nrf2 dependent since the induction of these enzymes were abolished in the presence of actinomycin D. These studies show that activation of Nrf2 and cytoprotective enzymes plays significant role in the adaptive response of cells against Cd toxicity.

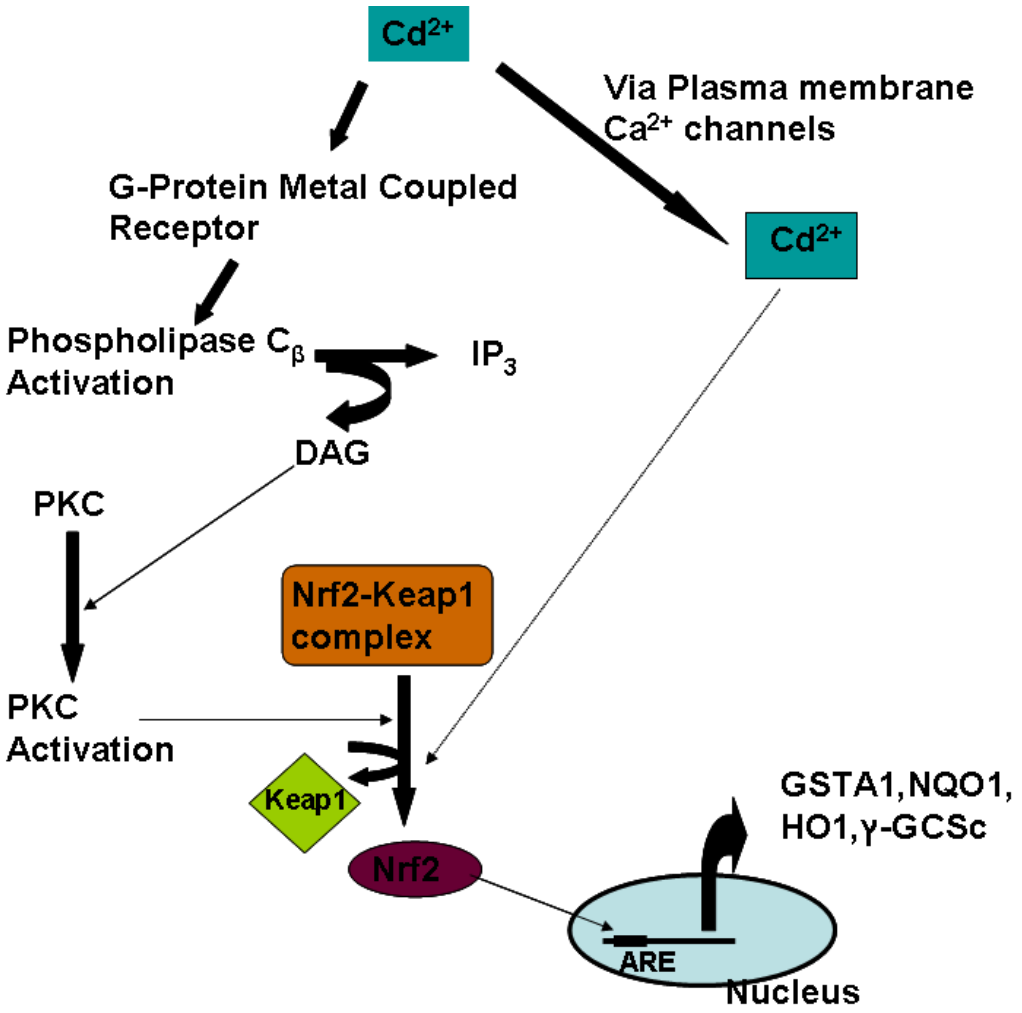

Fig.1.9 Schematic representation of the effects of Cd on the Nrf2-Keap1-ARE pathway The presence of cadmium can induce the activation of the Nrf2-Keap1-ARE pathway either directly by causing conformational change in Keap1 through the reaction with the reactive cysteine residues (Cys151, 273 and 288) resulting in the release of Nrf2 or indirectly through the PLC-IP_3 pathway by the activation of PKC by DAG with the consequent phosphorylation of Nrf2 at Ser40.

1.5. Chemoprevention

Chemoprevention (or chemoprotection) is the use of vitamins, minerals, pharmaceuticals or other chemicals to reduce, retard, block or reverse the incidence of cancer (Wattenberg, 1985). About 20 different classes of chemicals have been identified as having chemopreventive properties (Wattenberg, 1985). Some of these chemicals are phytochemicals present in food. Two broad categories of chemopreventive agents can be identified, the first class are compounds that can prevent or inhibit complete carcinogens and the second class is compounds that are active against tumour promoters. The inhibitors of carcinogens include compounds that can prevent carcinogen formation from precursor compounds e.g. ascorbic acid (Mirvish, 1981), compounds that can inhibit carcinogenesis (blocking agents) by preventing critical target sites in tissues from reacting with carcinogenic compounds (Miller, 1978), and compounds that act after exposure to carcinogen and suppress (suppressing agents) the expression of neoplasia cells (Fig.1.10).

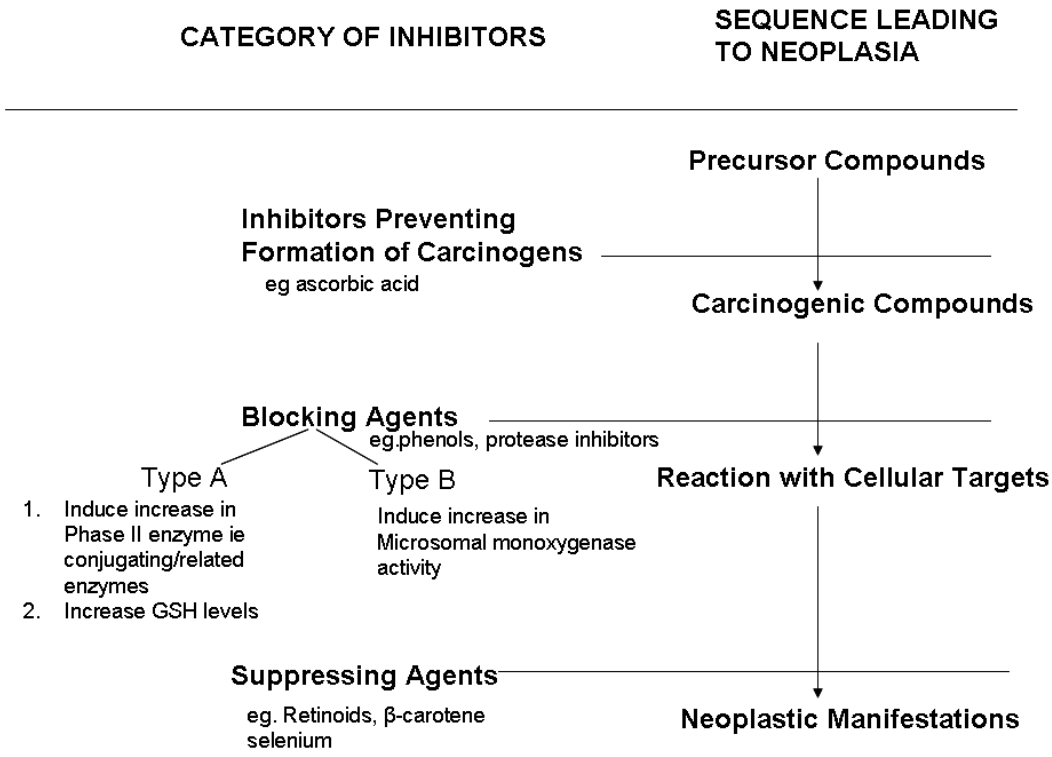

Source: Wattenberg (1985)

Fig.1.10.Classification of chemopreventive agents on the basis of the time at which they exert their protective effects

1.5.1. Garlic

The use of garlic (Allium sativum L.) as a medicinal plant is dated to the ancient time (Block, 1985). The plant uses as a cure for heart disease, tumours and headaches are documented in the Egyptian Codex Ebers, dating from 1550 BC. Epidemiologic studies have consistently shown a direct relationship between consumption of high amounts of garlic and a reduced risk of cancer at most sites in the body especially in the stomach and colon (Fleischauer and Arab, 2001).

The therapeutic effects of garlic include lowering of blood lipids, cardioprotection (Neil and Sigali, 1994) and antithrombotic effect (Block, 1985). Garlic contains a wide range of unique water and lipid soluble organosulfur compounds (OSCs) (Block, 1985) which have been identified as being responsible for the protective effect of garlic. The OSCs originate from γ-glutamyl cysteine (Amagase *et al.*, 2001) and are also responsible for the characteristic flavour and odour of garlic. Different in vitro and in vivo studies have revealed that the OSCs in garlic have antimutagenic, antioxidant, antiproliferative and apoptotic effects against carcinogenic processes (Thomson and Ali, 2003). The OSCs in garlic include allicin (DADSO); dially sulphide (DAS); diallyl disulfide (DADS); S-allyl cysteine (SAC); allyl mercaptan (AM) and dially trisulfide (DATS) (Fig.1.11). DADSO is the main thiosulfinate in crushed raw garlic (Lawson, 1996), DAS and DADS are lipid soluble compounds in crushed garlic and garlic oils and are formed from allicin (Lawson, 1996), SAC is a water soluble compound found in high amounts in aged garlic extract (Lawson 1996). AM is formed by the metabolism of DADS (Germain *et al*., 2002) and DADSO (Lawson, 1998). The

therapeutic action of garlic is enhanced by a unique aging process to form the aged garlic extract (AGE).

1.5.1.1. AGE

Aged garlic extract (AGE) is an odourless product obtained from long time (about 10 to 20months) extraction of fresh garlic at room temperature and has been shown to be highly bioavailable and biologically active (Moriguchi *et al*., 1997). The main OSCs in AGE are the water-soluble allyl amino acid derivatives such as S-allylcysteine (SAC) and S-allylmercaptocysteine (SAMC) both of which have antioxidant activity (Imai *et al*., 1994). SAC and SAMC are produced during the aging process thereby providing age with higher antioxidant property than the fresh and other garlic preparations (Imai *et al*., 1994). Other compounds in AGE are the stable lipid-soluble allyl sulfides such as dially sulphide (DAS), triallyl sulphide, diallyl disulfide (DADS) and dially polysulfides (Amagase, 1998). Allicin, the lipid-soluble volatile OSC, produced enzymatically when garlic is chopped or cut is absent in AGE (Freeman and Kodera, 1995). Due to the ageing process, the antioxidant properties of garlic are enhanced by modifying the unstable molecules such as allicin with antioxidant activity and also by increasing the stability and bioavailability of water-soluble OSCs such as SAC and SAMC (Borek, 2001). AGE also contains phenolic compounds such as allixin (Ide and Lau, 1997), flavonoids, saponins and essential macro- and micronutrients such as selenium (Amagase, 1998).

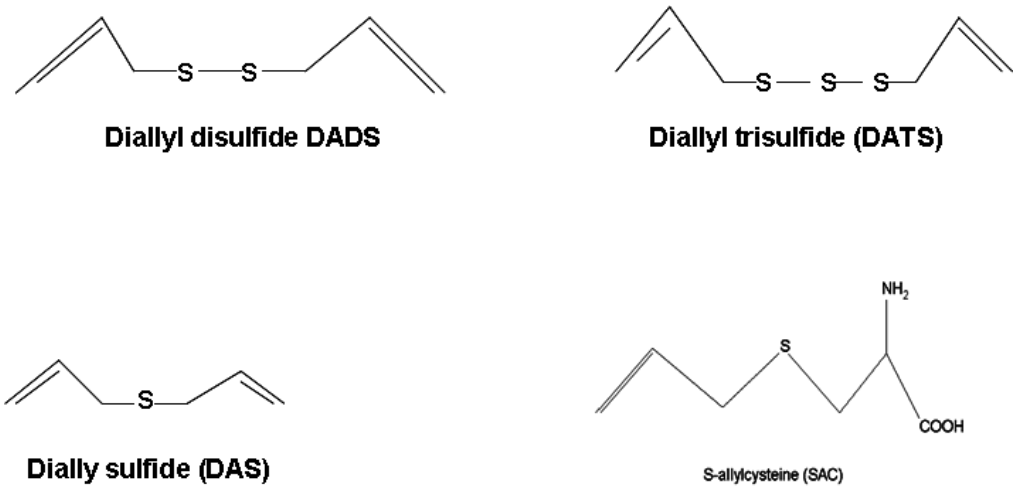

Fig.1.11. Structures of garlic organosulfur compounds

1.5.2. Garlic and the Nrf2-Keap1-ARE pathway

Garlic organosulfur compounds (OSCs) have been reported to induce the expression of cytoprotective genes through the Nrf2-Keap1-ARE pathway (Chen *et al*., 2004). The study shows that the presence of diallysulfide (DAS), diallyl disulfide (DADS) and diallyltrisulfide (DATS) produced a significant induction in NQO1 and HO-1 genes expression in HepG2 cells. These inductions were found to correlate with Nrf2 protein accumulation and ARE activation and no inductions were observed in Nrf2 nun mutant HepG2 cells (Chen *et al.,* 2004). In order to determine the mechanisms of action of these OSCs, the cells were treated with protein kinase inhibitors and the results reveal the involvement of calcium-dependent signalling pathway in DATS – induced ARE activity. Other studies have shown the induction of GST (Hatono *et al.,* 1996), glutathione reductase (Wu *et al*., 2001), and NQO1 (Singh *et al*., 1998) enzymes in animal and cellular models after treatment with OSCs.

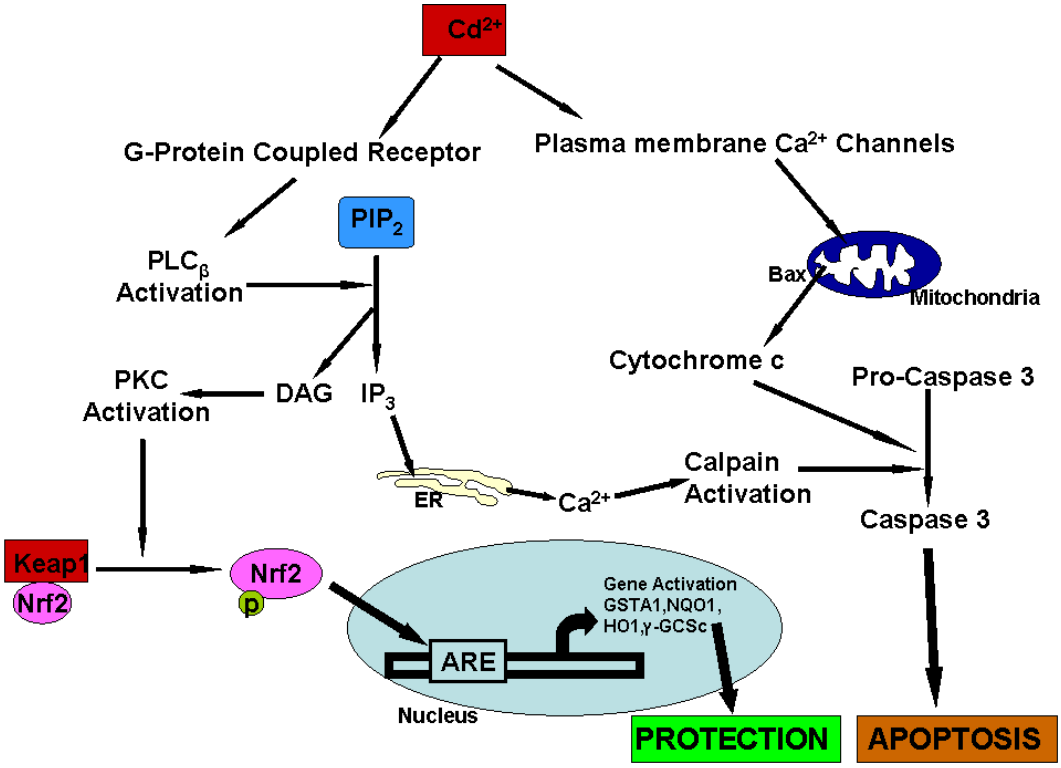

Fig.1.12. Proposed double edged-sword effects of Cd. Depending on dose and duration of exposure, Cd can induce an adaptive response in cells via the Nrf2-Keap1-ARE pathway especially at low dose. A higher dose of Cd can push the cells toward apoptotic cell death via the PLC-IP_3 pathway leading to alteration in intracellular Ca^{2+} or the mitochondrial-caspase dependent pathway. The balance between the two end points determines the net effect of Cd in a cell.

1.6. JUSTIFICATION FOR PROJECT

Due to the ubiquitous nature of Cd in the environment, the danger posed by this metal cannot be overemphasised. Having been shown to be highly toxic and carcinogenic in human, Cd should be a source of concern, and protection of the cell against this environmental toxicant should be a priority. Evidence has suggested that this heavy metal disrupts many metabolic processes in the cells; it induces apoptosis and necrosis, causes lipid peroxidation in membrane, destroys proteins and enzymes, competes with other metals for their binding site, alters signal transduction and promotes DNA damage. Despite the known toxicity of this technologically appealing but biologically hazardous metal, the **complete mechanism** by which this metal carries out its toxic effect is not yet clarified.

1.7. Aim

The aim of this present study was ultimately to elucidate the mechanism(s) of Cd induced toxicity in human cell lines and to evaluate the role of Nrf2 in adaptive response to Cd toxicity and the protective effect (if any) of antioxidants from garlic extracts against this toxicity. Therefore, to achieve this, this study has set the following objectives

1. To determine the involvement of oxidative stress in Cd toxicity
2. To evaluate the involvement of intracellular Ca^{2+} ion alteration via phospholipase C- Inositol-1, 4, 5-triphosphate (PLC-IP_3) in Cd induced toxicity.
3. To evaluate the role of the mitochondrial-caspase pathway in the aetiology of Cd toxicity.
4. To determine whether or not Cd toxicity alters the proteomic composition of cell lines and to evaluates the role of the altered

protein(s) in Cd toxicity thereby identifying protein biomarkers for Cd toxicity.

5. To determine the expressions of antioxidant response element (ARE) regulated genes in response to Cd toxicity.
6. To evaluate the translocation of Nrf2 protein from the cytosol into the nucleus in response to Cd toxicity
7. To determine the chemopreventive effect of garlic on Cd toxicity.

CHAPTER 2

MATERIALS AND METHODS

Chapter 2

2.0. Materials and Methods

2.1. Materials

2.1.2. Human Cell lines

Human hepatoma (HepG2) cells were obtained from America Type Culture Collection (ATCC). The cell line was used for this study simply because the liver is one of the major target organs of cadmium toxicity as the metal preferentially accumulates in the liver. Human hepatoma cell line (HepG2) has been an effective tool for the in vitro study of both the cytoprotective effect of modulators and the metabolisms and toxicity of xenobiotics because they tend to retain some of the functions of undiseased human hepatocytes (Knasmuller *et al*., 1998). They have also been reported to have the ability of retaining the activities of many drug metabolism and antioxidant enzymes (Knasmuller *et al.,* 2004) and so can correctly represent a normal liver cell for in vitro study.

Human astrocytoma (1321N1) cells were a gift from Dr. Eve Lutz, University of Strathclyde. The cells were used for this study since they are important in the defence system of the Central Nervous system (CNS) as they act more or less like a macrophage. Studying the effect of cadmium on this cell line can determine the impact of cadmium toxicity on the CNS.

Human embryonic kidney (HEK 293) cells were obtained from Dr.Corinne Spickett Laboratory, University of Strathclyde. The kidney is the most

targeted organ in cadmium toxicity; therefore, the use of this cell line will enable the elucidation of the mechanism(s) of cadmium toxicity in kidney.

2.1.3. Cell culture equipment

The cell culture hood was obtained from ICN Gelaine in England.

The cell culture incubator was supplied by Heraeus in Germany.

The carbon (IV) oxide (CO_2) cylinder was supplied by BOC gases (UK).

Micropipettes were obtained from Fisher Scientific (UK).

2.1.4. Cell culture Media and Reagent

Dulbecco's modified Eagle's medium (DMEM) was obtained from Sigma-Aldrich (UK).

Trypsin-EDTA Solution (1x) was obtained from Sigma-Aldrich (UK).

Penicillin-Streptomycin (10,000units penicillin; 10mg streptomycin/ml 0.9% NaCl) Solution was obtained from Sigma-Aldrich (UK).

Fetal Bovine Serum (FBS) was obtained from Sigma-Aldrich (Germany).

Sodium Pyruvate (11.0mg/ml sodium pyruvate in tissue culture water) was obtained from Sigma-Aldrich (UK).

Non-Essential Amino Acid (100x) Solution was obtained from Sigma-Aldrich (UK).

Hank's Balanced Salt Solution (HBSS) was obtained from Sigma-Aldrich (UK).

2.1.5. Cell Culture plastic wares

EasyFlask 75cm^2 Vent/Close tissue culture flasks were obtained from Fisher Scientific (UK).

The 6 and 24 wells cell culture plates were obtained from Fisher Scientific (UK).

96 well cell culture plates were obtained from Greiner Bio-one (UK).

Cell Scrapers were obtained from BD bioscience (UK).

2.1.6. Cells Counting

Ethanol was obtained from Sigma-Aldrich (Germany).

Trypsin-EDTA Solution (1x) was obtained from Sigma-Aldrich (UK).

Hank's Balanced Salt Solution (HBSS) was obtained from Sigma-Aldrich (UK).

Equipment

Bright-line haemocytometer was obtained from Sigma-Aldrich (Germany).

Olympus CK40 Microscope was from Olympus (Japan).

2.1.7. Cells extracts preparation reagent

Tris base [Tris (hydroxymethyl) aminomethane] was obtained .from Fisher Scientific (UK).

Ethylenediaminetetraacetic acid disodium salt (EDTA) was obtained from BDH Chemicals limited (Poole, England).

Sodium hydroxide (NaOH) was obtained from Fisher Scientific (UK).

Hydrochloric acid (HCl) was obtained from Reidd-de Haeu (Germany).

Sodium Chloride (NaCl) was obtained from Fisher Scientific (UK).

Potassium Chloride (KCl) was obtained from Fisher Scientific (UK)

Sodium phosphate dibasic (Na_2HPO_4) was obtained from Sigma-Aldrich (Germany).

Potassium dihydrogen orthophosphate (KH_2PO_4) was obtained from BDH Laboratory Supplies (England).

2.1.8. Cadmium Compound

Cadmium (II) Chloride ($CdCl_2$) was obtained from Acros Organics (USA). This cadmium compound was used in this work because it is one of the most soluble forms of Cadmium in the earth crust (table1.1) and therefore represents a large percentage of available form of cadmium for uptake in plants, fish and animals including human via food chain.

2.1.9. Cell Viability

Chemicals and Reagent

3-(4, 5-Dimethylthiazol-2-yl)-2, 5-diphenyltetrazolium bromide (MTT) was obtained from Sigma-Aldrich (Germany).

Dimethyl Sulfoxide (DMSO) was obtained from Sigma-Aldrich (Germany).

Equipment

Labsystems iEMS Reader MF (Microplate reader) was supplied by Labsystems and Life Sciences International Limited (UK).

96 well cell culture plates were obtained from Greiner Bio-one (UK

2.1.10. Lactate Dehydrogenase (LDH) Leakage Assay Reagent

Chemicals and Reagent

Invitro Toxicology Assay Kit (Lactate Dehydrogenase Based, TOX-7) was obtained from Sigma-Aldrich (UK).

Kit Components

1. LDH Assay Substrate Solution (25ml).
2. LDH Assay Cofactor Preparation.
3. LDH Assay Dye Solution (25ml).
4. LDH Assay Lysis Solution (10ml).

Hydrochloric acid (HCl) was obtained from Reidd-de Haeu (Germany).

Equipment

Labsystems iEMS Reader MF (Microplate reader) was supplied by Labsystems and Life Sciences International Limited (UK).

Aluminium foil was obtained from Terinex (Germay).

2.1.11. Reactive Oxygen Species (ROS) Assay Reagent

Chemical and Reagent

Dihydrofluorescein diacetate (H_2FDA) was obtained from Aldrich (UK).

Sodium hydroxide (NaOH) was obtained from Fisher Scientific (UK).

Hank's Balanced Salt Solution (HBSS) was obtained from Sigma-Aldrich (UK).

Dimethyl Sulfoxide (DMSO) was obtained from Sigma-Aldrich (Germany).

Equipment

Microplate Fluorescence Reader (FL600) was obtained from BIO-TEK

(Germany).

96 black well fluorescence plates were obtained from Fisher Scientific (UK).

2.1.12. Lipid Peroxidation Assay Reagent

Chemicals and Reagent

Tetramethoxy propane (TMP) was obtained from Sigma-Aldrich (UK).

Sodium Acetate was obtained from Formachem (Research International) Limited (UK).

Sodium Dodecyl Sulfate (SDS) was obtained from Sigma-Aldrich (Germany).

Tetraoxosulphate (VI) acid (H_2SO_4) was obtained from Fluka (Germany).

Thiobarbituric Acid (TBA) was obtained from Sigma-Aldrich (Germany).

Butylated hydroxytoluene (BHT) was obtained from Sigma-Aldrich (Germany)

Iron (III) chloride ($FeCl_3$) was obtained from Sigma-Aldrich (Germany).

Equipment

Student water bath was obtained from Griffin (UK).

Magnetic Stirrer was obtained from Stuart Magnetic Company Limited (UK).

DU 650 Spectrophotometer was obtained from Beckman (USA).

2.1.13. Single cell gel electrophoresis (Comet) assay reagent

Chemicals and Reagents

GenSieve LE agarose was obtained from Flowgen (UK).

Sodium hydroxide (NaOH) was obtained from Fisher Scientific (UK).

Ethylenediaminetetraacetic acid disodium salt (EDTA) was obtained from BDH Chemicals limited (Poole, England).

Hydrochloric acid (HCl) was obtained from Reidd-de Haeu (Germany).

Tris base [Tris (hydroxymethyl) aminomethane] was obtained .from Fisher Scientific (UK).

Sodium Chloride (NaCl) was obtained from Fisher Scientific (UK).

Ethidium bromide was obtained from Sigma (UK).

Triton x-100 was obtained from Sigma-Aldrich (Germany).

Ethanol was obtained from Sigma-Aldrich (Germany).

Equipment

0.8-1.0mm Microscopic Slide was obtained from VWR International (Germany).

Gel Electrophoresis Tank was supplied by Bethesda Research Laboratories (BRL).

Regulated DC Power Source (Model PAB) was supplied by Telonic Instrument Limited (UK).

UV Radiation Source machine was supplied by Vilber Lourmat (France).

ID Image Analysis Software (Version 3.0) was supplied Eastman Kodak

Company (USA).

37^{o}C Waterbath was from Grant Instruments (Cambridge) Limited (UK).

Microwave Oven was obtained from Electrolux (UK).

Comet Assay Scoring Software from Perspective Instrument (UK).

2.1.14. Apoptotic and Necrotic Studies Reagent

Chemicals and Reagents

Annexin V-Cy3 Apoptosis Detection Kit Plus (Cat. No K202-25) was obtained from BioVision (USA).

Kit Components

1. 1 x Binding Buffer

2. Annexin V-Cy3

3. SYTOX green dye

Equipment

Fluorescence microscopy was obtained from BD Bioscience (UK).

Flow Cytometry (FACS) was obtained from BD Bioscience (UK).

0.8-1.0mm Microscopic Slide was obtained from VWR International (Germany).

2.1.15. Reduced Glutathione Assay Reagent

Chemicals and Reagents

5, 5′-Dithiobis (2-nitrobenzoic acid) [Ellman Reagent] was obtained from Sigma-Aldrich (Germany).

5-Sulfosalicylic acid dehydrate was obtained from Sigma-Aldrich (Germany).

Disodium hydrogen orthophosphate dihydrate ($Na_2HPO_4.2H_2O$) was obtained from Sigma-Aldrich (Germany).

Sodium dihydrogen orthophosphate dihydrate ($NaH_2PO_4.2H_2O$) was obtained from Reidd-de Haeu (Germany).

Reduced Glutathione (GSH) was obtained from Sigma-Aldrich (Germany).

2.1.16. Glutathione S-transferase Assay Reagent

Chemicals and Reagents

Potassium dihydrogen orthophosphate (KH_2PO_4) was obtained from BDH Laboratory Supplies (England).

Dipotassium hydrogen orthophosphate (K_2HPO_4) was obtained from BDH Laboratory (England).

1-Chloro-2, 4-dinitrobenzene (CDNB) was obtained from Sigma-Aldrich (UK).

Reduced Glutathione (GSH) was obtained from Sigma-Aldrich (Germany).

2.1.17. Glutathione Reductase Assay Reagent

Chemicals and Reagents

Glutathione Reductase Assay Kit (Product Number GR-SA) was obtained from Sigma (USA).

Kit components

1. Glutathione Reductase Dilution Buffer (100ml)
2. Glutathione Reductase Positive Control (1unit)
3. β-Nicotinamide Adenine Dinucleotide Phosphate, Reduced (NADPH) (25mg).
4. Glutathione, oxidised, Disodium Salt (GSSG) (100mg).
5. 5, 5′-Dithiobis (2-nitrobenzoic acid) (DTNB) (50mg).
6. Glutathione Reductase Assay Buffer (125ml).

Equipment

Quartz cuvette was obtained from VWR International (UK).

DU 650 Spectrophotometer was obtained from Beckman (USA).

2.1.18. Glutathione Peroxidase Assay Reagent

Chemicals and Reagent

Glutathione peroxidase cellular activity assay kit (Product Code CGP-1) was obtained from Sigma-Aldrich (USA).

Kit Components

1. Glutathione Peroxidase Assay Buffer (120ml).

2. NADPH Assay Reagent (1.25ml).

3. Tert-Butyl Hydroperoxide (1ml)

Hydrogen peroxide was obtained from Sigma-Aldrich (Germany).

Sodium azide (NaN_3) was obtained from sigma-Aldrich (UK).

Equipment

1ml Quartz cuvette was obtained from VWR International (UK).
DU 650 Spectrophotometer was obtained from Beckman (USA).

2.1.19. Catalase Assay Reagent

Chemical and Reagent

Catalase Assay Kit (Product Number CAT 100) was obtained from Sigma-Aldrich (USA).

Kit Components

1. Assay Buffer 10x (500mM potassium phosphate buffer, pH 7.0) (100ml)

2. 3% (w/w) Hydrogen Peroxide Solution (10ml)

3. Enzyme Dilution Buffer (50mM potassium phosphate buffer, pH 7.0; 0.1% TRITON X-100)

Equipment

1ml Quartz cuvette was obtained from VWR International (UK).

DU 650 Spectrophotometer was obtained from Beckman (USA).

1.5ml Eppendorf tube was obtained from Greiner bio-one (UK).

2.1.20. Superoxide Dismutase (SOD) Assay Reagent

Chemical and Reagent

SOD determination assay kit (Product Number 19160) was obtained from Fluka (UK).

Kit Components

The kit contains; Water-soluble tetrazolium salt (WST), (2-(4-Iodophenyl)-3-(4-nitrophenyl)-5-(2,4-disulfophenyl)-2H-tetrazolium, monosodium salt) (5ml), Enzyme Solution (100µl), Buffer Solution (100ml) and Dilution Buffer (50ml).

Equipment

Labsystems iEMS Reader MF (Microplate reader) was supplied by Labsystems and Life Sciences International Limited (UK).

96 well cell culture plates were obtained from Greiner Bio-one (UK).

10, 100 and 200µl pipettes and a multi-channel pipette were obtained from Fisher Scientific (UK).

37^{o}C incubator (model IH-150) was obtained from Gallenhamp (UK).

2.1.21. Aldehyde Reductase Activity Assay Reagent

Chemical and Reagent

Disodium hydrogen orthophosphate dihydrate ($Na_2HPO_4.2H_2O$) was obtained from Sigma-Aldrich (Germany).

Sodium dihydrogen orthophosphate dihydrate ($NaH_2PO_4.2H_2O$) was obtained from Reidd-de Haeu (Germany).

p-Nitrobenzaldehyde (p-NBA) was obtained from Sigma- Aldrich (UK).

NADPH was obtained from Sigma-Aldrich (UK).

2.2. Methods

2.2.1. Cell Culture

HepG2 cells were grown in Dulbecco's modified Eagle's medium (DMEM) supplemented with 10% fetal bovine serum (FBS), 1% MEM nonessential amino acid solution (100x), 1% sodium pyruvate (11.0mg/ml sodium pyruvate in tissue culture sterile water) solution and 1% penicillin-streptomycin solution (10,000units penicillin; 10mg streptomycin/ml 0.9% NaCl). The cells were maintained at 35°C in a humidified atmosphere of 5% CO_2 and 95% air.

1321N1 cells were grown in Dulbecco's modified Eagle's medium (DMEM) and supplemented with 10% FBS and 1% penicillin-streptomycin (10,000units penicillin; 10mg streptomycin/ml 0.9% NaCl) solution. The cells were maintained at 35°C in a humidified atmosphere of 5% CO_2 and 95% air.

HEK 293 Cells were grown in Dulbecco's modified Eagle's medium (DMEM) supplemented with 10% FBS and 1% penicillin-streptomycin (10,000units penicillin; 10mg streptomycin/ml 0.9% NaCl) solution. The cells were maintained at 35°C in a humidified atmosphere of 5% CO_2 and 95% air.

2.2.2. Cells Counting by Haemocytometer

<u>70% ethanol</u>

70ml ethanol was made up to 100ml with distilled water.

Procedure

Cell preparation for counting

The cell culture media were removed from the cell culture flask and the cells were washed with 5ml HBSS.1ml of 1x trypsin-EDTA solution was added to the flask and left for 1minute in order to detach the cells from the flask. 5ml of fresh media were then added to the flask in order to dilute the trypsin. The media containing the detached cells were then removed into a sterile centrifuge tube and then centrifuged for 1min at 3000x*g*. 2ml of the cell culture media were then added to the cell pellet and resuspended thoroughly by pipetting. 10µl of the resuspended cell media were then transferred into a fresh eppendorf tube and an equal volume of HBSS added to give a 1 in 2 dilution.

Haemocytometer slide preparation

The slide and the glass cover slip of the haemocytometer were cleaned with 70% ethanol. The cover slip was then placed on top of the arrow head of the slide.

Counting cells

10µl of the 1 in 2 diluted cells suspension were transferred using micropipette into the arrow head of the haemocytometer slide and the solution was drawn under the cover slip. Excess solution was blotted with tissue paper without drawing from under the cover slip. The slide was then placed on the microscope stage with objective lens set at x10 and the slide was adjusted for proper focus. The cells in the four corner squares and the central square were counted. Each square is $1mm^2$ in area and depth of 0.1mm. Only the cells in a square or overlapping the top or left hand sides

were counted. Cells on the bottom and right hand sides of the square were not counted in order to avoid counting the same cell twice.

Analysis of cells count

The number of cells counted per ml (C; concentration of cells) was determined by the equation;

$C=n/v=$ total number of cells count $X\ 10^4X$ dilution factor

Number of square counted

n= total number of cells count

v=volume=10^{-4}ml

1mm x 1mm x 0.1mm= 0.1mm^3=volume

0.1mm^3=0.0001cm^3=$10^{-4}cm^3$= 10^{-4}ml

To determine how much media was to be used in order to make a specific concentration of cells, the equation $C_1V_1=C_2V_2$ was used.

2.2.3. Cell extract preparation for enzyme assay

Tris-Cl (80mM)(pH 7.5)

1.94g of Tris base [Tris (hydroxymethyl) aminomethane] [MW=121.14] was dissolved in 180ml distilled water (H_2O) and the pH was adjusted with hydrochloric acid (HCl) to 7.5. The solution was then made up to 200ml with distilled H_2O.

EDTA(10mM)(pH 8.0)

0.37g of EDTA (MW=372.24) was dissolved in 80ml distilled water and the pH adjusted with NaOH (0.1M) to 8.0. The solution was then made up to 100ml with distilled water.

TE(Tris/EDTA) Solution

50ml of Tris-Cl (80mM, pH 7.5) was added to 10ml of EDTA (10mM, pH 8.0).

TEN (Tris/EDTA/NaCl) Solutions

16g of NaCl was added to the TE Solution and the resulting solution made up to 100ml with distilled water and filter sterile.

Tris-Cl (250mM)(pH 7.5)

3.029g Tris was dissolved in 80ml distilled water and the pH adjusted to 7.5 by HCl. The solution was then made up to 100ml with distilled water and filter sterilised.

Phosphate Buffered Saline (pH 7.4)

8g $NaCl_2$; 0.2g KCl; 1.44g Na_2HPO_4; 0.24g KH_2PO_4 were dissolved in 800ml distilled water and the pH adjusted to 7.4 with HCl. The resulting solution was made up to 1litre with distilled water. The solution was autoclaved and store at room temperature.

Freeze-Thaw method

Cells in 6 well plates were harvested by washing with phosphate buffered saline (PBS), followed by resuspension in 300µl lysis buffer (TEN) (80mM Tris-HCl (pH 7.5), 16% NaCl, 10mM EDTA (pH 8.0)). Cells were allowed to sit on ice for 5min.The cells were scraped and centrifuged at 10,000 x *g* for 1 min after which time the supernatant was removed and the pellet resuspended in 100 µl 250 mM Tris-HCl (pH 7.5). The cells were then frozen at -80^0C for 5min and thawed rapidly at 37^oC for 5min. This process was repeated 5 times. The cells were then centrifuged at 10,000 x *g* for 5 min and

the supernatants were stored at -20^{o}C for enzyme analysis and protein determination.

2.2.4. Stock Cadmium (II) Chloride (100μM) Solution

1.833mg of Cadmium (II) Chloride ($CdCl_2$) (MW=183.31) was dissolved in 100ml Ultra High Quality (UHQ) water and filter sterilised.

2.2.5. Cell Viability study (MTT assay)

MTT Stock Solution (1.2mg/ml)

1.2mg of MTT was dissolved in 1ml DMEM freshly before use.

Principle

Cell viability was assessed by the MTT assay method (Mossman, 1983). The method was based on the conversion of soluble yellow coloured tetrazolium salt, [3-(4, 5-dimethyldiazol (-2-yl) - 2, 5-diphenyltetrazolium bromide] (MTT) into an insoluble purple coloured formazan by succinate dehydrogenase in the mitochondrion and cytosol of viable cells (Fig.2.1). The coloured compound formed has a characteristic absorption at 560nm wavelength and absorbance at this wavelength was used to monitor the viability of the cells.

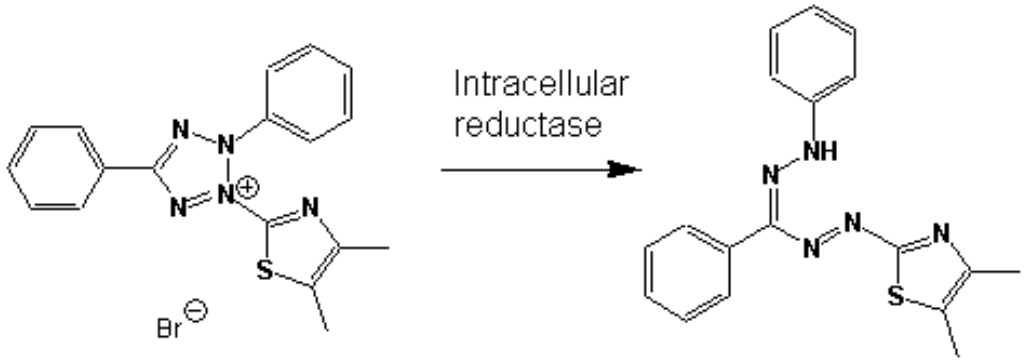

MTT (yellow) Formazan (purple)

Fig.2.1. Biochemistry of the MTT reaction in cell viability study. The reaction involves the reduction of a tetrazolium salt (MTT) by the action of intacellular reductases to form a purple coloured formazan.

Procedures

Cells were cultured in a 96 well plate at a concentration of 3 X10^5cells/ml and allowed to attach for 24hr. The cell monolayer was washed with phosphate buffered saline (PBS) after which addition of different concentrations of $CdCl_2$ diluted in DMEM followed. At the end of the incubation period, cells were washed again with PBS and 20µl of MTT prepared in DMEM (1.2mg/ml) were added. At the end of 4hr incubation, the media were aspirated and cells washed with PBS. Addition of 100µl of Dimethylsulfoxide (DMSO) was followed with gentle shaking for 10min in order to obtain complete dissolution. Absorbance was read at 560nm using the Labsystems iEMS microplate spectrophotometer and the background values were subtracted. Results were expressed as mean value of percentage of control.

2.2.6. LDH Leakage Assay

1X LDH Assay Cofactor (25ml)

25ml of tissue culture grade water was added to the bottle of lyophilised cofactors. The reconstituted cofactor preparation was stored at -0^{O}C in working aliquots in order to prevent repeated freeze/thaw.

Lactate Dehydrogenase Assay Mixture

5ml LDH Assay Substrate; 5ml LDH Assay Cofactor; 5ml of LDH Assay Dye Solution were added. The solution was prepared freshly prior to use.

Principle

The LDH assay was based on the method described by Decker and Lohmann-Matthes (1988). It involves measurement of lactate dehydrogenase (LDH) activity in the culture medium as a result of leakage from the cytoplasm of the cells due to membrane damage. The method was based on the conversion of lactate to pyruvate in the presence of LDH with parallel reduction of NAD. The reduced NAD (NADH) is used to convert a tetrazolium dye, INT (2-[4-Iodophenyl]-3-[4-nitrophenyl]-5-pheyltetrazolium chloride), into a coloured compound which can be monitored spectrophotometrically (Fig.2.2). Changes in absorbance were monitored at 490nm and background absorbance was monitored at 690nm.

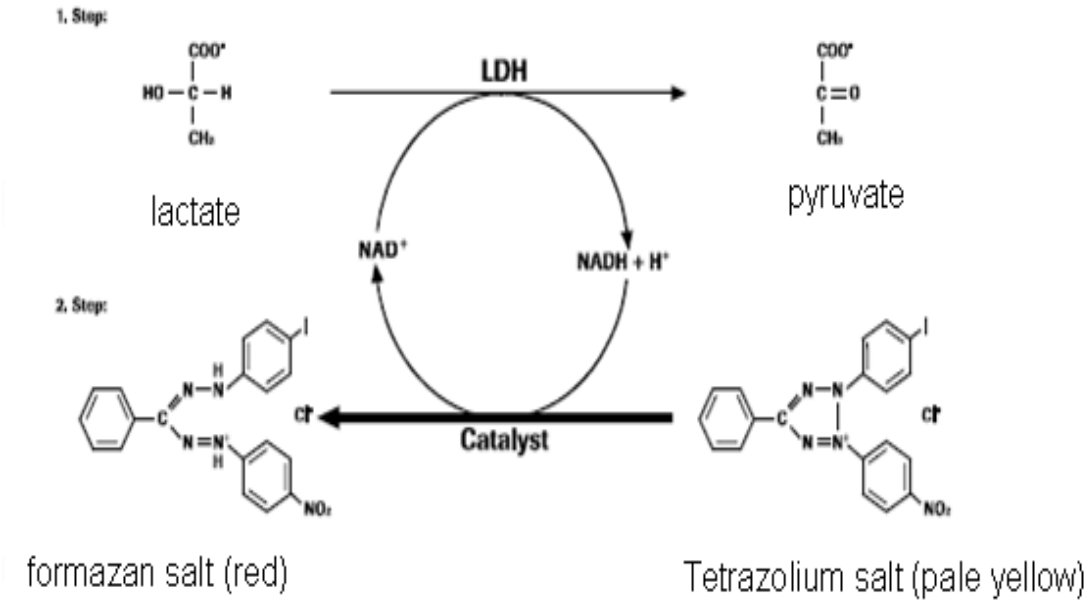

Fig.2.2. Biochemistry of the LDH reaction in the detection of cytotoxicity. The reaction is divided into 2 steps: the oxidation of lactate to pyruvate with concomitant reduction of NAD^+ to $NADH + H^+$ in an enzymatic reaction catalysed by LDH; the transfer of H/H^+ from $NADH+ H^+$ to the tetrazolium salt (INT) to form formazan.

Procedure

Cells culture preparation and treatment

Cells were cultured in 96 well plates at a concentration of 3X 10^5cells/ml and the cells were allowed to attach for 24hr. The cell monolayer was washed with PBS followed by the addition of different concentrations of $CdCl_2$ diluted in serum free DMEM. At the end of the incubation period, the medium was aspirated and centrifuged at 250x *g* for 4min.

LDH activity measurement

LDH activity in the aliquot of the supernatant was determined using LDH in vitro toxicology assay kit from sigma. The reaction was carried out in 96well plate containing 30µl of the supernatant and 60µl of the LDH assay mixture. The plate containing the reaction mixture was covered with aluminium foil and then incubated at room temperature for 20-30min. The reaction was terminated with 9µl 1N HCl. Absorbance was measured using Labsystems iEMS Reader MF (Microplate reader) at 490nm with background absorbance at 690nm. The background absorbance was subtracted from the absorbance at 490nm. Results were presented as mean value of percentage of control.

2.2.7. Assay for Reactive Oxygen Species (ROS)

Dihydrofluorescein diacetate (H_2FDA)(6mM) Stock

1.25mg H_2FDA (MW=418.41) was dissolved in 0.5ml DMSO on the day of the experiment and covered with aluminium foil.

H_2FDA (50µM) Working Solution

200µl of the H_2FDA stock was dissolved in 23.8ml Hank's Balanced Salt Solution (HBSS) just before use.

1M NaOH

1g of NaOH was dissolved in 25ml distilled water and was sterile filtered.

Principle

ROS assay was based on the protocol described by Hempel (1999) and modified by Fotakis *et al* (2005).The method was based on the conversion of nonfluorescent compound, dihydrofluorescein diacetate (H_2FDA), to the

fluorescent, fluorescein by reactive oxygen species. The fluorescent compound has characteristic excitation and emission at 488nm and 512nm respectively.

Procedure

Cells Culture and Treatment

Cells were cultured in 24 well plates at a density of 5.0×10^5 cells /well. The cells were allowed to attach for 24hr and then washed in PBS. The cells were then treated with different concentrations of $CdCl_2$ diluted in DMEM. After the incubation periods, the cell culture media were aspirated and cells were washed with PBS. 500µl of the working probe, H_2FDA (50µM), was added to the cells and the plates covered with aluminium foil. The cells were allowed to incubate for 30min. After the incubation period, the solution was aspirated and the cells were washed with PBS.

Conversion of fluorescein diacetate to fluorescein

500µl of 1M NaOH were added to the cells in other to extract the fluorescent product from the cells. The NaOH reacts with the fluorescein diacetate formed from H_2FDA to produce sodium acetate and the fluorescent compound, fluorescein. 100µl of the extract were then transferred to black 96 well plates and fluorescence intensity measured with Computer assisted Microplate Fluorescence Reader (FL600) at excitation of 488nm and emission of 512nm. Protein levels of the remaining extract were then carried out using Bradford method. The results were expressed as fluorescent intensity per mg protein and are presented as mean value of percentage of control.

2.2.8. Lipid Peroxidation Assay

Thiobarbituric Acid (TBA) (pH 3.8) Reagent

1.23g Sodium acetate (MW=82.03); 0.188g TBA (MW=144.15); 0.075g SDS (MW=288.38) were dissolved in 40ml distilled water and the pH adjusted to 3.8 with HCl. The solution was the made up to 50ml with distilled water.

2mM Butylated Hydroxytoluene (BHT)

22mg BHT; 27mg $FeCl_3$ were dissolved in 50ml ethanol.

1% H_2SO_4

1ml H_2SO_4 (MW=98.08) was diluted in 99ml distilled water.

10mM Tetramethoxypropane (TMP)

82.5µl of TMP was added to 50ml Concentrated H_2SO_4 and stirred in a magnetic stirrer for 2hours for hydrolysis.

1% H_2SO_4

1ml of H_2SO_4 was diluted in 99ml distilled water.

1mM TMP

0.5ml of stock TMP (10mM) was diluted with 4.5ml of 1% H_2SO_4.

Table.2.1. Standard TMP dilution preparation

1% H_2SO_4 (µl)	1mM TMP (µl)	TMP concentration (µM)
1000	0	0
999	1	1
998	2	2
997	3	3
996	4	4
995	5	5
994	6	6
993	7	7
992	8	8
991	9	9
990	10	10

Principle

Thiobarbituric acid reactive species (TBARS) assay was used to measure the extent of malondialdehyde (MDA) formed as a result of membrane lipid damage. The assay was based on the formation of a pink coloured complex in a reaction between malondiadehyde, formed during lipid peroxidation, and thiobarbituric acid (TBA) (Fig.2.3). The complex formed has a characteristic absorbance at 532nm.

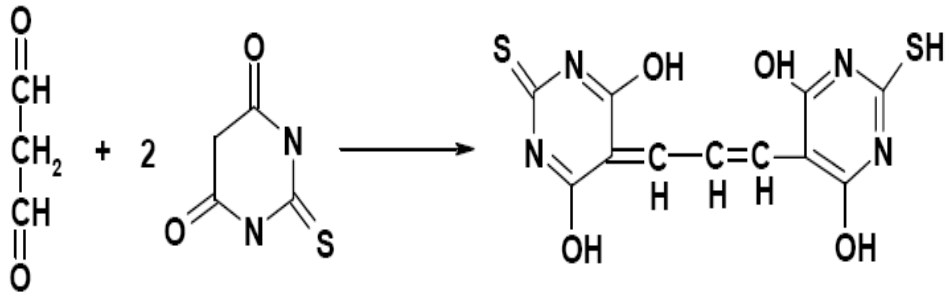

MDA TBA MDA-TBA$_2$ adduct (pink)

Fig.2.3. The reaction between Malondialdehyde (MDA) and Thiobarbituric acid (TBA). MDA reacts with TBA to form a pink coloured MDA-TBA$_2$ adduct with characteristic absorption at 532nm.

Procedure

Cells were cultured in 6 well plates at a density of 2.0 x 10^6cells/well and left to attach for 24hr. The cells were then treated with different concentrations of $CdCl_2$ diluted in DMEM. After the incubation period, the cell extracts were then prepared as described above. 500µl of cell extract was added to 1000µl TBA reagent (0.375% TBA, 0.3M Sodium acetate and 0.15% SDS) and 50µl BHT (a chain breaking antioxidant used to prevent amplification of the lipid peroxidation reaction during the assay) and the mixture was incubated for 60min at 90^{o}C in a waterbath (Table.2.2). The mixture was allowed to cool in ice after the incubation and then centrifuged at 5000x*g* for 10min. 1ml of the supernatant was removed and absorbance read at 532nm. A standard reaction was prepared by adding 500µl of each of the standard TMP dilutions (Table.2.1) to 1000µl TBA reagent. The amount of MDA formed was extrapolated from a standard MDA curve and result was expressed as µmol MDA/ml/mg protein.

Table.2.2.Lipid Peroxidation Reaction Mixture

	Blank	Sample	Standard
TBA	1000µl	1000µl	1000µl
TMP(MDA standard)	0	0	500µl
Cells extract	0	500µl	0
Distilled water	500µl	0	0

2.2.9. Reduced Glutathione (GSH) level determination

4% Sulfosalicylic acid

4g of Sulfosalicylic acid (MW=254.22) was dissolved in 100ml distilled water.

1M $Na_2HPO_4.2H_2O$

44.48g of $Na_2HPO_4.2H_2O$ (MW=177.99) was dissolved in 250ml distilled water.

1M $NaH_2PO_4.2H_2O$

39.002g of $NaH_2PO_4.2H_2O$ (156.01) was dissolved in 250ml distilled water.

0.1 M Sodium phosphate buffer (pH 7.4)

77.4ml of $Na_2HPO_4.2H_2O$ mixed with 22.6ml of $NaH_2PO_4.2H_2O$

1mM 5-5′-Dithiobis (2-nitrobenzoic acid)(DTNB) [Ellman reagent]

40mg of Ellman reagent was dissolved in 100ml of 0.1M Sodium phosphate buffer (pH 7.4).

13mM GSH Stock

40mg of GSH (MW=307.3) was dissolved in 100ml of 0.1M Sodium phosphate buffer (pH 7.4).

Table.2.3. Standard GSH preparation

Stock GSH(µl)	Ellman reagent(µl)	0.1M Sodium phosphate buffer(pH 7.4)	Amount of GSH(µg)
0	900	100	0.00
1	900	99	0.4
2	900	98	0.8
4	900	96	1.6
5	900	95	2.0
10	900	90	4.0
20	900	80	8.0
40	900	60	16.0
50	900	50	20.0

Principle

GSH level was determined spectrophotometrically according to the method of Jollow *et al* (1974). The method was based on the formation of 5-thio-2-nitrobenzoic acid (TNB) (a stable yellow coloured compound) in a reaction between Ellman reagent (5, 5′-dithiobis (-2-nitrobenzoic acid) (DTNB) and GSH (Fig.2.4). The coloured compound has a characteristic absorption at 412nm and it is proportional to the concentration of GSH. The amount of

GSH in the sample was extrapolated from a standard GSH curve and result was expressed as μg/ml/mg protein.

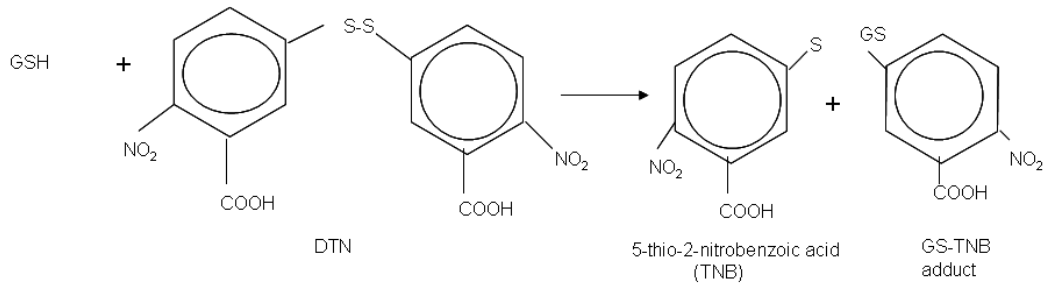

Fig.2.4. The reaction between GSH and Ellman reagent. GSH reacts with Ellman reagent to form a stable yellow coloured compound, 5-thio-2-nitrobenzoic acid with characteristic absorbance at 412nm.

Procedures

Cell sample preparation

Cell extracts were prepared according to the procedures as described in section 2.2.3. Equal volume of 4% Sulfosalicylic acid was added to the cell extract in order to deprotenise the sample by removing other sulhydryl group containing proteins which can interfere with the reaction. The mixture was then centrifuged at 17,000x*g* for 15min at 2^{o}C.

Assay mixture

100μl of the supernatant was added to 900μl of Ellman reagent in a 1ml cuvette and absorbance was measured at 412nm. The sample blank contains 100μl of 4% Sulfosalicylic acid and 900μl Ellman reagent while the zero blank contains 100μl of 0.1M Sodium phosphate buffer (pH 7.4) and 900μl of Ellman reagent (Table. 2.4). The absorbance of the sample blank was

subtracted from the absorbance of the sample and the amount of GSH in each sample was obtained from extrapolation from the standard curve (Table.2.3).

Table.2.4. GSH Assay Mixture

Reagent	Sample (µl)	Sample Blank(µl)	Zero Blank(µl)
Cell extracts	100	0	0
Ellman Reagent	900	900	900
4% Sulfosalicylic acid	0	100	0
0.1M Sodium Phosphate buffer(Ph7.4)	0	0	100

2.2.10. Glutathione S-transferase Activity Determination

1M K_2HPO_4

17.423g of K_2HPO_4 was dissolved in 100ml distilled water

1M KH_2PO_4

13.609g of KH_2PO_4 (MW=136.09) was dissolved in 100ml of distilled water.

0.1M Potassium Phosphate buffer (pH 6.5)

38.1ml of K_2HPO_4 was added to 61.9ml of KH_2PO_4.

0.1M GSH

30.73mg of GSH (MW=307.3) was dissolved in 1ml of 0.1M Potassium phosphate buffer (pH 6.5).

20mM 1-chloro-2, 4-dinitrobenzene (CDNB)

0.4052g of CDNB was dissolved in 100ml 0.1M Potassium phosphate buffer (pH 6.5).

Principle

GST activity in the cell sample was assessed spectrophotometrically according to the method of Habig *et al* (1974). The method was based on the conjugation of 1-chloro-2 4-dinitrobenzene (CDNB) with reduced glutathione (GSH) in a reaction catalysed by GST (Fig.2.5). Increase in absorbance was monitored for 3min at 30sec intervals at wavelength of 340nm.Results were expressed as μmol/min/ml/mg protein.

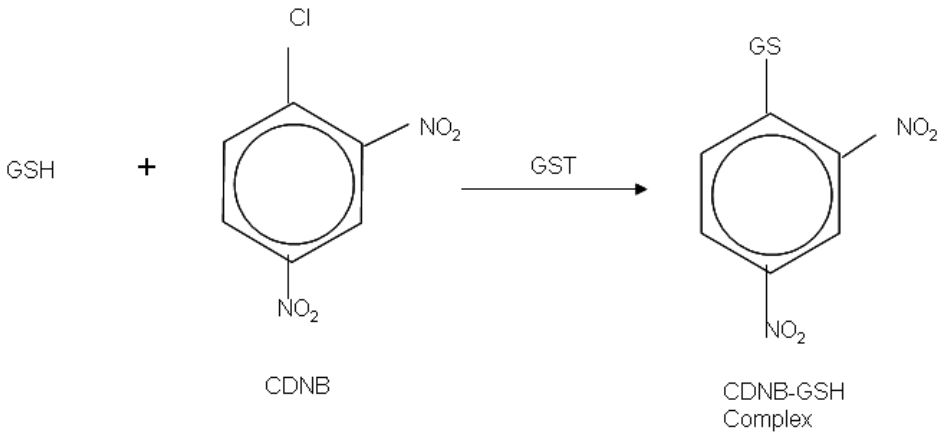

Fig.2.5. GST catalysed reaction. GST catalysed conjugation reaction between GSH and 1-chloro-2, 4-dinitrobenzene (CDNB).

Procedures

Cell sample preparation

Cell extracts were prepared according to the procedures as described in section 2.2.3.

Assay mixture

10µl of 0.1M GSH was added to 50µl of 20mM CDNB and 930µl of 0.1M Potassium Phosphate Buffer (pH 6.5). The mixture was incubated for 15min at 37^{o}C. After the incubation, 10µl of the cell extract was added to the reaction mixture in a quartz cuvette and changes in absorbance were monitored for 3min at 1min interval. The blank mixture contain 10µl GSH, 50µl of 20mM CDNB and 940µl 0.1M Potassium Phosphate Buffer. GST activity was expressed as µmol/min/ml/mg protein.

GST activity calculation

GST activity was calculated using the formula below;

$$\text{GST activity} = \frac{\text{Change in absorbance per min} \times \text{Total reaction volume}}{9.6 \times \text{Volume of sample}}$$

Total reaction mixture=1ml

Volume of sample= 10µl

9.6mM^{-1}cm^{-1}= extinction coefficient for CDNB-GSH complex at 340nm.

Table.2.5. GST Assay Mixture

Reagent	Sample(µl)	Blank(µl)
0.1M GSH	10	10
20mM CDNB	50	50
0.1M Potassium PhosphateBuffer(pH 6.5)	930	940

Incubate for 15min at 37^{o}C

Cell extracts	10	0

2.2.11. Glutathione Reductase Activity Determination

Glutathione Reductase Dilution Buffer

The solution contains 100mM potassium phosphate buffer (pH 7.5); 1mM EDTA and 1mg/ml bovine serum albumin.

Glutathione Reductase Assay Buffer

The solution contains 100mM potassium phosphate buffer (pH 7.5) and 1mM EDTA.

(2mM) β-Nicotinamide adenine dinucleotide phosphate, reduced (NADPH)

1.85mg of NADPH was dissolved in 1ml Assay Buffer. The solution was prepared freshly on the day of the experiment and stored at 4^{o}C.

2mM GSSG

1.42mg of GSSG was dissolved in 1ml Assay Buffer and store at 25^{o}C.This solution was used within 7 days when stored at 2-8^{o}C.

Principle

Glutathione reductase activity was determined spectrophotometrically according to method of Carlberg and Mannervik (1977).The assay was based on the reduction of GSSG to GSH by NADPH in a reaction catalysed by glutathione reductase (Fig.2.6). Decreases in absorbance were monitored at 340nm.

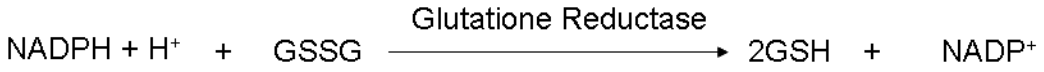

Fig.2.6. Glutathione reductase catalysed reaction. Glutathione reductase catalysed the reduction of oxidised glutathione in the presence of NADPH as cofactor

Procedures

Cell sample preparation

Cell extracts were prepared according to the procedures as described in section 2.2.3.

Assay Mixture

The reaction mixture contains 500µl of 2mM GSSG; 440µl of assay buffer (100mM potassium phosphate buffer, pH 7.5; 1mM EDTA) and 10µl cell extracts in a 1ml quartz cuvette. The reaction was started by the addition of 50µl of 2mM NADPH and the reaction mixtures were mixed by inversion (Table. 2.6). The blank reaction contains 500µl 2mM GSSG; 450µl of assay buffer and 50µl NADPH. Decrease in NADPH absorbance was monitored for

2min at 10sec intervals at 340nm. Results were expressed as units/ml/mg protein.

Glutathione Reductase Activity Calculation

Glutathione reductase (GR) activity was calculated using the formular below;

$$\text{GR activity (units/ml)} = \frac{(\Delta A_{sample} - \Delta A_{blank}) \text{ X (dilution factor)}}{\varepsilon^{mM} \text{ X (volume of sample in ml)}}$$

$\varepsilon^{mM} = 6.22 mM^{-1}cm^{-1}$ for NADPH

ΔA_{sample}= change in absorbance of sample per min.

ΔA_{blank} = change in absorbance of blank per min.

One unit of GR activity is defined as the amount of enzyme that catalysed the oxidation of 1.0µmole NADPH at 25^{o}C at pH 7.5.

Table.2.6. Glutathione Reductase Activity Assay Mixture

Solution	Sample (µl)	Blank (µl)
2mM GSSG	500	500
Assay Buffer(100mM potassium phosphate buffer,pH7.5; 1mM EDTA)	440	450
Cell Extracts	10	0
2mM NADPH	50	50

2.2.12. Glutathione Peroxidase Activity Determination

NADPH Assay Reagent

This solution contains 5mM NADPH; 42mM GSH and 10units/ml glutathione reductase.

Glutathione Peroxidase Assay Buffer

This solution contains 50mM Tris HCl, pH 8.0; 0.5mM EDTA.

30mM tert-Butyl Hydroperoxide Solution

This solution was prepared by diluting 21.5 μl of reagent to a total volume of 5ml with distilled water.

0.2mM H_2O_2

1μl of 8.77M H_2O_2 stock was added to 43.86ml distilled water.

1mM NaN_3

1.302mg of NaN_3 (MW=65.01) was added to 20ml distilled water.

Principle

Glutathione Peroxidase activity was measured spectrophometrically according to the method of Wendel (1980). The assay was based on the oxidation of reduced glutathione (GSH) to oxidised glutathione (GSSG) in a reaction catalysed by glutathione peroxidase and coupled to the reduction of GSSG to GSH in a reverse reaction catalyzed by glutathione reductase using NADPH as a cofactor (Fig.2.7). Decrease in absorbance was monitored at 340nm.

$R\text{-}OOH + 2GSH \rightarrow R\text{-}OH + GSSG + H_2O$

$GSSG + NADPH + H^+ \rightarrow 2GSH + NADP^+$

Fig.2.7. Glutathione peroxidase catalysed reaction. Glutathione catalysed the oxidation of glutathione in the presence of peroxides. The reaction is coupled to the reduction of oxidised glutathione back to GSH in a reaction catalysed by glutathione reductase

Procedures

Cell sample preparation

Cell extracts were prepared according to the procedures as described in section 2.2.3.

Assay Mixture

The reaction mixture contains 930µl of assay buffer (50mM Tris HCl, pH 8.0; 0.5mM EDTA), 50µl NADPH assay reagent (5mM NADPH; 42mM GSH; 10units/ml glutathione reductase) and 10µl of cell extracts in a 1ml quartz cuvette. The reaction mixture was mixed by inversion and 10µl of 30mM tert-Butyl Hydroperoxide solution was added to start the reaction. The blank contains 940µl of assay buffer; 50µl NADPH and 10µl of 30mM tert-Butyl Hydroperoxide (Table.2.7). For HepG2 cells extract, the reaction mixture contains 920µl assay buffer (50mM Tris HCl, pH 7.0; 0.5mM EDTA), 50µl NADPH assay reagent (5mM NADPH; 42mM GSH; 10units/ml glutathione reductase); 10µl of cell extracts and 10µl of 1mM NaN_3. The reaction was started with 10µl of 0.2mM H_2O_2 (Table.2.8). The blank contains 930µl of assay buffer; 50µl NADPH; 10µl NaN_3 and 10µl of 0.2mM H_2O_2. The decrease in NADPH absorbance was monitored at 340nm for 1min at 15sec intervals. Results were expressed as µmol/min/ml/mg protein.

Glutathione Peroxidase Activity Calculation

Glutathione Peroxidase activity in the cells extracts was calculated using the formular below;

$$\text{Activity/cell extract (μmol/min/ml=units/ml)} = \frac{[\Delta A_{blank} - \Delta A_{sample}]X\ DF}{6.22\ X\ V}$$

$6.22=\varepsilon^{mM}$ for NADPH

DF=dilution factor

V=sample volume in ml

One unit of glutathione peroxidise is defined as the amount of enzyme that catalysed the formation of 1.0μmol of $NADP^+$ from NADPH per minute at pH 8.0 at 25°C in a coupled reaction in the presence of reduced glutathione, glutathione reductase and tert-butyl hydroperoxide.

Table.2.7. Glutathione Peroxidase Activity Assay Mixture for 1321N1 and HEK 293 cells

Solution	Blank (μl)	Sample (μl)
Assay Buffer(50mM Tris HCl, pH 8.0; 0.5mM EDTA)	940	930
NADPH reagent (5mM NADPH; 42mM GSH; 10units/ml glutathione reductase)	50	50
Cell extracts	0	10
30mM tert-Butyl Hydroperoxide	10	10

Table.2.8. Glutathione Peroxidase Activity Assay Mixture for HepG2 Cells

Solution	Blank (µl)	Sample (µl)
Assay Buffer(50mM Tris HCl, pH7.0; 0.5mM EDTA)	930	920
NADPH reagent (5mM NADPH; 42mM GSH; 10units/ml glutathione reductase)	50	50
Cell extracts	0	10
1mM NaN_3	10	10
0.2mM H_2O_2	10	10

2.2.13. Catalase Activity Determination

Assay buffer (10x)

This solution contains 500mM potassium phosphate buffer, pH 7.0

1x Assay buffer

2ml of the 10x assay buffer was dissolved in 18ml with water. The resulting solution contains 50mM potassium phosphate buffer, pH 7.0. The solution is stored at room temperature.

20mM H_2O_2

200µl of 3% H_2O_2 was diluted to 10ml with 1x assay buffer. This solution was stored at 4^{o}C and was used within 6 days.

Principle

Catalase activity was determined spectrophotometrically according to the method of Aebi (1973) using the catalase assay kit (Product Number CAT 100) from Sigma. The method was based on the decomposition of hydrogen peroxide to water and oxygen by catalase (Fig.2.8). Decrease in absorbance of hydrogen peroxide was monitored at 240nm.

$$2H_2O_2 \rightarrow 2H_2O + O_2$$

Fig.2.8. Catalase catalysed reaction. Catalase catalysed the reduction of hydrogen peroxide to molecular water and oxygen

Procedures

Cell sample preparation

Cell extracts were prepared according to the procedures as described in section 2.2.3.

Assay Mixture

The assay mixture contains 50µl cell extracts and 450µl 1X assay buffer (50mM potassium phosphate buffer; pH 7.0) in a 1ml quartz cuvette. The mixture was mixed by inversion and the reaction was started by adding 500µl of 20mM H_2O_2 solution (Table.2.9). The blank reaction mixture contains 500µl 1x assay buffer (50mM potassium phosphate buffer, PH7.0) and 500µl of 20mM H_2O_2. Decrease in absorbance was monitored at 240nm for 30seconds at 5second intervals. Catalase activity was expressed as units/ml/mg protein.

Catalase Activity Calculation

Catalase activity in the cells extracts was calculated using the formula below;

$$\text{Units/ml} = \frac{[\Delta A/\text{min(Blank)} - \Delta A/\text{min(Sample)}] \times d \times 1}{V \times 0.0436}$$

d= dilution factor

V= volume of sample in the reaction

0.0436= ε^{mM} for hydrogen peroxide

One unit of catalase is defined as the amount of enzyme that catalyses the decomposition of 1.0μmole of hydrogen peroxide to oxygen and water per minute at pH7.0 at 25°C when the substrate concentration is 10mM H_2O_2

Table.2.9. Catalase Activity Assay Mixture

Solution	Blank (μl)	Sample(μl)
Cell extracts	0	50
1x Assay Buffer (50mM potassium phosphate buffer, pH 7.0)	500	450
20mM H_2O_2	500	500

2.2.14. Superoxide Dismutase Activity Determination

1x Water Soluble Tetrazolium Salt (WST) (2-(4-Iodophenyl)-3-(4-nitrophenyl)-5-(2,4-disulfophenyl)-2H- tetrazolium,monosodium salt)

1ml of WST was dissolved in 19ml of buffer solution.

Enzyme Working Solution

The enzyme solution was centrifuged for 5sec at 1,000x*g* and mixed by pipetting. 15µl of the solution was then diluted with 2.5ml of dilution buffer.

Principle

Superoxide dismutase activity was assayed using the SOD assay kit (Product code 19160) from Fluka (UK). The method was based on the ability of SOD to remove superoxide anion formed by xanthine oxidase (XO) and thereby prevent it from converting water soluble tetrazolium salt, (WST-1) (2-(4-Iodopheyl)-3-(4-nitrophenyl)-5-(2, 4-disulfophenyl)-2H-tetrazolium, monosodium salt), into a coloured compound, formazan (Fig.2.9). Absorbance of WST-1 was monitored at 450nm and is a measure of SOD activity.

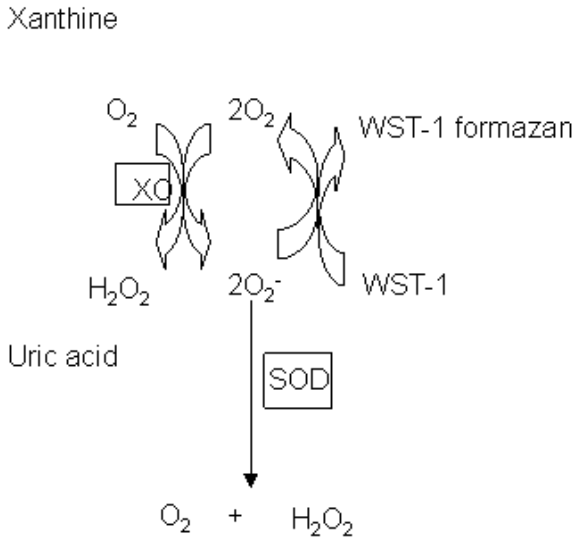

Fig.2.9. **SOD catalysed reaction**. SOD catalysed the oxidation of superoxide anions into molecular oxygen and hydrogen peroxide thereby inhibiting the formation of a dye (WST-1formazan)

Procedures

Cell sample preparation

Cell extracts were prepared according to the procedures as described in section 2.2.3.

Assay Mixture

The reaction was carried out in 96well plates and contains 20µl cell extracts; 200µl of WST and 20µl of enzyme working solution in the sample reaction well. The sample blank reaction well contains 20µl cell extracts; 200µl WST and 20µl of dilution buffer. The enzyme reaction well contains 20µl ultra high quality water (UHQ); 200µl of WST working solution and 20µl enzyme working solution. While the enzyme blank reaction well contains 20µl ultra high quality water (UHQ); 200µl WST working solution and 20µl of dilution buffer (Table.2.10). The plate was incubated for 20min at 37^{o}C and absorbance was read at 450nm with the Labsystems iEMS microplate spectrophotometer. SOD activity was expressed as the rate of inhibition of WST reduction/mg protein.

SOD activity calculation

SOD activity in the cell extracts was calculated using the formula below;

$$\text{SOD activity (inhibition rate \%)} = \frac{\{[(A_{blank1} - A_{blank3}) - (A_{sample} - A_{blank2})\}}{(A_{blank1} - A_{blank3})} \times 100$$

A_{blank1}= Enzyme reaction mixture

A_{blank3} = Enzyme blank reaction mixture

A_{sample} = Sample reaction mixture

A_{blank2} = Sample blank reaction mixture

Table.2.10. SOD Activity Assay Mixture

Solution	Sample (µl)	Blank1(µl)	Blank2(µl)	Blank3(µl)
Cells extracts	20	0	20	0
UHQ	0	20	0	20
WST working solution	200	200	200	200
Enzyme working solution	20	20	0	0
Dilution buffer	0	0	20	20

2.2.15. Aldehyde Reductase Activity Determination

0.1M $Na_2HPO_4.2H_2O$

1.78g of $Na_2HPO_4.2H_2O$ (MW=177.99) was dissolved in 100ml distilled water. The solution was autoclaved before use.

0.1M $NaH_2PO_4.2H_2O$

1.56g of $NaH_2PO_4.2H_2O$ (MW=156.01) was dissolved in 100ml distilled water. The solution was autoclaved before use.

100mM Sodium Phospate Buffer (pH 6.6)

9.375ml 0.1M $Na_2HPO_4.2H_2O$; 15.625ml $NaH_2PO_4.2H_2O$; were mixed together.

25mM p-Nitrobenzaldehyde

19mg p-Nitrobenzaldehyde (MW=151.1) was dissolved in 2.5ml Methanol (the mixture was heated to 50°C to dissolve) and 2.5ml of 100mM sodium phosphate buffer (pH 6.6) was added.

5mM NADPH

2.1mg NADPH (MW=833.4); 0.5ml 100mM sodium phosphate buffer (pH 6.6) were added together.

Principle

AKR activity in the cell extracts was assessed spectrophotometrically according to the method of Iwata *et al (*1990).The method was based on monitoring the decrease in absorbance of NADPH at 340nm in the presence of p-Nitrobenzaldehyde (pNBA) (Fig.2.10).

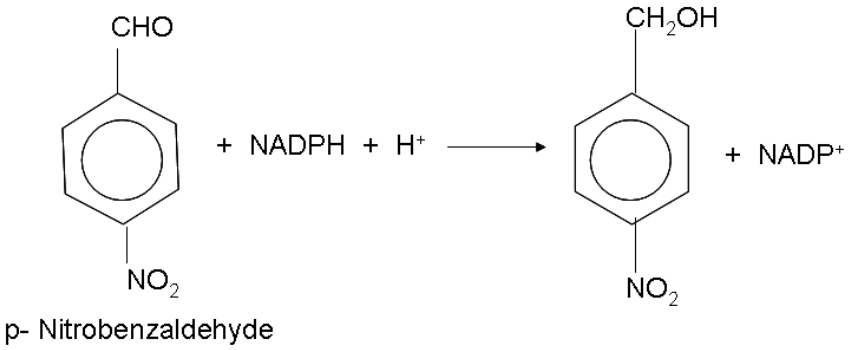

Fig.2.10. AKR catalysed reaction. AKR catalysed the reduction of p-nitrobenzaldehyde with a corresponding oxidation of NADPH.

Procedures

Cell sample preparation

Cells extracts were prepared according to the procedures as described in section 2.2.3.

Assay Mixture

The reaction consists of 940µl 100mM $NaPO_4$ Buffer (pH 6.6); 40µl 25mM p-Nitrobenzaldehyde; 10µl 5mM NADPH in 1ml quartz cuvette. The reaction was started by the addition of 10µl cell extract. Changes in absorbance were monitored for 2min at 30sec interval. Results were expressed as units/min/mg protein.

One unit of AKR was defined as the amount of enzyme that catalysed the oxidation of 1µmoleNADPH at 37^{o}C .Results was expressed as units/min/mg protein.

2.2.16. Protein Gels and Western Blots

4 x Resolving buffer

90.8g of Tris base; 2g of SDS; made up to 450ml with distilled water and the pH was adjusted to 8.8 with concentrated HCl. The solution was then made up to 500ml with distilled water and filtered through the Whatman # 1 filter paper.

4 x Stacking buffer

15.14g Tris base; 1g SDS; made up to 200ml with distilled water and the pH was adjusted to 6.8 with concentrated HCl. The solution was made up to 250ml with distilled water and filtered through the Whatman # 1 filter paper.

10 x Running buffer

30.28g Tris base; 144g Glycine; 10g SDS; made up to 1litre with distilled water.

1x Running buffer

100ml of 10x running buffer was made up to 1litre with distilled water (1:10 dilution).

2 x Lysis buffer

3.13ml Tris-Cl (pH 6.8); 2g SDS; 9ml Glycerol (heated to make it less viscous); 5ml Mercaptoethanol (added freshly on the day of use); 1ml Bromophenol (0.1%,v/v) (added freshly on the day of use); made up to 50ml with distilled water.

SDS-Polyacrylamide Gel Electrophoresis

Principle

Electrophoresis studies the movement of charged molecules in an applied electric field. In SDS-PAGE, proteins are separated based on their molecular weight in an applied electric field. SDS is an anionic detergent that denatures protein by disrupting their secondary, tertiary and quaternary structures thereby producing a linear polypeptide chain surrounded by negatively charged SDS molecules. Mercaptoethanol further helps in the denaturation process by reducing the disulfide bonds. The denatured proteins thus travel along the polyacrylamide gel (stationary phase) (Fig.2.11) according to their molecular weight. The pore sizes retard the movement of the large protein while the smaller proteins travel further along the gel.

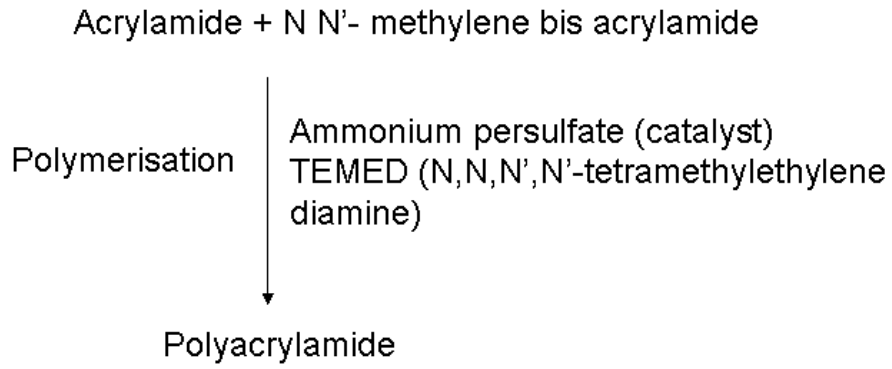

Fig.2.11. Biochemistry of acrylamide polymerisation. Acrylamide in the presence of ammonium persulfate catalyst and TEMED polymerised with bis-acrylamide to form polyacrylamide

Sample preparation

Cells were cultured in a 6 well plate as previously described in section 2.2.1. The cells were the treated with different concentrations of $CdCl_2$. After the incubation period, cells were washed with ice-cold PBS and the cells were then scraped in 100µl of 2x lysis buffer with a rubber policeman into an eppendorf tube. The sample was boiled in a boiling waterbath for 5min and then centrifuged briefly for 1min at 1,000x*g*. Protein levels in the cell lysate were determined according to the protocol described by Bradford (1976) using the bovine serum albumin (BSA) as standard.

Procedures

Resolving Gel (10% Gel)

30% acrylamide/bisacrylamide solution	6.6ml
4 x resolving buffer	5ml
Distilled water	8.2ml
Ammonium persulfate (100mg/ml)	100µl

TEMED	10µl

Stacking Gel (5% Gel)

30% acrylamide/bisacrylamide solution	1.64ml
4 x stacking buffer	2.5ml
Distilled water	5.86ml
Ammonium persulfate (100mg/ml)	60µl
TEMED	10µl

Gel plates were washed and wiped dry with ethanol. The plates were then assembled using the rubber spacers in between plates. Care was taken to avoid leakages. 10% Gel (Resolving Gel) was then poured into the assembled plates leaving about 1cm space at the top. The gel was then overlaid with water saturated isobutanol and left to polymerise. After polymerization, the isobutanol was poured out and the space between the plates was dried up with paper towel. 5% gel (Stacking Gel) was then poured on top of the resolving gel and combs were inserted. The gel was then left to polymerise. After polymerization, the combs were removed and the plates were placed in ATTO gel apparatus (model-AE6450) from ATTO Corporation, Japan and the tank was filled with 1x running buffer. Each gel well was then loaded with approximately 9µg sample and the gel was run at 125V and 200mA.

Western Blot

1x Transfer Buffer

14.4g glycine; 3.0g Tris base; 200ml Methanol; made up to 1litre with distilled water.

10x TBS

100ml of 1M Tris.Cl (pH 7.5); 375ml of 4M NaCl; made up to 1litre with distilled water.

1x TBSTween

100ml of 10x TBS; 2ml of Tween 20 (0.2% v/v); made up to 1litre with distilled water.

Blocking Solution

5g dried skimmed milk powder was dissolved in 100ml 1x TBSTween.

Procedure

In Western blotting, the gel containing the proteins was transferred to a nitrocellulose membrane. For each gel to be transferred, 4pieces of Whatman 3MM paper and 1 piece of nitrocellulose membrane were cut to the size of the gel and together with 2 sponges were all soaked in 1x Transfer Buffer and then assembled in form of a sandwich (Fig.2.12). The sandwich was set up in such a way that the sponge was on the black (-ve)side of the plastic holder followed by 2 layers of Whatman paper, the gel containing the proteins, nitrocellulose membrane, 2layers of Whatman paper and sponge in that order. The assembled sandwich was then placed in transfer tank (Bio-Rad gel apparatus) filled with 1x Transfer Buffer and transfer was carried out for 2hr at 300mA. After the transfer, the nitrocellulose membrane was removed into a clean plastic container containing the blocking solution and left for 2hours or overnight in order to block the protein-binding sites present on the membranes. After the incubation, the blocking solution was removed and antibody diluted in fresh blocking solution (1: 2000) was added to the

membrane and was allowed to incubate for at least 2hours on a shaker. The nitrocellulose membrane was then washed with 1x TBSTween for 4times (5min each). The secondary antibody diluted in blocking solution (1: 2000) was added to the washed membrane and then incubated for 1hour with gentle shaking. After the incubation, the membrane was washed 3times (5min each) in 1xTBSTween and once in TBS. The blot was then developed using ECL.

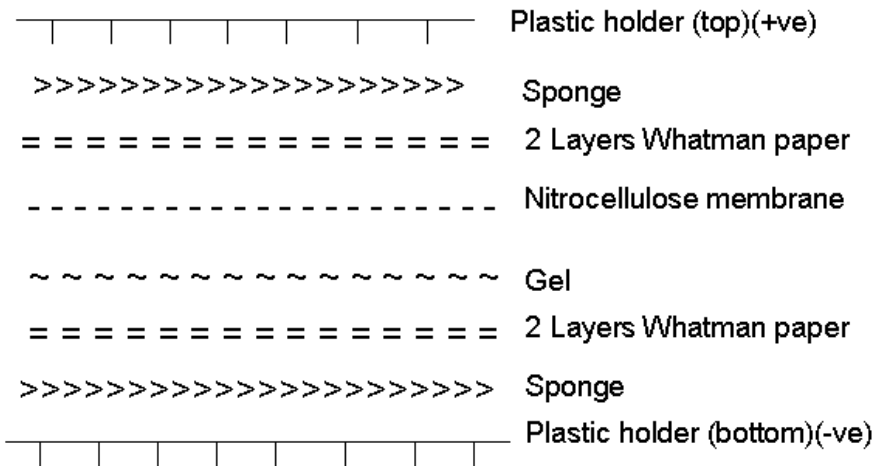

Fig.2.12. Western Blot transfer sandwich

Antibody Detection using Enhanced Chemiluminescence (ECL)

250mM Luminol

0.22g Luminol (Fluka, cat no 09253) was dissolved in 5ml DMSO. The solution was kept in the dark at -20^{o}C in 500µl aliquots.

90mM Coumaric acid

0.07g Coumaric acid (Sigma, cat no C-9008) was dissolved in 5ml DMSO and the solution was kept in the dark at -20°C in 500µl aliquots.

ECL 1 Solution

1ml of 250mM Luminol solution; 0.44ml of 90mM Coumaric acid solution; 10ml of 1M Tris-Cl (pH 8.5); was made up to 100ml with distilled water.

ECL 2 Solution

64µl of H_2O_2 (30%); 10ml of 1M Tris-Cl (pH 8.5); was made up to 100ml with distilled water.

Both solutions were kept in the dark at 4°C. Equal volumes of both solutions were mixed together just before use and poured over the membrane. Bands were detected using the computer assisted intelligent dark box image reader (LAS3000) from Fujifilm Company and images were stored as 8bits image format. The intensities of the bands were quantified with "image j" analysis software (www.imagejdev.org) and compared relative to internal control.

2.2.17. Protein Determination

(1.0mg/ml) Bovine Serum Albumin (BSA)Stock

1.0mg of BSA was dissolved in 1ml distilled water and the solution stored at -20°C.

0.1mg/ml BSA working solution

1ml of the BSA stock solution was made up to 10ml to give a 1 in 10 dilution. This solution was kept on ice until used.

BSA standard dilution

Serial dilution of the stock solution was prepared in distilled water as shown in table below.

Table.2.11. BSA standard dilution for protein determination

Volume (µl) of BSA stock solution	Amount (µg)	Distilled water(µl)	Bradford reagent(µl)
0	0	800	200
2	0.2	798	200
5	0.5	795	200
10	1.0	790	200
20	2.0	780	200
50	5.0	750	200
100	10.0	700	200
200	20.0	600	200
Sample (10µl)		790	200

Principle

Protein determination was performed according to the Bradford method (1976). The method was based on the formation of dye-protein complex solution between Bradford reagent and protein with a characteristic absorbance at 595nm.

Procedure

Several serial dilutions of BSA stock (0.1mg/ml) were prepared and made up to 800µl with distilled water in eppendorf tubes. The samples were diluted appropriately to allow the absorbance to fall within the standard range and 10µl were made up to 800µl with distilled water in an eppendorf tube. A blank tube (zero blank) contains 800µl distilled water and sample blank contains 800µl sample buffer .200µl of Bradford reagent (Bio-Rad, UK) was added to each tube and the mixtures were vortexed or inversed several times to allow for uniform solution. The mixtures were allowed to standard for at least 5min and absorbance was taken at 595nm in a pre-warmed spectrophotometer. The amount of protein in the sample was extrapolated from the standard curve of absorbance versus microgram protein (Table.2.11).

2.2.18. ATP Determination

(1.1mg/ml) ATP Standard Stock

1.1mg ($2.2x10^{-6}$mole) ATP (Product code FL-AAS; Sigma) was dissolved in 1ml sterile water and the solution was stable for 2weeks when stored frozen at -20^{o}C.

ATP Standard Dilution for Calibration Curve

ATP standard solutions for the calibration curve were prepared by making serial dilutions of ATP standard stock solution with sterile water. 25µl of the stock are made up to 1ml with sterile distilled water (1 in 40 dilutions) to give a solution containing 5.5 $x10^{-8}$mole ATP. This solution was then diluted serially in 1 in 10 dilutions to give solution containing different amounts of ATP as shown in table 2.12 below

Table.2.12. Standard ATP Dilution Preparation

ATP stock solution							ATP standard
10^{-8} moles ATP	10^{-9} moles ATP	10^{-10} moles ATP	10^{-11} moles ATP	10^{-12} moles ATP	10^{-13} moles ATP	H_20	Conc. (moles ATP)
50µl						450µl	10^{-9}
	50µl					450µl	10^{-10}
		50µl				450µl	10^{-11}
			50µl			450µl	10^{-12}
				50µl		450µl	10^{-13}
					50µl	450µl	10^{-14}

ATP Assay Mix (Product code FL-AAM) stock solution

One vial of the lyophilized powder containing luciferase, luciferin, $MgSO_4$, DTT,EDTA, BSA and tricine buffer salts was dissolved in 5ml of sterile water to generate a stock solution of pH 7.8.The solution was mixed by gentle inversion and allowed to stand in ice for 1hour to allow complete dissolution. This solution is stable for 2weeks when stored in the dark between 0-5^{o}C.

ATP Assay Mix Dilution Buffer (Product code FL-AAB)

One vial of the lyophilised powder containing MgSO4, DTT, EDTA, bovine serum albumin and tricine buffer salts was dissolved in 50ml of sterile water. The solution is stable for at least 2weeks when stored at 0-5^{o}C.

ATP Assay Mix Working Solution

1ml of the ATP assay mix stock solution was diluted with 24ml of ATP assay mix dilution buffer.

Principle

The assay was based on the production of light by the consumption of ATP in a reaction catalysed by firefly luciferase (Fig.2.13; Leach, 1981). The amount of light emitted was measured by the luminometer and it is proportional to the amount of ATP present.

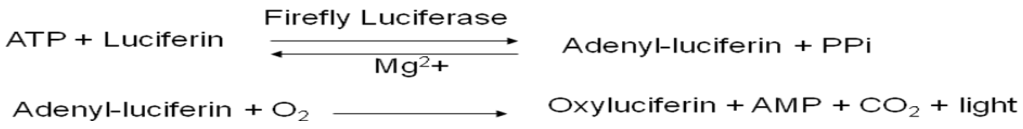

Fig.2.13. Luciferase catalysed reaction. ATP is consumed in the presence of luciferase to produce light with the emission of CO_2. The intensity of the light emitted is a measure of ATP level.

Procedure

Cell sample preparation

Cell extracts were prepared according to the procedures as described in section 2.2.3.

Assay Mixture

The reaction was carried out in black 96 well plates.100µl of ATP assay mixture working solution was added into each well and swirled. The solution was allowed to stand for 3minutes at room temperature in order to hydrolyse any endogenous ATP that may be present. After the incubation

period, 100µl of sample or standard was added and the plate was swirled briefly and the amount of light produced was measured immediately with luminometer (Galaxy lumistar, model). A reaction blank was produced by adding 100µl of sterile water to the ATP assay mixture working solution (Table.2.13). The amount of ATP was extrapolated from the standard curve (Table.2.12) and was expressed as moles ATP/ml/mg protein.

Table. 2.13. ATP assay mixture

	Standard (µl)	Sample(µl)	Blank (µl)
ATP assay mixture working solution	100	100	100
ATP standard	100	0	0
Sample	0	100	0
Sterile water	0	0	100

2.2.19. Single Cell Gel Electrophoresis (Comet) assay

Lysis Buffer (pH 10)

73.05 g NaCl (2.5M) (MW=58.44); 18.612 g EDTA (0.1M) (MW=372.24 g); 0.6057 g Tris (0.01M) (MW=121.14) were dissolved in 400ml distilled water and pH adjusted to 10 with NaOH. The solution was then made up to 500ml with distilled water and Triton X-100 (1%v/v) was then added to the solution freshly before used. The solution was stored at room temperature.

0.4M Tris-Cl (pH 7.5)

12.114 g Tris base (MW=121.14) was dissolved in 200ml distilled water and pH was adjusted to 7.5 with HCl. The Solution was made up to 250ml with distilled water.

Electrophoresis Buffer (pH 13)

0.744 g EDTA (1mM) (MW=372.24); 24 g NaOH (300mM) (MW=40) was added to 1800ml distilled water and pH adjusted to 13 with HCl. The solution was then made up to 2000 ml with distilled water.

96% Ethanol

960 ml ethanol was made up to 1000 ml with distilled water.

Stock Ethidium Bromide (20 μg/ml)

10 mg Ethidium bromide was dissolved in 50ml distilled water.

Ethidium Bromide (2 μg/ml) Working Solution

1 ml of ethidium bromide stock solution was mixed with 9ml distilled water.

1% Agarose (Normal Melting Agarose (NMA))

1 g Agarose was dissolved in 100 ml Millipore High Quality water and microwave heated to near boiling until the agarose dissolved.

0.5% Agarose (Low Melting Point Agarose (LMPA))

0.5 g Agarose was dissolved in 100 ml Phosphate Buffer Saline (PBS) solution and the solution was microwaved to near boiling until the agarose dissolved. The solution was placed in a 37^{o}C waterbath prior to use.

Phosphate Buffered Saline (pH 7.4)

8g $NaCl_2$; 0.2g KCl; 1.44g Na_2HPO_4; 0.24g KH_2PO_4 were dissolved in 800ml distilled water and the pH adjusted to 7.4 with HCl. The resulting solution was made up to 1litre with distilled water. The solution was autoclaved and stored at room temperature.

Principle

The Comet assay was performed according to the method of Singh *et al* (1988). The method was based on the formation of a comet, a distinct head and tail, by the migration of denatured and fragmented DNA out of the cells in an applied electric field. The undamaged DNA moves slowly and remains within the nucleoid to form the head while the damaged DNA migrates faster to form the tail. The degree of DNA migration out of the head is used as a measure of DNA damage.

Procedures

Base Slides Preparation

Slides were dipped in methanol and were sterilised by burning them over a blue flame. The slides were then pre-coated by dipping them into the hot NMA agarose. The agarose on the underside of the slides were wiped off with tissue paper and the slides were placed in the microscopic slide tray on a flat surface. The slides were then allowed to dry overnight at room temperature.

Cell Sample preparation

Cells were plated in EasyFlask 75cm^2 Vent/Close tissue culture flasks at a density of 2x 10^6cells/flask and allowed to attach for 24hr. Cells were then

treated with different concentrations of $CdCl_2$ for 24hr. After the incubation, the cell monolayer was washed with PBS and the cells were trypsinised with a very low concentration of trypsin (0.1%) for 2minutes at 37°C. DMEM supplemented with 10% FBS was added to inhibit the action of trypsin. The cell suspension was pipetted into a 15ml centrifuge tube and centrifuged at 1000x*g* for 2min to obtain cell pellets. The pellets were kept on ice before use.

Sample Slides Preparation

The cell pellet was resuspended in PBS and approximately 10,000 cells/10 µl were mixed with 75 µl of LMPA agarose at 37°C. This solution was rapidly pipetted and spread uniformly on NMA agarose pre-coated slides and the slides were then covered with coverslips to allow the mixture to spread homogenously on the slides. The cells-LMPA agarose mixture was allowed to solidify by placing the slides on an ice-cold microscopic tray for 5minutes. After the solidification, the coverslips were removed and an additional 75µl of LMPA agarose was layered on top of the mixtures. The slides were again covered with coverslips and the agarose allowed to solidify for an additional 5minutes on ice. The coverslips were removed after the agarose solidified and the slides were then immersed into the lysis buffer (pH 10) for 2hours at 4°C and protected from light.

Electrophoresis of Sample Slides

After the 2hr incubation, the slides were rinsed with distilled water and then placed side by side in a horizontal electrophoresis tank. The tank was then filled with freshly prepared electrophoresis buffer (pH 13) until the liquid level completely covered the slides and no bubbles formed over the agarose. The slides were allowed to sit in the buffer for 40minutes at room

temperature in order to allow the unwinding of the DNA. Electrophoresis was then carried out for 30min at 24volts and 300mA using the Regulated DC Power Supply (Model PAB) as the source of power and the process was performed under dim light in order to prevent any DNA damage that may arise as a result of fluorescent white light. After electrophoresis, the slides were gently lifted up and placed in the drain tray. The slides were then rinsed three times carefully with Neutralization buffer (0.4M Tris-Cl (pH 7.5) at 4^{o}C each time for 5min. The slides were then stained with ethidium bromide (2μg/ml) and left for 5min. The stained slides were then dipped in chilled distilled water and covered with coverslips. The slides are then scored using computer assisted image analysis. The slides are preserved by dipping them in 96% ethanol and they were air-dried and stored in a dry environment.

Scoring Slides and Evaluation of DNA damage

For the quantitative and qualitative evaluation of single cell gel electrophoresis , the slides were rehydrated by staining with ethidium bromide (2μg/ml) and then examined under a computer assisted ID image analysis software (Version 3.0) linked to a Kodak digital camera and the images were scored using the comet assay IV software from Perspective Instruments, UK. The extent of DNA damage in the cells was scored by measuring the head and tail length, head and tail intensity, tail migration and tail moments. Generally, 20 to 50 cells were randomly analysed per sample.

2.2.20. Statistical analysis

Statistical analysis of results was performed with one-way analysis of variance (ANOVA) unless otherwise stated. Comparison between groups was performed with Dunnett's test. Statistical analysis was done using the excel and prism software

CHAPTER 3

The Effects of Cadmium on Three Model Human Cell Lines

Chapter 3

3.0. The Effects of Cadmium on Three Model Human Cell Lines

3.1. Introduction

Acute exposure to cadmium has been reported to target mainly the kidney, liver and intestine (Friberg *et al.*, 1986). Chronic exposure has been shown to be carcinogenic to various tissues and organs in the body including liver, kidney, lung, prostate and the hematopoietic system (Waalkes, 2000) leading to its classification as a category I human carcinogen (IARC, 1993). There is currently no effective treatment for Cd toxicity.

At the molecular level, cadmium has a variety of adverse effects on cells and tissues, including damage to DNA, protein and membranes, but no single mechanism has been established to account for these. One of the proposed mechanisms of toxicity is via increased levels of damaging reactive oxygen species (ROS) (Liu *et al.*, 2009). Increased levels of superoxide anion, nitric oxide, hydrogen peroxide and hydroxyl radicals have been observed in the liver of animals exposed to cadmium (Galan *et al.*, 2001), and treatment of cultured cells with cadmium enhances the production of ROS (Hart *et al.*, 1999). ROS production by Cd is not direct, however. One mechanism proposed is that Cd displaces iron and copper from cellular binding sites, an action which then leads to increased ROS production via the Fenton reaction (Robertson and Orrenius, 2000). In another mechanism, Cd-induced lysosomal damage has been proposed as responsible for increased ROS generation (Fotakis *et al.*, 2005). In this model, myeloperoxidases released from the lysosome catalyse the production of hypochlorous acid from hydrogen peroxide and chloride ions. The resulting hypochlorous acid is

converted to superoxide anion. ROS can damage protein, DNA and lipids, and in cell lines can affect mitochondrial function and initiate apoptosis and necrosis (Galan, et al., 2001; Oh and Lim, 2006).

Mammalian cells contain several antioxidant molecules and enzymes that can protect against ROS and chemical insult. Of the non-enzymatic defences, glutathione (GSH) can provide significant protection against ROS. However, Cd is known to bind with high affinity to thiol (SH) groups including GSH, leading to depletion in GSH levels. A deficiency in GSH may account for some of the observed increase in ROS in Cd-treated cells (Liu, et al., 2009). It is known that GSH depletion can lead to increased Cd sensitivity (Nzengue *et al.*, 2008), and that artificial elevation of intracellular GSH levels can protect against Cd toxicity (Aiba *et al.*, 2008). However chronic exposure to Cd can lead to an elevation in intracellular GSH levels (Kamiyama *et al.*, 1995). This increase is thought to be part of an adaptive response that may help to protect cells against subsequent challenge with Cd (Liu, *et al*., 2009).

Cells also possess a range of antioxidant enzymes such as catalase, superoxide dismutase (SOD), glutathione peroxidase and glutathione reductase that can contribute to removing ROS or restoring GSH levels. In addition, many cells are equipped with enzymes that can detoxify reactive carbonyls that are produced as a consequence of oxidative stress, including aldehydic lipid peroxidation and glycoxidation products (Ellis, 2007). These protective enzymes include aldo-keto reductase (AKR) that catalyse the reduction of aldehydes to alcohols (Jin and Penning, 2007) and glutathione S-transferase (GST) that conjugate GSH to a range of molecules including aldehydes (Hayes *et al.*, 2005).

The aim of the work described in this chapter is to compare the toxicity of Cd in three different human cell lines, and to correlate these with levels of ROS following cadmium treatment in order to establish whether increased ROS production is always associated with Cd toxicity. In addition, the endogenous levels of key protective molecules and enzymes in each cell type are evaluated, as well as the effect of low and high doses of Cd on these activities and molecules. Defining this response provides a route for the identification of potential biomarkers of cadmium exposure in different cell types. In addition, an understanding of how protection against Cd can be enhanced may lead to approaches for therapeutic intervention, with the aim of preventing long-term damage.

3.2. Materials and Methods

3.2.1. Materials

Three human cell lines; Hepatoma (HepG2) cells(Aden *et al.*, 1979), 1321N1 human astrocytoma (Clark *et al.*, 1975) cells and HEK 293 human embryonic kidney cells(Graham *et al.*, 1977) were used in this work. The reasons for selecting these cell lines have been highlighted in section 2.1.2.

3.2.2. Methods

The general methods used are as described in Chapter 2

3.2.2.1. Inhibitors studies for cell viability

10mM Aminotriazole stock

8.4mg of aminotriazole (MW=84.08; Sigma) was dissolved in 10ml distilled water.

10mM Mercaptosuccinate stock

15mg of mercaptosuccinate (MW=150.15; Sigma) was dissolved in 10ml distilled water.

10mM N, N-bis(-2-chloroethyl)-N-nitrosourea (BCNU)

21.41mg of BCNU (MW=214.1; Sigma) was dissolved in 10ml ethanol.

Procedure

1321N1 and HEK 293 cells were used for inhibitor studies. The cells were seeded in 96 well plates at a density of 10^5 cells/ ml and allowed to attach for 24hr. The media were removed and 100µl of 1mM inhibitor was added to the well and allowed to incubate for 30min. After the incubation, the media were

removed and cell monolayer was washed with PBS. 100µl of 5, 10, 25 and 50µM $CdCl_2$ was added and incubated for 24hr. MTT assay was then carried out as previously described in section 2.2.5.

3.3. Results

3.3.1 Effects of Cadmium chloride on cell viability

Three cell lines were selected to represent models of target tissues for cadmium toxicity: the hepatoma cell lines HepG2; the astrocytoma cell line 1321N1; and human embryonic kidney cells HEK 293. Cells were treated with varying concentrations of cadmium chloride for 2, 4 and 24 hours and the effect on cell survival was measured with the MTT assay, which measures metabolic activity (viability). The results show decreased cell viability in all the three cell lines and these decreases were dose and time dependent (Fig 3.1). The effect of $CdCl_2$ was more pronounced at 24hr compared to 2 and 4hr exposure. Though all the cell lines show decreased cell viability at the different times of exposure, significant decreases were observed at 24hr at all the doses of exposure in all the cell lines. The results reveal a 10.7, 7.58 and 3.0-fold decrease in HepG2 (Fig.3.1A), 1321N1 (Fig.3.1B) and HEK 293 (Fig.3.1C) cell viability respectively following treatment with 50μM $CdCl_2$. IC_{50} values were obtained with the MTT assay after 24hr exposure to $CdCl_2$ (0-50μM) using the prism software nonlinear regression. HepG2 cells, with an IC_{50} of 13.96μM are the most sensitive to the toxic effect of cadmium when compared with 1321N1 (IC_{50}=19.92μM) and HEK 239 (IC_{50}=221.8μM), and this differential sensitivity is particularly apparent at lower concentrations (Fig.3.2).

3.3.2. Effects of $CdCl_2$ on cell membrane integrity

Disruptions of cell membrane integrity was used to assess the cytotoxicity of $CdCl_2$ in HepG2, 1321N1 and HEK 293 cells exposed to 5, 10 and 50μM $CdCl_2$ for 2, 4 and 24hr. The assessment was carried out by using the LDH leakage assay. The LDH leakages in HepG2 show dose and time dependent effect

(Fig3.3A). Significant increases of 2.5, 2.21 and 2.17-fold in LDH leakages were observed after 24hrs in HepG2 cells exposed to 5, 10 and 50μM $CdCl_2$ respectively (Fig3.3A). Significant increases in LDH leakages were also observed at 2 and 24hr exposure to 5, 10 and 50μM $CdCl_2$ and at 4hr exposure to 50μM $CdCl_2$ in 1321N1 cells (Fig3.3B). The highest (4-fold) increase in LDH leakage in 1321N1 cells was observed at 24hr exposure to 50μM (Fig3.3B). In HEK 293 cells, significant increases in LDH leakages were also observed at 24hr exposure to $CdCl_2$ at all the concentrations used (Fig.3.3C). No significant differences were observed at 2 and 4hr exposure (Fig.3.3C). The highest (10.7-fold) increase in LDH leakage in HEK 293 cells was observed at 24hrs exposure to 50μM $CdCl_2$ (Fig.3.3C). Comparison analysis shows that treatment with $CdCl_2$ leads to a dose-dependent increase in LDH leakage in 1321N1 and HEK 293 cell lines at 24hr exposure. HepG2 appeared more sensitive at lower concentrations (5 and 10μM) of exposure at 24hr, but HEK 293 cells released more LDH at higher concentrations (Fig 3.4). The LDH leakage assay seems to be a very sensitive cytotoxic test for $CdCl_2$ as significant increases were observed in all the cell lines at all the concentrations used after 24hr exposure. It is therefore apparent that 5 uM $CdCl_2$ can induce the release of LDH in all the cell lines via membrane damage but the concentration seems not to have appreciable effects on the MTT assay in 1321N1 and HEK 293 cell lines at 24hr exposure.

Figure3.1. Dose and time-dependent effects of $CdCl_2$ on cell viability

A.

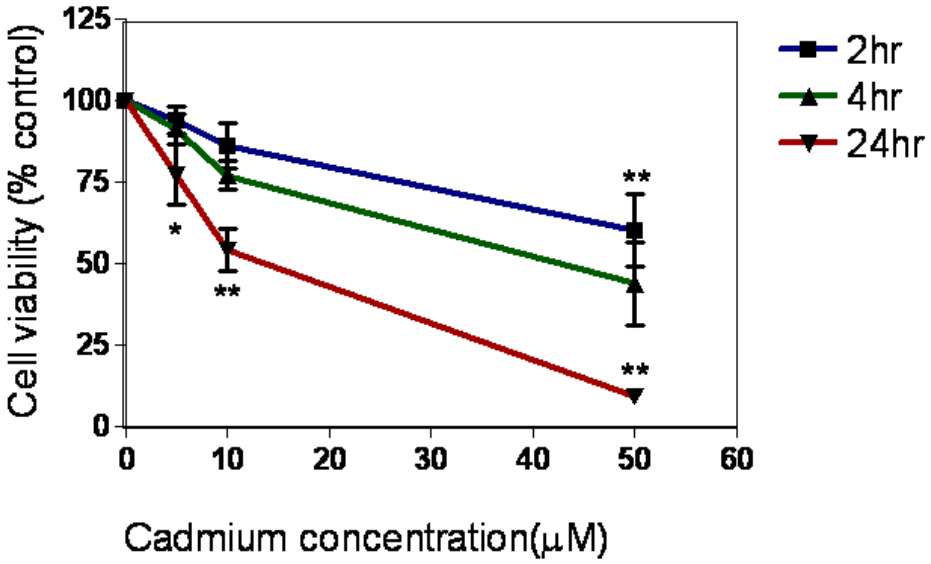

B.

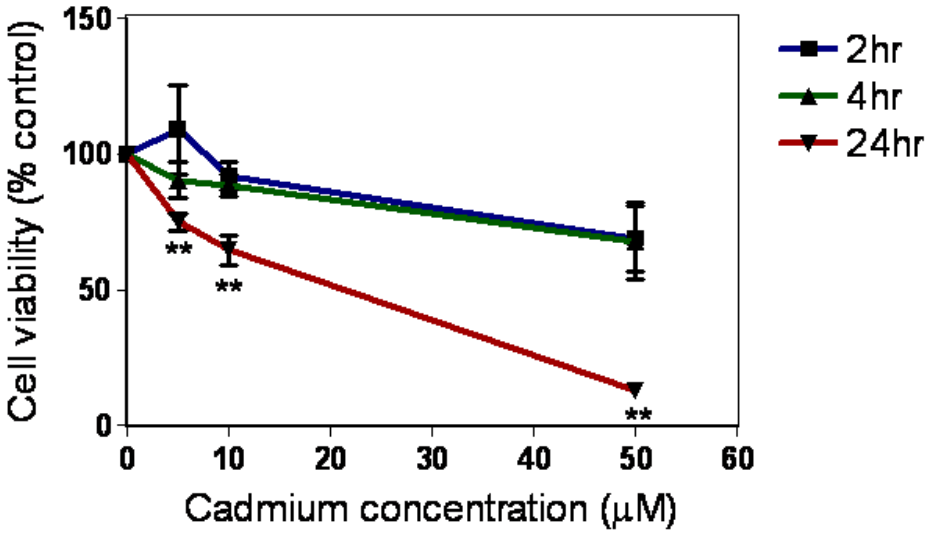

C.

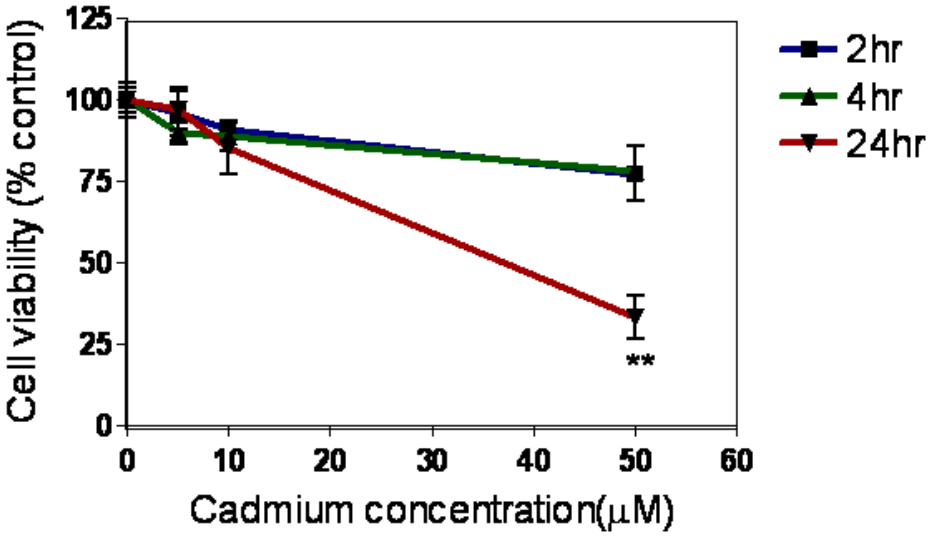

(A) HepG2, (B) 1321N1 and (C) HEK 293 cells were exposed to 5, 10 and 50μM $CdCl_2$ for 2, 4 and 24hr and cell viability was assessed with the MTT assay as described in Materials and Methods. Data represent the mean value (n=6 individual experiments done in triplicate) of percentage control ±SD. Asterisks indicate significant compared with untreated control (***$p<0.005$ **$p<0.01$ *$p<0.05$) using one-way ANOVA with Dunnett's post test.

Figure3.2. Comparison of the effects of $CdCl_2$ on HepG2, 1321N1 and HEK 293 cell viability after 24hr exposure

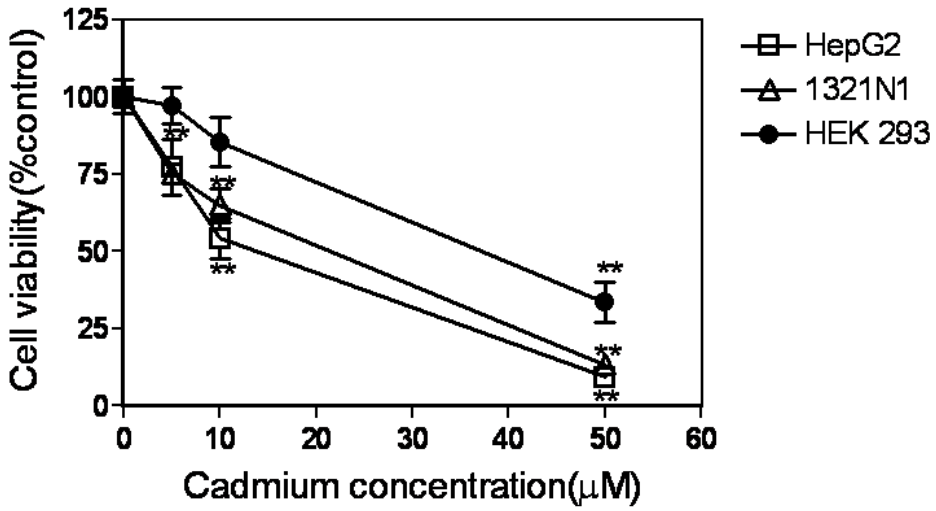

HepG2, 1321N1 and HEK 293 cells were exposed to 5, 10 and 50μM $CdCl_2$ for 24hr and cell viability was assessed with the MTT assay as described in Materials and Methods. Data represent the mean value (n=6 individual experiments done in triplicate) of percentage control ±SD. Asterisks indicate significant compared with untreated control (***$p<0.005$ **$p<0.01$ *$p<0.05$) using one-way ANOVA with Dunnett's post test.

Figure3.3. Dose and time-dependent effects of $CdCl_2$ on LDH leakage

A.

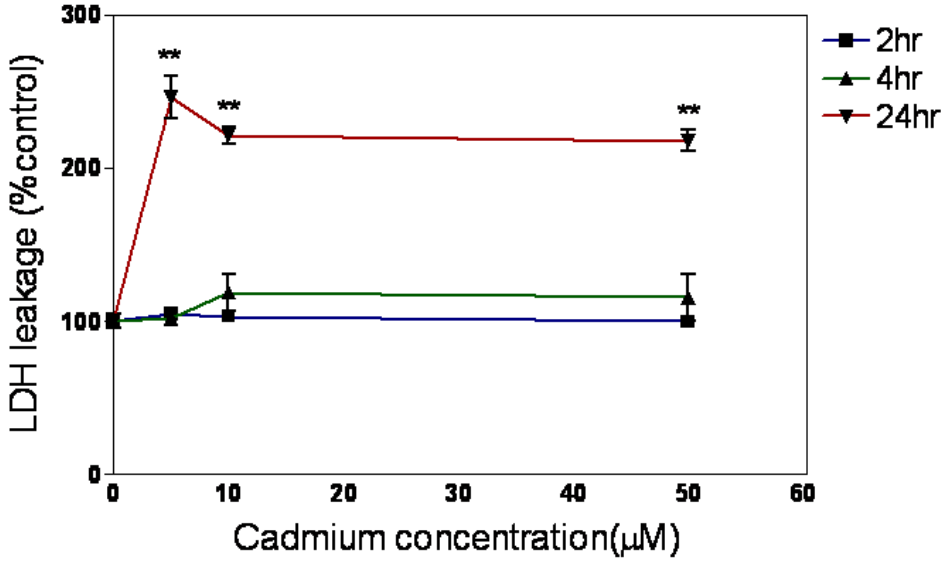

B.

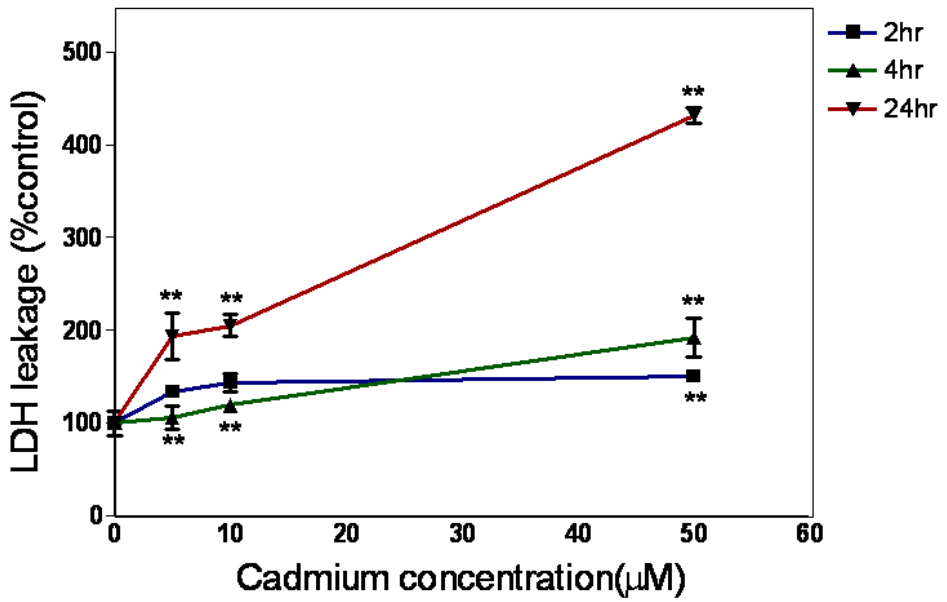

C.

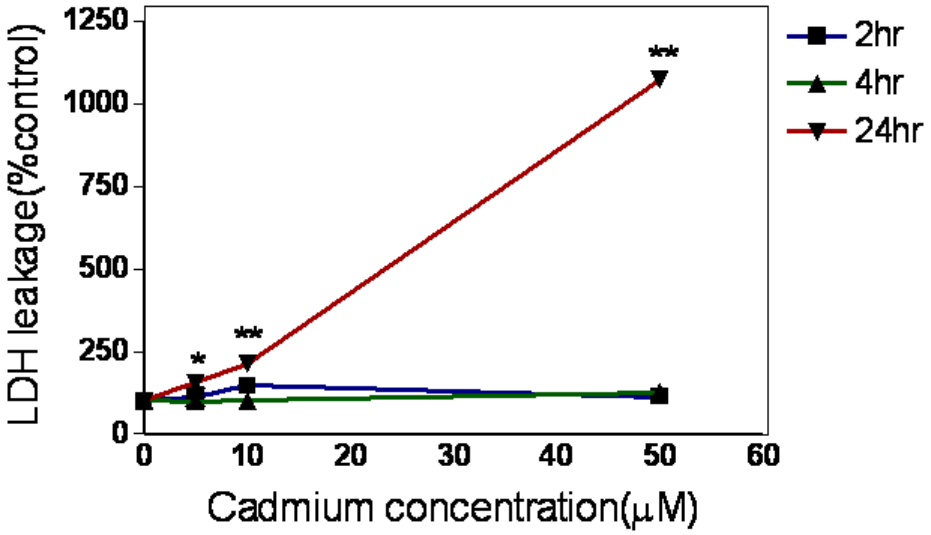

(A) HepG2, (B) 1321N1 and (C) HEK 293 cells were exposed to 5, 10 and 50μM $CdCl_2$ for 2, 4 and 24hr and cytotoxicity was assessed with the LDH leakage assay as described in Materials and Methods. Data represent the mean value (n=6 individual experiments done in triplicate) of percentage control±SD. Asterisks indicate significant compared with untreated control (***p<0.005 **p<0.01 *p<0.05) using one-way ANOVA with Dunnett's post test.

Figure 3.4 Comparison of the effects of $CdCl_2$ on HepG2, 1321N1 and HEK 293 cells LDH leakage after 24 hr exposure

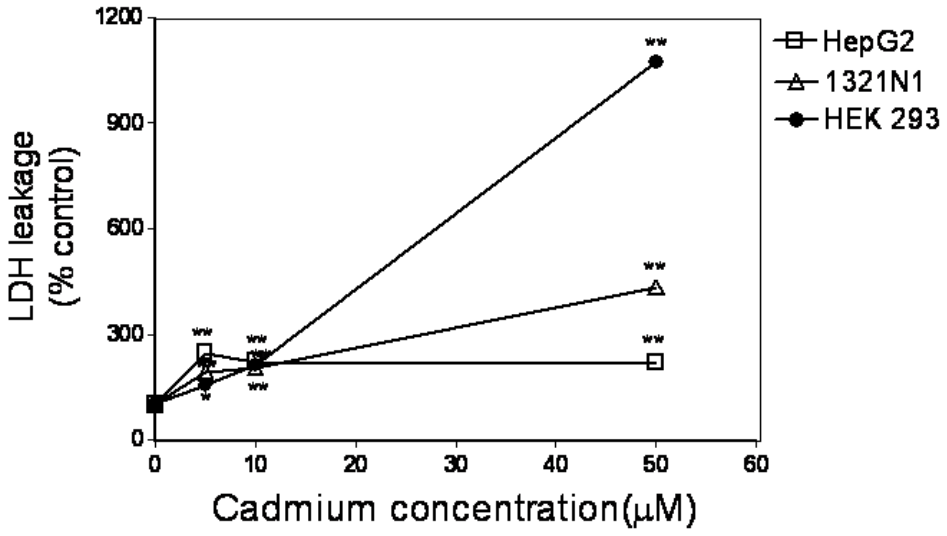

HepG2, 1321N1 and HEK 293 cells were exposed to 5, 10 and 50μM $CdCl_2$ for 24hr. Cytotoxicity was assessed with the LDH leakage assay as described in Materials and Methods. Data represent the mean value (n=6 individual experiments done in triplicate) of percentage control ±SD. Asterisks indicate significant compared with untreated control (***$p<0.005$ **$p<0.01$ *$p<0.05$) using one-way ANOVA with Dunnett's post test.

3.3.3. Effects of cadmium chloride on cellular redox status

To determine the effect of Cd exposure on redox status in the three cell lines under study, reduced GSH levels were measured after 2, 4 and 24 hours exposure (Fig 3.5). In HepG2 cells, there was no significant change in GSH levels following $CdCl_2$ treatment for 24hr. However, exposure to 5 and 10μM $CdCl_2$ for 4hr resulted in significant reduction in GSH levels in HepG2 (Fig.3.5A). The non significant change at 24hr exposure to 50μM $CdCl_2$ in this cell line may be as a result of the adaptive response of the HepG2 cells to the significant initial depletion observed at 2hr. Similarly, exposure of HEK 293 cells to 10 and 50μM $CdCl_2$ for 4hr resulted in significant decrease of 4.11 and 2.45-fold respectively (Fig.3.5C).There was a significant increase in GSH levels after 2hr exposure to 5 μM $CdCl_2$ and no significant change at 4hr in 1321N1 cells (Fig.3.5B). Also exposure of HEK293 cells and 1321N1 cells to 50μM $CdCl_2$ for 24hr resulted in a significant decrease in GSH levels in both cell lines (Fig 3.6). This suggests that GSH is being depleted, possibly leading to the observed decrease in viability in these cells at this concentration of Cd.

One of the consequences of GSH depletion is an increased susceptibility to oxidative stress, and this redox imbalance can lead to increased levels of reactive oxygen species (ROS). The effect of $CdCl_2$ treatment on levels of intracellular ROS in the three cell lines was measured using dihydrofluorescein diacetate (Hempel, et al., 1999). Treatment of HepG2 cells with 5, 10 and 50 μM $CdCl_2$ for 24 hours resulted in a significant increase of 1.7, 2.97 and 2.9-fold in ROS levels respectively (Fig 3.7A). There was no significant increase in ROS levels in HepG2 cells after 2 and 4hr treatment with 5, 10 and 50μM $CdCl_2$. This correlates with the no significant loss in HepG2 cell viability (Fig.3.1A) and LDH leakage (Fig.3.3A) observed at these

time of exposure Also there was no significant increase in ROS levels in 1321N1 cells (Fig.3.7B) and HEK293 cells (Fig.3.7C) following treatment with up to 50 μM $CdCl_2$ for 2, 4 and 24hr. These set of data indicate that although elevated ROS are associated with Cd-induced loss of viability in HepG2 cells at 24hr exposure, ROS levels do not appear to be associated with Cd-induced toxicity in 1321N1 and HEK 293 cells (Fig.3.8A), and there is no correlation between reduced GSH levels and ROS levels in any of the cell lines.

3.3.4. Effects of cadmium chloride on cellular lipid peroxidation

The effect of Cd-induced changes in redox status on the peroxidation of cellular lipids in the three cell lines was estimated by measuring changes in malondialdehyde (MDA) levels (Fig.3.8B). HepG2 cells showed a significant increase in MDA levels following exposure to 10 (2.3-fold) and 50 μM (3.6-fold) $CdCl_2$ for 24 hours, which correlates well with the increased ROS levels observed above (Fig.3.8A). Significant increases (4-fold) in MDA levels following exposure to 50 μM $CdCl_2$ were also observed in both 1321N1 cells and HEK 293 cells. These increases in MDA levels do not correlate with ROS levels but do correlate with the depletion of GSH levels (Fig.3.6). This indicates that GSH depletion may lead to the peroxidation of lipids but without any measurable change in ROS levels after 24 hours.

Figure3.5. Dose and time-dependent effects of $CdCl_2$ on GSH level

A.

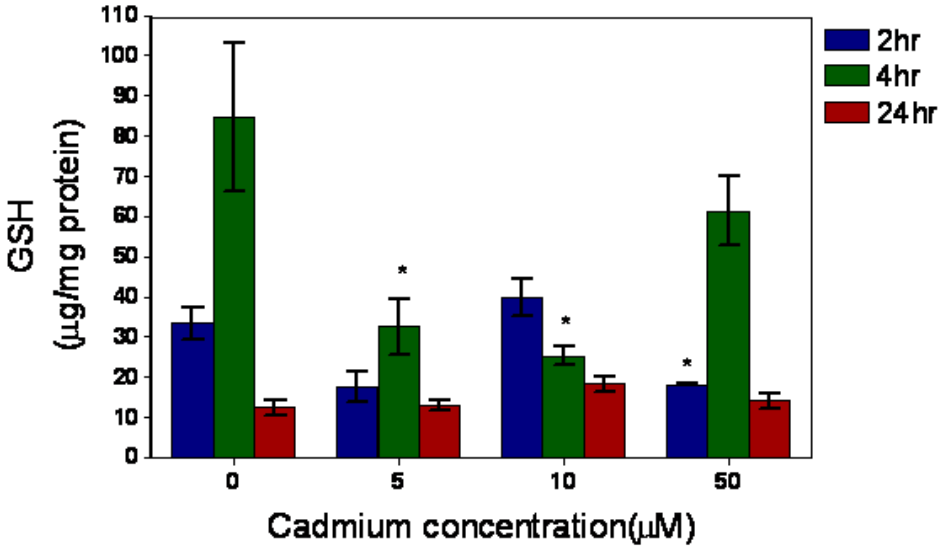

B.

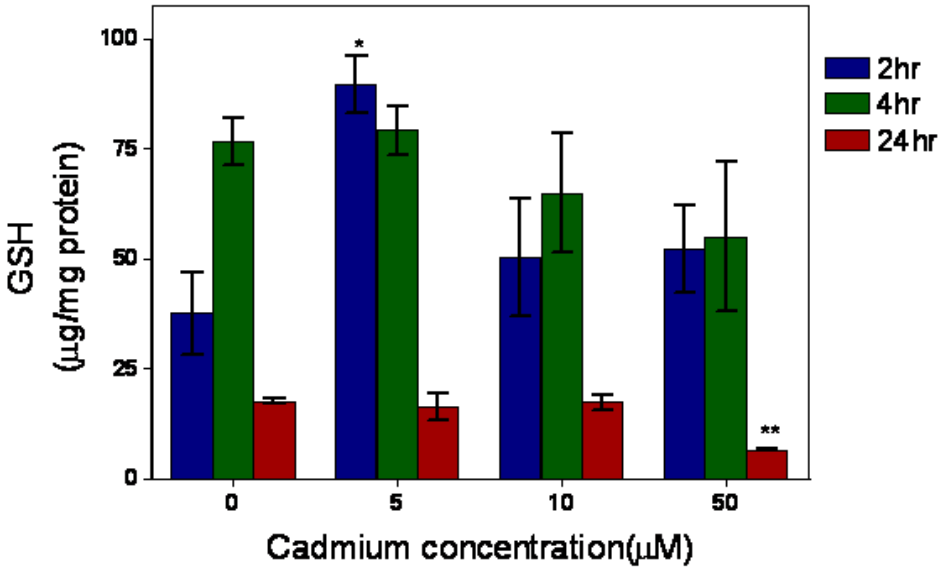

C.

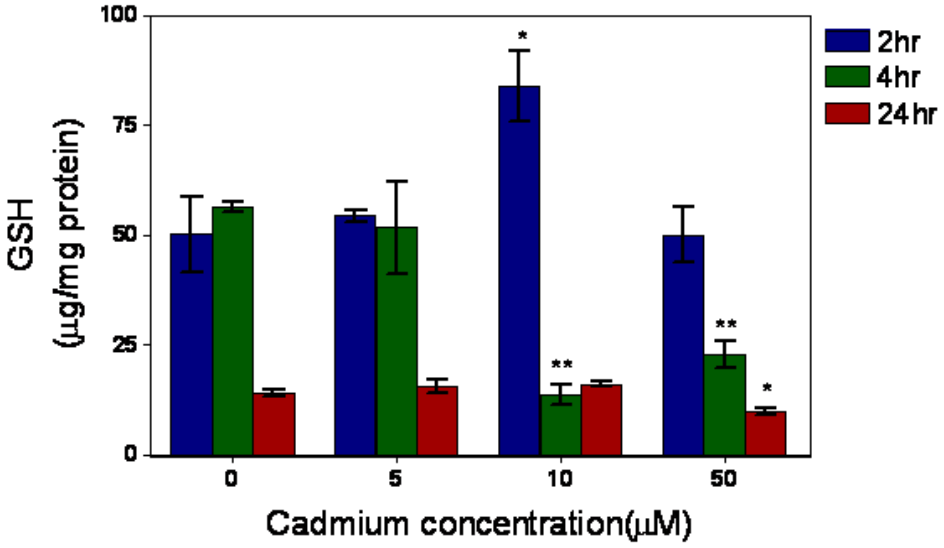

(A) HepG2, (B)1321N1 and (C) HEK 293 cells were treated with 5, 10 and 50µM $CdCl_2$ for 2, 4 and 24hr and GSH levels was determined with Ellman reagent (5, 5′-dithiobis(-2-nitrobenzoic acid) as described in Materials and Methods . Data represent the mean value (n=3 individual experiments done in triplicate) of percentage control±SD. Asterisks indicate significant compared with untreated control (***p<0.005 **p<0.01 *p<0.05) using one-way ANOVA with Dunnett's post test.

Figure3.6. Comparison of the effects of $CdCl_2$ on the GSH levels in HepG2, 1321N1 and HEK 293 cells after 24hr exposure

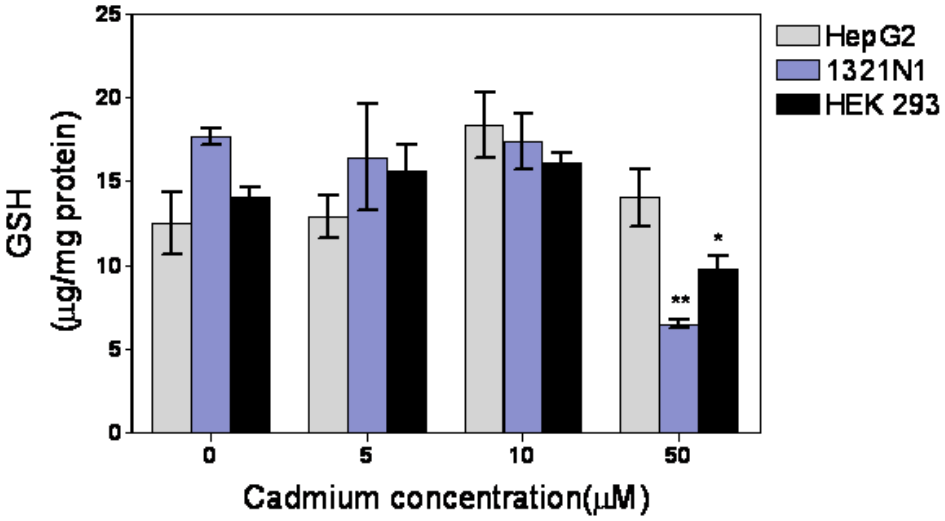

HepG2, 1321N1 and HEK 293 cells were treated with 5, 10 and 50µM $CdCl_2$ for 24hr and GSH levels was determined with Ellman reagent (5, 5'-dithiobis(-2-nitrobenzoic acid) as described in Materials and Methods. Data represent the mean value (n=3 individual experiments done in triplicate) of percentage control±SD. Asterisks indicate significant compared with untreated control (***$p<0.005$ **$p<0.01$ *$p<0.05$) using one-way ANOVA with Dunnett's post test.

Figure3.7. Dose and time-dependent effects of $CdCl_2$ on reactive oxygen species (ROS) production

A.

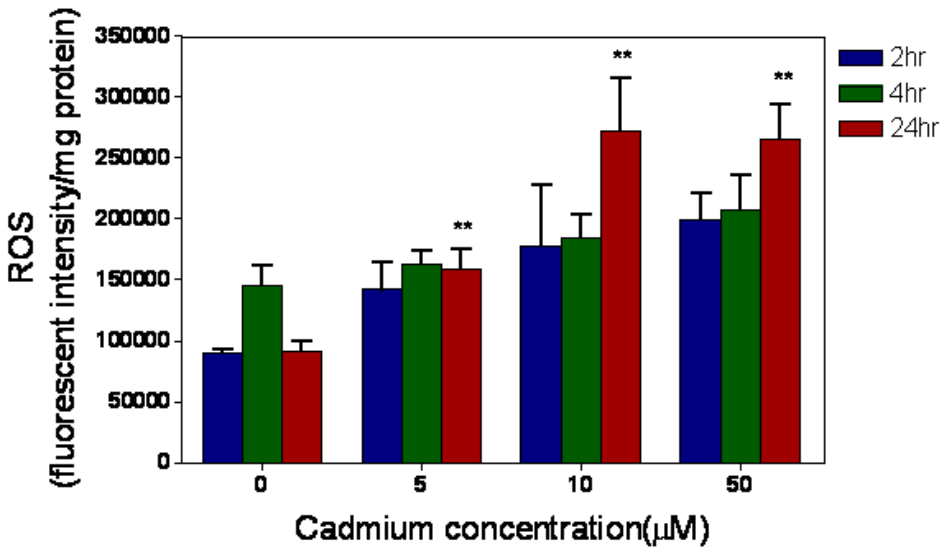

B.

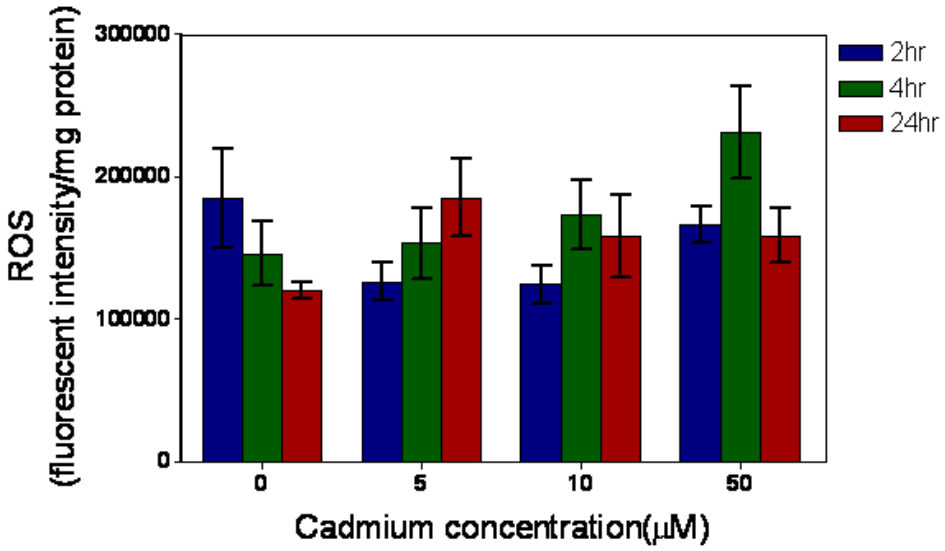

C.

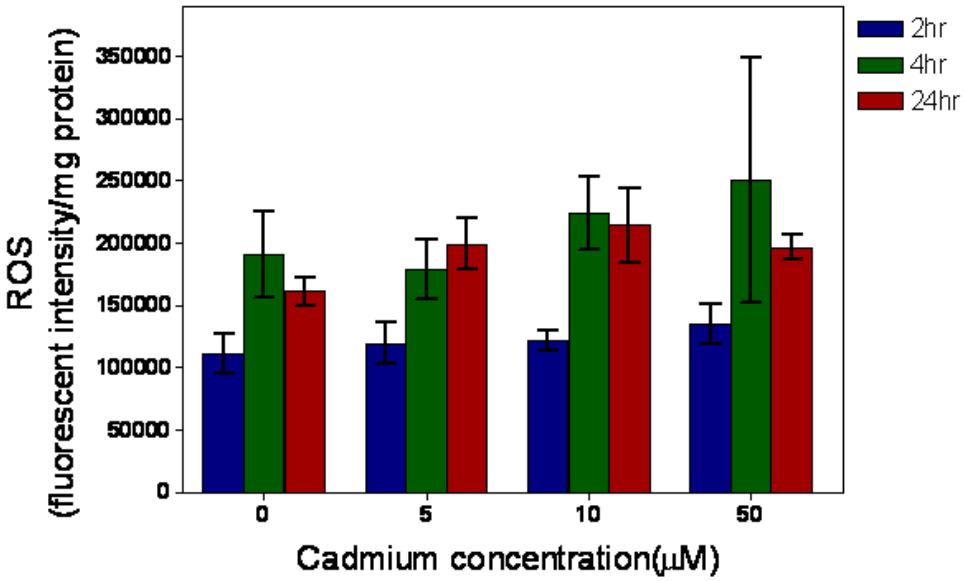

(A) HepG2, (B) 1321N1 and (C) HEK 293 cells were treated with 5, 10 and 50μM $CdCl_2$ for 2, 4 and 24hr and ROS production was determined with dihydrofluorescence diacetate as described in Materials and Methods. Data represent the mean value (n=6 individual experiments done in triplicate) of percentage control ±SD. Asterisks indicate significant compared with untreated control (***p<0.005 **p<0.01 *p<0.05) using one-way ANOVA with Dunnett's post test.

Fig.3.8 Comparison of the effects of $CdCl_2$ on ROS production and lipid peroxidation in HepG2, 1321N1 and HEK 293 cells after 24hr exposure

A.

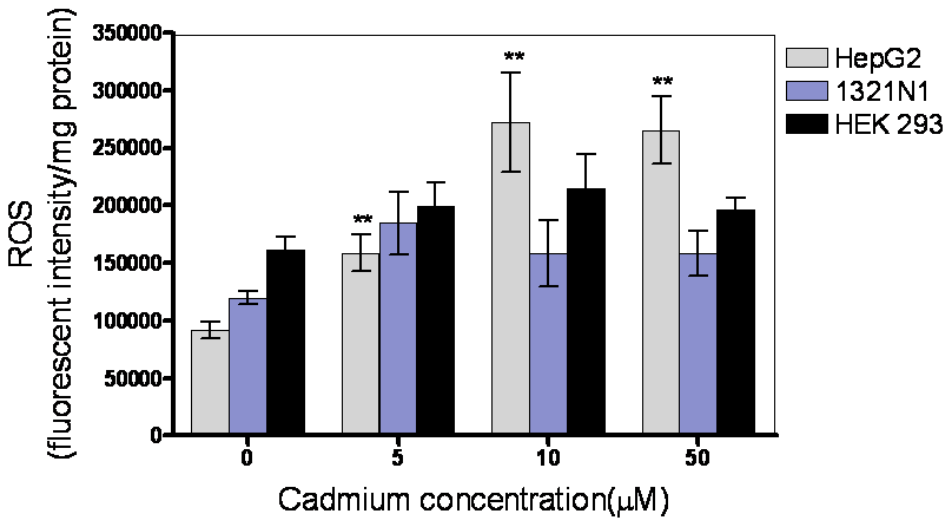

B.

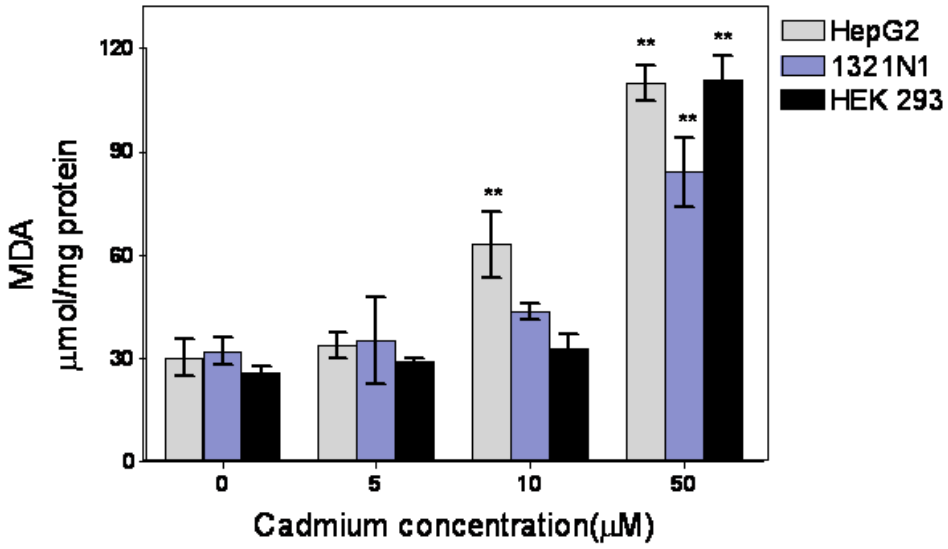

Cells were treated with 5, 10 and 50μM $CdCl_2$ for 24hr and (A) ROS production and (B) lipid peroxidation was determined with dihydrofluorescein diacetate and TBARS assay respectively as described in Materials and Methods. Data represent the mean value (n=6 individual experiment done in triplicate) of percentage control±SD. Asterisks indicate significant compared with untreated control (***p<0.005 **p<0.01 *p<0.05) using one-way ANOVA with Dunnett's post test.

3.3.5. Effects of Cadmium chloride on Catalase activities

To evaluate the constitutive and inducible protective mechanisms present within the three cell lines, the levels of key antioxidant enzymes in the three cell lines were determined and the effect of treatment with Cd was evaluated.

The basal level of catalase activity in untreated cells was highest in 1321N1 cells and lowest in HEK293 cells at 24hr (Fig.3.10). The results show 1.52 and 1.35-fold significant increases in catalase activities at 10 and 50μM $CdCl_2$ at 4hr exposure in HepG2 cells (Fig.3.9A). Decreased activities were observed at 2hr in HepG2 (Fig.3.9A). There was also a significant 3.54 and 17-fold increased in catalase activity in HepG2 cell following 24hr treatment with 10 and 50 μM $CdCl_2$ compared to untreated cells (Fig.3.9A). There was no significant increase in catalase activity in 1321N1 cells following 4 and 24hr $CdCl_2$ exposure (Fig.3.9B). However, 1.5 and 1.9-fold significant increases were observed at 2hr exposure to 10 and 50μM $CdCl_2$ in 1321N1 cells (Fig.3.9B). HEK293 cells showed a small but significant 2-fold increased in catalase activity following 24hr treatment with 50 μM $CdCl_2$ (Fig.3.9C). No significant change in catalase activity was observed after 2 and 4hr exposure in HEK 293 cells (Fig.3.9C). Of the three cell lines, only HepG2 cells appeared able to respond to the lower levels (10 μM) of Cd after 24hr (Fig.3.10) and only 1321N1 cells appeared able to respond to lower (10μM) and higher (50μM) levels of Cd after 2hr (Fig.3.9B). These set of data suggest that increased catalase activities in HepG2 cells was time and dose dependent.

Figure 3.9 Dose and time-dependent effects of $CdCl_2$ on catalase activities

A.

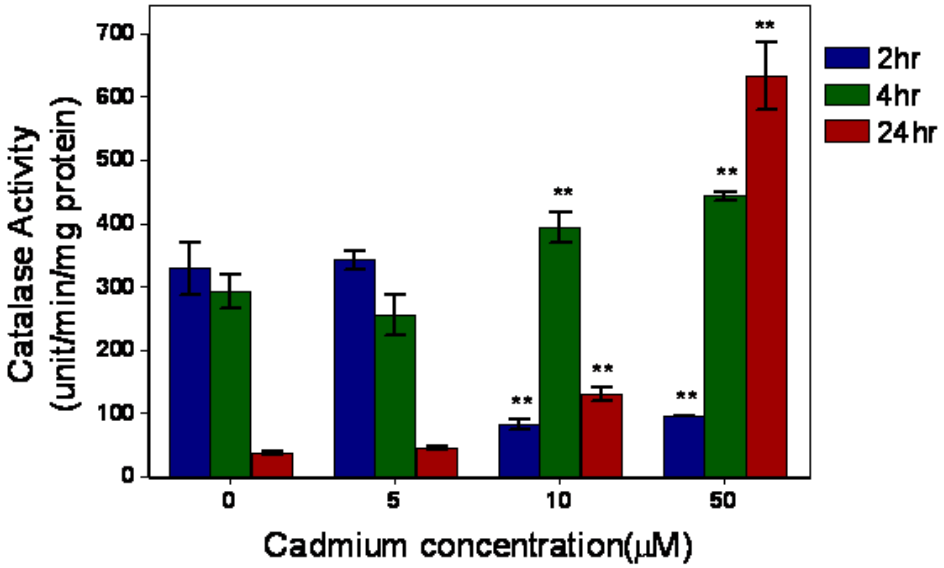

B.

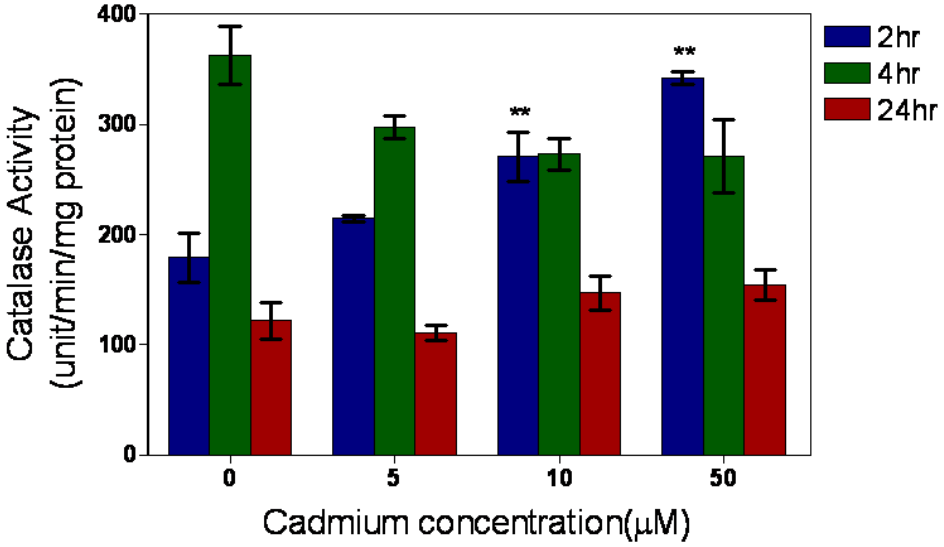

C.

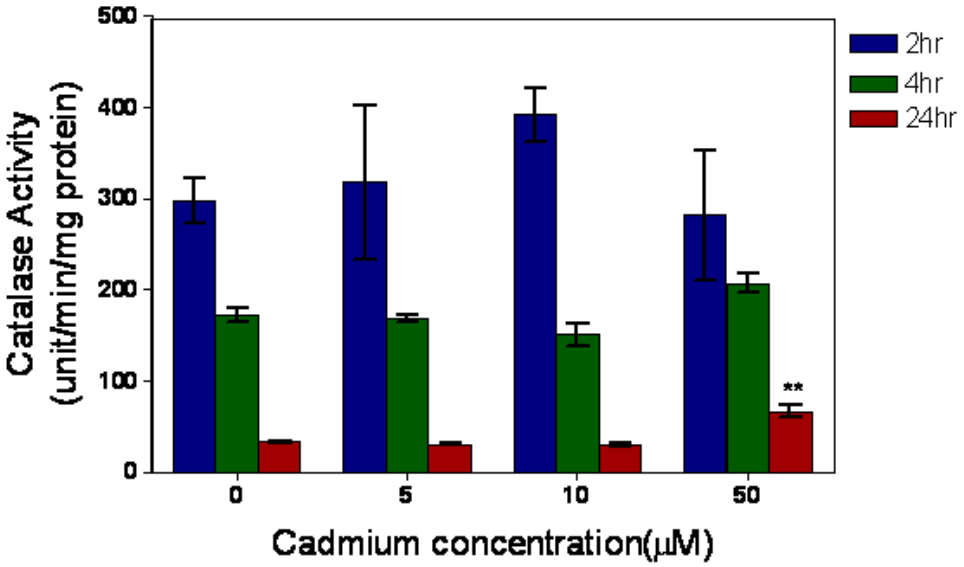

(A) HepG2, (B) 1321N1 and (C) HEK 293 cells were treated with 5, 10 and 50μM $CdCl_2$ for 2, 4 and 24hr and catalase activities was assayed in the whole cell extracts as described in Materials and Methods. Data represent the mean value (n=3 individual experiments done in triplicate) of percentage control±SD. Asterisks indicate significant compared with untreated control (***p<0.005 **p<0.01 *p<0.05) using one-way ANOVA with Dunnett's post test.

Figure 3.10 Comparison of the effects of $CdCl_2$ on catalase activities in HepG2, 1321N1 and HEK 293 cells after 24hr exposure

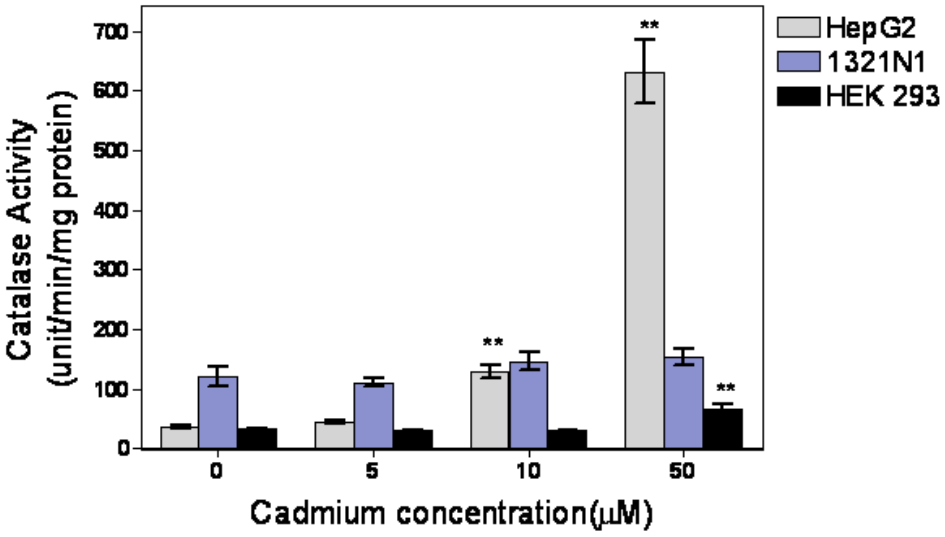

HepG2, 1321N1 and HEK 293 cells were exposed to 50μM $CdCl_2$ for 24hr and catalase activities was determined as described in Materials and Methods. Data represent the mean value (n=3 individual experiments done in triplicate) of percentage control±SD. Asterisks indicate significant compared with untreated control (***$p<0.005$ **$p<0.01$ *$p<0.05$) using one-way ANOVA with Dunnett's post test.

3.3.6. Effects of catalase inhibitor (aminotriazole) on cell viability in $CdCl_2$ exposed cells

In order to assess the role of catalase in enhancing cell viability in $CdCl_2$ exposed cells, cells were pretreated with 1 mM aminotriazole for 30 min before 24 hr exposure to 5, 10, 25 and 50μM $CdCl_2$. MTT assays were performed after this exposure. The results show no significant difference in the viability of 1321N1 cells between the aminotriazole pre-treated cells and cells exposed to $CdCl_2$ alone (Fig 3.11A). As expected there was a significant decrease in 1321N1 cell viability in 10 μM (1.2-fold), 25 μM (1.3-fold) and 50 μM (2.2-fold) $CdCl_2$ treated cells when compared to control in the absence of inhibitor. However, there was no significant difference in cell viability in aminotriazole pre-treated cells when compared with control except at 50 μM $CdCl_2$ exposed 1321N1 cells where a 2.1-fold difference was observed (Fig.3.11A). In HEK 293 cells, aminotriazole did not significantly alter viability when compared with cells exposed to $CdCl_2$ alone (Fig.3.11B). However, the presence of aminotriazole significantly decreased cell viability by 1.38- ad 1.37-fold at 25 and 50μM $CdCl_2$ respectively in HEK 293 cells (Fig.3.11B). These sets of data seem to suggest that catalase does not play a significant role in enhancing cell viability in $CdCl_2$ exposed 1321N1 and HEK 293 cells at low concentrations of Cd. However, there is no evidence in this work that the inhibitor actually cause the inhibition of the enzyme.

Figure3.11. Effects of catalase inhihibitor (Aminotriazole) on cell viability in $CdCl_2$ exposed cells

A.

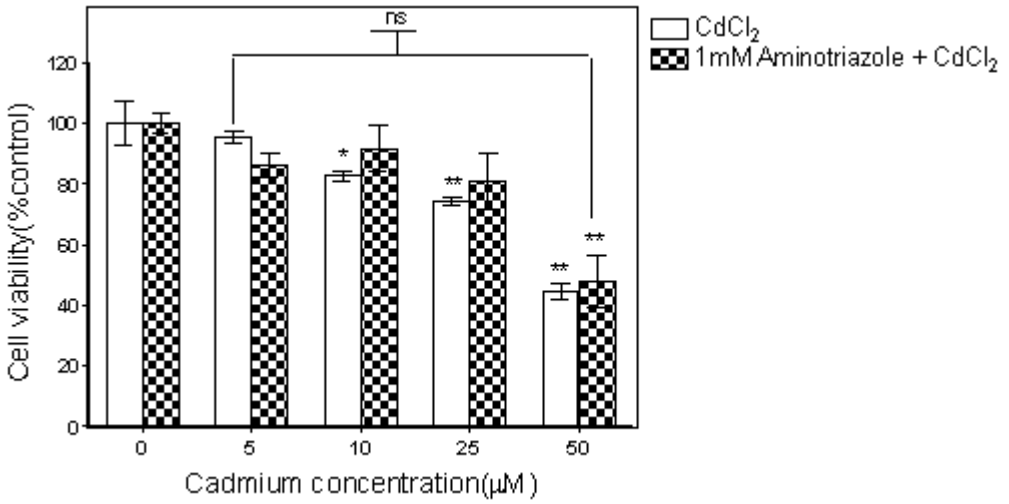

B.

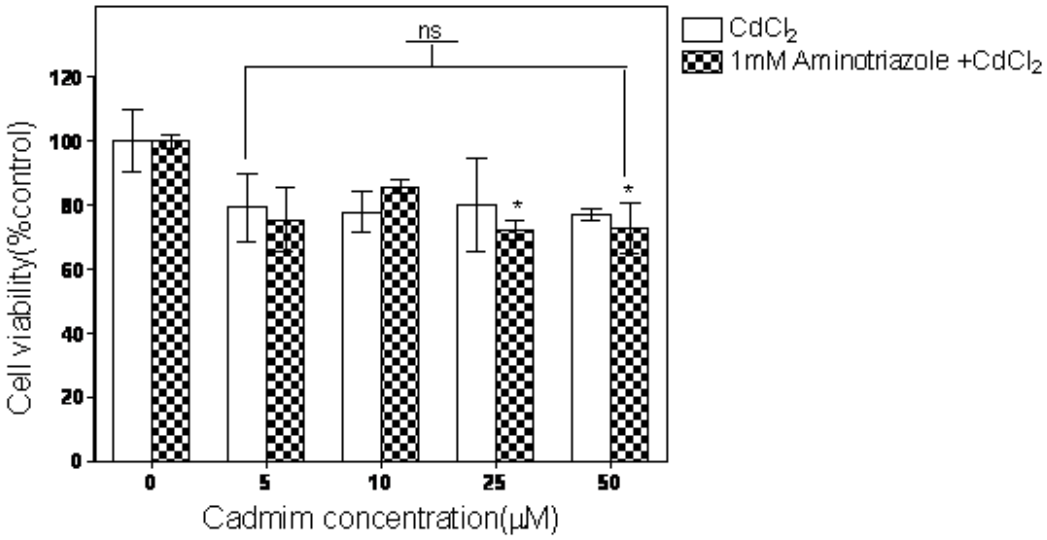

(A) 1321N1 and (B) HEK 293 cells were pre-treated with 1mM aminotriazole for 30min before exposure to 5, 10, 25 and 50µM $CdCl_2$ for 24hrs. Cells viability was determined by MTT assay as described in Materials and Methods. Data represent the mean value (n=3 individual experiments done in triplicate) of percentage control±SD. Asterisks indicate significant compared with untreated control (***$p<0.005$ **$p<0.01$ *$p<0.05$); ns (non significant) using one-way ANOVA with Dunnett's post test; Significant compared with Cd alone at the respective concentration (#$p<0.05$) using unpaired student's t-test.

3.3.7. Effects of Cadmium chloride on the Superoxide dismutase activities

Basal Superoxide dismutase (SOD) activity was highest in HepG2 cells and lowest in HEK 293 cells (Fig.3.12). Exposure of HepG2 cells to cadmium for 24hr resulted in a significant increase in SOD activity at 50 μM (2-fold) (Fig 3.12). There was also a 2-fold increase in SOD activity in HEK293 cells exposed to 50 μM Cd for 24hr but no significant change was observed in 1321N1 cells (Fig.3.12). This indicates that HepG2 and HEK293 cells appear to be responding to Cd exposure at higher concentrations, but that only HepG2 cells are responding to the lower concentrations (10 μM) of Cd tested.

Figure3.12. Comparison of the effects of $CdCl_2$ on superoxide dismutase activities in HepG2, 1321N1 and HEK 293 cells after 24hr exposure

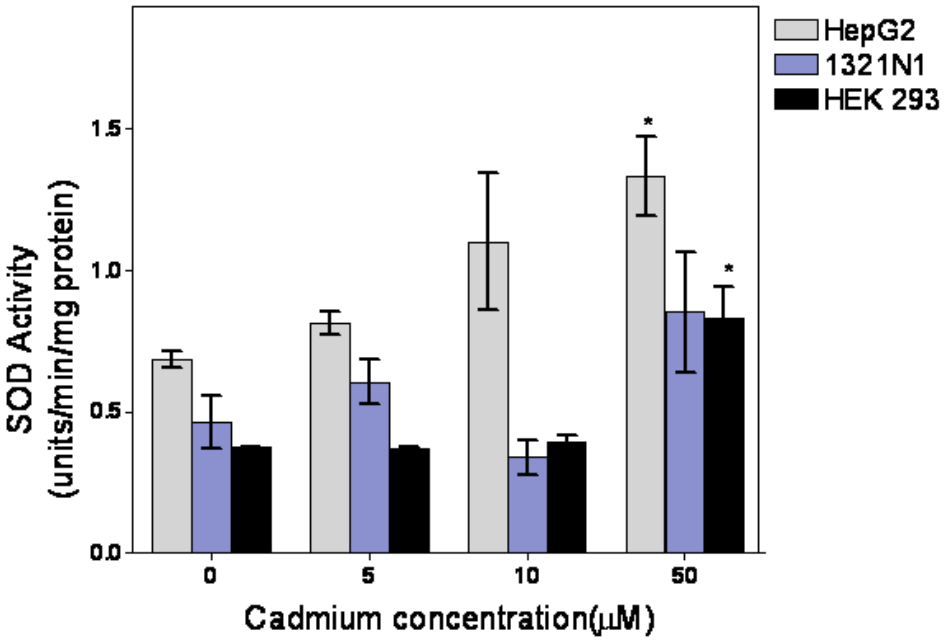

HepG2, 1321N1 and HEK 293 cells were exposed to 50μM $CdCl_2$ for 24hr and SOD activities was determined as described in Materials and Methods. Data represent the mean value (n=3 individual experiments done in triplicate) of percentage control±SD. Asterisks indicate significant compared with untreated control (***p<0.005 **p<0.01 *p<0.05) using one-way ANOVA with Dunnett's post test.

3.3.8. Effects of Cadmium chloride on the glutathione peroxidase activities

The basal glutathione peroxidase (GPx) activity was highest in HEK293 cells and lowest in 1321N1 cells (Fig.3.14). A significant increase in activities was observed in HepG2 (1.73-fold) and 1321N1 (1.57-fold) at 4hr exposure to 50 μM $CdCl_2$ (Fig.3.13A&B) but decreased activity was observed in HEK 293 cells at the same concentration and time of exposure (Fig.3.13C). Exposure to cadmium chloride caused a significant increase in activities in all three cell lines at 50μM after 24hr exposure (Fig.3.14). Increased activities were also observed at 10 μM in HepG2 and HEK 293 cell lines and at 5 μM in 1321N1 cells at 24hr exposure (Fig.3.14). However, induction was greatest in HEK293 cells (14-fold increase) following 24hr treatment with 50μM $CdCl_2$.

Figure3.13. Dose and time-dependent effects of $CdCl_2$ on glutathione peroxidase activities

A.

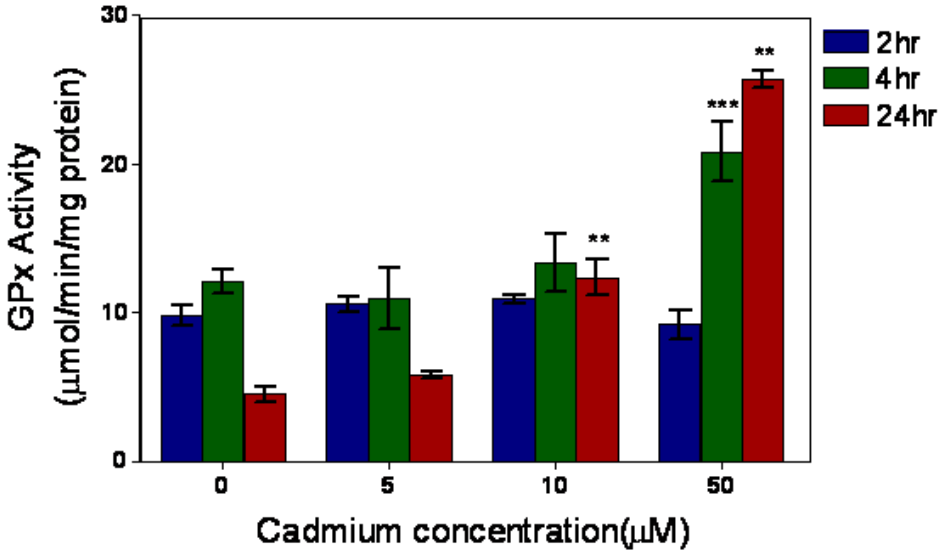

B.

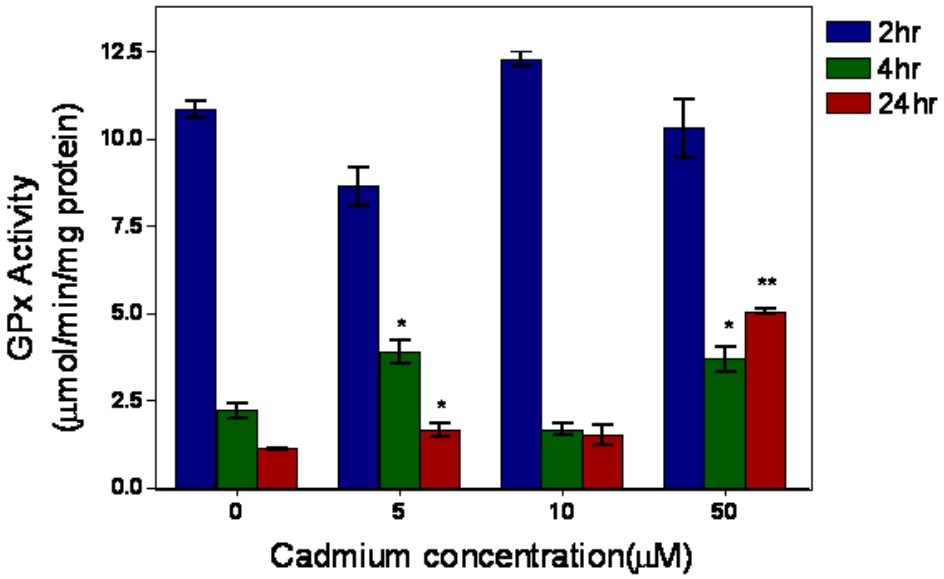

C.

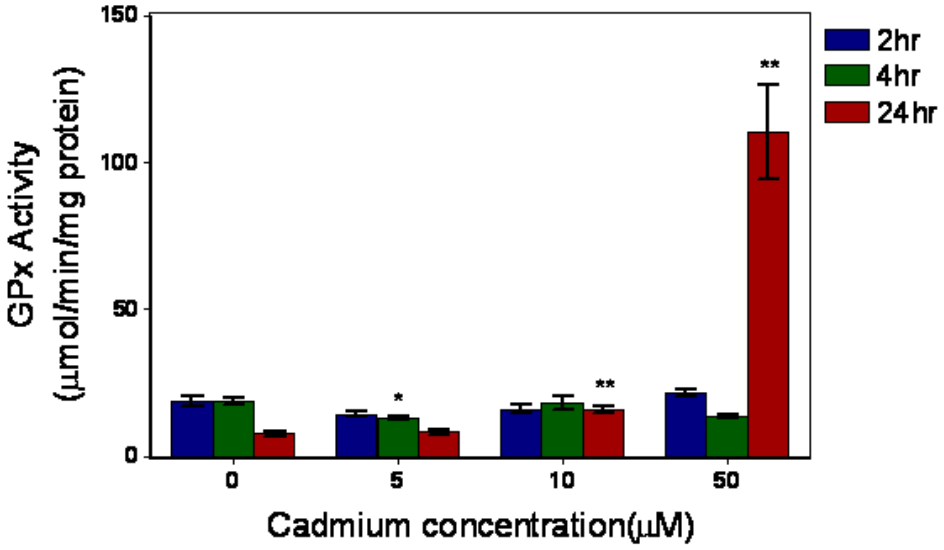

(A) HepG2, (B) 1321N1 and (C) HEK 293 cells were treated with 5, 10 and 50µM $CdCl_2$ for 2, 4 and 24hr and GPx activities was assayed in the whole cell extracts using H_2O_2 as substrate for HepG2 and t-Bu-OOH for 1321N1 and HEK 293 cells as described in Materials and Methods. Data represent the mean value (n=6 individual experiments done in triplicate) of percentage control±SD Asterisks indicate significant compared with untreated control (***$p<0.005$ **$p<0.01$ *$p<0.05$) using one-way ANOVA with Dunnett's post test.

Figure3.14. Comparative effects of $CdCl_2$ on GPx activities in HepG2, 1321N1 and HEK 293 cells

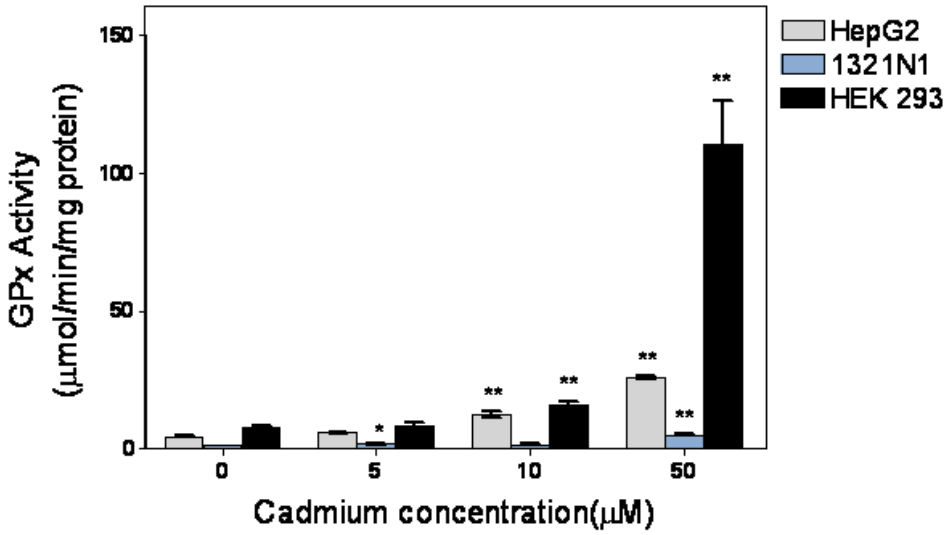

HepG2, 1321N1 and HEK 293 cells were exposed to 50µM $CdCl_2$ for 24hr and GPx activities were determined as described in Materials and Methods. Data represent the mean value (n=3 individual experiments done in triplicate) of percentage control±SD. Asterisks indicate significant compared with untreated control (***p<0.005 **p<0.01 *p<0.05) using one-way ANOVA with Dunnett's post test.

3.3.9. Effects of Glutathione peroxidase (GPx) inhibitor (Mercaptosuccinate) on cell viability in $CdCl_2$ exposed cells

To further assess the role of the GSH redox cycle in protection against $CdCl_2$ induced toxicity, the effect of GPx in Cd exposed cells were evaluated by pre-treating cells with 1 mM mercaptosuccinate for 30 min before 24 hr exposure to 5, 10, 25 and 50μM $CdCl_2$. The results show that the presence of mercaptosuccinate did not impair cell viability in 1321N1 cells when compared with cells exposed to $CdCl_2$ alone (Fig.3.15A). Similarly, the presence of the inhibitor did not impair cell survival at all the $CdCl_2$ concentrations of exposure in HEK 293 cells when compared with cells exposed to $CdCl_2$ alone (Fig3.15B). Taken together, these results seem to suggest that GPx does not play important role in protecting of 1321N1 and HEK 293 cells against Cd toxicity. However, there is no evidence in this present work that shows that the inhibitor actually inhibits GPx.

Figure3.15. Effects of GPx inhibitor (mercaptosuccinate) on cell viability in $CdCl_2$ exposed cells

A.

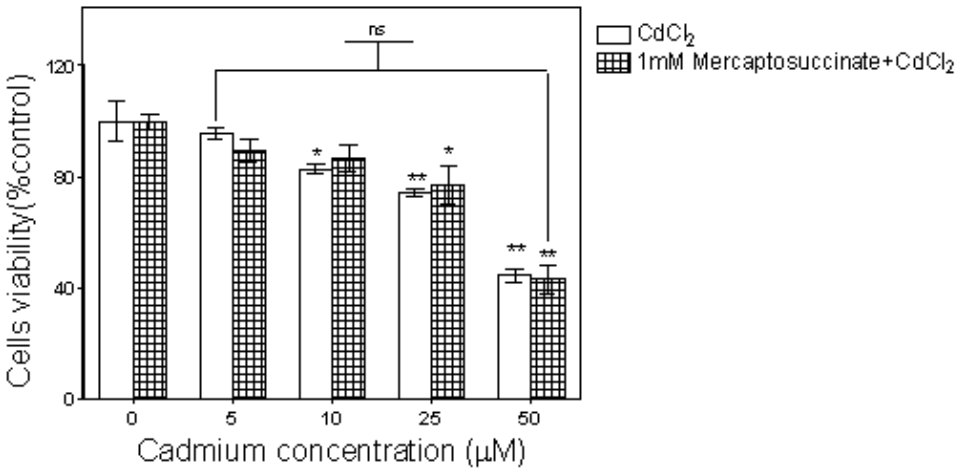

B.

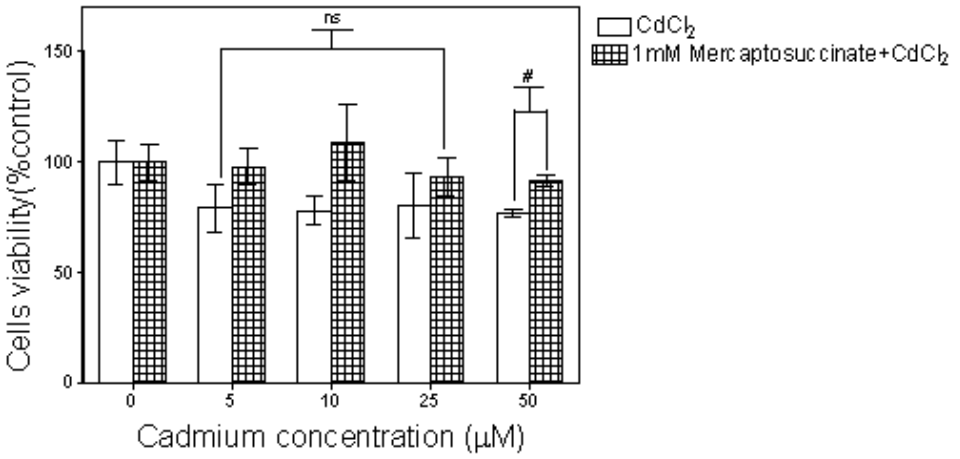

(A) 1321N1 and (B) HEK 293 cells were pre-treated with 1mM Mercaptosuccinate 30min before exposure to 5, 10, 25 and 50µM $CdCl_2$ for 24hr. Cells viability was determined by MTT assay as previously described in Materials and Methods. . Data represent the mean value (n=6 individual experiment done in triplicate) of percentage control±SD. Asterisks indicate significant compared with untreated control (***p<0.005 **p<0.01 *p<0.05); ns (non signifant) using one-way ANOVA with Dunnett's post test; Significant compared with Cd alone at the respective concentration (#p<0.05) using unpaired student's t-test.

3.3.10. Effects of Cadmium chloride on the glutathione reductase activities

Basal glutathione reductase (GRed) activity was highest in HepG2 cells (Fig.3.16). Treatment with 5, 10 and 50μM $CdCl_2$ for 24hr does not cause any significant change in glutathione reductase activity in HepG2 cells. In 1321N1 cells, there was a significant reduction in GR activity at 5μM (2.2-fold) and 10μM (2.4-fold) but activity significantly increased at 50μM (2-fold of control) after 24hr exposure (Fig.3.16). A significant increase in GR activity was also observed in HEK293 cells following treatment with 50μM $CdCl_2$ (1.8-fold) for 24hr. This correlates with the increases observed with catalase and SOD activities in HEK293 at this concentration.

Figure3.16. Comparative effects of $CdCl_2$ on glutathione reductase activities in HepG2, 1321N1 and HEK 293 cells

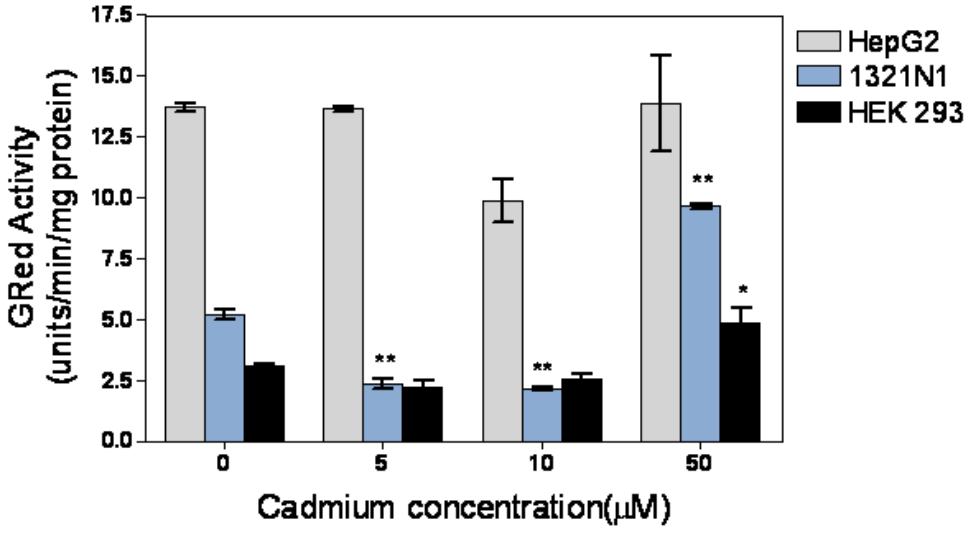

HepG2, 1321N1 and HEK 293 cells were exposed to 5, 10 and 50μM $CdCl_2$ for 24hr and GRed activities were determined as previously described in Materials and Methods. Data represent the mean value (n=6 individual experiments done in triplicate) of percentage control±SD. Asterisks indicate significant compared with untreated control (***p<0.005 **p<0.01 *p<0.05) using one-way ANOVA with Dunnett's post test.

3.3.11. Effects of Glutathione reductase (GRed) inhibitor (BCNU) on cell viability in $CdCl_2$ exposed cells

To define the involvement of GRed in the protection of cells against $CdCl_2$ induced toxicity, 1321N1 and HEK 293 cells were pre-treated with 1 mM N,N-bis(-2-chloroethyl)-N-nitrosourea (BCNU) for 30min before exposure to 5, 10, 25 and 50 μM $CdCl_2$ for 24hr. The results show that the presence of BCNU significantly reduced 1321N1 cell viability at 5μM (17.7-fold), 10μM (23.55-fold), 25μM (25.49-fold) and 50μM (16.29-fold) when compared to the presence of $CdCl_2$ alone (Fig.3.17A). The results also show that the presence of inhibitor does not affect HEK 293 cell viability at 5, 10 and 25μM $CdCl_2$ but significantly decreased (5.5-fold) cell viability at 50μM $CdCl_2$ when compared with HEK 293 cells exposed to $CdCl_2$ alone (Fig.3.17B). The results show that glutathione reductase may play an important role in protecting 1321N1 against Cd toxicity; it may also be involved in protecting HEK 293 cells at higher Cd concentrations (50μM). However, there is no evidence in this work that the inhibitor actually inhibits GRed.

Figure3.17. Effects of GRed inhihibitor (BCNU) on cell viability in $CdCl_2$ exposed cells

A.

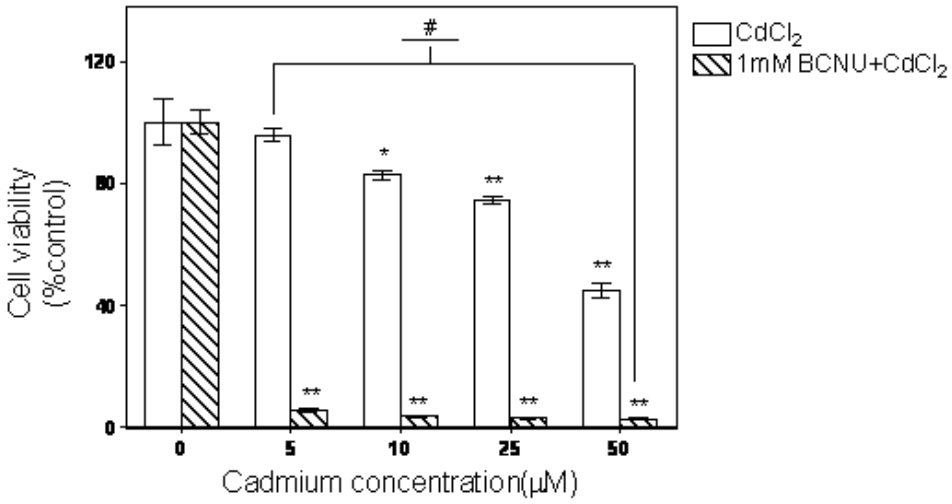

B.

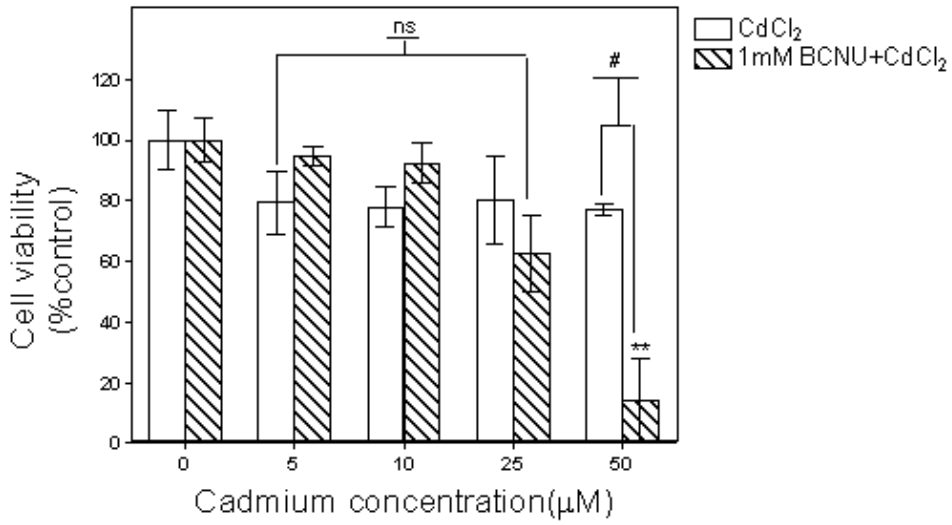

(A) 1321N1 and (B) HEK 293 cells were pre-treated with 1mM BCNU 30min before exposure to 5, 10, 25 and 50μM $CdCl_2$ for 24hr. Cell viability was determined by MTT assay as previously described in Materials and Methods. Data represent the mean value (n=3 individual experiments done in triplicate) of percentage control±SD. Asterisks indicate significant compared with untreated control (***$p<0.005$ **$p<0.01$ *$p<0.05$); ns (non significant) using one-way ANOVA with Dunnett's post test; Significant compared with Cd alone at the respective concentration (#$p<0.05$) using unpaired student's t-test.

3.3.12. Elevation of aldehyde-metabolizing enzymes

Aldehyde products of lipid peroxidation such as 4-hydroxynonenal and acrolein are among the most cytotoxic consequences of elevated ROS (Ellis, 2007). Aldehydes can be removed by conjugation to GST and reduction by AKR. The effect of Cd treatment on levels of GST activity was measured using CDNB as substrate in control and treated cells, and it is apparent that the basal level of GST is highest in HEK293 cells and lowest in 1321N1 (Fig.3.19). There were significant increases in GST after 4hr exposure to 5μM (1.3-fold), 10μM (3.28-fold) and 50μM $CdCl_2$ and after 2hr exposure to 10μM (1.28-fold) and 50μM (1.71-fold) in HEK 293 cells (Fig.3.18C). There was a significant increase in GST activity in HepG2 cells after 24hr exposure to 5, 10 and 50μM $CdCl_2$ concentrations, with a maximum increase of 4.3-fold using 50 μM $CdCl_2$ (Fig.3.18A). The results also show significant increase in GST activity at 10 and 50 μM Cd after 24hr exposure and at 50 μM Cd at 4hr in 1321N1 cells (Fig3.18B). The increase in 1321N1 cells (3.8-fold) and HEK 293 cells (2.9-fold) was also significant following 24hr exposure to 50μM $CdCl_2$, indicating that one or more GST enzymes is being induced. However, only HepG2 cells responded to the lower concentrations of Cd at 24hr.

Basal aldo-keto reductase activity was highest in 1321N1 cells and lowest in HEK293 cells (Fig.3.20). Treatment with $CdCl_2$ cause a significant increase in aldehyde reductase activity in all three cell lines at all the concentrations used in this work. The highest increase (4-fold) was in 1321N1 cells at 50 μM (Fig.3.20).

Figure3.18. Dose and time-dependent effects of $CdCl_2$ on glutathione S-transferase activities

A.

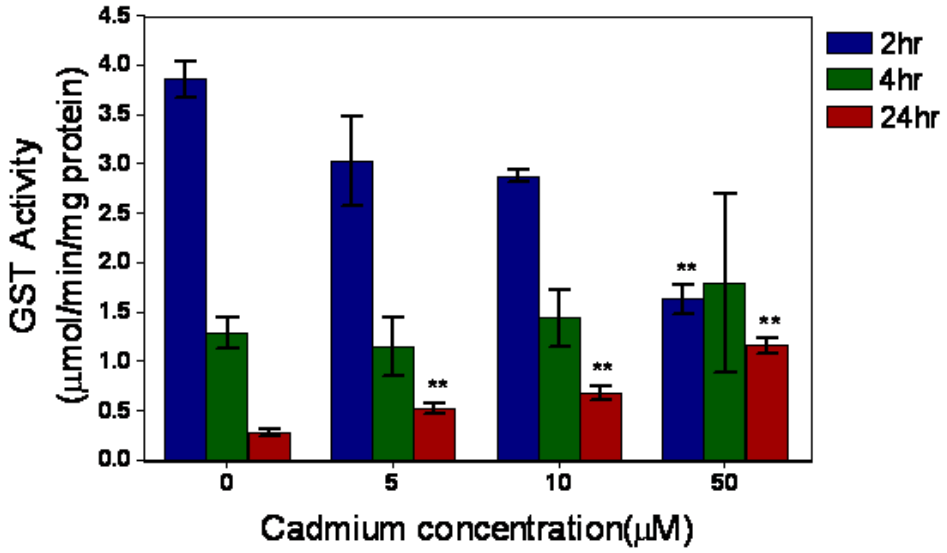

B.

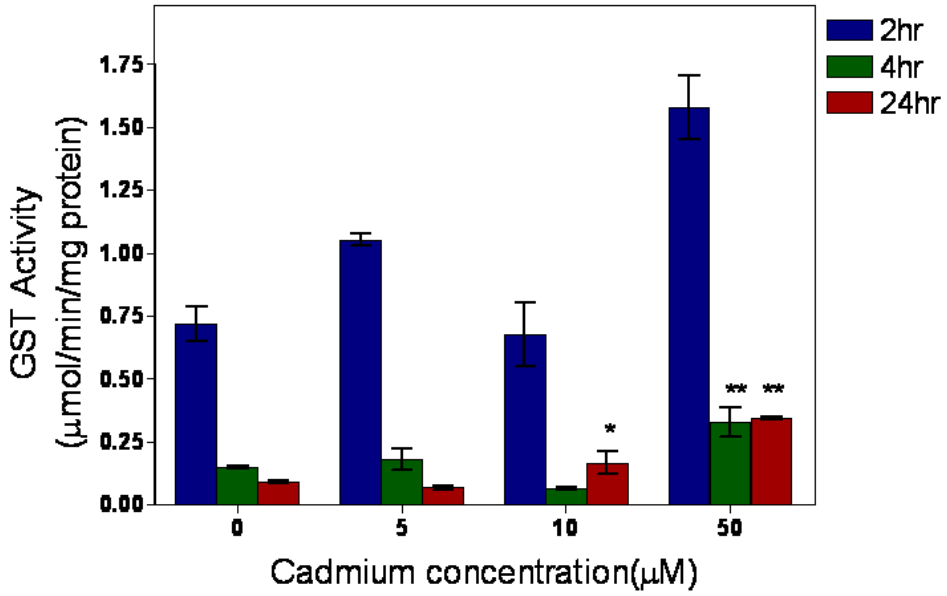

C.

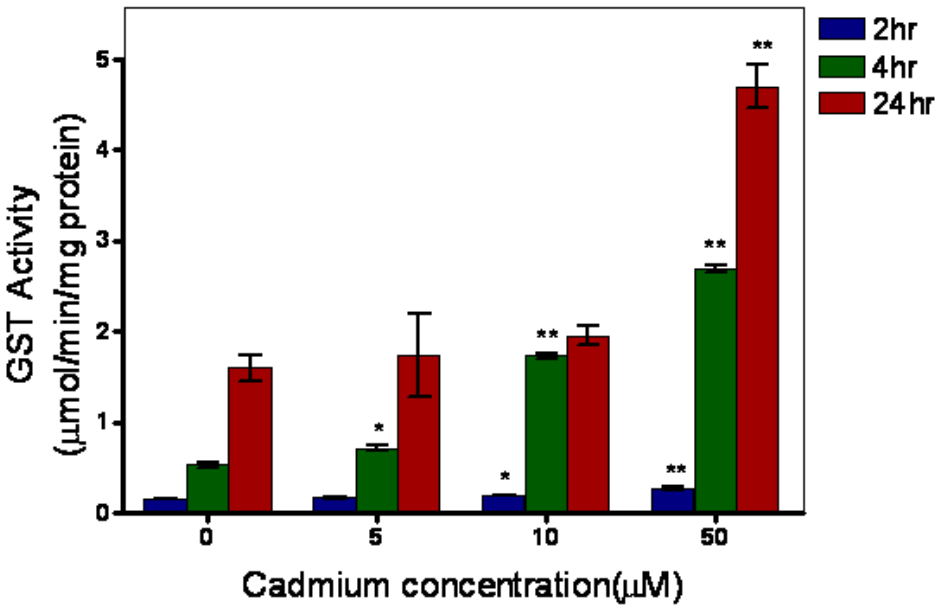

(A) HepG2, (B) 1321N1 and (C) HEK 293 cells were treated with 5, 10 and 50µM $CdCl_2$ for 2, 4 and 24hr and GST activities were determined in the whole cell extracts with CDNB as described in Materials and Methods. Data represent the mean value (n=6 individual experiments done in triplicate) of percentage control±SD. Asterisks indicate significant compared with untreated control (***p<0.005 **p<0.01 *p<0.05) using one-way ANOVA with Dunnett's post test.

Figure 3.19. Comparative effects of $CdCl_2$ on glutathione S-transferase activities in HepG2, 1321N1 and HEK 293 cells

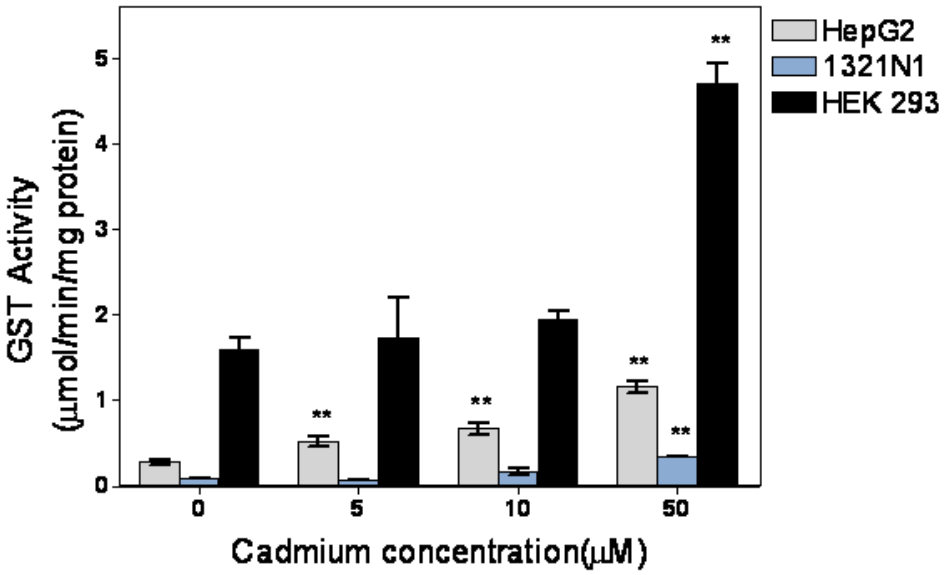

HepG2, 1321N1 and HEK 293 cells were exposed to 50µM $CdCl_2$ for 24hr and GST activities were determined with CDNB as described in Materials and Methods. Data represent the mean value (n=6 individual experiments done in triplicate) of percentage control±SD. Asterisks indicate significant compared with untreated control (***p<0.005 **p<0.01 *p<0.05) using one-way ANOVA with Dunnett's post test.

Figure 3.20. Comparative effect of $CdCl_2$ on aldo-keto reductase activities in HepG2, 1321N1 and HEK 293 cells

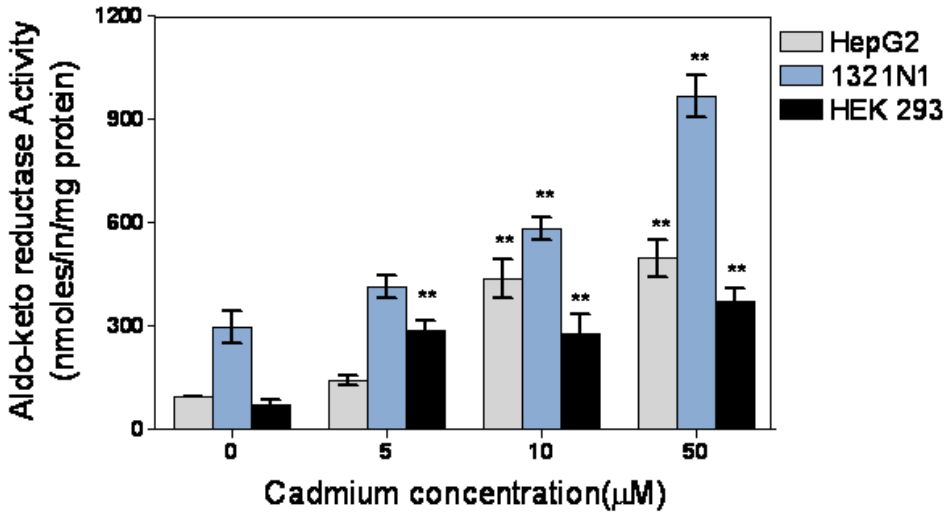

HepG2, 1321N1 and HEK 293 cells were exposed to 50μM $CdCl_2$ for 24hr and AKR activities were determined as described in Materials and Methods. Data represent the mean value (n=3 individual experiments done in triplicate) of percentage control±SD. Asterisks indicate significant compared with untreated control (***p<0.005 **p<0.01 *p<0.05) using one-way ANOVA with Dunnett's post test.

3.4. Discussion

In this study we have examined a cell-dependent differential sensitivity to Cd toxicity. Using the MTT viability assay, HepG2 hepatoma cells are the most sensitive compared to HEK293 kidney and 1321N1 astrocytoma cells and the effects of Cd on cell viability was time and dose dependent in all the cell lines (Fig.3.1). However the LDH leakage assay shows HEK293 cells to be more sensitive to cell membrane disruption at higher concentrations of cadmium (Fig.3.4). The effect of $CdCl_2$ on the viability of HepG2 cells has been investigated previously, where a similarly high sensitivity of HepG2 cells to $CdCl_2$ was observed (IC_{50} = 15 μM) (Fotakis and Timbrell, 2006). Our results are the first to show that 1321N1 cells are equally sensitive to Cd as HepG2 cells, and this supports previous work showing that primary astrocytes are sensitive to $CdCl_2$ (Yang *et al.*, 2008). This is important because it demonstrates that this type of brain cell is potentially at risk from Cd damage. Astrocytes provide metabolic support to neurons, and can also contribute towards the repair of damaged neurons. Given their sensitivity to Cd, the role of astrocytes may be compromised following Cd exposure, leading to deleterious consequences for brain function and development (Gabbiani *et al.*, 1967; Yang, et al., 2008). Other cells in brain, such as neuronal cells of the cortex and hypothalamus and neuron-glia cultures are also sensitive to Cd (Yang *et al.*, 2007b), but astrocytes are crucial to survival and repair of all these cell types. HEK 293 cells in comparison are more resilient than either HepG2 or 1321N1 cells at low concentrations of cadmium, but as shown previously, $CdCl_2$ decreases viability in a time and dose dependent manner, and causes significant cell damage at high concentrations (Mao *et al.*, 2007). Overall, these results indicate a differential

sensitivity, likely due to differences in the underlying protective mechanisms present in each cell type.

The present work shows a correlation between basal intracellular GSH levels and cell cycle progression in all the three cell lines. Markovich *et al* (2007) reported that GSH is localised mainly in the nucleus in the early phase of cell proliferation in 3T3 fibroblasts followed by redistribution in the cytoplasm as the cells reach confluence. In agreement with this earlier report, the present shows that the basal levels of intracellular GSH were lower at 2hr and 24hr when compared with 4hr (Fig.3.5). This may be due to the fact that most of the GSH was concentrated in the nucleus at 2hr following cell plating which is the early phase of cell growth when the cells are actively dividing. At 4hr, the GSH becomes redistributed into the cytoplasm as the cells move toward confluence and this may account for the higher intracellular GSH levels observed at this time when compared to 2hr. At 24hr when the cells no longer proliferate exponentially ie at confluence, GSH becomes uniformly distributed between the nucleus and the cytoplasm. To investigate the effect of Cd on the intracellular GSH levels, the present work shows that treatment with high levels of Cd leads to significant depletion of GSH in HEK293 and 1321N1 cells at 24hr, and that these cells are not able to increase GSH levels response to low levels of Cd (Fig3.5B&C). HepG2 cells on the other hand do not show a significant change in GSH levels at 24hr but significant decrease was obtained at 2hr and 4hr at 5μM (Fig.3.5A). This shows that the long time (24hr) exposure to Cd induced an adaptive response in the HepG2 cells leading to enhanced GSH production as earlier observed in rat liver exposed to Cd (Kamiyama *et al*., 1995). It is possible that Cd treatment is responsible for triggering an increase in GSH production in these cells, which can

compensate for any depleting effect of Cd or the effect of elevated ROS seen in these cells. In contrast, in the other two cell lines, ROS levels do not appear to increase at all periods of exposure following Cd treatment, even when GSH is depleted, suggesting that other constitutive cellular antioxidant defence mechanism in these latter two cell lines are able to counter any increase in Cd-dependent ROS production (Fig.3.7B&C). In this present study, Cd exposure does not cause enhanced ROS production in 1321N1 and HEK 293 cells. This shows that ROS production may not be involved in Cd toxicity in these two cell lines. This is supported by cell viability assay performed in the presence of catalase inhibitor, aminotriazole (Fig.3.11). The present work shows that 1mM aminotriazole does not alter cell viability in the presence of Cd in 1321N1 and HEK 293 cells (Fig.3.11). The non significant difference in cell viability in the presence and absence of catalase inhibitor shows that superoxide anion and H_2O_2 may not play a key role in Cd induced toxicity in both cell lines laying credence to the non significant change in ROS levels observed in both cell lines. However, there is no evidence in this work that aminotriazole actually inhibits catalase activities. Therefore further work is required in order to actually ascertain the role of catalase in Cd toxicity.

Several previous studies have shown that increased intracellular ROS leads to the oxidation of membrane-derived lipids giving rise to aldehydes, 70% of which are malondialdehyde (MDA) (Esterbauer *et al.*, 1982). In our study, it appears that although ROS levels are not increased significantly in HEK293 and 1321N1 cells, there is evidence of significant peroxidation of lipids over the 24 hour period following exposure to toxic levels of $CdCl_2$ (Fig.3.8B). These data correlate with the drop in GSH levels seen following 50 μM Cd

treatment in these cell types (Fig.3.6), indicating that significant GSH depletion has taken place. It also suggests that there is no correlation between measurable ROS levels and GSH levels at 24 hours in HEK293 and 1321N1 cells, but there is a correlation between decreased GSH levels observed and the degree of lipid peroxidation that has taken place. In contrast, the high levels of ROS observed in HepG2 cells correlate with increased MDA levels but changes in GSH levels do not correlate with ROS levels.

The activity of several antioxidant enzymes in each of the cell lines was investigated. Enzymes such as catalase, SOD and glutathione peroxidase are known to be key protective enzymes. In terms of basal activities, HepG2 have highest SOD and glutathione reductase activities, 1321N1 have the highest catalase and aldo-keto reductase activities and HEK293 has the highest GST and GPx activities at 24hr.

It is apparent that the constitutive levels of glutathione reductase are significantly higher in HepG2 cells than in the other two cell types (Fig.3.16). This suggests that HepG2 is intrinsically more capable of modulating its GSH/GSSG ratio to maintain GSH levels, and this may explain why there is no observable change in GSH levels in this cell line even at high concentrations of Cd. Despite this, HepG2 cells are still sensitive to Cd exposure, suggesting that the maintenance of GSH levels is not the predominating factor in Cd-sensitivity. The observed impaired 1321N1 and HEK 293 cell viability (especially at high concentration) in the presence of BCNU suggests the involvement of GSH redox cycle in maintaining the levels of GSH in response to the depleted GSH levels at 50μM. However, this

work did not show whether BCNU actually inhibits GRed activity. Further work is required in order to actually define the role of GRed in Cd toxicity in these cell lines.

HepG2 cells respond to Cd by increasing the activity of catalase, SOD, GPx, GST and AKR, being the most responsive of the three lines with a 17-fold increase in catalase activity in HepG2 cells at higher concentrations of Cd. The other two cell lines are able to increase GPx, GST, GRed and AKR activities. This responsiveness suggests either those oxidants are being produced within these cells leading to increased expression of the relevant enzymes; or that Cd can induce expression of these enzymes directly. Of all the activities examined GPx and AKR are the most responsive and good markers of Cd exposure. In contrast, SOD activity does not appear to be very responsive to Cd treatment. This further confirms the catalase inhibitor study that shows that superoxide and hydrogen peroxide may not be very important in Cd toxicity in HEK 293 and 1321N1 especially at low concentrations of Cd.

The significant increase in GST activities at all the concentrations tested in HepG2 cells shows that GST conjugation is likely to be a major mechanism of detoxification of reactive molecules produced in HepG2 cells following 24hr Cd exposure. Given that 1321N1 cells and HEK293 cells have lower glutathione reductase activities and hence are more susceptible to GSH depletion, the observed increased GST activities at 50 μM Cd in these cells may explain the depletion in GSH levels at this concentration. Increased aldo-keto reductase activities observed in all the three cell lines indicate that the cells are also responding by inducing carbonyl-metabolizing enzymes in

order to deal with the elevated levels of lipid peroxidation products that have arisen as a consequence of Cd exposure. This is the first report of this class of enzymes responding to Cd.

Exposure to cadmium is known to cause changes in the activities of several other protective enzymes and proteins. Decreased enzymes activities have been observed after short-term acute exposure to cadmium in both *in vitro* and *in vivo* studies. However, exposure to Cd can also result in enhanced activities of heme oxygenase (Koizumi *et al.*, 2008), metallothionein (Durnam and Palmiter, 1981), and heat shock proteins (Williams and Morimoto, 1990). This adaptive response is mediated through changes in transcription (Koizumi, *et al.*, 2008), most likely via the interaction of the transcription factor Nrf2 with an Antioxidant Response Element (He *et al.*, 2008) or through other pathways using factors such as Ap1 (Liu *et al.*, 2002) and NFkB (Yang *et al.*, 2007a). The involvement of Nrf2 in mediating the observed responses to Cd, particular the elevation in GPx and AKR activities is currently the focus of further investigations.

In conclusion, Cd-induced ROS formation observed in HepG2 cells indicates that ROS may play an important role in cadmium induced toxicity in this cell line. However, another mechanism of toxicity is likely to be involved in the other two cell lines and this is likely to include GSH depletion that is independent of ROS production. The increase in activities of several antioxidant enzymes examined in this work is a reflection of the cells response to Cd toxicity. At low concentrations of exposure, free radicals generated are not toxic but may serve as signalling molecules to trigger an adaptive response within the cells, leading to increased expression of several

protective enzymes. A more detailed profile of expressed proteins and enzymes will allow common factors of Cd exposure to be identified, and to be compared to signatures of other stressors. Knowledge of these protective pathways may lead to the development of new treatments that can enhance their levels within cells.

CHAPTER 4

The Role of Intracellular Ca^{2+} and Mitochondrial-Cytochrome c Dependent Pathway in Cadmium-induced Cell Death in Human Cell Lines

Chapter 4

4.0. The Role of Intracellular Ca^{2+} and Mitochondrial-Cytochrome c Dependent Pathway in Cadmium-induced Cell Death in Human Cell Lines

4.1. Introduction

Despite the known toxicity of cadmium, the exact mechanism of action is yet to be fully elucidated. The mode of toxicity appears to be dependent both on dose and duration of exposure, and also varies depending on the cell type. Under a defined set of conditions cell death may be variously necrotic or apoptotic; and if apoptotic then this may be directed through one of several different pathways. Typically, low dose (10μM) short-term exposure (less than 6hours) leads to apoptosis in a variety of cell types, whereas high dose (50μM) long-term exposure leads to necrosis.

One of the several mechanisms proposed for cadmium toxicity is via an alteration in the intracellular Ca^{2+} ion level (Misra *et al*., 2002). Increased Ca^{2+} levels can activate several different signalling pathways leading to either apoptosis or necrosis (Orrenius & Nicotera, 1994). Alterations in calcium homoeostasis and cellular functions mediated by calcium have therefore been highlighted as mechanisms for the toxic action of cadmium as well as certain other toxic metals (Yamagami *et al*. 1998).

One of the cytosolic target proteins for Ca^{2+} is a cysteine protease, Calpain, a protein involved in mediating necrotic, and also apoptotic cell death

(Wang, 2000). Apart from calpain activation, changes in intracellular Ca^{2+} as a consequence of cadmium exposure also modulate the activation and function of the executioner caspase 3 (Juin *et al*. 1998). Caspases, belonging to a family of aspartate proteases have been implicated in apoptosis (Thornberry and Lazebnik, 1998). Two independent pathways are involved in the activation of caspase 3: 1, the receptor-intermediated caspase 8 pathway and 2, the mitochondrial- cytochrome c intermediate caspase 9 activation (Nunez *et al*., 1998).

In the previous chapter the effect of cadmium chloride on 3 different cell lines was investigated. The results show that cadmium toxicity was time and dose-dependent in human hepatoma HepG2, human astrocytoma 1321N1 and human embryonic kidney HEK 293 cell lines but pronounced effects were observed after 24hr exposure. The present study was therefore carried out with the aim of defining the role of intracellular Ca^{2+}, calpain and mitochondrial-caspase dependent pathways in the aetiology of cadmium induced toxicity in HepG2, 1321N1 and HEK 293 cell lines at 24hr exposure that produces the pronounced effect. The response of HepG2 and HEK 293 cells to Cd has been previously investigated by several groups, but the involvement of these pathways is not clear. In addition, the response of 1321N1 cell lines is not known. A comparison of changes within cells may reveal potential areas where intervention could prevent the toxic effects of cadmium exposure.

To achieve this aim, this study has set the following objectives;

1. To determine the involvement of the phospholipase C-Inositol 1, 4, 5-triphosphate (PLC-IP_3) pathway in cadmium induced cell death via intracellular Ca^{2+} alteration by;
    - Assessing the viability of the cells in the presence of $CdCl_2$ following pretreatment with or without U73122 (a phospholipase C specific inhibitor) and U73343 (inactive analog of U73122, which only slightly inhibits PLC and therefore used as negative control).
    - Measuring the intracellular Ca^{2+} levels in the presence and absence of U73122.
    - Determining calpain activities in the presence and absence of U73122
2. To determine the role of the mitochondrial-caspase dependent pathway in cadmium induced cell death by;
    - Determining caspase 3 activities and expression level in the cells after cadmium exposure.
    - Determining the expression levels of cytochrome c in the cytosolic fractions after $CdCl_2$ exposure.
    - Determining the expression levels of Bax protein in the mitochondrial fractions after $CdCl_2$ exposure.

4.2. Materials and Methods

4.2.1. Cell Culture

HepG2, 1321N1 and HEK 293 Cells were cultured as previously described in section 2.2.1.

4.2.2. Apoptotic and Necrotic Studies

Materials

The Materials used are as listed in section 2.1.14.

Principle

The method was based on the translocation of phospholipids, phosphatidylserine (PS), from the internal surface of the plasma membrane to the cell surface after the initiation of apoptosis and the monitoring of nucleic acids damage in necrosis. The PS can thus be detected by staining with fluorescent conjugate of annexin V. The annexin V protein has a strong natural affinity for PS and so can be used in monitoring the translocation of PS to the external cell surface which is the characteristic of apoptotic cells. The SYTOX green dye is impermeable to live and apoptotic cells but gives an intense green fluorescence by binding to cellular nucleic acids in necrotic cells.

Cells Sample Preparation

Cells were seeded in 6well plates at a concentration of $1x\ 10^6$ cells/well and the cells were allow to attach for 24hr. Cells were then treated with different concentrations of $CdCl_2$ for 24hr. After the incubation period, the cells media were collected in 15ml centrifuge tubes and the cells were then detached by adding very low concentration of trypsin (0.1%) for 1minutes. The detached

cells were collected into the 15ml centrifuge tube containing the aspirated media and then centrifuged at 1000x*g* for 5min. After centrifugation, the media were aspirated and the cells were washed in PBS. The cells were counted using the Bright-line haemocytometer. Approximately 1x 10^5cells were then collected by centrifugation at 1000x*g* for 5min.

Cells Staining

The collected cells were re-suspended in 500µl Binding Buffer. 5 µl of Annexin V-Cy3 dye and 1 µl of SYTOX Green dye were then added to the resuspended cells and thoroughly mixed by pipetting. The mixture was then incubated in the dark for 10minutes at room temperature.

Fluorescence Microscopic Examination of Stained cells

In order to determine the nature of cell death caused by the exposure of HepG2, 1321N1 and HEK 293 cells to 5, 10 and 50µM $CdCl_2$, 50 µl of the stained cells were mounted on a 0.8-1.0mm Microscopic Slide and then covered with coverslip. The slides were then placed upside down to allow for the uniform distribution of the cells. The slides can be stored in the dark or wrapped with aluminium foil until use. The slides were then viewed under the fluorescence (confocal) microscope in an upside down position at a magnification of 40x using TRITC filter (red coloured filter) for Annexin V-Cy3 and FITC filter (green coloured filter) for SYTOX. Apoptotic cells show red fluorescence and the necrotic cells show green fluorescence while the live cells show little or no fluorescence. The images were converted to 8/24bits for storage.

Flow Cytometry (FACS) Analysis Method

Cells exposed to 5, 10 and 50μM $CdCl_2$ for 24hr were further analysed with the BD FACSCanto™ FlowCytometer (Model-1) from BD Bioscience (USA) in other to determine the percent distribution of apoptotic and necrotic cells. The stained cells were analysed with the FACS machine. The FL1 (FITC) channel was used for the SYTOX green dye at excitation wavelength of 488nm and emission wavelength of 530nm. The FL2 (PE) channel was used for the Annexin V-Cy3 at excitation wavelength of 543nm and emission wavelength of 570nm. The gates for the forward scatter (FSC) were selected based on the fluorescence peaks obtained with the negative control (unstained) and positive control (annexin V-Cy3 stained) in the annexin V channel (FL2 channel) and the gates for the sideward scatter (SSC) were selected based on the fluorescence peaks obtained with the negative control (unstained) and positive control (SYTOX green stain) in the SYTOX channel (FL1 channel). The cell population was separated into four groups: live, early apoptotic, late apoptotic and necrotic cells. A total of 10,000 events were used in the analysis. Results were analysed with the BD FACSDiva flow Jo software. Each cell population was expressed as percentage of the 10,000 events.

4.2.3. Cell viability-Inhibitor study

100μM U73122 Stock

4.64 mg of U73122 (MW=464.7; Product code U6756)) was dissolved in100 μl DMSO (0.1%) and made up to 100 ml with sterile distilled water. The solution was prepared freshly before use.

100 μM U73343 Stock

4.64mg of U73343 (MW=466.7; Product code U6881) was dissolved in 100μl DMSO (0.1%) and made up to 100ml with sterile distilled water. The solution was prepared freshly before use.

Procedures

Cells were seeded in 96 well plates at a concentration of 10^5cells/ml and left for 24hr to attach. Cells were then treated with different concentrations (0-10μM) of U73122 and its inactive analogue U73343 for 30 min at 37°C. Other sets of cells were treated with 5 μM U73122 for 30 min and the medium was removed after the incubation period and the cells were washed with PBS before treatment with different $CdCl_2$ concentration for 24hr. MTT assay was performed as described in section.2.2.5.

4.2.4. Calpain Activity Determination

Calpain activity was determined using the Calpain Activity Assay kit, Fluorogenic (Cat. No QIA120) from Calbiochem (UK). The kit component contains the following; Standard, 100μl of 1mM 7-Amino-4-methylcoumarin (AMC) Standard; Substrate, 60μl Suc Leu-Leu-Val-Tyr-AMC; Activation Buffer, 20ml buffer containing Ca^{2+}; Inhibition Buffer,10ml buffer containing BAPTA (calcium chelator); Reduction Reagent, 100μl 0.5M TCEP; Assay Buffer; Cell Lysis Buffer, 10ml CytoBuster™ Protein Extraction Reagent (Cat.No.71009).

AMC Standard Dilution for Calibration Curve

AMC standard solutions for the calibration curve were prepared by making serial dilutions of 1mM AMC standard stock solution with assay buffer. 5μl

AMC stock was made up to 500µl with assay buffer (1 in 100) to give 10µM solution. Serial dilution of this solution was made by pipetting into different tubes 200µl of assay buffer and 200µl of the 10µM solution was transferred into the first tube to give a solution of 5µM AMC. The solution was vortex and 200µl of this solution was transferred to the next tube (2.5µM). Serial dilutions were continued by transferring 200µl to consecutive tubes. The blank tube contains only assay buffer.

Diluted Substrate

30µl of substrate was diluted with 2.97ml assay buffer (1 in 100 dilution).

Activation Buffer, Final

20µl of reducing reagent (TCEP) was added to 5ml activation buffer just before use.

Principle

The assay was based on the cleavage of synthetic calpain substrate, Suc-LLVY-AMC in the presence of calpain , Ca^{2+} and the reducing agent TCEP to release AMC which can be monitored fluorometrically at an excitation wavelength of approximately 360-380nm and emission wavelength of approximately 440-460nm. Calpain activity was quantified either in terms of relative fluorescence units (RFU) (RFU/ml/mg protein) or extrapolated from the AMC calibration curve (µM AMC/min/mg protein).

Procedures

Sample preparation

Cells were plated in 6well plates at concentration of 10^5cells/ml and were allowed to grow to 90% confluent. The cells were then treated with different concentrations of $CdCl_2$ for 24hr. After the incubation period, the medium was aspirated and the cells layer was washed with ice-cold PBS. 500µl lysis buffer was added to the cells and the cells were allowed to stand on ice for 30min. The cells were scraped into 1.5ml eppendorf tubes and vortexed. The cell suspensions were then centrifuged at 14,000x*g* for 5min and the supernatant was collected and stored as the cell lysates. Further dilutions of the samples were done in assay buffer. The protein content of the cell lysates was measured according to Bradford method.

Assay mixture

For each sample, 100µl activation buffer, final (20 µl TCEP and 5 ml activation buffer) and 100µl of inhibition buffer were pipetted into separate wells in a 96-well plate and 50µl of the sample were added to each well of the activation buffer, final and the inhibition buffer (Table.4.1). The standard wells contain 100µl activation buffer, final and 50µl of the serially diluted AMC standard and the blank well contain100µl activation buffer and 50µl assay buffer (Table.4.1). 50µl diluted substrate was then added to all the wells and incubated for 15min at room temperature (Table.4.1). Fluorescence was then read at an excitation wavelength of 360-380nm and emission wavelength of 440-460nm.The corrected fluorescence was obtained by subtracting the value of the blank from that of the sample and standard. The fluorescence obtained from the inhibition buffer was subtracted from that of

the activation buffer, final. The results were expressed as μM AMC/min/mg protein.

Table.4.1. Calpain assay mixture

	$Sample_A$ (μl)	$Sample_I$ (μl)	Standard (μl)	Blank (μl)
Activation buffer, final	100	0	100	100
Inhibition buffer	0	100	0	0
Sample	50	50	0	0
Assay buffer	0	0	0	50
AMC standard	0	0	50	0

$Sample_A$= Activation sample

$Sample_I$=Inhibition sample

4.2.5. Caspase 3 Activity Determination

Caspase 3 activities were determined with the CaspACE™ Assay System, Colorimetric kit (Product code G7220) from Promega (USA). The kit consists of the following components;2 x100μl Caspase-3 Substrate, Ac-DEVD-pNA (10mM) (product code G724A); 125μl Caspase-3 Inhibitor, Z-VAD-FMK (20mM) (product code G723A); 20ml Cell Lysis Buffer (product code G726A).; 100μl pNA Standard (100mM) (product code G725A) and 5ml Caspase Assay Buffer (product code G595B).

Caspase Assay Buffer

This contains 312.5mM HEPES (pH 7.5); 31.25 %(w/v) sucrose; 0.3125% (w/v) (3-[(3-cholamido-propyl)-dimethylamimonio]-1-propane-sulfonate),CHAPS.

100mM DTT

1.54g DTT (MW=154.25) was dissolved in 100ml sterile water.

Preparation of pNA Stock Solutions

Serial dilutions of the 10mM pNA stock solution were prepared in DMSO according to table 4.2 and 4.3.

Table.4.2. Preparation of pNA Stock Solutions

pNA Stock Solution				
10Mm	**1mM**	**100µM**	**DMSO**	**Final pNA Solution**
10µl	-	-	90µl	1mM
-	10µl	-	90µl	100µM
-	-	10µl	90µl	10µM

Table.4.3. Preparation of pNA Calibration Curve

pNA Stock Solution					**pNA Standard**	
10 µM	**100 µM**	**1 mM**	**DMSO**	**Deionised water**	**µM**	**pmol/µl**
-	-	-	20µl	80µl	0	0
10µl	-	-	10µl	80µl	1	1
20µl	-	-	0	80µl	2	2
-	5µl	-	15µl	80µl	5	5
-	10µl	-	10µl	80µl	10	10

-	-	5µl	15µl	80µl	50	50
-	-	10µl	10µl	80µl	100	100

Principle

The assay was based on production of yellow-coloured p-nitroaniline (pNA) upon cleavage of Ac-DEVD-pNA, a colorimetric substrate, by caspase-3 (DEVDase). The pNA produced was monitored spectrophotometrically at 405nm and is a measure of caspase-3 activity.

Procedures

Sample preparation

Cells were seeded in a 6well plate at a concentration of 10^6cells/ml and allowed to attach for 24hr. At 90% confluent, the cells were treated with $CdCl_2$ in order to induce apoptosis. Replicate well plates were prepared for each $CdCl_2$ concentration to inhibit apoptosis by adding 7.5 µl Z-VAD-FMK (final concentration of 50µM) inhibitor at the same time $CdCl_2$ was added and the cells were incubated for 24hr at 37°C in a humidified 5% CO_2 atmosphere. The cells were washed with ice-cold PBS and the cells were scraped into the eppendorf tubes with rubber policeman. The harvested cells were centrifuged at 450xg for 10minutes at 4°C. The cell pellet was kept on ice and resuspended in cell lysis buffer (product code G726A). The cells were lysed by freeze-thaw and then incubated on ice for 15minutes. The cell lysates were then centrifuged at 15,000x*g* for 20min at 4°C and the supernatants were collected and stored at -70°C until use. Protein determination of the extracts was performed with Bradford method.

Assay mixture

The assay mixture was set up in a 96well plate and contained 32 µl caspase assay buffer; 2 µl DMSO and 10 µl 100 mM DTT in the entire well (Table.4.4). The negative control well contains 20µl untreated cell extract; the induced apoptosis well contains 20µl $CdCl_2$ treated cell extract and the inhibited apoptosis well contains 20µl Z-VAD-FMK /$CdCl_2$ treated cell extract. The reaction volumes were made up to 98µl with deionised water. The reaction was started by adding 2µl of the DEVD-pNA Substrate (10mM stock) to the entire well and the plate was covered with aluminium foil (Table.4.4). The plate was incubated for 4hr at 37°C and absorbance was measured at 405nm.Results were expressed as µM pNA liberated/ml/mg protein.

Table.4.4. Caspase assay reaction mixture

	Blank	**Negative Control**	**Induced Apoptosis**	**Inhibited Apoptosis**
Caspase Assay Buffer	32µl	32µl	32µl	32µl
DMSO	2µl	2µl	2µl	2µl
DTT, 100mM	10µl	10µl	10µl	10µl
Untreated cell extract	-	20µl	-	-
Induced apoptosis extract	-	-	20µl	-
Inhibited apoptosis extract	-	-	-	20µl
Deionized water	54µl	34µl	34µl	34µl
DEVD-pNA (10mM)	2µl	2µl	2µl	2µl

Relative Absorbance Determination

A_A= (mean induced apoptosis sample A_{405}) – (mean blank A_{405})

A_N= (mean negative control sample A_{405}) – (mean blank A_{405})

A_I = (mean inhibited apoptosis sample A_{405}) – (mean blank A_{405})

$\Delta A = (A_A - A_N) - (A_I - A_N)$

Caspase-3 activity calculation

Caspase-3 activity (μM pNA liberated/hour)

$$= \frac{\Delta A - (\text{Y intercept of pNA std. Curve})}{\text{Incubation time in hours}} \times \frac{100\mu l \text{ (sample volume)}}{\text{(slope of pNA std curve)}}$$

$$\text{Specific activity of caspase-3} = \frac{\mu M \text{ pNA liberated per hour}}{\mu g \text{ protein}}$$

4.2.6. Intracellular Ca^{2+} level determination

100 μM U73122 Stock

4.64 mg of U73122 (MW=464.7; Product code U6756)) was dissolved in100 μl DMSO (0.1%) and made up to 100ml with sterile distilled water. The solution was prepared freshly before use.

100μM N, N,N′,N′-Tetrakis(2-pyridylmethyl)ethylenediamine (TPEN) Stock

2.12 mg of TPEN (MW=424.6; Product code 028k1095) was dissolved in 50 μl DMSO (0.1%) and made up to 50ml in DMEM.

Ca^{2+}-free Kreb-Ringer HEPES (KRH) Buffer (pH 7.4)

The buffer contains 3.828g NaCl (131mM); 0.16g $MgSO_4$ (1.3mM); 0.186g KCl (5mM); 0.027g KH_2PO_4 (0.4mM); 0.54g glucose (6mM); 2.383g HEPES (20mM); made up to 500ml with sterile distilled water.

3μM Fura -2AM

0.15mg of Fura-2AM was dissolved in 50ml Ca^{2+}-free KRH (pH7.4). The solution was prepared freshly before use.

Principle

Intracellular ca^{2+} was measured according to the method described by Faurskov and Bjerregaard (2002). The method was based on the formation of a complex between Ca^{2+} and calcium specific membrane permeant dye, fura-2AM. The complex was monitored at fluorescence excitation wavelengths of 340 and 380nm and emission wavelength of 510nm. The fluorescence ratio F340/F380 was used as an indicator of intracellular Ca^{2+}.

Procedure

Cell treatment and Intracellular Ca^{2+} measurement

Cells were seeded in 96well plates at a concentration of 10^6 cells/ml and were allowed to attach for 24hr. The cells were then treated with different concentrations of $CdCl_2$ for 24hr. In an inhibitor study, 5μM U73122 [1-(6-(17β-3-methoxyestra-1,3,5(10)-trien-17-yl)amino)hexyl)-1H-pyrrrole-2,5-dione was loaded on the cells for 30min before $CdCl_2$ treatment. After the incubation period, cells were washed thrice with Ca^{2+}-free Krebs-Ringer-HEPES(KRH) buffer (131mM NaCl, 1.3mM $MgSO_4$, 5mM KCl, 0.4mM KH_2PO_4, 6mM glucose, 20mM HEPES, pH 7.4).The cells were then loaded

with 3μM Fura-2 AM at 37°C for 1hr. 50μM TPEN [tetrakis-(2-pyridylmethyl)-ethylenediamine], an inhibitor of heavy metals except Ca^{2+} , were loaded on the cells 10min before the end of Fura-2 AM loading. After incubation, the cells were washed thrice with Ca^{2+} free-KRH buffer and then incubated in the buffer for additional 30min. Fluorescence was measured on a Luminescence spectrophotometer, model at 340 and 380nm excitation wavelength and 510nm emission wavelength. Intracellular Ca^{2+} was expressed as the fluorescence ratio (F_{340}/F_{380}).

4.2.7. Preparation of Subcellular Fractions

Materials and Methods

Beckman centrifuge (Avanti™J-30I) from Beckman (USA).

Homogeniser (Model T25basic) from IKA Labortechnik (UK).

Homogenising Buffer

The buffer contains the following;

2.383g HEPES -KOH(20mM; pH7.5); 1.712g Sucrose (10mM); 0.3728g KCl (10mM); 0.1535g $MgCl_2$ (1.5mM); 0.186g EDTA (1mM); 0.19g EGTA (1mM); 0.077g DTT (1mM); 0.087g PMSF (1mM); 1g Aprotinin (2mg/ml); 5g Leupeptin (10mg/ml); 2.5g Pepstatin (5mg/ml) made up to 500ml with sterile distilled water.

Lysis Buffer

The buffer contains 3.029g Tris-Cl (50mM; pH7.4); 4.383g NaCl (150mM); 2.5ml Triton-X (0.5%,v/v); 3.804g EGTA (20mM); 0.077g DTT (1mM); 0.092g Sodium orthovanadate (1mM).

Principle

Cells fractions were prepared by the differential centrifugation method. This method of separation was based on the fact that cell organelles of different sizes, shapes and densities sediment at different rates when subjected to centrifugal force at a given speed and time.

Procedures

HepG2, 1321N1 and HEK 293 cells were seeded in 2 x 175cm^3 tissue culture flasks and was allowed to grow to 90% confluent. The cells were then treated with 5 and 10μM $CdCl_2$ for 24hours. After the incubation period, the cells were washed with ice-cold PBS and harvested by scraping with a rubber policeman in PBS. The harvested cells were then centrifuged at 1,000xg for 3min at 4°Cand the pellets were resuspended in 1ml ice cold homogenising buffer (20mM HEPES-KOH,pH 7.5; 10mM Sucrose; 10mM KCl; 1.5mM $MgCl_2$; 1mM EDTA; 1mM EGTA; 1mM DTT; 1mM PMSF; 2mg/ml Aprotinin; 10mg/ml Leupeptin; 5mg/ml Pepstatin) and homogenised with the homogeniser (Model T25basic) in order to break the cell membrane to release the cell contents. The cell homogenate was centrifuged in Beckman centrifuge (Avanti™J-30I) at 3,000x*g* for 5min at 4°C and the pellets were retained and resuspended in the lysis buffer (50mM Tris-HCl, pH7.4; 150mM NaCl; 0.5% (v/v) Triton X-100; 20mM EGTA; 1mM DTT; 1mM Sodium Orthovanadate) as the **nuclear fraction** and stored at -70°C until used for western blots. The supernatant was removed and centrifuged at 10,000x*g* for 10min at 4°C and the pellets obtained were resuspended in lysis buffer and retained as the **mitochondrial fraction.** The fraction was stored at -70°C until further use. The supernatant was removed and centrifuged further at

100,000x*g* for 1hour at 4°C. The supernatant was removed and retained as the **cytosolic fraction.**

4.2.8. Protein Gels and Western Blots

Sample preparation

100µl of the cell fraction was mixed with 200µl of the 2x lysis buffer before boiling in a waterbath for 5min as previously described in section 2.2.18.

Procedures

SDS PAGE and Western Blots of the cells fractions were carried out as described in section 2.2.18. Amersham ECL DualVue Western blotting markers (Code; RPN810, MW range 15-150KDa) were obtain from GE Healthcare (UK) and used as 1 in 5000 dilution. Caspase 3, Bax and cytochrome c antibodies were obtained from Santa Cruz Biotech.Inc and diluted as indicated in table 4.5. The Loading of the cytosolic, nuclear and mitochondrial proteins in the SDS PAGE were normalised using different antibodies as listed in table 4.6.

Table 4.5. Apoptosis indicator antibodies

Antibodies	Catalogue number	Company	Dilution (μl)
Caspase 3 (H-277)	Sc-7148	Santa Cruz Biotechnology, Inc.	1:1000
Bax (N-20)	Sc-493	Santa Cruz Biotech. Inc.	1: 500
Cytochrome c(H-104)	Sc-7159	Santa Cruz Biotech. Inc.	1:500

Table.4.6. Antibodies for cell fractions normalisation

Cells fractions	Antibodies	Catalogue number	Company	Dilution (μl)
Cytosol	GAPDH	Sc-25778	Santa Cruz Biotech.Inc.	1:2000
Nuclear	Lamina B	Sc-6216	Santa Cruz Biotech. Inc	1:1000
Mitochondrial	Tom40	Sc-11025	Santa Cruz Biotech.Inc	1:1000

4.3. Results

4.3.1. Cadmium chloride- induced apoptotic and necrotic cells death

To evaluate the type of cell death induced by cadmium chloride in the three cell lines, the cells were exposed to the different $CdCl_2$ concentrations for 24hr. Cells were stained with apoptosis-specific annexin V–Cy3 dye and the necrosis-specific SYTOX green dye. The results in Figure 4.1 show that $CdCl_2$ induces apoptosis in all the cell lines at the lower concentrations of exposure used (5μM). At 10 μM, the majority of HepG2 cells are apoptotic with a few necrotic cells. However, few of the 1321N1 cells are apoptotic at 10μM. Higher concentrations (50μM) give rise to necrotic cell death in all cells (Fig.4.1). This reveals distinct dose-dependent differences in modes of toxicity between the cell lines. To investigate apoptosis in more detail, cells were exposed to 5, 10 and 50μM $CdCl_2$ for 24hours and analysed using BD FACSCanto™ FlowCytometer. Results reveal significant 435-, 448- and 526-fold increase in the population of HepG2 cells in the late apoptotic stage after treatment with 5, 10 and 50μM $CdCl_2$ respectively when compared with control (Fig.4.2). Also, in HepG2 cells, there were significant 14-, 16- and 19-fold increases in the necrotic cells population when compared with control (Fig.4.2). In 1321N1 cells, the population of necrotic cells significantly increased by 10-, 26- and 29-fold when compared with the control after exposure to 5, 10, and 50μM $CdCl_2$ respectively (Fig.4.3). The results also show a significant 3.4-fold increase in necrotic cells population in HEK 293 cells after exposure to 50μM $CdCl_2$ (Fig.4.4). The increase (3-fold) in necrotic population observed at 10μM $CdCl_2$ was not significant. This set of results indicates that HEK 293 cells are the least susceptible of all the cell lines to $CdCl_2$ induced cell death

Figure4.1. Cadmium chloride-induced apoptotic and necrotic cell death

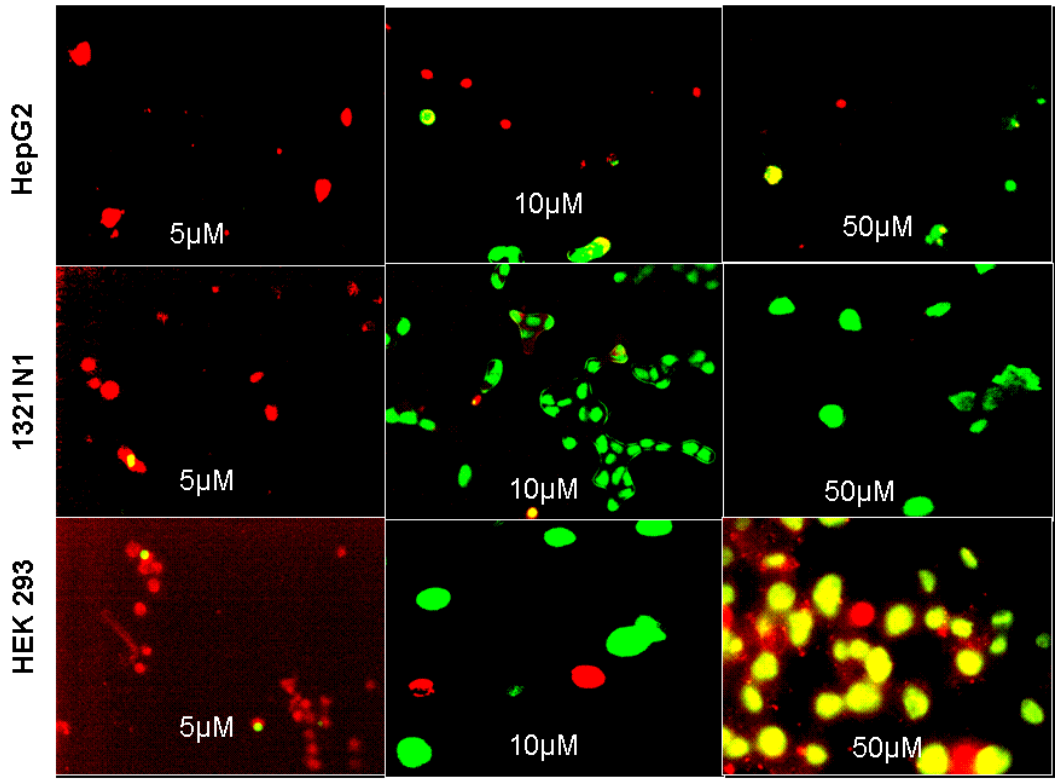

Cadmium chloride-induced apoptosis and necrosis cell death was detected in HepG2, 1321N1 and HEK 293 cells by Fluorescence microscope using AnexinV-Cy3 and SYTOX staining. Cells were treated with 5, 10 and 50µM $CdCl_2$ for 24hours and then stained with AnnexinV-Cy3 and SYTOX Green dye. The stained cells were then fixed on microscopic slide and view under the fluorescence microscope using the TRITC (red) filter for AnnexinV-Cy3 stain and FITC (green) filter for the SYTOX green dye. The cells are divided into apoptotic cells with red fluorescence, necrotic cells with green fluorescence and live cells with little or no fluorescence.

Figure 4.2. The effects of $CdCl_2$ on percentage distribution of apoptotic and necrotic cells in HepG2.

A.

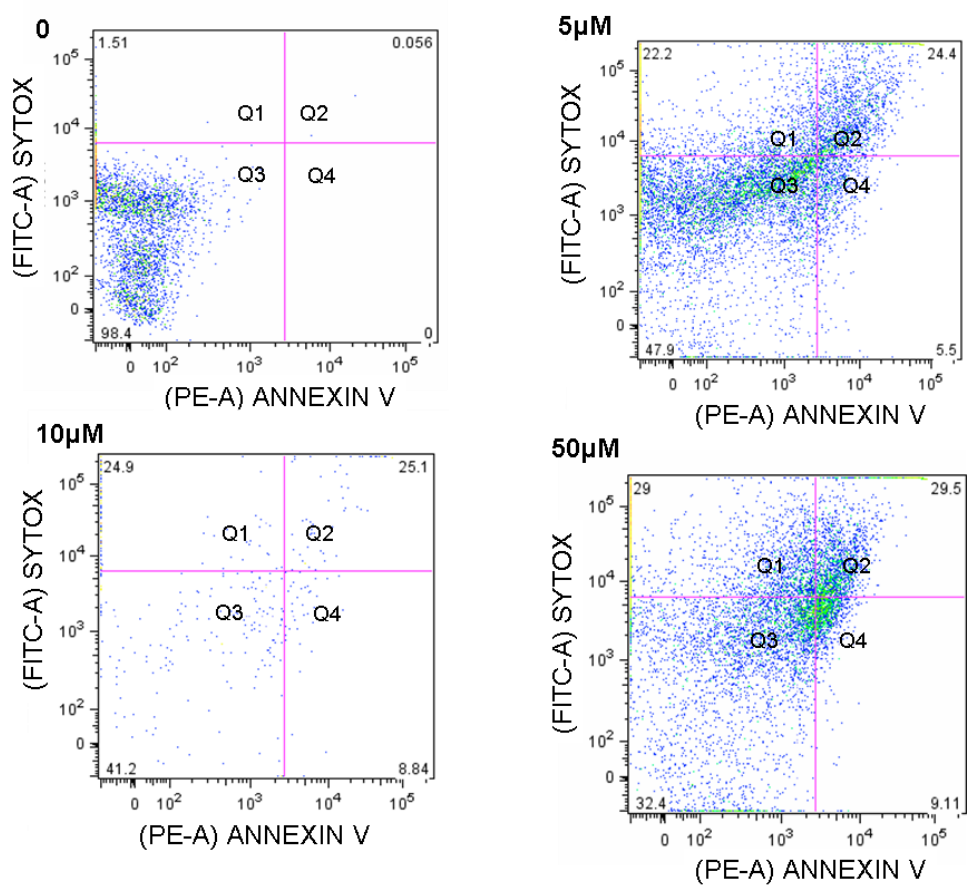

B

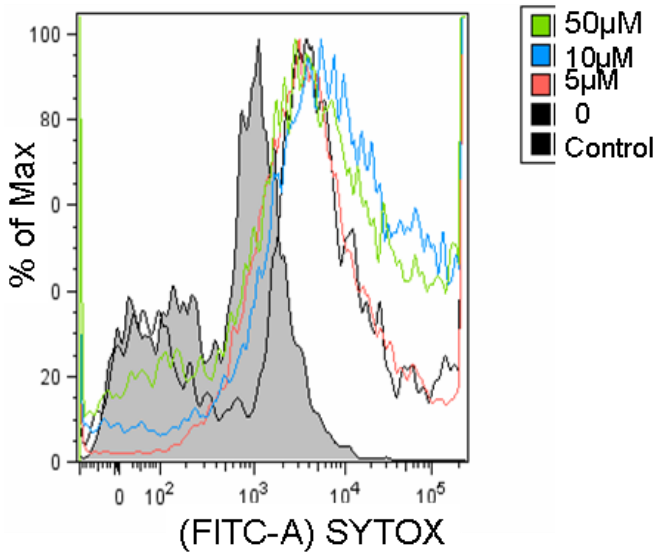

C.

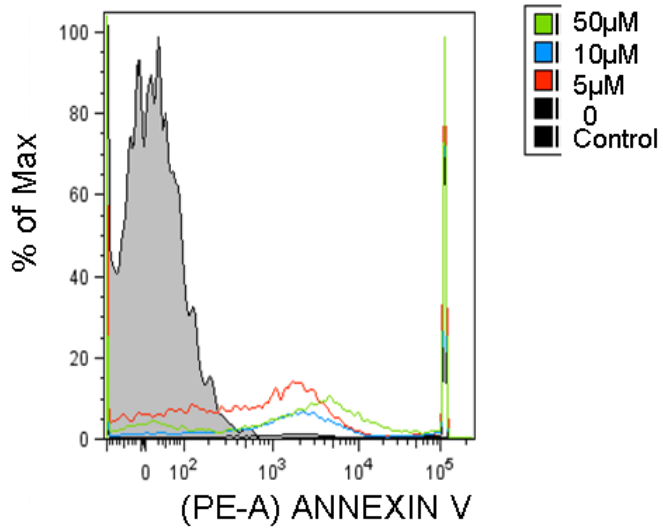

D

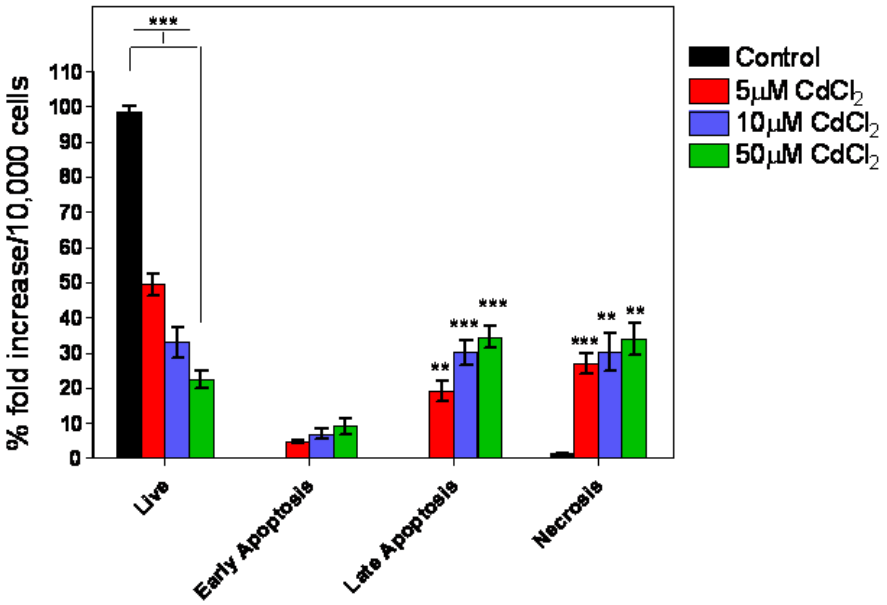

HepG2 cells were treated with 5, 10 and 50µM $CdCl_2$ for 24hr and the cell distribution was analysed by flowcytometry using AnnexinV-Cy3 and SYTOX uptake. The FL1 filter was used for the SYTOX (FITC) fluorescence and the FL2 filter was used for the AnnexinV (PE) fluorescence. Data were expressed as (A) dot plots and (B, C & D) histogram representing one of the six independent values (n=6) and asterisks indicate significant compared with untreated control (***p<0.005 **p<0.01 *p<0.05) using one-way ANOVA with Dunnett's post test.Q1, necrotic cells; Q2, late apoptotic cells; Q3, live cells; Q4, early apoptotic cells.

Figure4.3. The effects of $CdCl_2$ on percentage distribution of apoptotic and necrotic cells in 1321N1

A.

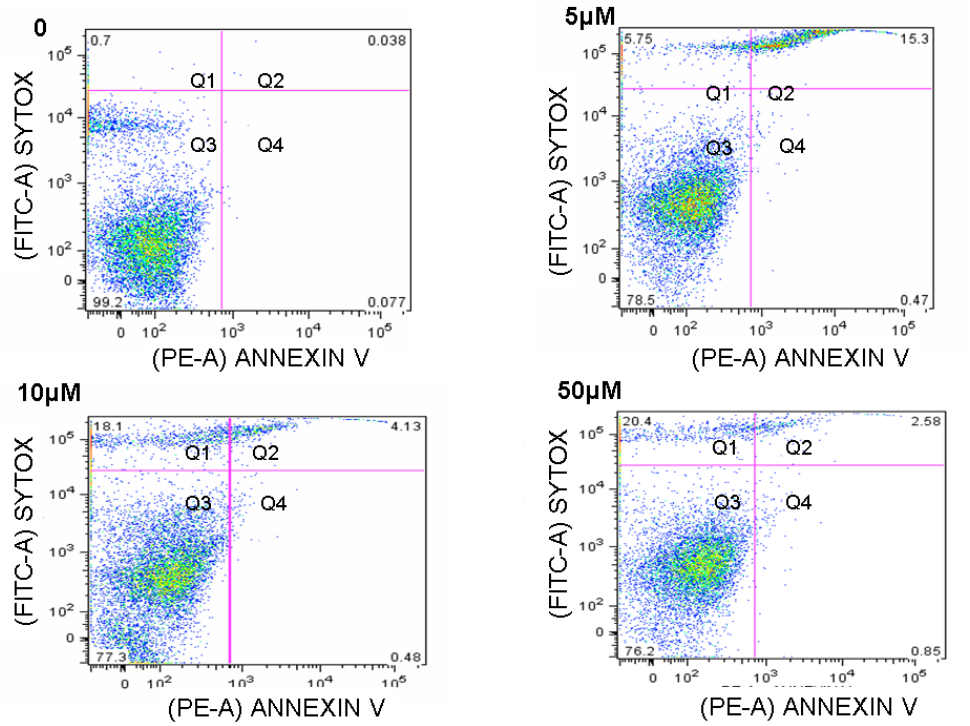

B.

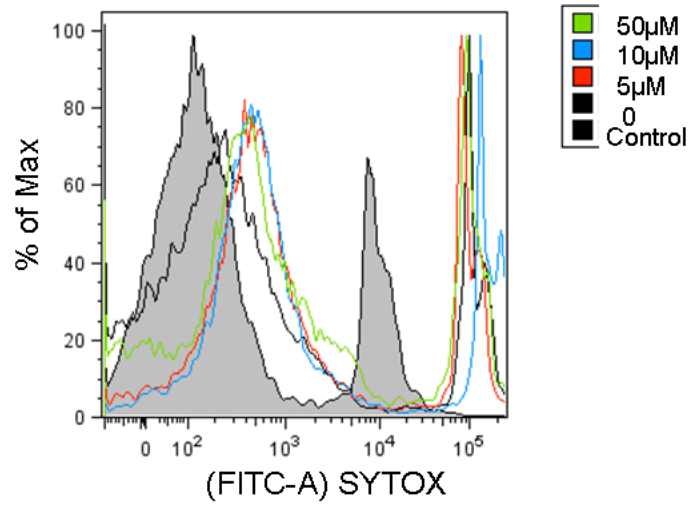

C.

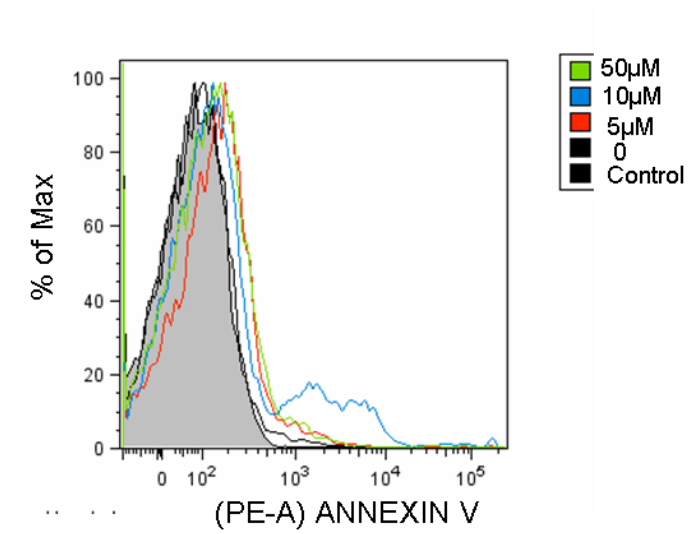

D.

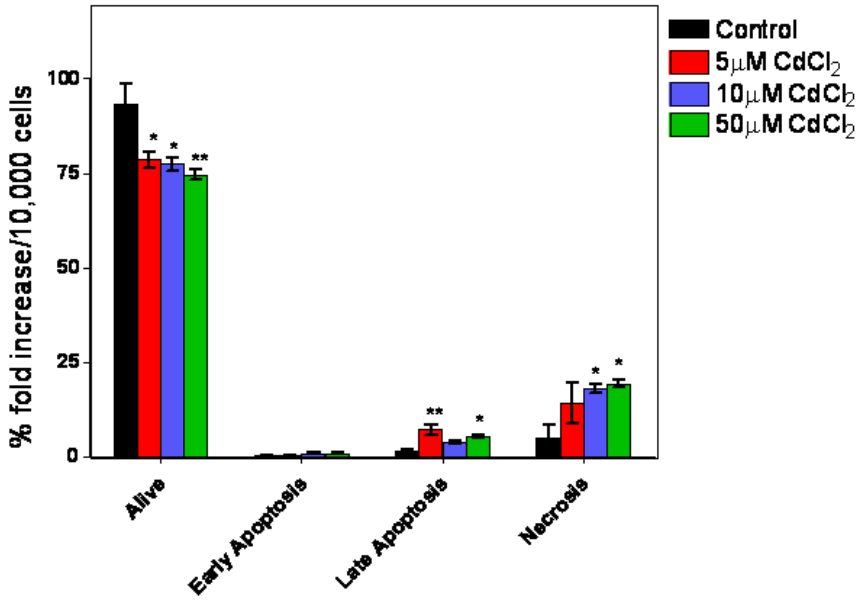

321N1 cells were treated with 5, 10 and 50µM $CdCl_2$ for 24hr and the cell distribution was analysed by flowcytometry using AnnexinV-Cy3 and SYTOX uptake. The FL1 filter was used for the SYTOX (FITC) fluorescence and the FL2 filter was used for the AnnexinV (PE) fluorescence. Data were expressed as (A) dot plots and (B, C & D) histogram representing one of the six independent values (n=6) and asterisks indicate significant compared with untreated control (***p<0.005 **p<0.01 *p<0.05) using one-way ANOVA with Dunnett's post test.Q1, necrotic cells; Q2, late apoptotic cells; Q3, live cells; Q4, early apoptotic cells.

Figure4. 4. The effects of $CdCl_2$ on percentage distribution of apoptotic and necrotic cells in HEK 293 cells

A.

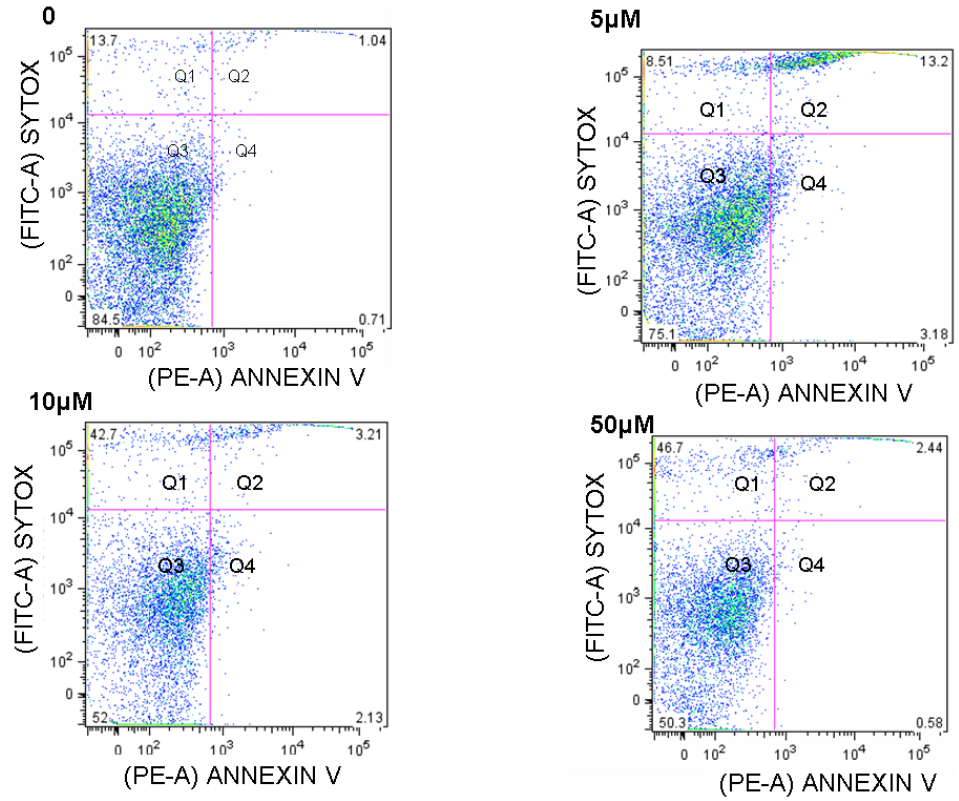

B.

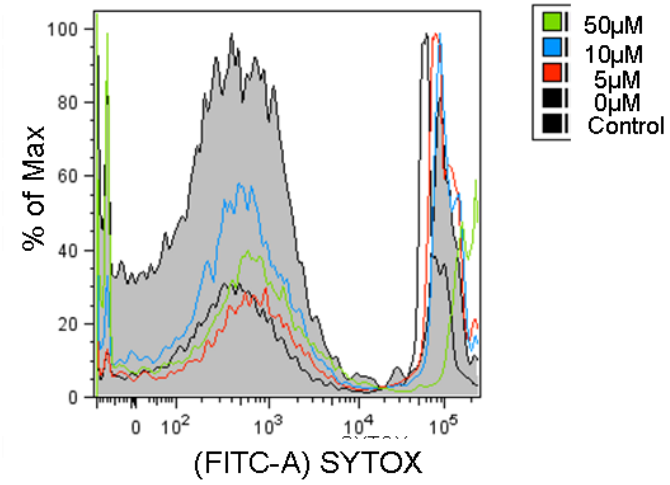

C.

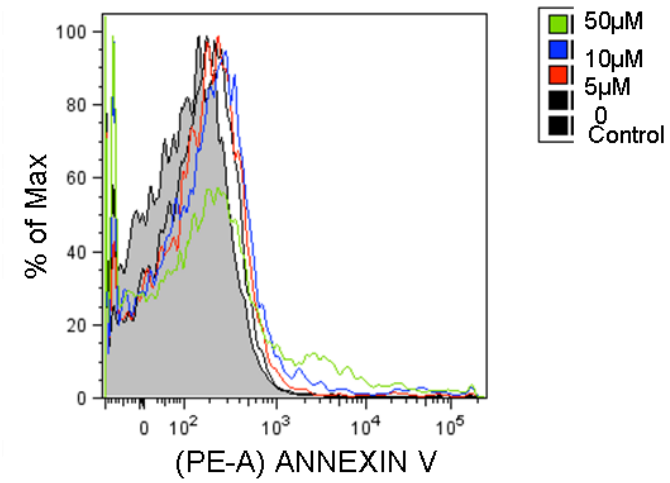

D.

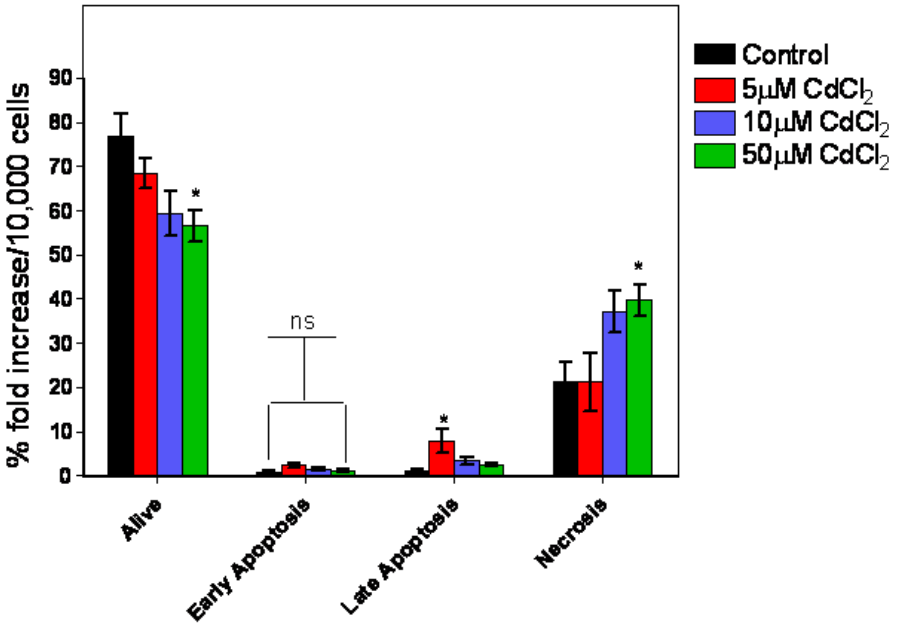

HEK 293 cells were treated with 5, 10 and 50µM $CdCl_2$ for 24hr and the cell distribution was analysed using AnnexinV-Cy3 and SYTOX uptake. The FL1 filter was used for the SYTOX (FITC) fluorescence and the FL2 filter was used for the AnnexinV (PE) fluorescence. Data were expressed as (A) dot plots and (B, C & D) histogram representing one of the six independent values and asterisks indicate significant compared with untreated control (***$p<0.005$ **$p<0.01$ *$p<0.05$); ns (non significant) using one-way ANOVA with Dunnett's post test.Q1, necrotic cells; Q2, late apoptotic cells; Q3, live cells; Q4, early apoptotic cells.

4.3.2. Effect of Cd on Indicators of Apoptosis

Apoptosis leads to several changes in the mitochondria, typically in Bax, Bcl and release of cytochrome c. In addition, ATP levels decrease. To compare the effect of Cd on these parameters, cells were treated with apoptosis inducing levels of Cd (5 and 10μM) and the levels of Bax and cytochrome c were examined. The results show that Bax levels increased significantly at 5 and 10μM in all three cell lines (Fig.4.5). Cytochrome c levels also increased in all three cell lines after 24hours (Fig.4.6). In addition, ATP levels decreased in the cells after 8hours but returned to higher levels after 24hours (Fig.4.7). These results seem to suggest the involvement of the mitochondrial dependent pathway in the apoptotic cell death observed in all the three cell lines.

4.3.3. Cadmium chloride induced caspase-3 activation and expression

One of the main pathways of apoptosis includes the activation of the executioner caspase 3. The effect of cadmium treatment on caspase 3 activation and expression was investigated. Cells were exposed to 5 and 10μM $CdCl_2$ for 24hr and caspase-3 activity was determined (Fig.4.8).There was a 30 to 40-fold increased in caspase-3 activity in HepG2 cells in the presence of 5 and 10μM $CdCl_2$ after 24hours.This increase was also observed in the other cell lines but to much lower levels. Western blot analysis also show increased in expression of the activated caspase 3 (p17subnit) in all three cell lines after exposure to 5 and 10μM $CdCl_2$ (Fig.4.9). These set of results seem to suggest that caspase-3 activation may play an important role in $CdCl_2$ induced apoptosis in all the three cell lines.

4.3.4. Effect of phospholipase C inhibitor on caspase 3 activation

In order to determine the role of PLC-IP_3 pathway in caspase 3 activation, cells were pretreated with the phospholipase C inhibitor U73122 for 30min before exposure to cadmium for 24hours and activated caspase 3 expressions was analysed by western blot (Fig.4.9). U73122 did not abolished activated caspase 3 (p17subunit) expressions in HepG2 and 1321N1 cells (Fig.4.9A & B). However, the presence of U73122 results in decreased in activated caspase 3 (p17subunit) expressions in HEK 293 cells (Fig. 4.9C). These results suggest a possible link between PLC-IP_3 pathway and caspase 3 activation in Cd-induced cell death in HEK 293 cells probably via calpain activation.

Figure4.5. Levels of Bax protein in the mitochondrial fractions of cadmium chloride exposed cells.

A.

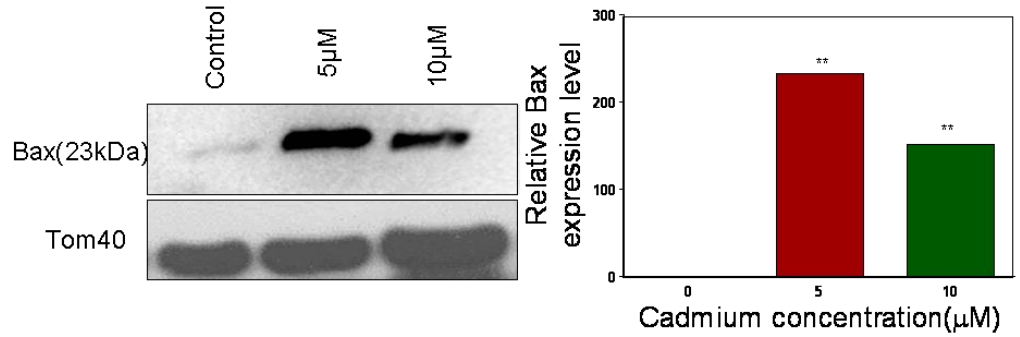

B.

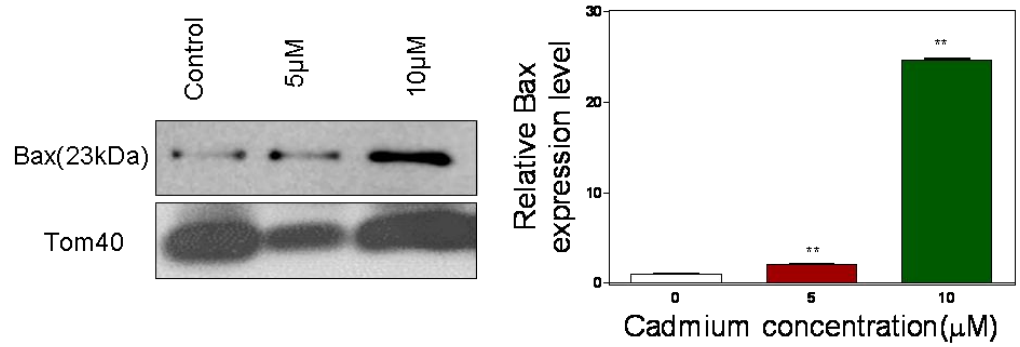

C.

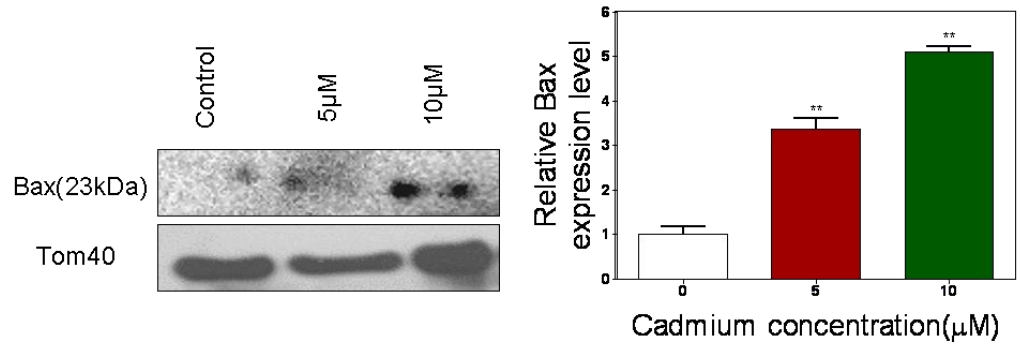

(A) HepG2, (B) 1321N1 and (C) HEK cells were treated with 5 and 10µM $CdCl_2$ for 24hr and mitochondrial fractions were prepared as described in Materials and Methods. Western blot expression of Bax protein was carried out on the mitochondrial fractions and Tom40 was used as an internal

control for normalization and loading of samples on 10% SDS-PAGE gel. The protein concentrations of the loaded samples were determined by Bradford method and approximately 12μg of samples were loaded.The protein bands were quantified by image J and expressed relative to untreated control.Data represent the mean value (n=3) relative to control ±SD. Asterisks indicate significant compared with untreated control (***$p<0.005$ **$p<0.01$ *$p<0.05$) using one-way ANOVA with Dunnett's post test.

Figure4.6. Expression levels of cytochrome c in the cytosolic fraction of $CdCl_2$ exposed cells.

A.

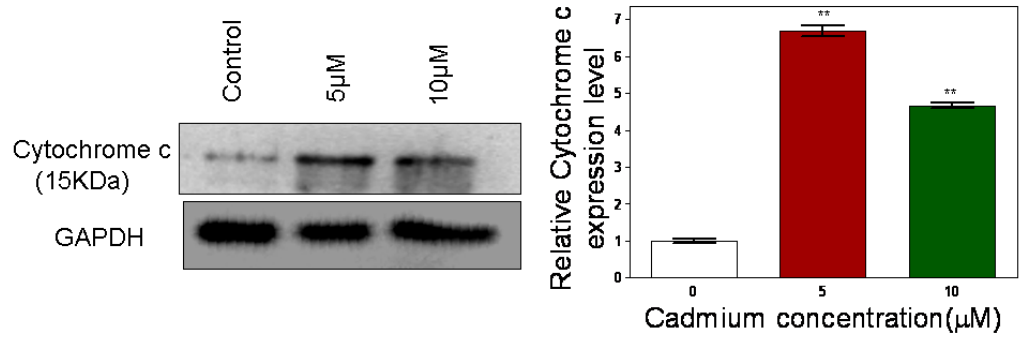

B.

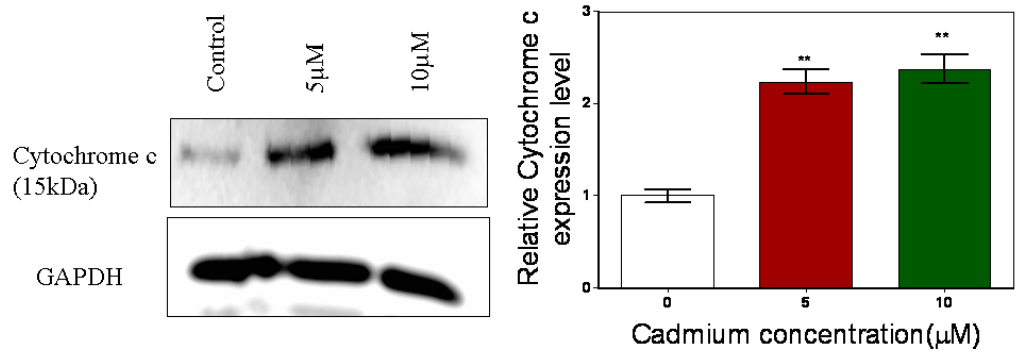

C.

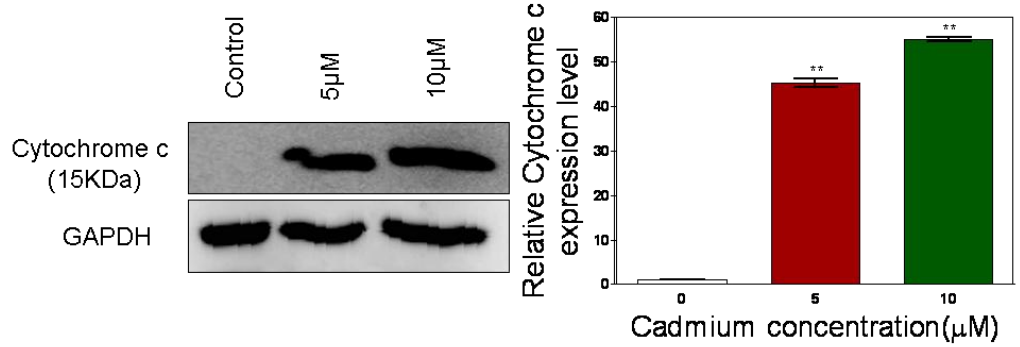

(A) HepG2, (B) 1321N1 and (C) HEK cells were treated with 5 and 10µM $CdCl_2$ for 24hr and cytosolic fractions were prepared as described in Materials and Methods. Western blot expression of cytochrome c protein was carried out on the cytosolic fractions and GAPDH was used as an internal

control for normalization and loading of samples on 10% SDS-PAGE gel. The protein concentrations of the loaded samples were determined by Bradford method and approximately 9μg of samples were loaded.The protein bands were quantified by image J and expressed relative to untreated control.Data represent the mean value (n=3) relative to control ±SD. Asterisks indicate significant compared with untreated control (***$p<0.005$ **$p<0.01$ *$p<0.05$) using one-way ANOVA with Dunnett's post test.

Figure4.7. Effects of $CdCl_2$ on ATP levels in exposed cells.

A.

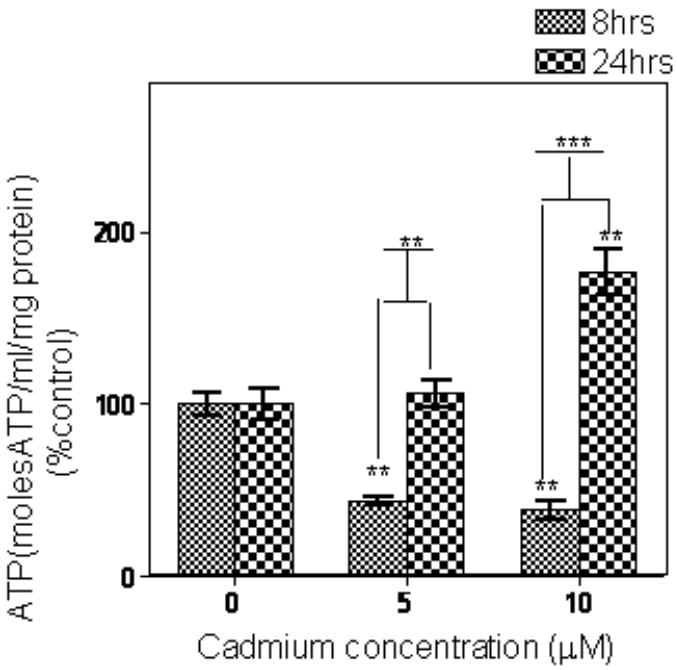

B.

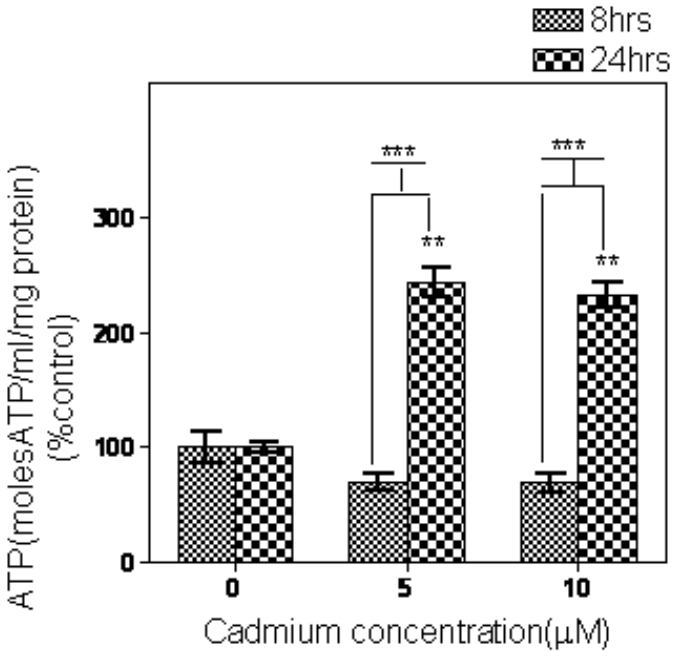

C.

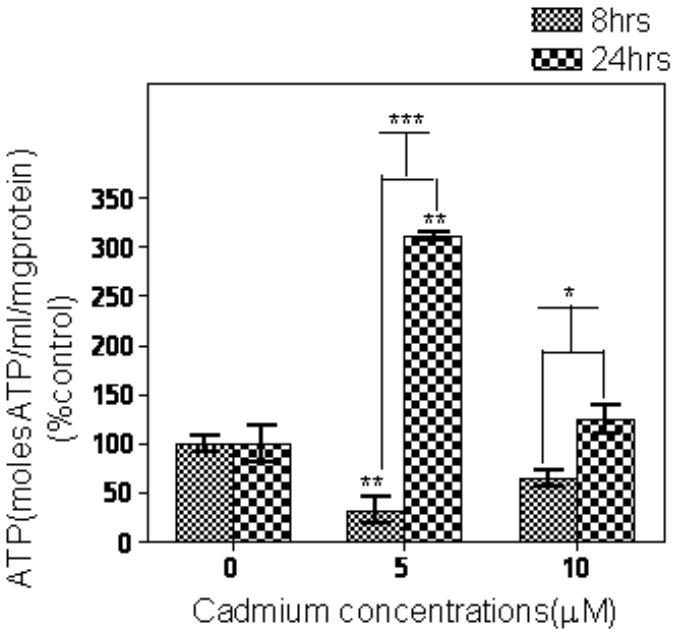

(A) HepG2, (B) 1321N1 and (C) HEK 293 cells were exposed to 5 and 10μM $CdCl_2$ for 8 and 24hr and ATP levels in the cell extracts were determined by luciferase firefly reaction as described in Materials and Methods. Data represent the mean value (n=6 individual assay done in triplicate) of percentage control±SD. Asterisks indicate significant compared with untreated control (***$p<0.005$ **$p<0.01$ *$p<0.05$) using one-way ANOVA with Dunnett's post test and significant compared between different time of Cd treatment at the respective concentration using unpaired student's t-test.

Figure4.8. Effect of $CdCl_2$ on caspase 3 activities in exposed cells

A.

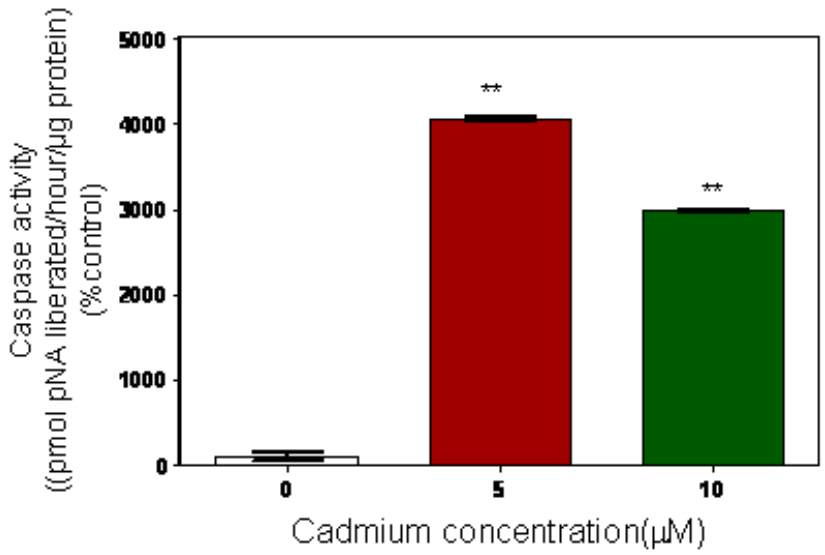

B.

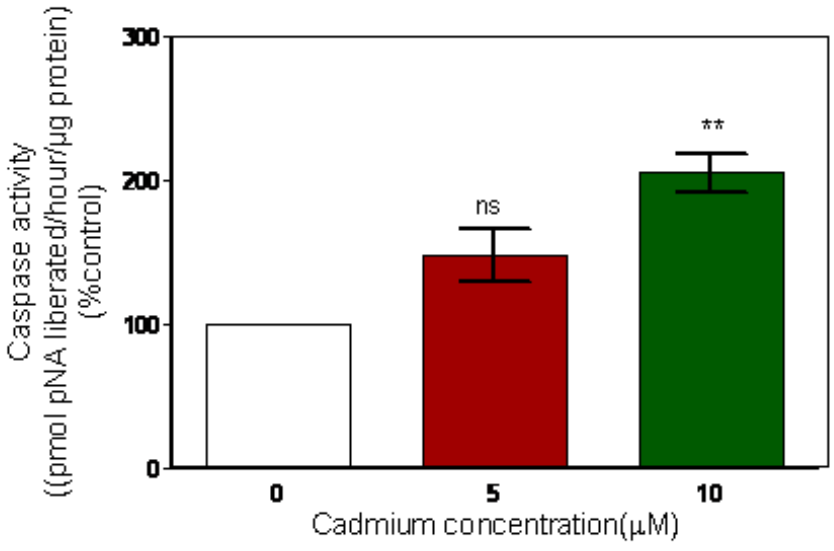

C.

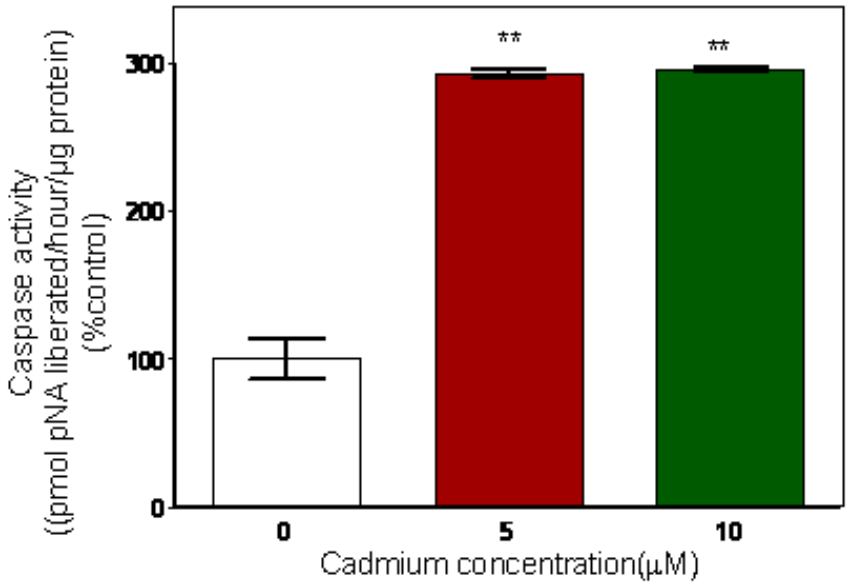

(A) HepG2, (B) 1321N1 and (C) HEK 293 cells were exposed to 5 and 10µM $CdCl_2$ for 24hr and Caspase-3 activities in the cell extracts were determined colorimetrically using Ac-DEVD-pNA as synthetic substrate as described in Materials and Methods. Data represent the mean value (n=3 individual assay done in triplicate) of percentage control±SD. Asterisks indicate significant compared with untreated control (***p<0.005 **p<0.01 *p<0.05) using one-way ANOVA with Dunnett's post test.

Figure4.9. Effect of $CdCl_2$ on caspase-3 protein expression in exposed cells

A.

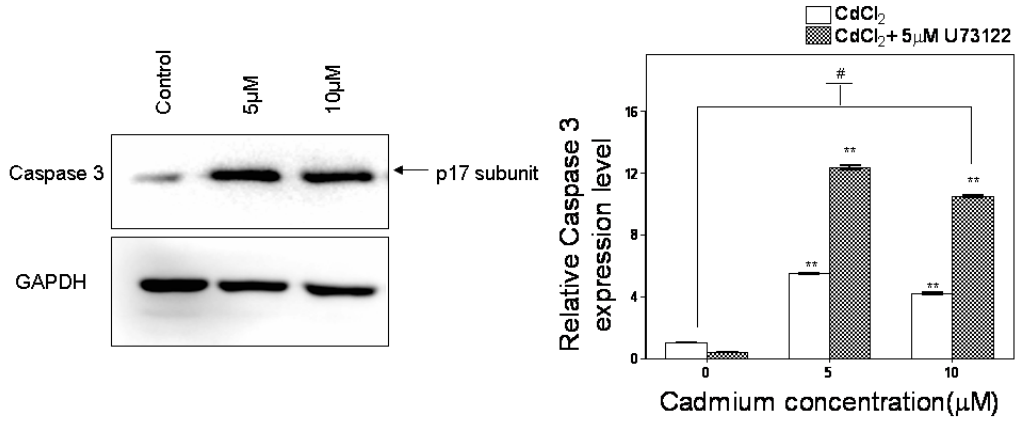

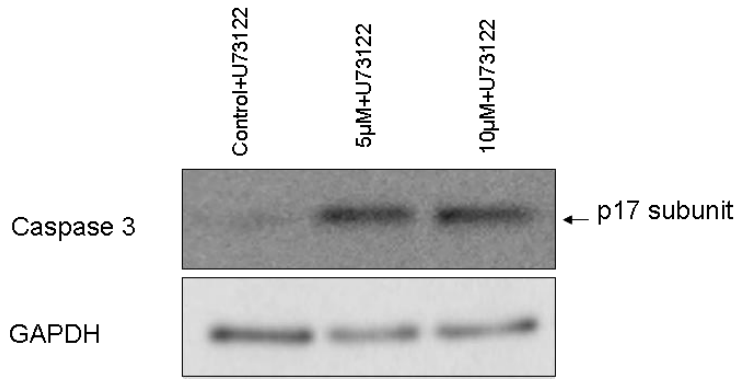

B.

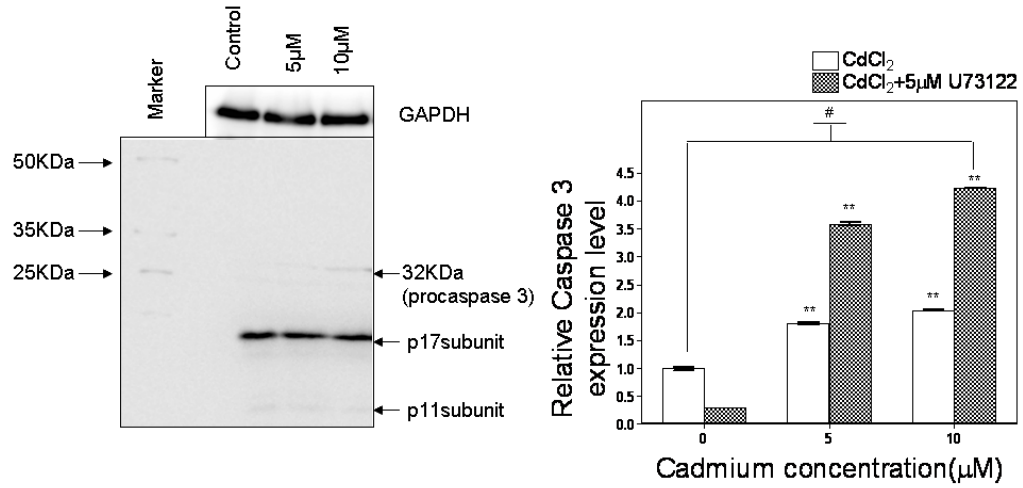
Marker
Control
5μM
10μM
GAPDH
50KDa
35KDa
25KDa
32KDa
(procaspase 3)
p17subunit
p11subunit
CdCl2
CdCl2+5μM U73122
Relative Caspase 3
expression level
Cadmium concentration(μM)

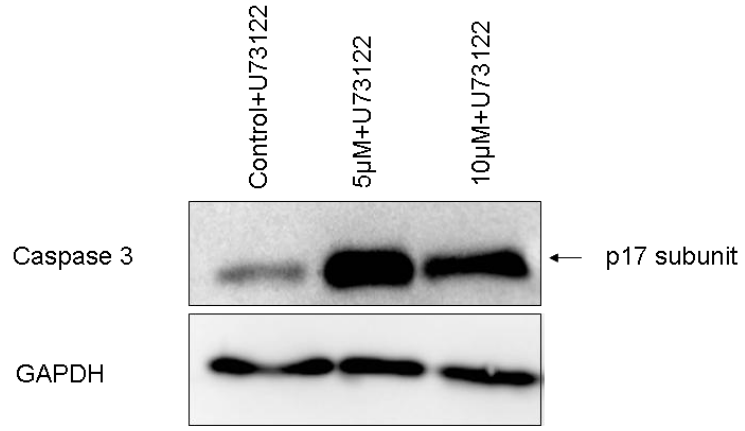
Control+U73122
5μM+U73122
10μM+U73122
Caspase 3
p17 subunit
GAPDH

C.

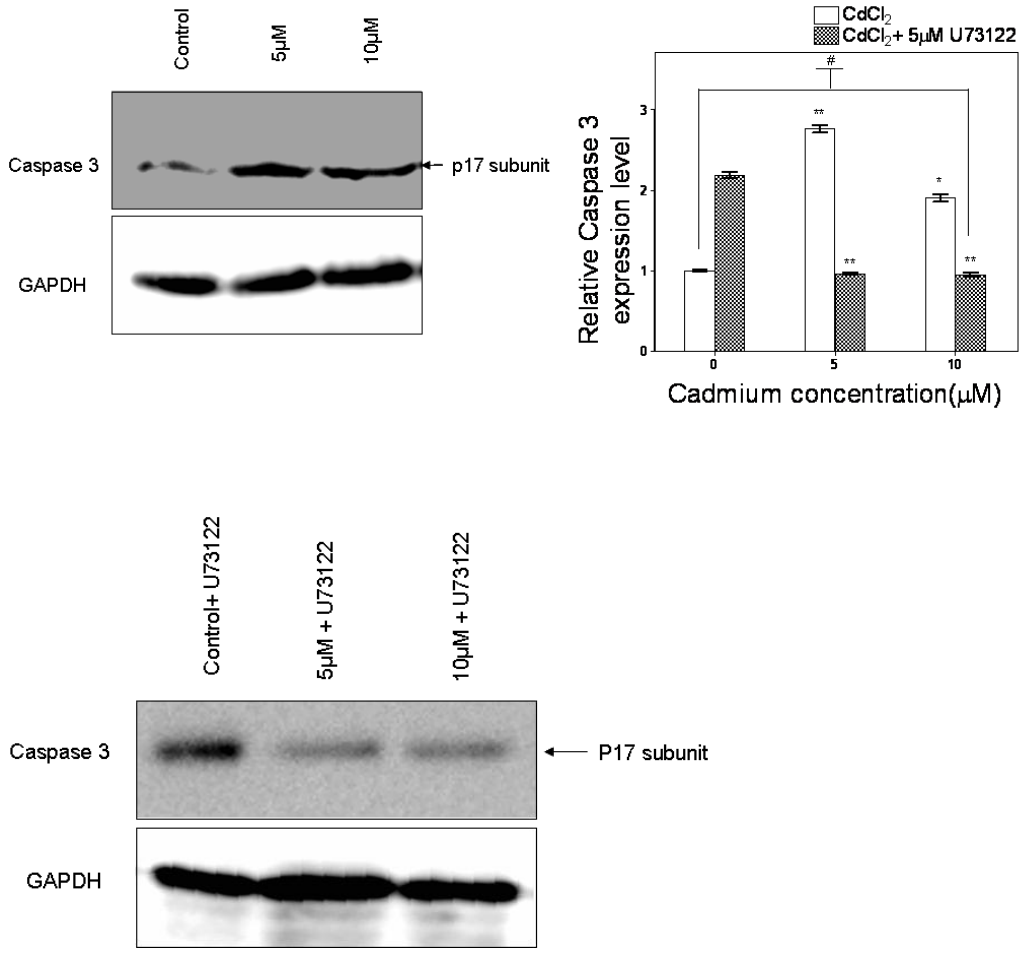

(A) HepG2, (B) 1321N1 and (C) HEK cells were treated for 24hr with 5 and 10μM $CdCl_2$ in the presence and absence of 5μM U73122 and western blot analysis of the whole cell extracts were performed using specific caspase 3 antibodies as described in Materials and Methods. GAPDH was used as an internal control for normalisation and loading of samples on 10% SDS-PAGE gel. The protein concentrations of the loaded samples were determined by Bradford method and approximately 9μg of samples were loaded. Protein bands were quantified by image J relative to untreated control and Data represent the mean value (n=3) relative to control ±SD. Asterisks indicate significant compared with untreated control (***p<0.005 **p<0.01 *p<0.05) using one-way ANOVA with Dunnett's post test; Significant compared with Cd alone at the respective concentration (#p<0.05) using unpaired student's t-test.

4.3.5. Effect of U73122 and U73343 on cell viability

In order to determine the concentration(s) of U73122 that will not have an appreciable effect on cell viability, cells were exposed to a range (2, 5, 8 and 10 μM) of U73122 and its inactive analogue U73343 for 30 min, and MTT assay was performed after the exposure. The results show no significant change in cell viability in HepG2 and 1321N1 cells at all the concentrations of U73122 when compared with control (Fig.4.10A&B). However, a 1.25-fold significant decrease in viability was observed in HEK 293 cells at 10 μM U73122 when compared with control (Fig.4.10C). U73343 on the other hand shows 1.32 and 1.36-fold increased cell viability in HepG2 cells when compared with control (Fig.4.10A). The results show that U73343 enhanced cell viability in HepG2 and HEK 293 cells when compared to U73122 treated cells. These set of data seem to suggest that U73122 in the range of 2 to 8μM has no effect on cell viability and can be used to study the role of PLC-IP3 pathways in the toxic effect of toxic compounds.

4.3.6. Effect of U73122 on cell viability after cadmium chloride exposure

In order to determine the effect of PLC-IP_3 pathway on cell viability, cells were pretreated with 5μM U73122 for 30min before 24hr exposure to 5, 10 and 50μM $CdCl_2$. The results of the MTT assay show that the presence of U73122 does not enhance HepG2 (Fig.4.11A) and 1321N1 (Fig.4.11B) cell survival. The presence of U73122 significantly impairs HepG2 cell viability by 1.69, 1.96-fold at 5 and10 μM respectively (Fig.4.11A). Also the presence of U73122 significantly impairs 1321N1 cell survival by 1.54 and 1.58-fold at 10 and 50 μM respectively. In contrast, the presence of U73122 enhances HEK 293 cell survival (Fig.4.11C). Increase (1.67-fold) in HEK 293 cell viability in the presence of U73122 was significant at 50μM when compared with the

absence of the inhibitor (Fig.4.11C) .These set of data seem to suggest that PLC-IP_3 pathway may be involved in the observed cell death in HEK 293 cells.

4.3.7. Cadmium chloride induced calpain activation

One of the ways in which caspase 3 may be activated is via the action of the protease calpain. To assess the possible role of calpain activation in mediating apoptotic and necrotic cell death following $CdCl_2$ exposure, HepG2, 1321N1 and HEK 293 cells were treated with 5 and 10μM $CdCl_2$ for 24hr and calpain activity was determined (Fig.4.12). The results show no significant increased in calpain activity in HepG2 and 1321N1 cells at 5 and 10μM $CdCl_2$ (Fig.4.12A&B). However, the increased in calpain activity in HEK 293 cells was significant but only at 10μM (Fig.4.12C). These results indicate that activation of calpain may be important in cadmium-mediated apoptosis in HEK 293 cells but not in HepG2 and 1321N1 cells.

4.3.8. Effect of phospholipase C inhibitor on calpain activation

To confirm the involvement of PLC-IP_3 pathway in calpain activation, cells were further pretreated with the phospholipase C inhibitor U73122 for 30min before exposure to 5 and 10μM $CdCl_2$ for 24hours. Significant decreased (21 and 22-fold at 5 and 10μM $CdCl_2$ respectivly) in calpain activity were observed in HEK 293 in the presence of U73122 and 15 and 13-fold decreased at 5 and 10μM $CdCl_2$ in 1321N1 cells (Fig.4.12B &C). Decreased in activities were not significant in HepG2 cells (Fig.4.12A). These results further demonstrate the involvement of PLC-IP_3 pathway in Cd induced toxicity in HEK 293 cells.

4.3.9. Effect of Cadmium treatment on Ca^{2+} levels

One mechanism of calpain activation is via an increase in intracellular calcium levels. To investigate this, cells were treated with $CdCl_2$ for 24hours and Ca^{2+} levels were measured. The results in Figure 4.13 show that Ca^{2+} levels rose significantly (1.2, 1.3 and 1.5-fold at 5, 10 and 50μM $CdCl_2$ respectively) in HEK 293 cells (Fig.4.13C). There was no significant increased in Ca^{2+} levels in HepG2 (Fig.4.13A) or 1321N1 (Fig.4.13B) cells. These set of data seem to suggest that the activation of calpain observed in HEK 293 cells may be dependent on increased calcium levels.

4.3.10. Effect of phospholipase C inhibitor on Ca^{2+} release

A rise in intracellular calcium levels can be mediated by phospholipase C activation. To test whether this pathway is important in cadmium-dependent apoptosis, cells were pretreated with the phospholipase C inhibitor U73122 for 30min before exposure to cadmium for 24hours. Treatment with U73122 in the presence of cadmium led to decreased in calcium ion levels in all cell lines (Fig.4.13). The decreases were significant at all the cadmium chloride concentrations used in HEK 293 cells (Fig.4.13C) but were not significant in HepG2 cells (Fig.4.13A). Significant decreased were also observed at 10 and 50μM $CdCl_2$ in 1321N1 cells (Fig.4.13B). These results seem to suggest the involvement of PLC-IP_3 pathway in intracellular Ca^{2+} alteration in Cd-induced toxicity in HEK 293 cells.

Fig.4.10. Effect of U73122 and U73343 on cell viability

A.

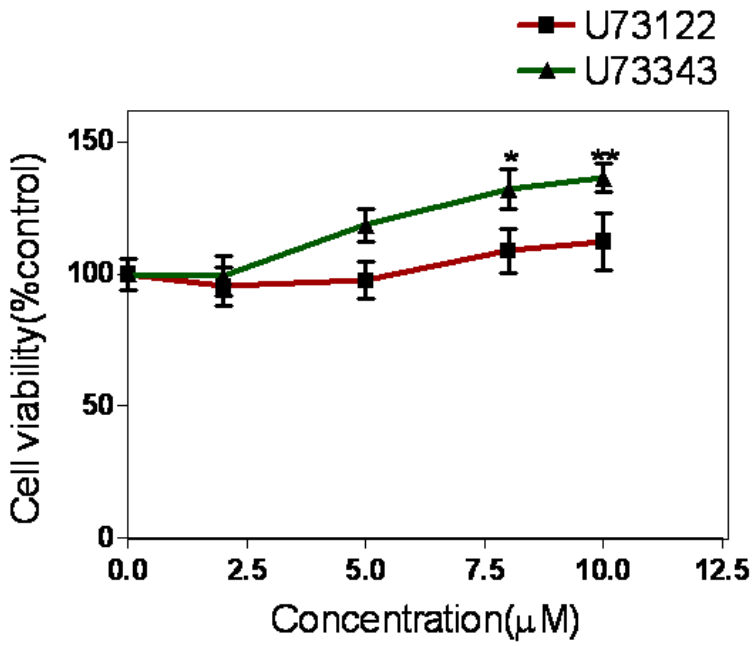

B.

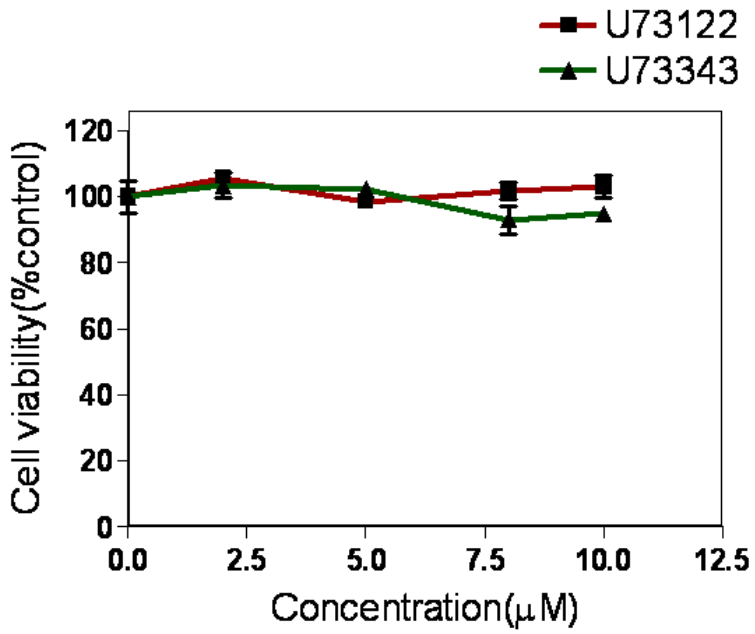

C.

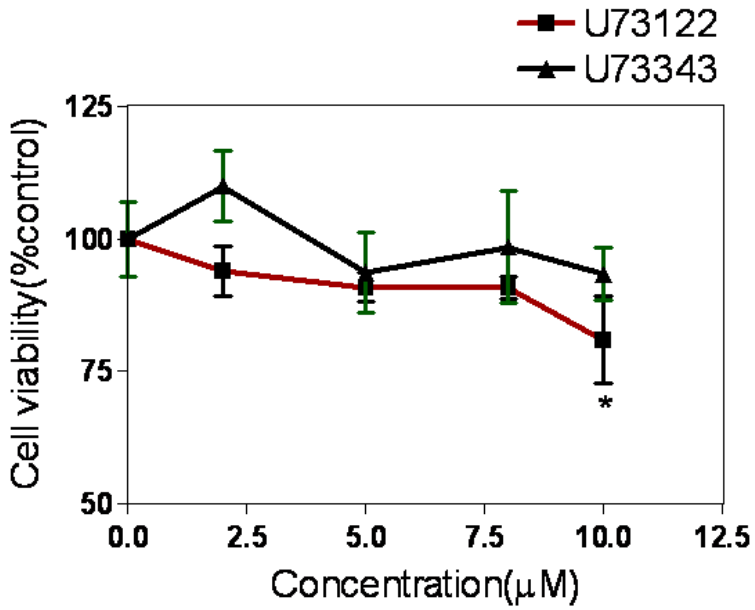

(A) HepG2, (B) 1321N1 and (C) HEK 293 cells were exposed to 0-10μM of U73122 and U73343 for 30min and cell viability was determined by MTT assay as described in Materials and Methods. Data represent the mean value (n=6 individual assay done in triplicate) of percentage control±SD. Asterisks indicate significant compared with untreated control (***p<0.005 **p<0.01 *p<0.05) using one-way ANOVA with Dunnett's post test.

Figure4.11. Effect of U73122 on cell viability in cells exposed to $CdCl_2$

A.

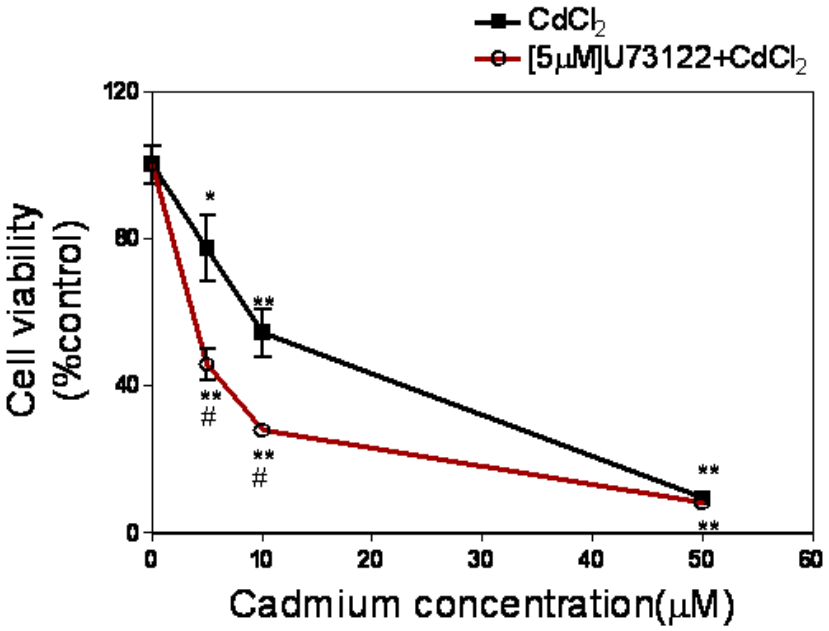

B.

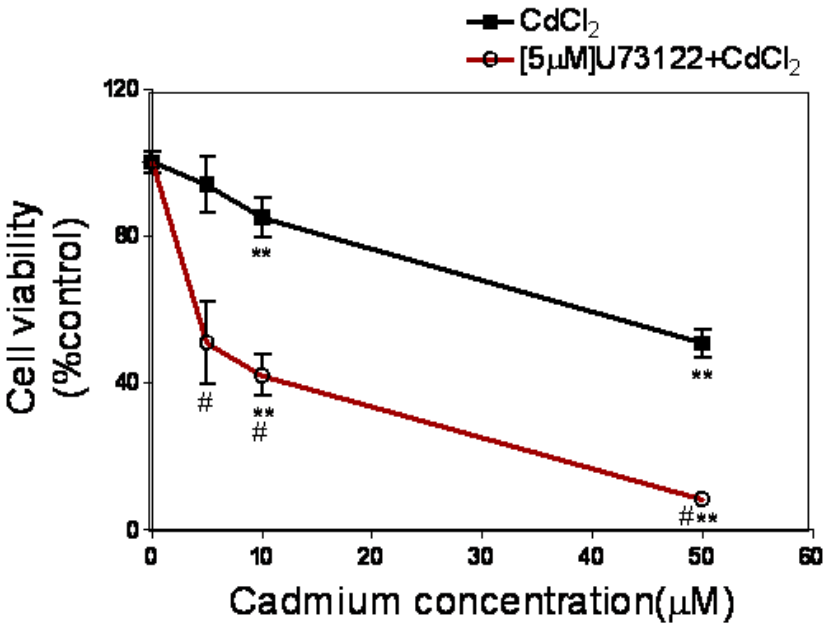

C.

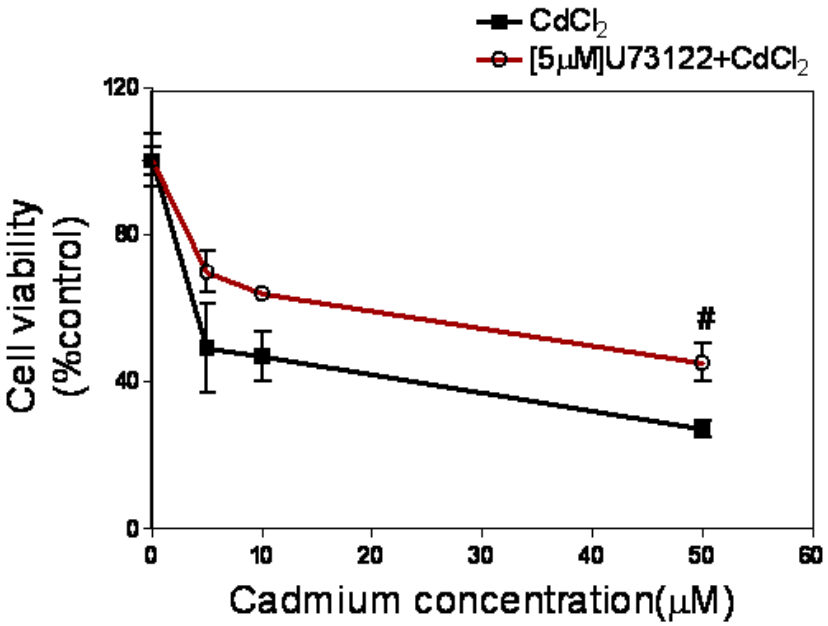

(A)HepG2, (B) 1321N1 and (C) HEK 293 cells were pretreated with 5μM U73122 for 30min before exposure to 0-50μM $CdCl_2$ for 24hr and cells viability was determined by MTT assay as described in Materials and Methods. Data represent the mean value (n=6 individual assay done in triplicate) of percentage control±SD. Asterisks indicate significant compared with untreated control (***p<0.005 **p<0.01 *p<0.05) using one-way ANOVA with Dunnett's post test. Significant compared with Cd alone at the respective concentration (#p<0.05) using unpaired student's t-test.

Fig.4.12. Effect of $CdCl_2$ on calpain activities in $CdCl_2$ exposed cells

A.

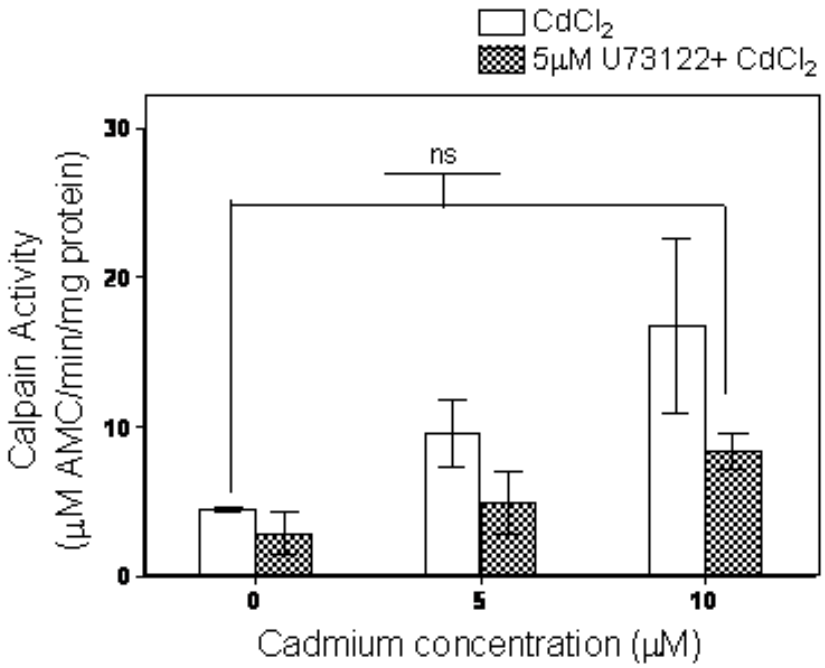

B.

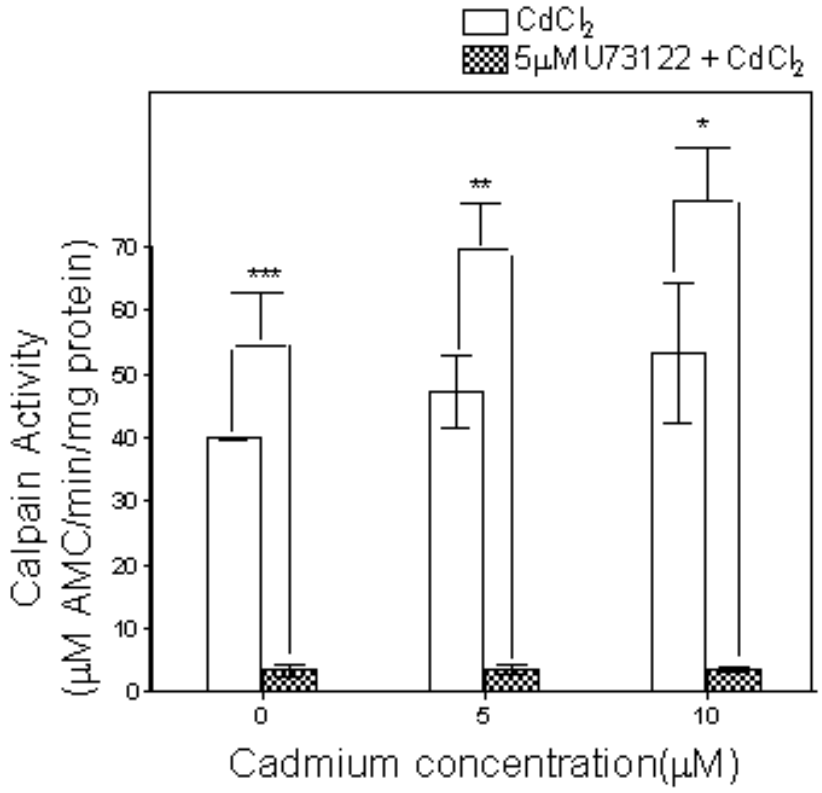

C.

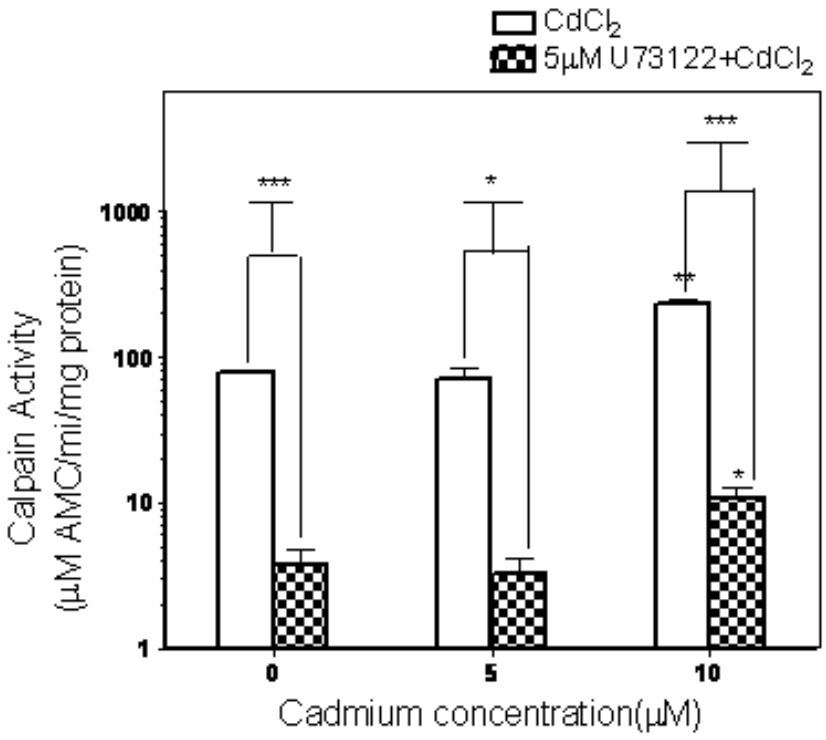

(A) HepG2, (B) 1321N1 and (C) HEK 293 cells were treated with 5 and 10µM $CdCl_2$ for 24hours in the presence and absence of 5µM U73122 and calpain activities were determined in the cell extracts fluorimetrically using synthetic calpain substrate, Suc-LLVY-AMC as described in Materials and Methods. Data represent the mean value (n=3 individual assay done in triplicate) of percentage control±SD. Asterisks indicate significant compared with untreated control (***p<0.005 **p<0.01 *p<0.05); ns (non significant) using one-way ANOVA with Dunnett's post test and significant compared with Cd alone at the respective concentration using unpaired student's t-test.

Fig.4.13. Effect of $CdCl_2$ on the Levels of intracellular Ca^{2+} in $CdCl_2$ exposed cells

A.

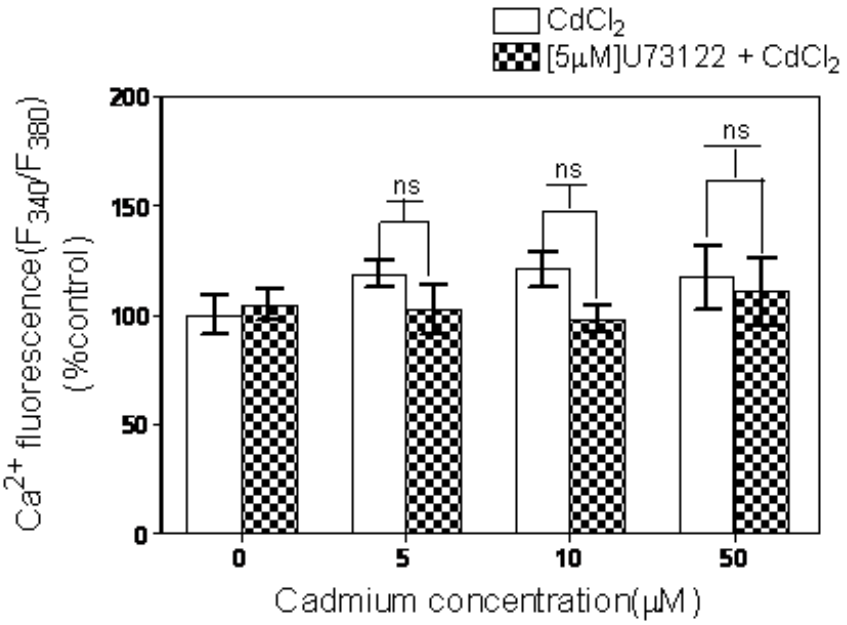

B.

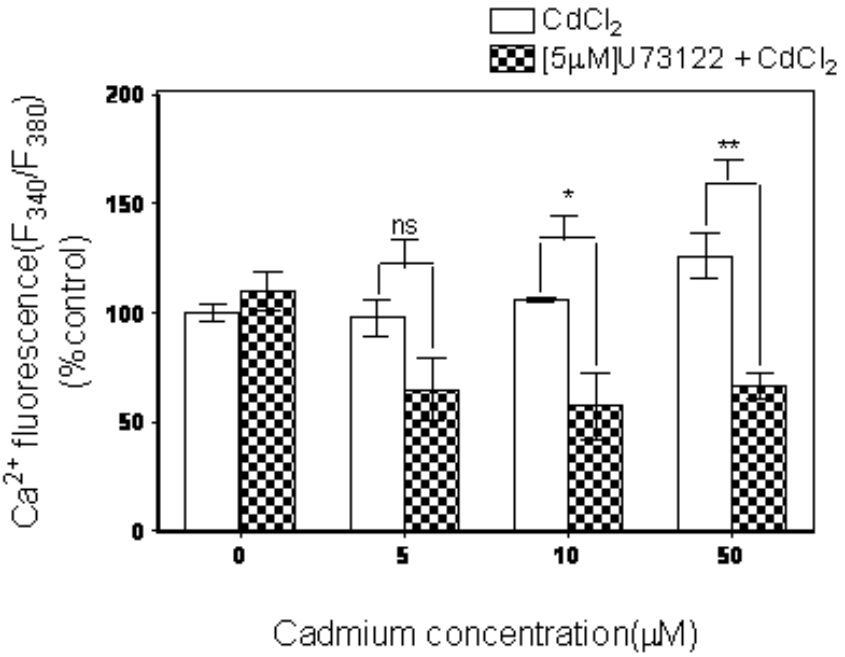

C.

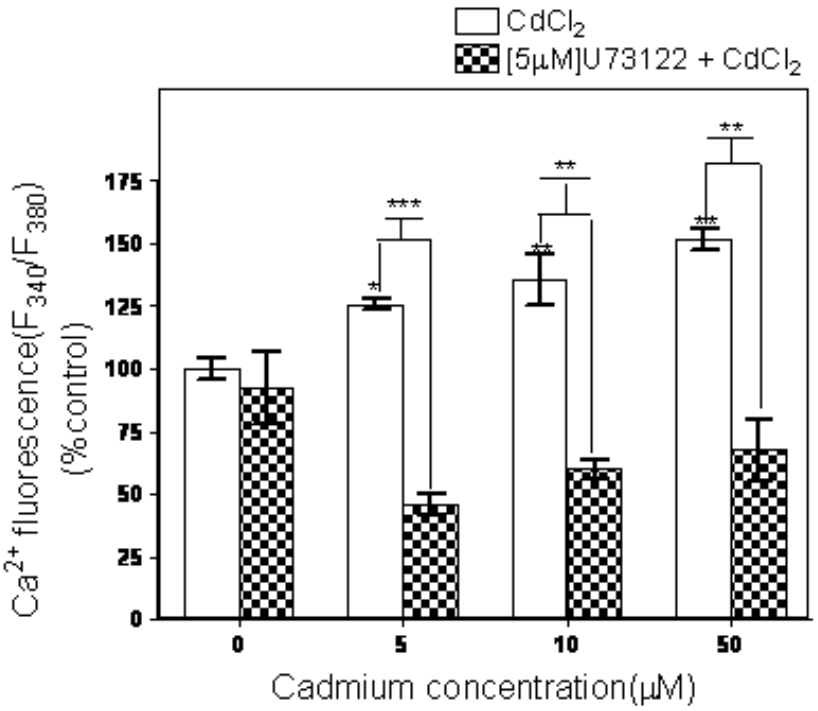

A) HepG2, (B) 1321N1 and (C) HEK 293 cells were treated with $CdCl_2$ for 24hr and also pretreated with 5µM U73122 for 30min before $CdCl_2$ treatment. Intracellular Ca^{2+} levels were determined by fluorescence with Fura-2AM at excitation wavelength of 340nm and 380nm and emission wavelength of 510nm as described in Materials and Methods. Intracellular Ca^{2+} was expressed as the fluorescence ratio (F_{340}/F_{380}).Data represent the mean value (n=6 individual assay done in triplicate) of percentage control±SD. Asterisks indicate significant compared with untreated control (***$p<0.005$ **$p<0.01$ *$p<0.05$); ns (non significant) using one-way ANOVA with Dunnett's post test and significant compared with Cd alone at the respective concentration using unpaired student's t-test.

4.3.11. Effect of Cd on DNA fragmentation

To assess the genotoxic effect of $CdCl_2$, HepG2; 1321N1 and HEK 293 cells were exposed to 5, 10 and 50μM $CdCl_2$ for 24hr and comet assay was performed under alkaline conditions. The results obtained show significant increases of 1.21 and 1.25-fold in DNA tail intensity at 10 and 50μM $CdCl_2$ respectively in HepG2 cells (Fig.4.14). Significant increases of 1.44 and 1.31-fold in DNA tail intensity was also obtained at 50μM in 1321N1 and HEK 293 cells respectively (Fig.4.14).The results seem to suggest that Cd-induced DNA damage in a dose dependent manner but the effect is most pronounced in HepG2 cells.

Fig.4.14. Effect of $CdCl_2$ on DNA fragmentation in exposed cells

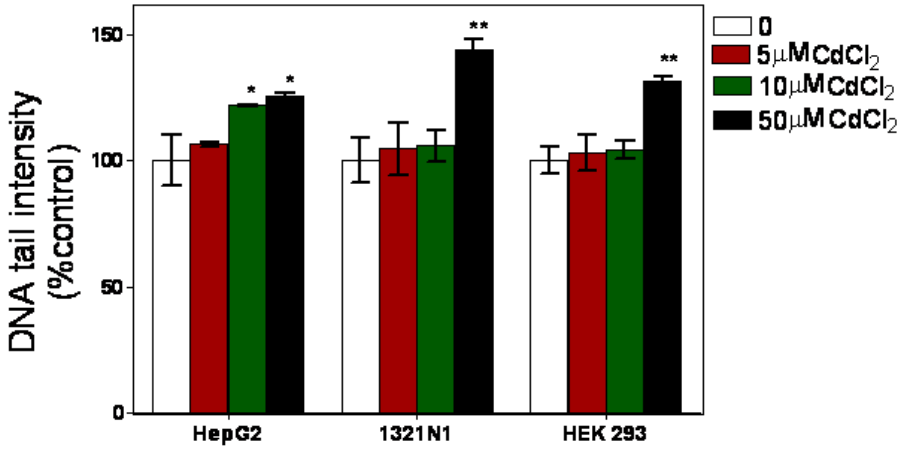

Cells were exposed to 5, 10 and 50μM $CdCl_2$ for 24hr and DNA damage was evaluated by comet assay as described in Materials and Methods. The results were expressed as DNA tail intensity percentage of control. Data represents the mean value (n=6) as a percentage of control ±SD. Asterisks indicate significant compared with untreated control (***p<0.005 **p<0.01 *p<0.05) using one-way ANOVA with Dunnett's post test.

4.4. Discussion

Several *in vivo* (Habeebu *et al*., 1998, Xu *et al*., 1996 & 1999) and *in vitro* studies (Tanimoto *et al*., 1993, Watjen *et al*., 2002) have shown that cadmium induces apoptosis and necrotic cell death (Li *et al*., 2000) in mammalian cells. The present study confirms these earlier reports as cadmium was found to induce apoptotic and necrotic cell death in three cell lines used in this work (Fig.4.1). Flow cytometry analysis revealed an increase in the number of necrotic cells compared to the apoptotic cells as the $CdCl_2$ concentrations increased in all the three cell lines (Fig.4.2; 4.3 & 4.4). Although cadmium has been reported in many studies to induce toxicity by apoptotic cell death, the actual mechanism involved in this process is yet to be clearly understood.

The mitochondrial-dependent apoptosis pathway has been implicated in several studies of cadmium toxicity in vitro. For example, Caspase -9 activation has been reported in cadmium treated HL60 leukemia cells (Kondoh *et al*., 2002) and Bax has been reported to be induced in primary epithelial lung cells as a result of cadmium exposure (Lag et al., 2002). In the apoptotic events involving the mitochondrial-dependent pathway, Bax protein is mobilised into the mitochondrial membrane resulting in the release of cytochrome c and the consequent activation of executioner caspase, caspase 3. Cadmium has been previously reported to induce both caspase-dependent and independent apoptotic pathways (Shih *et al*., 2003). Therefore to further elucidate the role of mitochondrial-dependent pathways in $CdCl_2$ induced cell death, the alterations in the expression of Bax, an apoptotic protein were examined by Western blot. The induced expression of Bax protein in the mitochondrial fractions of all the three cell lines (Fig.4.5) further supports the involvement of mitochondrial dependent pathways in

$CdCl_2$ induced toxicity in these cell lines. Cytochrome c is released into the cytosol during apoptosis as a result of the permeability transition pores formed in the mitochondrial membrane by the apoptotic Bax protein. The increase in cytochrome c expression levels observed in HepG2 and HEK 293 cytosolic fractions after cadmium exposure(Fig 4.6) and the corresponding increase in caspase-3 activities (Fig.4.8) observed in the three cell lines further lay credence to the involvement of mitochondrial-dependent pathway in cadmium cell death in these three cell lines.

Cadmium can induce different apoptotic pathways depending on the cell types. Therefore effects of Cd on intracellular Ca^{2+} ions levels were examined in order to define the involvement of PLC-IP_3 pathway in cadmium toxicity.

One mechanism proposed for cadmium toxicity is the alteration in intracellular Ca^{2+} ion (Misra *et al*., 2002). Cadmium has been reported to activate a G protein coupled metal-binding receptor to activate phospholipase C (PLC) with the release of Inositol-1, 4,5-triphosphate (IP_3) (Misra et al., 2002).

In the present study, $CdCl_2$ caused a significant increase in intracellular Ca^{2+} in HEK 293 cells but not in the other cell lines (Fig.4.13). The presence of PLC inhibitor, U73122, abolished this increased in HEK 293 cells (Fig.4.13C). Also the presence of U73122 enhances HEK 293 cells survival (Fig.4.11C) indicating the involvement of PLC-IP_3 pathway in Cd toxicity in this cell line. No differences in Ca^{2+} levels were observed in the presence and absence of inhibitor in HepG2 cells (Fig.4.13A).

The release of Ca^{2+} from the IP_3- sensitive pool has been speculated to be responsible for the responses of Ca^{2+} of the astrocytes in the CNS to a large number of signalling molecules such as acetylcholine, histamine (McCarthy and Salm, 1991). The present study however shows that the PLC-IP_3 pathway may be involved in intracellular Ca^{2+}alteration in $CdCl_2$ induced toxicity in HEK 293 but not in HepG2 and 1321N1 cell lines. To further elucidate the involvement of intracellular Ca^{2+} ions in the toxicity of $CdCl_2$, calpain activity was examined in the three cell lines (Fig.4.12). Calpain belongs to a family of Ca^{2+} dependent cystein proteases that is widely expressed (Henkart, 1996). Calpain has been previously reported in many studies to participate in apoptosis as a result of increased Ca^{2+} ions (Squier and Cohen, 1997). The significant increase in calpain activity observed at 10μM $CdCl_2$ in HEK 293 cells in the absence of U73122 and the corresponding decrease in activity in the presence of the inhibitor (Fig.4.12C) further support the involvement of PLC-IP_3 pathway in Cd-induced toxicity in this cell line. The nonsignificant changes observed in calpain activity in HepG2 cells both in the presence and absence of inhibitor further confirm that this pathway may not be involved in Cd toxicity in this cell line. Similarly, although 1321N1 cells shows significant differences in intracellular Ca^{2+} and calpain activity in the presence and absence of U73122, this did not resulted in significant increased in Ca^{2+} and calpain activity, thereby eliminating the involvement of this pathway in Cd induced toxicity in this cell line. It has been reported that calpain can activate caspase 3 thereby providing a link with the mitochondrial caspase 3 dependent pathways in apoptosis (Lee *et al*., 2006 &2007). The present study shows that there was a significant increase in expression of caspase 3 in absence of U73122 in HEK 293 cells. This increase was abolished in the presence of U73122 (Fig.4.9C) suggesting the

involvement of calpain in caspase 3 expression and caspase dependent apoptosis. However, the mechanism involved needs further elucidation. Both HepG2 and 1321N1 cells show increased caspase 3 expression in the presence and absence of the inhibitor (Fig4.9A&B) indicating that calpain may not be involved in caspase 3 expression and caspase 3 dependent apoptosis in these two cell lines. This present result was in agreement with previous work that shows that the calpain inhibitor inhibited DNA fragmentation induced by cadmium (Li *et al.,* 2000). Apart from DNA fragmentation, calpain is also said to activate other proteases such as Ca^{2+}/Mg^{2+}-dependent endonuclease and fodrin, both of which are involved in apoptosis in U937 cells (Vanags *et al.,* 1996).

Apoptosis is a highly regulated process that involves a number of ATP-dependent steps such as caspase activation, bleb formation, chromatin condensation and formation of apoptotic bodies (Kass *et al*., 1996, Richter *et al*., 1996). ATP level has been reported to increase during apoptosis in cervical (HeLa), phenochromocytoma (PC12) and human leukemic monocyte lymphoma (U937) cell lines (Zamaraeva *et al*., 2005). It has been reported in several studies that ATP elevation is required for apoptosis and that the depletion of ATP determines the switch from apoptosis to necrosis (Leist *et al*., 1997).The observed increased in ATP levels in the three cells at 24hr (Fig.4.7) further support these earlier reports and correlates with the apoptotic cell death observed in this study. The transient decrease in ATP initially observed at 8hr (Fig.4.7) shows that cadmium increases the metabolic processes in the cells leading to an increase in energy consumption. The increase in metabolic rate therefore resulted in enhanced ATP production as observed after 24hr exposure. The observed increase in ATP corresponds with increased DNA fragmentation (Fig.4.15), caspase -3

(Fig.4.8) and calpain activation (Fig.4.14) which are indices of apoptosis observed at 24hr exposure.

It has already been reported that an increase in intracellular Ca^{2+} ion in astrocytes cells from cerebral cortex is evoked by ATP (Bruner and Murphy, 1993). This increase in intracellular Ca^{2+} ions by ATP has been shown to correlate with increased inositol triphosphate degradation and IP_3 production in astrocytes (Pearce *et al*., 1989). However, the significant increase in ATP levels at 24hr exposure (Fig.4.7B) in 1321N1 cells observed in this work does not correspond with an increase in intracellular Ca^{2+} in the absence of U73122 indicating that ATP may not be involved in Cd induced increase in Ca^{2+} ions level in these cells .

Previous work has shown that cadmium enhances DNA damage by inhibiting DNA repair (Hartwig and Schwerdtle, 2002) and also enhances reactive oxygen species (ROS) production (Chao and Yang, 2001). The present results show that high cadmium concentration (50μM) caused significant increase in DNA tail intensity in all the three cell lines (Fig.4.14). These results were in agreement with earlier studies that reported that cadmium at high cytotoxic concentrations induced DNA damage (Beyersmann and Hechtenberg, 1997; Hartwig, 1994).

These sets of results show that PLC-IP_3 pathway may cause increase Ca^{2+} ions level in the presence of Cd in HEK 293 cells and this may account for the increased calpain activity observed in this cell. However, intracellular Ca^{2+} ion alteration may not be the major pathway in cadmium induced toxicity in

HepG2 and 1321N1 cells but mitochondrial-dependent caspase-3 activation may play a role in Cd induced toxicity in all the three cell lines.

CHAPTER 5

Nrf2 Mediated Adaptive Response to Cadmium Exposure Involves Protein Kinase C

Chapter 5

5.0. Nrf2 Mediated Adaptive Response to Cadmium Exposure Involves Protein Kinase C

5.1. Introduction

As described earlier, cadmium, a heavy metal known to be carcinogenic, is an environmental and industrial toxicant and exposure to this metal has been linked with various cancers and conditions (Waalkes, 2000). As shown in Chapter 3, cadmium disrupts the redox homeostasis of the cells, generating ROS and inducing oxidative stress (Chapter 3). This results in damages to the macromolecules such as protein, DNA and Lipids. Cadmium toxicity depletes the GSH level by binding to the cysteinyl sulfhydryl group to form Cd-GSH complex which further attenuates ROS production with the consequent damage to the cell macromolecules (Chapter 3)

In order to cope with environmental insults, cells have devised means of dealing with cadmium. This includes inducing a range of enzymes that can deal with problems of oxidative stress and glutathione depletion, catalysed by enzymes such as GST, NQO1 and UDP-glucuronosyl transferase (UGTs). The expression of the genes encoding these enzymes has been reported to be transcriptionally regulated by electrophiles through an antioxidant-response element (ARE) present at the regulatory regions of the genes. The ARE has also been reported to be present in the promoter regions of genes encoding antioxidant enzymes such as γ-glutamylcysteine synthase (γ-GCS), and heme oxygenase-1 (HO1) (Wild *et al*. 1999; McMahon *et al*. 2001; Jaiswal, 2004). Both phase 2 and antioxidant enzymes work together to induce

cytoprotective responses that protect cells from the deleterious effects of xenobiotics and other environmental insults.

Nrf2, a basic region-leucine zipper (bZip)-type transcription factor (Moi *et al*., 1994), has been implicated in the transcriptional regulation of ARE-dependent genes (Itoh *et al*., 1997). Several studies have demonstrated that the activation of the Nrf2 pathway protects cells against toxic substances (Cho *et al*., 2002) and thus offers beneficial effects against oxidative stress-induced human disease, cancers and conditions (Zang, 2006). In an unstressed condition, Nrf2 is sequestered in the cytoplasm by Keap1 but in the presence of stress as observed in oxidative stress, the Nrf2-Keap1 complex breaks up leading to the migration of Nrf2 into the nucleus with the consequent transactivation of the antioxidant responsive element. The mechanism(s) by which Nrf2 regulates the expression of Nrf2-dependent genes are becoming increasingly clearer; however, the mechanism by which Nrf2 is released from the Nrf2-Keap1 complex is still controversial (Numazawa *et al*., 2003). Some reports have concluded that the release of Nrf2 from the Nrf2-Keap1 complex is facilitated by the phosphorylation of Nrf2 on ser40 by protein kinase C (PKC) (Huang *et al*., 2000). PKC belongs to the serine/threonine protein kinases family and is found to be regulated by Ca^{2+} or lipids. Diacylglycerol (DAG), formed during lipid biosynthesis and degradation, binds to PKC to activate the latter and, depending on the PKC isoform this can lead to cell proliferation and apoptosis.

Cadmium has been reported previously to bind to a specific G protein coupled metal binding receptor to activate phospholipase C (PLC) with the consequent release of Ca^{2+} and DAG. The released DAG can then activate

PKC with the consequent translocation of Nrf2 from the cytoplasm into the nucleus. Some investigations have also revealed the involvement of Ca^{2+} in the translocation of Nrf2 from the cytoplasm to the nucleus (Kang *et al*., 2005).

In the previous Chapters, I have shown that cadmium induces apoptosis and necrosis in HepG2, 1321N1 and HEK 293 after exposure to the metal, and this leads to altered antioxidant enzyme activities. It is also clear that Cd elevates intracellular Ca^{2+} level via PLC-IP_3 pathway in HEK 293 cells. However, the role of PKC in the translocation of Nrf2 protein from cytoplasm to the nucleus in response to cadmium exposure has not been defined. In this study the role of Nrf2 in mediating the adaptive response of HepG2, 1321N1 and HEK 293 cell lines to Cd has been evaluated. The involvement of PKC in this response was also elucidated.

5.2. Materials and Methods

5.2.1. Cell Culture

HepG2, 1321N1 and HEK 293 Cells were cultured as previously described in section 2.2.1.

5.2.2. Cell fractions preparation

Nuclear and cytosolic fractions were prepared as previously described in section 4.4.9

5.2.3. Protein Gels and Western Blots

Sample preparation

100µl of the cell fraction was mixed with 200µl of the 2x lysis buffer before boiling in waterbath for 5min as previously described in section 2.2.18.

Procedures

SDS PAGE and Western Blots of the cells fractions were carried out as described in section 2.2.18. The antibodies used were diluted as stated in Table 5. 1

Table 5.1. Antibodies for western blot

Antibodies	Catalogue number	Company	Dilution (μl)
GAPDH	Sc-25778	Santa Cruz Biotech.Inc	1:5000
Lamina B	Sc-6216	Santa Cruz Biotech.Inc	1:5000
Nrf2	Sc-13032	Santa Cruz	1:2000
HO1		Santa Cruz Biotech.Inc	1:2000
NQO1	Sc-25591	Santa Cruz Biotech.Inc	1:1000
Keap 1	Sc-33569	Santa Cruz Biotech.Inc	1:2000
γ-GCSc	Sc-22667	Santa Cruz Biotech.Inc.	1:1000
PKCα	Sc-208	Santa Cruz Biotech. Inc.	1:500
PKCδ	Sc-937	Santa Cruz Biotech.Inc	1:500
p-PKCδ	Sc-23770-R	Santa Cruz Biotech. Inc.	1:500

5.2.4. RNA isolation

SV Total RNA Isolation System (Cat.No Z3100

Total RNA was isolated with the SV Total RNA Isolation system (Cat.No Z3100) from Promega, USA, the components of which are listed in Table 5.2 below.

Table.5.2. SV Total RNA Isolation System Components

Components	Volume/Pack
RNA Lysis Buffer(4M guanidine isothiocyanate, GTC; 0.01M Tris, pH7.5)	50ml
RNA Dilution Buffer (blue buffer)	20ml
B-mercaptoethanol (48.7%)	2ml
DNase I (lyophilized)	1vial
$MnCl_2$ (0.09M)	250µl
Yellow Core Buffer	2.5ml
DNase Stop Solution (concentrated) (5M GTC; 10Mm Tris-HCl, pH 7.5)	5.3ml
RNA Wash Solution (concentrated) (162.8 mM potassium acetate; 27.1 mM Tris-HCl, pH7.5 at 25°C)	58.8ml
Nuclease-Free Water	13ml
Spin Column Assemblies and Elution Tubes (5 each/pack)	50packs

RNA Lysis Buffer

1 ml of β-mercaptoethanol was added to 50 ml of RNA Lysis Buffer.

RNA Wash Solution

100 ml of 95% ethanol was added to 58.8 ml concentrated RNA Wash Solution.

DNase Stop Solution

8 ml of 95% ethanol was added to the 5.3ml DNase Stop Solution.

95% ethanol

95 ml ethanol was made up to 100 ml with sterile water.

Spin Column Assemblies

This consists of the Spin Basket and 2 ml Collection Tube. The Spin Column Assemblies were made by putting the Spin Basket in the Collection Tube.

Procedures

Cells were seeded in 6well plates at a density of 10^6cells/well**.** The cells were allowed to attach and then treated with 5, 10 and 50 μM $CdCl_2$ for 24hr. The cells were washed with ice-cold, sterile 1xPBS and RNA isolation was performed using the SV Total RNA Isolation System (Cat. No Z3100) from Promega (USA). 175 μl RNA Lysis Buffer was added to each well and the cells were scraped with a sterile rubber policeman into sterile eppendorf tubes. The lysates were passed through 20-gauge needles to shear the genomic DNA. 350 μl of RNA Dilution Buffer (blue coloured) were added to the lysates and mixed by inverting the tubes 3-4times. The tubes were

incubated in a waterbath at 70°C for 3min and then centrifuged at 12,000-14,000 x *g* for 10min at 20-25°C. The clear supernatants were transferred into fresh eppendorf tubes and 200 µl 95% ethanol prepared in sterile water were added to the supernatant and mixed by pipetting 3-4times. The mixture was then transferred into the spin column assembly and centrifuged at 12,000-14,000 x *g* for one minute. The liquid in the collection tubes was discarded and 600 µl of RNA Wash Solution was added to the spin column assembly and centrifuged at 12,000-14,000x*g* for 1minute. The collection tubes were emptied and placed in a rack. 50 µl freshly prepared DNA incubation mix (40 µl Yellow Core Buffer; 5 µl 0.09M $MnCl_2$; 5 µl DNase I enzyme) per sample was added to the membrane inside the spin basket of the spin column assembly and incubated for 15minutes at 20-25°C. After the incubation, 200 µl of DNase Stop Solution was added to the spin basket and centrifuged at 12,000-14,000x*g* for 1minute. 600 µl RNA wash solution was added to the spin basket and centrifuged at 12,000-14,000 x *g* for 1minute. The liquid in the collection tubes was emptied and 250 µl RNA wash solution was added to the spin basket and centrifuged at 16,000x*g* for 2minutes. The spin basket was then transferred into 1.5ml Elution Tube and 100µl Nuclease-Free Water was added to the membrane of the spin basket and centrifuged at 12,000-14,000x*g* for 1minute. The liquid in the elution tube was then retained as purified RNA and stored at -70°C .

Determination of RNA Yield and Quality

RNA yield was determined spectrophotometrically at 260nm, where 1 absorbance unit (A_{260}) equals 40µg of single-stranded RNA/ml.
RNA purity was also estimated spectrophotometrically from the relative absorbance at 230, 260 and 280nm (i.e., A_{260}/A_{280} and A_{260}/A_{230}). A_{280} is the

absorbance due to protein contamination and A_{230} is the absorbance due to DNA contamination. Pure RNA has an A_{260}/A_{280} ratio between 1.7-2.1 and a A_{260}/A_{230} ratio of 1.8-2.2.

RNA integrity

0.5M EDTA (pH 8.0)

93.05g EDTA disodium salt (MW=372.2) was dissolved in 400ml deionised water and the pH was adjusted to 8.0 with NaOH. The solution was made up to 500ml with water.

50x TAE

242g Tris base (MW=121.14) was dissolved in 750ml deionised water and 57.1ml glacial acetic acid and 100ml of 0.5M EDTA (pH 8.0) were added. The solution was made up to 1L with deionised water.

1x TAE

Iml of 50x TAE was made up to 50ml with deionised water.

1% agarose

0.4g agarose (Flowgen, UK) was dissolved in 40ml of 1x TAE buffer and heated in a microwave oven until the agarose dissolved.

Agarose gel electrophoresis

The integrity of the purified RNA is determined by running the isolated RNA in 1% TAE agarose gel electrophoresis. The dissolved agarose (1%) was cooled to 50^{o}C and ethidium bromide was added to make a final concentration of 0.5µg/ml. The warm agarose was poured into the gel caster

and a comb was inserted. The gel was then allowed to set for 20-30min and the comb removed. The gel was then placed in the electrophoresis tank and the tank was filled with 1x TAE buffer. RNA Samples were then mixed with loading buffer (10x stock solution: 25% Ficoll, 0.25% Bromophenol blue) and the samples were loaded into the wells.The gel was run at 100V and visualized under ultraviolet light.

5.2.5. Quantitative Reverse Transcriptase-Polymerase Chain Reaction (qRT-PCR)

Reverse-transcriptase (cDNA) reaction (First-Strand cDNA Synthesis)

M-MLV Reverse Transcriptase (200u/µl).

PCR Nucleotide Mix (dNTP mix) (10mM)

Random Primers (500µg/ml)

M-MLV Reverse Transcriptase Buffer (5x)

Procedures

10µl RNA (about 0.5µg) and 1µl Random primer (46ng final concentration) was added together in a sterile eppendorf tube and incubated for 5minutes at 70^{o}C. The mixture was quickly cooled on ice for 5minutes after the incubation and 5µl M-MLV reverse transcriptase buffer (5 x); 1.25µl PCR nucleotide mix (0.5mM final concentration); 6.75µl Nuclease free water and 1µl M-MLV reverse transcriptase (added last) was added. The mixture was incubated for 10min at 25^{o}C and the PCR reaction was performed in 2-steps at the following conditions; incubation at 42^{o}C for 50minutes (step-1) and inactivation at 70^{o}C for 15minutes (step-2). The cDNA produced was stored at -20^{o}C.

Second- Strand cDNA Synthesis and Polymerase Chain Reaction Amplification

H_2O, PCR grade

$MgCl_2$ (25 mM) stock

PCR primer mix (100 μM)

LightCycler® DNA Master SYBR Green I (10x conc.)

cDNA template

Procedure

Amplification and detection of cDNA was performed with the LightCycler®DNA Master SYBR Green I (Roche Applied Science, Germany) using the LightCycler®2.0 System. The PCR mix contains: 12.8μl PCR grade H_2O; 1.2μl $MgCl_2$ (1.5mM final concentration); 2μl primer mix (1μl forward primer and 1μl reverse primer, final conc. 0.5μM); 2μl LightCycler®DNA Master SYBR Green I (10x) in a total volume of 18μl. The components were mixed by gentle pipetting up and down and then transferred into LightCycler ®Capillary. 2μl of cDNA was then added and the capillary sealed with a stopper. The capillary was spun with LC Carousel Centrifuge and then transferred into the LightCycler®Sample Carousel for PCR run.

LightCyler®2.0 System Protocol

The PCR parameters for a LightCycler®2.0 System PCR run with the LightCycler® DNA Master SYBR Green I are shown below in Table 5.3 and the pimers used for the PCR run are as listed in Table 5.4.

Table.5.3. PCR programme for LightCycler®2.0 System

Analysis Mode	Cycles	Segment	Target Temperature	Hold Time	Acquisition mode
			Denaturation		
None	1	1	95°C	30s	None
			Amplification		
Quantification	45	Denaturation	95°C	0s	None
		Annealing	Primer dependent	5s	None
		Extension	72°C	Amplicon[bp]/25s	Single
			Melting Curve		
Melting Curves	1	Denaturation	95°C	0s	None
		Annealing	65°C	15s	None
		Melting	95°C	0s	continuous
			Cooling		
None	1		40°C	30s	None

Table.5.4.Oligonucleotides for PCR Reaction

Oligonucleotide	Sequence	Annealing temperature (^oC)	Amplicon size (bp)
GAPDH(forward) GAPDH(reverse)	5′-GGAGTCAACGGATTTGGT-3′ 5′-GTGATGGGATTTCCATTG-3′	46.4	206
GSTA1(forward) GSTA1(reverse)	5′-TCTGCCCGTATGTCCACCT-3′ 5′-GCTCCTCGACGTAGTAGAGAAGT-3′	53	185
Nrf2(forward) Nrf2(reverse)	5′-ACACGGTCCACAGCTCATC-3′ 5′-TGTCAATCAAATCCATGTCCTG-3′	51	83
NQO1(forward) NQO1(reverse)	5′-ATGTATGACAAAGGACCCTTCC-3′ 5′-TCCCTTGCAGAGAGTACATGG-3′	53	88

The oligonucleotides were synthesised by Eurofins MWG operon (UK).

Relative Quantification of mRNA levels

The levels of the targeted mRNA were quantified using the "Comparative C_T Method ($\Delta\Delta C_T$ Method) as described by Applied Biosystems (UK).

Arithmetic Formula:

The amount of targeted genes normalised to endogenous reference genes such as GAPDH and relative to calibrator (control) genes is given by;

$$2^{-\Delta\Delta C_T}$$

C_T= the cycle threshold value at a constant level of fluorescence. The threshold fluorescence is the point at which the fluorescence rises appreciably above the background fluorescence. The level of fluorescence for C_T was taken as 1.0 for all calculations.

$\Delta C_T = C_{T\ target} - C_{T\ reference}$

$\Delta\Delta C_T = \Delta C_{T\ test\ sample} - \Delta C_{T\ calibrator\ sample}$

5.2.6. MTT assay for Inhibitors study

The inhibitors and their target proteins are as listed in Table 5.5

20 mM Bisindolymaleimide VIII.acetate (BMA)(stock)

1mg of BMA (MW=458.5; Simga, UK) was dissolved in 109.5µl distilled water.

10 µM BMA working solution

10µl of the 20mM BMA stock was made up to 20ml in culture media.

20 mM Rottlerin (Stock)

1mg of rottlerin (MW=516.6; Sigma, UK) was dissolved in 96.79µl DMSO.

10 µM Rottlerin working solution

10µl of 20mM rottlerin stock was made up to 20ml in culture media.

20 mM L-threo-dihydrosphingosine (Safingol) (stock)

1mg of safingol (MW=301.5; Sigma, UK) was dissolved in 165µl DMSO.

10 µM Safingol working solution

10µl of 20mM safingol was made up to 20ml with culture media.

20 mM PD98059 (Stock)

1mg of PD98059 (MW=267.3; Sigma, UK) was dissolved in 187µl DMSO.

10 µM PD98059 working solution

10µl of 20mM PD98059 was made up to 20ml with culture media.

Procedures

Cells were seeded in 96 well plates at a density of 10^3cells/ml. The cells were allowed to reach 80% confluent before the administration of 10μM inhibitor for 1hr. After the incubation period, the media were removed and different concentrations of $CdCl_2$ (0-50μM) were added to the cells for 24hr. MTT assay was performed according to the method described in section 2.2.4 under the materials and methods. Cell viability was expressed as percentage of control.

5.2.7. Western blot analysis for inhibitors study

Cells were seeded in 96 well plates for 24hr prior to treatment. After reaching 90% confluence, cells were exposed to 10μM BMA and 10μM rottlerin for 1hr prior to 24hr treatment with $CdCl_2$. The cytosolic and nuclear fractions were prepared as described in section 4.2.9 and western blot analysis was performed as described in section 4.2.10.

Table.5.5. PKCs and ERK1/2 MAPK Inhibitors

Inhibitors	Molecular weight	Target Protein
Bisindolymaleimide VIII. Acetate. (BMA)	458.5	Protein Kinase C (broad spectrum inhibitor)
L-Threo-dihydrosphingosine (Safingol)	301.5	PKCα
Rottlerin	516.6	PKCδ
PD98059	267.3	ERK1/2 MAPK

5.3. Results

5.3.1. Effects of $CdCl_2$ on the expression of Nrf2-dependent enzymes

In order to assess the response of protective enzymes to Cd exposure, HepG2, 1321N1 and HEK 293 cells were exposed to 5, 10 and 50μM $CdCl_2$ for 24hr and Western blots were carried out on whole cell extracts using NQO1, HO1 and γ- GCSc antibodies. The results show an increase in expression of these antioxidant enzymes in all cell lines as the concentration of $CdCl_2$ increases (Fig.5.1). This indicates an adaptive response to $CdCl_2$ insult in all the cell lines.

5.3.2. Effects of $CdCl_2$ on Nrf2 protein translocation

In order to evaluate the role of Nrf2 in mediating the adaptive response of the cells to Cd exposure, Nrf2 expression was monitored in the nuclear and cytosolic fractions of HepG2, 1321N1 and HEK 293 cell lines after 24hr exposure to 5, 10 and 50μM $CdCl_2$. The results show an increase in nuclear Nrf2 levels with increased $CdCl_2$ concentrations in all the cell lines (Fig.5.2B, 5.3B & 5.4B). These increases were found to correlate with the corresponding decrease in cytosolic Nrf2 levels (Fig.5.2A, 5.3A & 5.4A). The results show 5.89, 9.36 and 16-fold increases in nuclear Nrf2 levels in HepG2 cells at 5, 10 and 50μM $CdCl_2$ respectively when compared with the cytosolic fractions (Fig.5.2C). There were significant increases of 1.83, 12.62 and 22.95-fold in nuclear Nrf2 levels in 1321N1 cells at 5, 10 and 50μM $CdCl_2$ when compared with the cytosolic level (Fig.5.3C). A significant increase of 6.48 and 12.78-fold was also observed in the nuclear fraction of HEK 293 cells at 10 and 50μM $CdCl_2$ when compared with the cytosolic fractions (Fig.5.4C). Also increased levels of Keap1 protein was observed in the cytosolic fraction of all the three cell lines cells as the $CdCl_2$ concentrations increased (Fig.5.2A, 5.3A

& 5.4A). These sets of data indicate that Nrf2 translocates from the cytosol to the nucleus in the presence of Cd and this translocation may be due to the release of Nrf2 from the Nrf2-Keap1 complex.

Figure.5.1. Effects of different concentrations of $CdCl_2$ on HO1, NQO1 and γ-GCSc expressions after 24hr exposure

A.

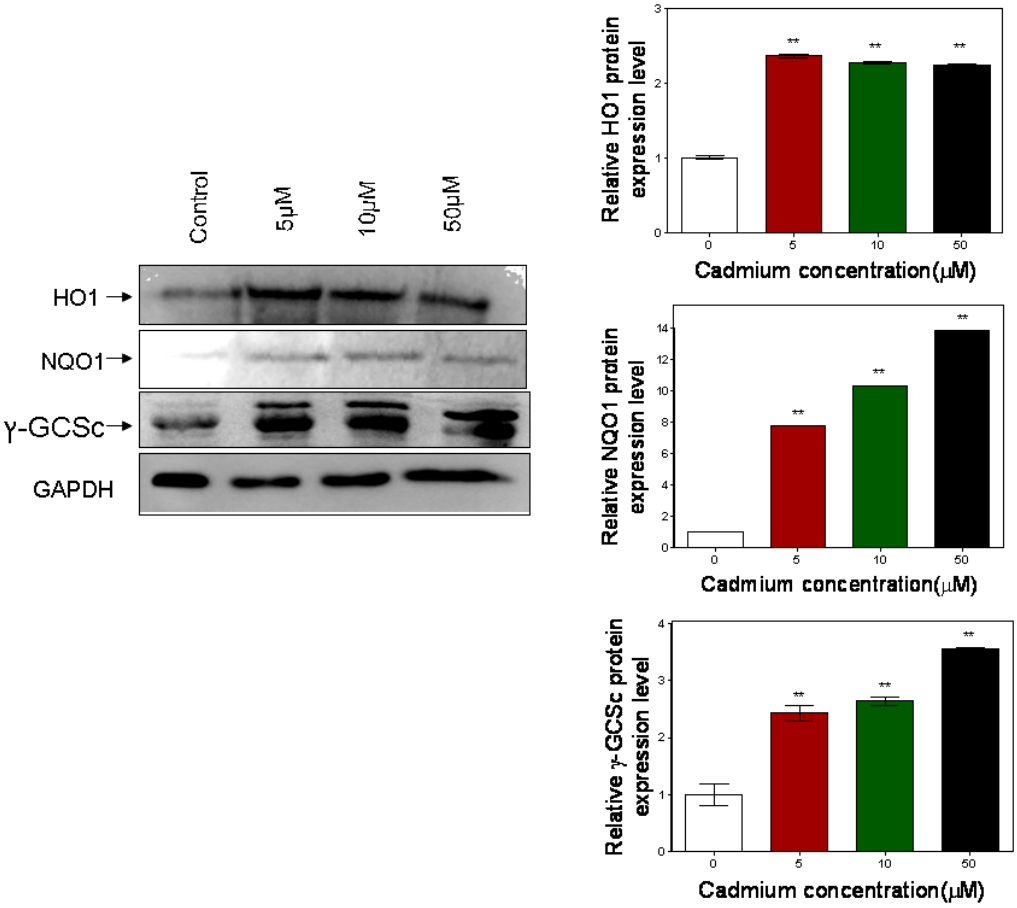

B.

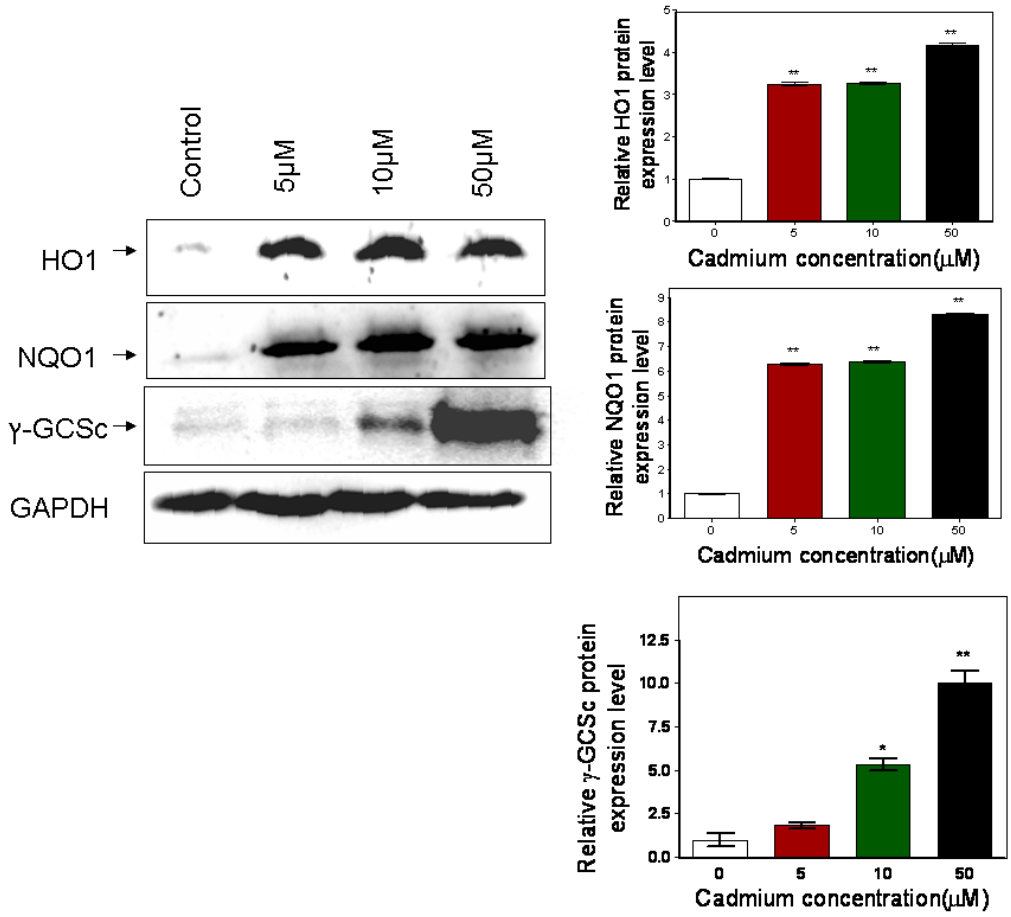
Control
5μM
10μM
50μM
HO1
NQO1
γ-GCSc
GAPDH
Relative HO1 protein expression level
Cadmium concentration(μM)
Relative NQO1 protein expression level
Cadmium concentration(μM)
Relative γ-GCSc protein expression level
Cadmium concentration(μM)

C.

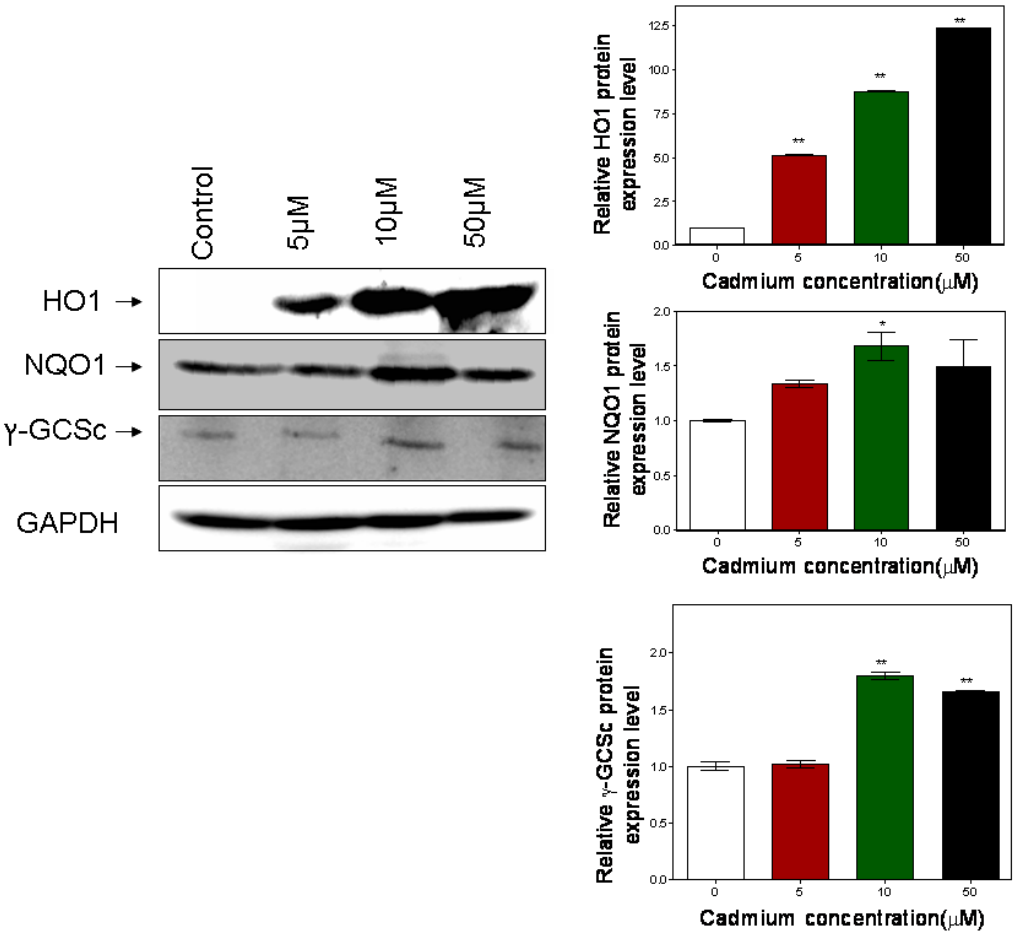

(A) HepG2, (B) 1321N1 and (C) HEK 293 cells were treated with 5, 10 and 50μM $CdCl_2$ for 24hr. HO1, NQO1 and γ-GCSc expression levels were determined in the whole cell extracts by western blot using specific HO1, NQO1 and γ-GCSc antibodies. GAPDH was used as an internal control for normalisation and loading of samples on 10% SDS-PAGE gel. The protein concentrations of the loaded samples were determined by Bradford method and approximately 9μg of samples were loaded. Protein bands were quantified by image J relative to untreated control and Data represent the mean value (n=3) relative to control ±SD. Asterisks indicate significant compared with untreated control (***p<0.005 **p<0.01 *p<0.05) using one-way ANOVA with Dunnett's post test.

Figure.5.2. Effects of different concentrations of $CdCl_2$ on Keap1 and Nrf2 expression in the cytosolic and nuclear fractions of HepG2 cells

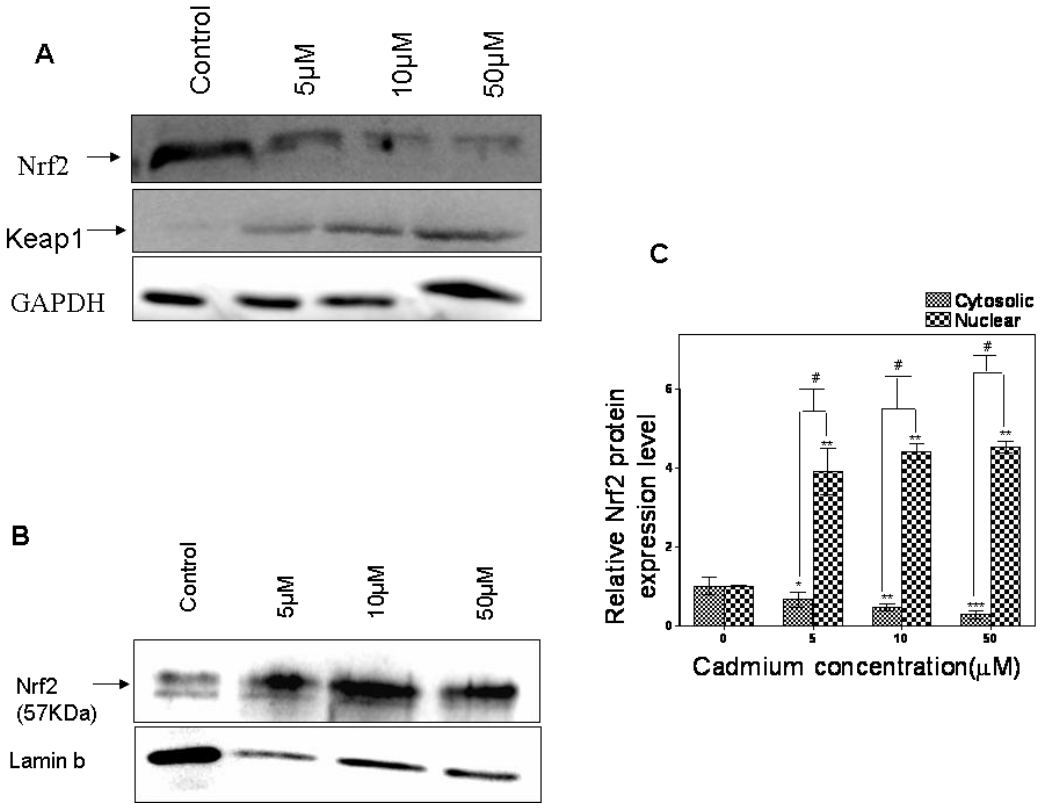

HepG2 cells were treated with 5, 10 and 50μM $CdCl_2$ for 24hr and cells fractions were prepared by differential centrifugation as described in Materials and Methods. Nrf2 protein expression levels were determined in the (A) cytosolic and (B) nuclear fractions by western blot using specific Nrf2 antibodies.Keap1 protein expression levels were determined in the (A) cytosolic fraction. Lamin b was used as an internal control for the normalisation and loading of nuclear fraction and GAPDH was used for the normalisation and loading of cytosolic fraction on 10% SDS-PAGE gel. The protein concentrations of the loaded samples were determined by Bradford method and approximately 9μg of samples were loaded. Protein bands were quantified by image J relative to untreated control. Relative Nrf2 expression was represented as (C) histogram and Data represent the mean value (n=3) relative to control ±SD. Asterisks indicate significant compared with untreated control (***$p<0.005$ **$p<0.01$ *$p<0.05$) using one-way ANOVA with Dunnett's post test; Significant between the nuclear and cytosolic fractions (#$p<0.005$) were compared using unpaired student's t-test.

Figure.5.3. Effects of different concentrations of $CdCl_2$ on Keap1 and Nrf2 expression in the cytosolic and nuclear fractions of 1321N1 cells

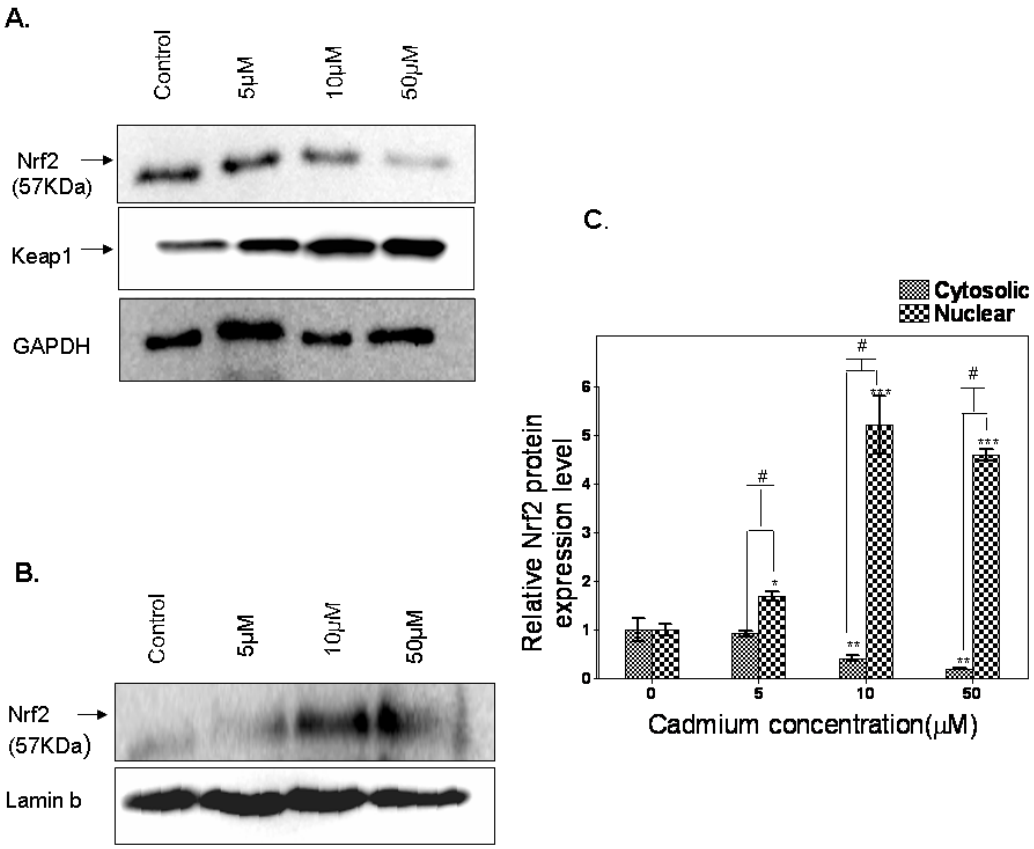

1321N1 cells were treated with 5, 10 and 50μM $CdCl_2$ for 24hr and cells fractions were prepared by differential centrifugation as described in Materials and Methods. Nrf2 protein expression levels were determined in the (A) cytosolic and (B) nuclear fractions by western blot using specific Nrf2 antibodies.Keap1 protein expression levels were determined in the (A) cytosolic fraction. Lamin b was used as an internal control for the normalisation and loading of nuclear fraction and GAPDH was used for the normalisation and loading of cytosolic fraction on 10% SDS-PAGE gel. The protein concentrations of the loaded samples were determined by Bradford method and approximately 9μg of samples were loaded. Protein bands were quantified by image J relative to untreated control. Relative Nrf2 expression was represented as (C) histogram and Data represent the mean value (n=3) relative to control ±SD. Asterisks indicate significant compared with untreated control (***$p<0.005$ **$p<0.01$ *$p<0.05$) using one-way ANOVA with Dunnett's post test; Significant between the nuclear and cytosolic fractions (#$p<0.005$) were compared using unpaired student's t-test.

Figure.5.4. Effects of different concentrations of $CdCl_2$ on Keap1 and Nrf2 expression in the cytosolic and nuclear fractions of HEK 293 cells

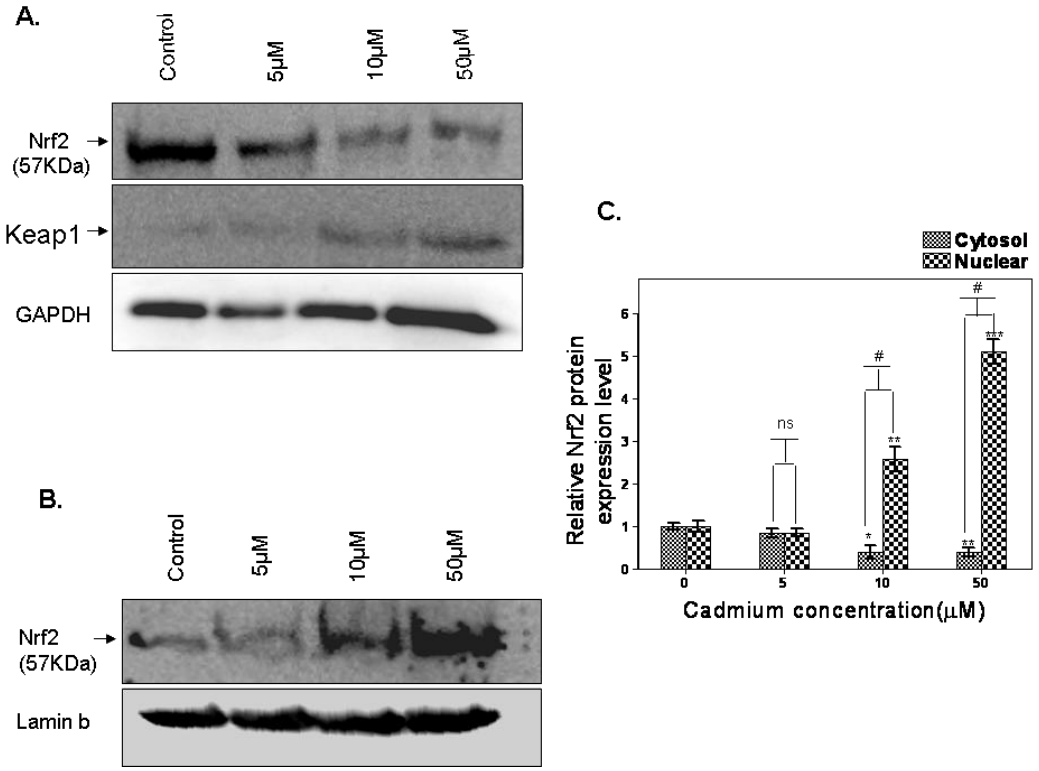

HEK 293 cells were treated with 5, 10 and 50μM $CdCl_2$ for 24hr and cells fractions were prepared by differential centrifugation as described in Materials and Methods. Nrf2 protein expression levels were determined in the (A) cytosolic and (B) nuclear fractions by western blot using specific Nrf2 antibodies.Keap1 protein expression levels were determined in the (A) cytosolic fraction. Lamin b was used as an internal control for the normalisation and loading of nuclear fraction and GAPDH was used for the normalisation and loading of cytosolic fraction on 10% SDS-PAGE gel. The protein concentrations of the loaded samples were determined by Bradford method and approximately 9μg of samples were loaded. Protein bands were quantified by image J relative to untreated control. Relative Nrf2 expression was represented as (C) histogram and Data represent the mean value (n=3) relative to control ±SD. Asterisks indicate significant compared with untreated control (***$p<0.005$ **$p<0.01$ *$p<0.05$); ns (non significant) using one-way ANOVA with Dunnett's post test; Significant between the nuclear and cytosolic fractions (#$p<0.005$) were compared using unpaired student's t-test.

5.3.3. Effects of $CdCl_2$ on Nrf2 mRNA level

To assess the effect of $CdCl_2$ exposure on Nrf2 mRNA levels in 1321N1 and HEK 293 cell lines, the cells were exposed to 5, 10 and 50μM $CdCl_2$ for 24hr and Nrf2 mRNA was quantified by qRT-PCR using Nrf2 specific oligonucleotide. The results show 1.61, 3 and 1.33-fold increase in Nrf2 mRNA levels in 1321N1 cells at 5, 10 and 50μM $CdCl_2$ respectively (Fig.5.5A). Similar increases of 3.09, 3.90 and 2.73-fold were obtained in HEK 293 cells Nrf2 mRNA levels at 5, 10 and 50μM $CdCl_2$ respectively (Fig.5.5B). The increased Nrf2 mRNA levels in 1321N1cells were significant at 5 and 10μM $CdCl_2$ and at 5, 10 and 50 μM in HEK 293 cells. The melting and amplification curves (Fig.5.6) show that the qRT-PCR was very efficient and that only the Nrf2 gene was amplified. These sets of data seem to show that 1321N1 and HEK 293 cells respond to Cd exposure by enhancing Nrf2 gene transcription.

Figure.5.5. Nrf2 mRNA levels after $CdCl_2$ exposure.

A.

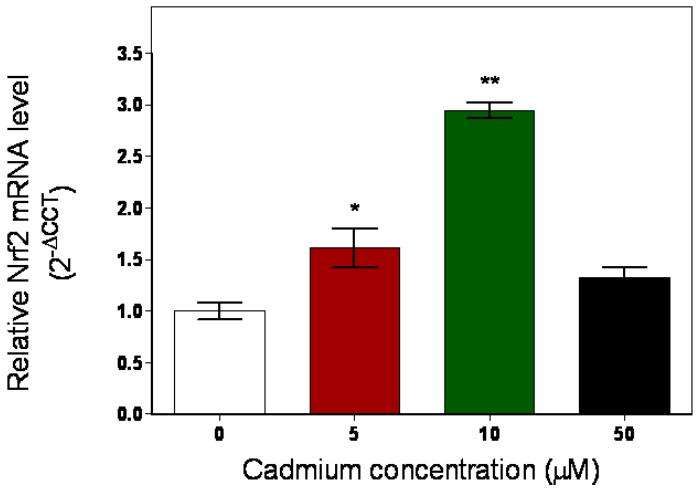

B.

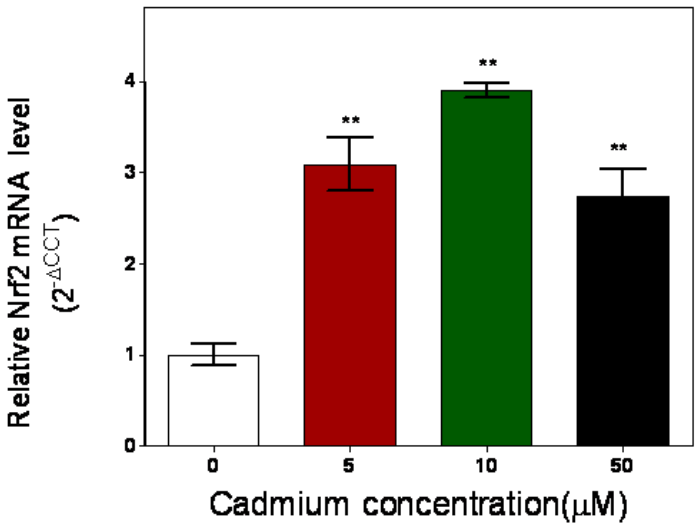

(A) 1321N1 and (B) HEK 293 cells were treated with 5, 10 and 50μM $CdCl_2$ for 24hr and total mRNA was isolated using SV Total RNA Isolation System. Nrf2 mRNA level was quantified by QRT-PCR using the LightCyler SYBRgreen I as described in Materials and Methods. Nrf2 mRNA was normalised to GAPDH mRNA and expressed relative to untreated control. Relative mRNA expression levels were calculated by the delta-delta Ct ($2^{-\Delta\Delta CT}$) method. Data represent the mean value (n=6 individual assay done in triplicate) relative to control ±SD. Asterisks indicate significant compared with untreated control (***p<0.005 **p<0.01 *p<0.05) using one-way ANOVA with Dunnett's post test.

Figure.5.6. Melting and amplification Curves of Nrf2 genes in 1321N1 cells after 24hr exposure to $CdCl_2$.

A.

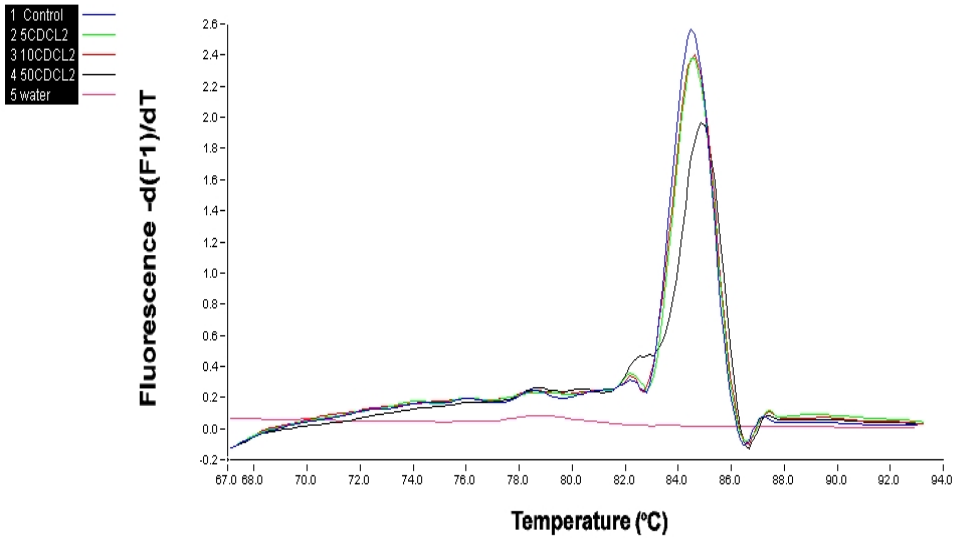

B.

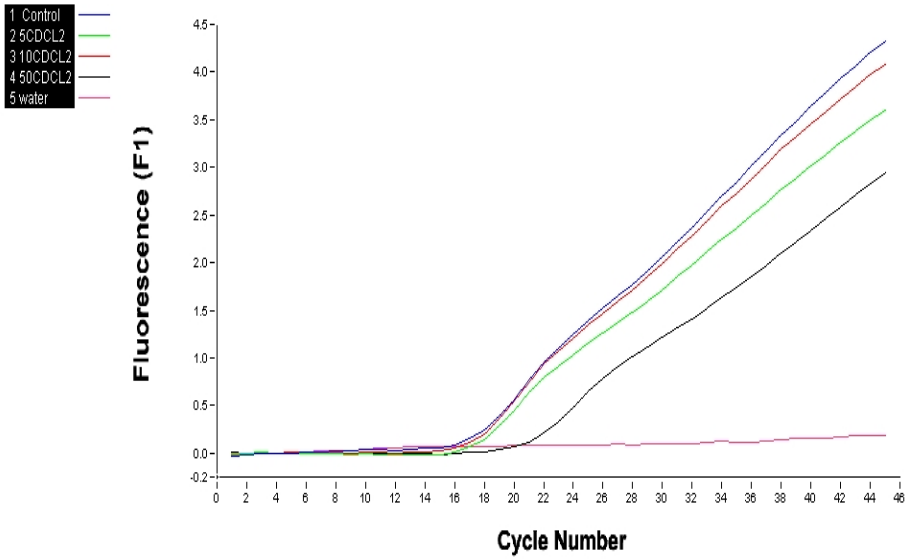

(A)Melting and (B) amplification curves for Nrf2 genes in 1321N1 cells.

5.3.4. Effects of $CdCl_2$ on GSTA1 mRNA expression

In order to assess the effect of Cd on GSTA1 mRNA levels, cells were exposed to 5, 10 and 50μM $CdCl_2$ for 24hr and total mRNA was isolated. Quantitative RT-PCR was then performed on the isolated RNA using GSTA1 specific oligonucleotide primers. The quantification was carried out using a LightCycler®2.0 System. The results show a significant 3-fold increase in GSTA1 mRNA level at 50μM $CdCl_2$ and a significant 2.58 and 7.21-fold increase at 5 and 10μM $CdCl_2$ respectively in 1321N1 cells (Fig.5.7A). There were also significant 2.94, 2.59 and 4.61-fold increases in GSTA1 mRNA levels at 5, 10 and 50μM $CdCl_2$ in HEK 293 cells (Fig.5.7B). These results indicate that GSTA1 may play important role in cytoprotection in 1321N1 cells exposed to Cd as the gene transcription was induced at all concentrations of Cd exposure.

5.3.5. Effects of $CdCl_2$ on NQO1 mRNA expression

In an attempt to define the involvement of NQO1 in the adaptive response of cells exposed to Cd, 1321N1 and HEK 293 cells were exposed to 5, 10 and 50μM $CdCl_2$ for 24hr and the level of NQO1 mRNA was quantified by qRT-PCR. The results show significant increases in NQO1 mRNA levels at all the concentrations of $CdCl_2$ exposure in 1321N1 cells (Fig.5.8A).The highest (4.6-fold) NQO1 mRNA level in 1321N1 was observed at 10μM of $CdCl_2$ exposure (Fig.5.8A). Similarly, there was a significant increase in NQO1 mRNA levels in HEK 293 cells following exposure to 5 (5.46-fold), 10 (10-fold) and 50μM (5.4-fold) $CdCl_2$ (Fig.5.8B).These results therefore suggested that induction of NQO1 gene transcription may be involved in the adaptive response of these cell lines to Cd.

Figure.5.7. GSTA1 mRNA levels after $CdCl_2$ exposure.

A.

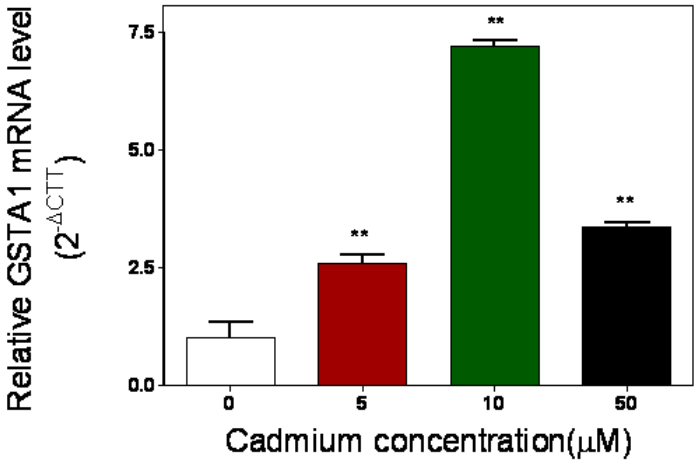

B.

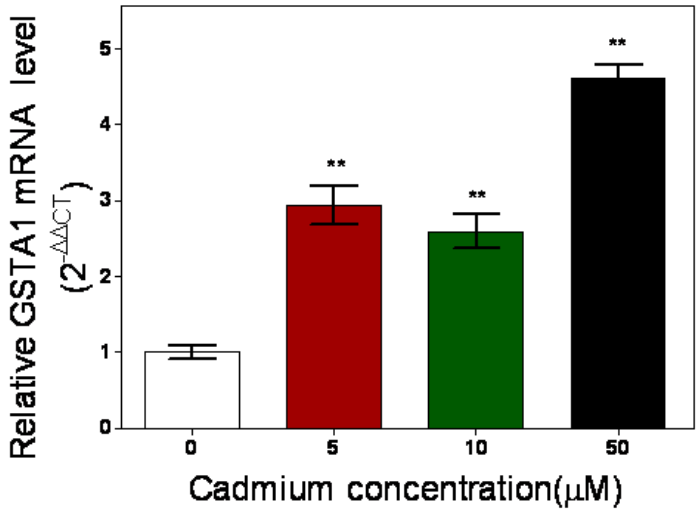

(A) 1321N1 and (B) HEK 293 cells were treated with 5, 10 and 50μM $CdCl_2$ for 24hr and total mRNA was isolated using SV Total RNA Isolation System. GSTA1 mRNA level was quantified by QRT-PCR using the LightCyler SYBRgreen I as described in Materials and Methods. GSTA1 mRNA was normalised to GAPDH mRNA and expressed relative to untreated control. Relative mRNA expression levels were calculated by the delta-delta Ct ($2^{-\Delta\Delta CT}$) method. Data represent the mean value (n=6 individual assay done in triplicate) relative to control ±SD. Asterisks indicate significant compared with untreated control (***$p<0.005$ **$p<0.01$ *$p<0.05$) using one-way ANOVA with Dunnett's post test.

Figure5.8. NQO1 mRNA levels after $CdCl_2$ exposure

A.

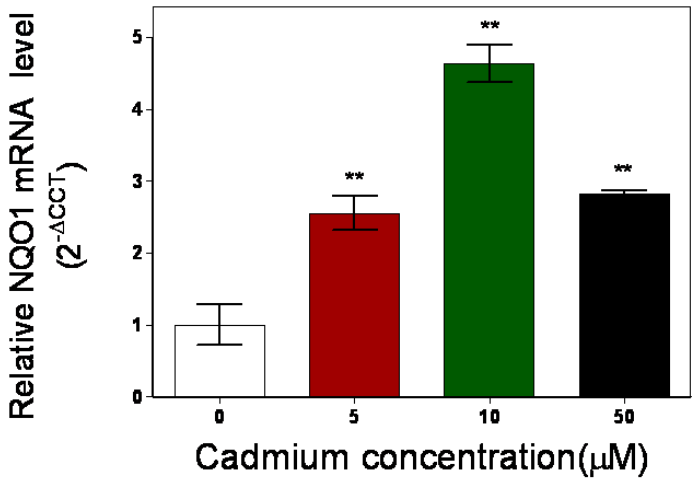

B.

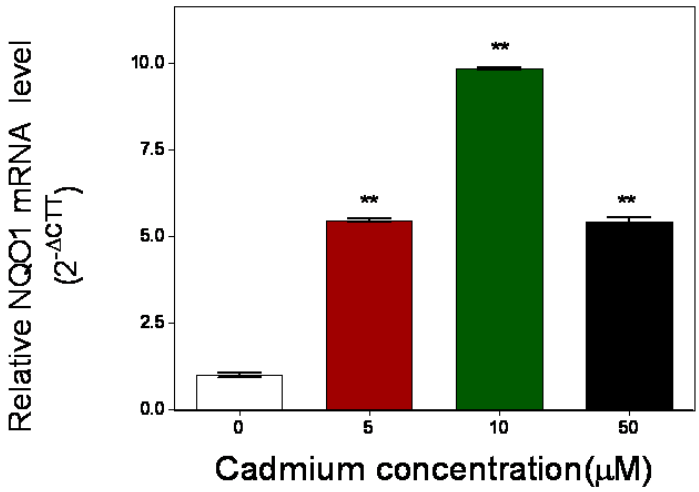

(A) 1321N1 and (B) HEK 293 cells were treated with 5, 10 and 50μM $CdCl_2$ for 24hr and total mRNA was isolated using SV Total RNA Isolation System. NQO1 mRNA level was quantified by QRT-PCR using the LightCyler SYBRgreen I as described in Materials and Methods. NQO1 mRNA was normalised to GAPDH mRNA and expressed relative to untreated control. Relative mRNA expression levels were calculated by the delta-delta Ct ($2^{-\Delta\Delta CT}$) method. Data represent the mean value (n=6 individual assay done in triplicate) relative to control ±SD. Asterisks indicate significant compared with untreated control (***p<0.005 **p<0.01 *p<0.05) using one-way ANOVA with Dunnett's post test.

5.3.6. Effects of broad spectrum PKC inhibitor (BMA) on Nrf2 translocation after $CdCl_2$ treatment

In order to investigate the involvement of protein kinase C (PKC) on the translocation of Nrf2 from the cytosol into the nucleus, the localization of Nrf2 was examined in both the nucleus and the cyotosol in cells pre-treated and unpretreated with BMA before $CdCl_2$ exposure. The results show that the presence of BMA caused 2.46, 1.96 and 3.17-fold increase in cytosolic Nrf2 at 5, 10 and 50μM $CdCl_2$ respectively in HepG2 cells when compared with its absence (Fig.5.9A). The presence of BMA also caused a reduction in nuclear Nrf2 proteins by 2.17 and 17.8-fold at 10 and 50μM $CdCl_2$ in HepG2 (Fig.5.9B).The results also show 4.36, 9.17 and 3.64-fold increase in Nrf2 expression in the cytosol of the BMA pre-treated 1321N1 cells at 5, 10 and 50 μM $CdCl_2$ respectively when compared to the cells exposed to $CdCl_2$ only (Fig.5.10A). However, corresponding decreases of 3.66, 2.17 and 7.80-fold in nuclear Nrf2 protein levels at 5, 10 and 50μM $CdCl_2$ respectively were obtained in the presence of BMA when compared with its absence (Fig.5.10B). HEK 293 cells showed a 5.11, 1.32 and 1.33-fold increase in Nrf2 levels in the cytosol of 10μM BMA pre-treated cells after exposure to 5, 10 and 50μM $CdCl_2$ respectively when compared with its absence (Fig.5.11A). A 2.37 and 3.3-fold decrease in nuclear Nrf2 protein levels at 10 and 50μM $CdCl_2$ was obtained in the presence of BMA when compared with its absence (Fig.5.11B). This set of data seems to suggest that PKC may be involved in mediating Nrf2 translocation from the cytosol into the nucleus following Cd-treatment in the three cell lines.

Figure 5.9.Effects of broad spectrum PKC inhibitor, bisindolylmaleimide (VIII) acetate (BMA), on Nrf2 protein expression in the cytosolic and nuclear fractions of HepG2 cells after Cd exposure

A.

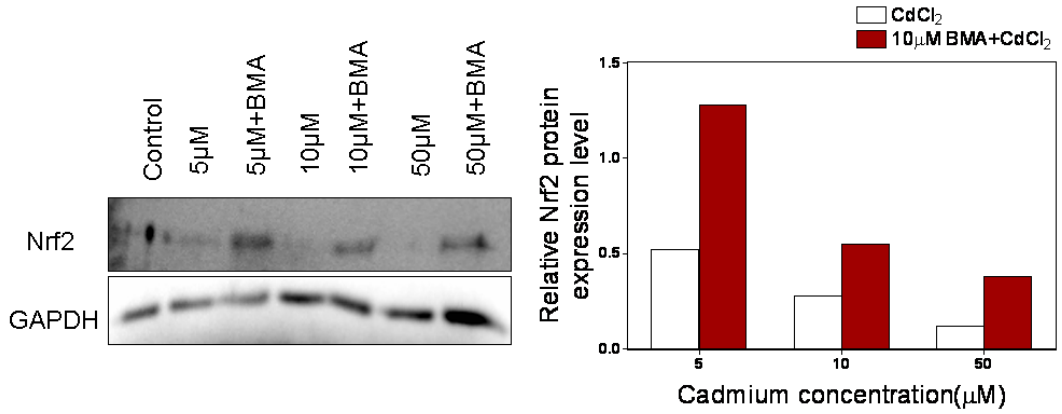

B.

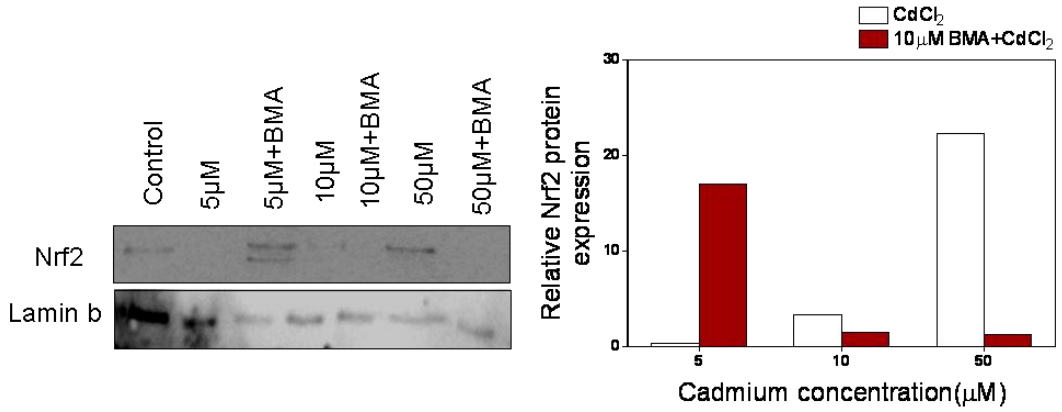

HepG2 cells were pre-treated with 10µM BMA for 1hour followed by treatment with 5, 10 and 50µM $CdCl_2$ for 24hr in both the BMA pre-treated and unpretreated cells. (A) Cytosolic and (B) Nuclear fractions were prepared by differential centrifugation and Western blot analyses were carried out using Nrf2 specific antibody as described in Materials and Methods. Lamin b was used as an internal control for the normalisation and loading of nuclear fraction and GAPDH was used for the normalisation and loading of cytosolic fraction on 10% SDS-PAGE gel. The protein concentrations of the loaded samples were determined by Bradford method and approximately 12µg of samples were loaded. Protein bands were quantified by image J relative to untreated control. Relative Nrf2 expression was represented as histogram.

Figure 5.10.Effects broad spectrum PKC inhibitor, bisindolylmaleimide (VIII) acetate (BMA), on Nrf2 protein expression in the cytosolic and nuclear fractions of 1321N1 cells after Cd exposure

A.

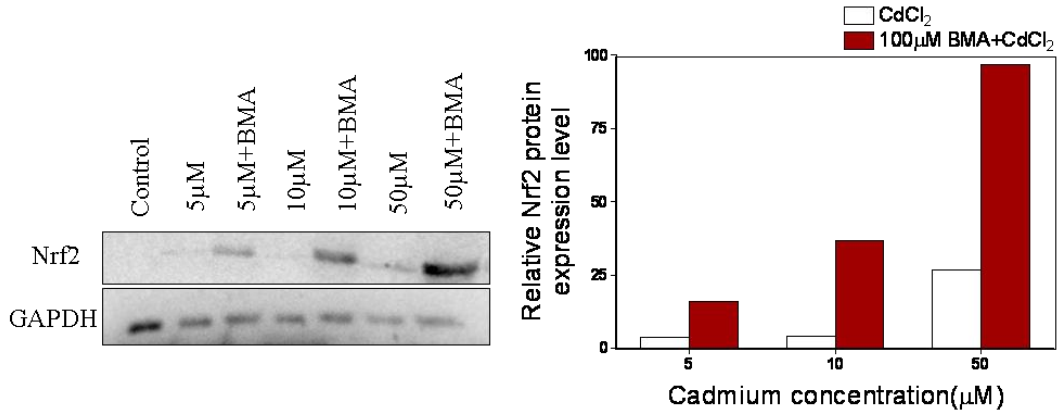

B.

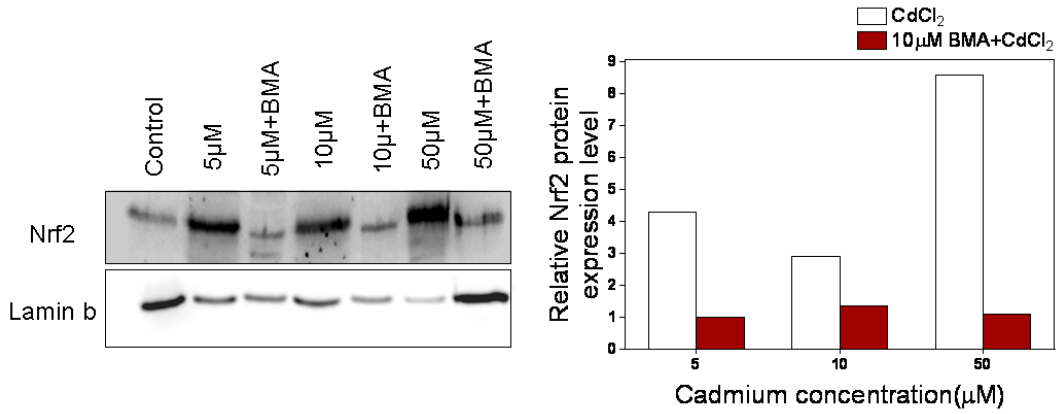

1321N1 cells were pre-treated with 10μM BMA for 1hour followed by treatment with 5, 10 and 50μM $CdCl_2$ for 24hr in both the BMA pre-treated and unpretreated cells. (A) Cytosolic and (B) Nuclear fractions were prepared by differential centrifugation and Western blot analyses were carried out using Nrf2 specific antibody as described in Materials and Methods. Lamin b was used as an internal control for the normalisation and loading of nuclear fraction and GAPDH was used for the normalisation and loading of cytosolic fraction on 10% SDS-PAGE gel. The protein concentrations of the loaded samples were determined by Bradford method and approximately 12μg of samples were loaded. Protein bands were quantified by image J relative to untreated control. Relative Nrf2 expression was represented as histogram.

Figure 5.11.Effects broad spectrum PKC inhibitor, bisindolylmaleimide (VIII) acetate (BMA), on Nrf2 protein expression in the cytosolic and nuclear fractions of HEK 293 cells after Cd exposure

A.

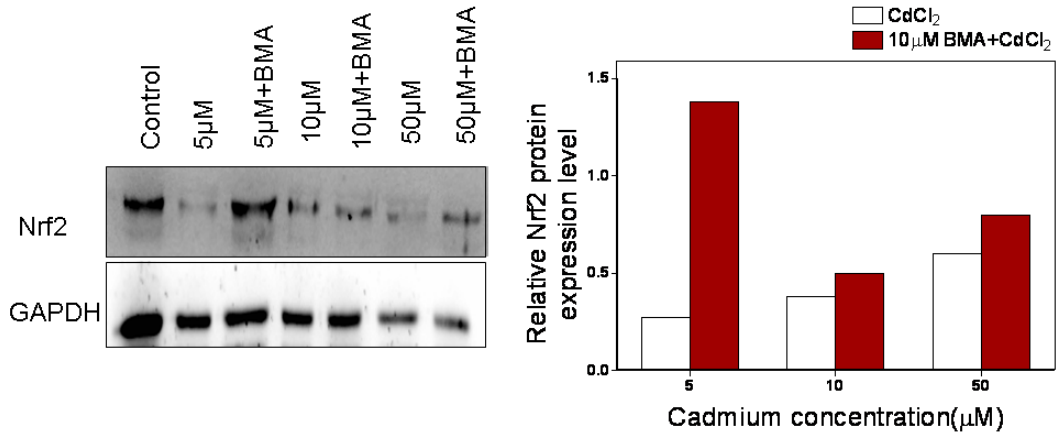

B.

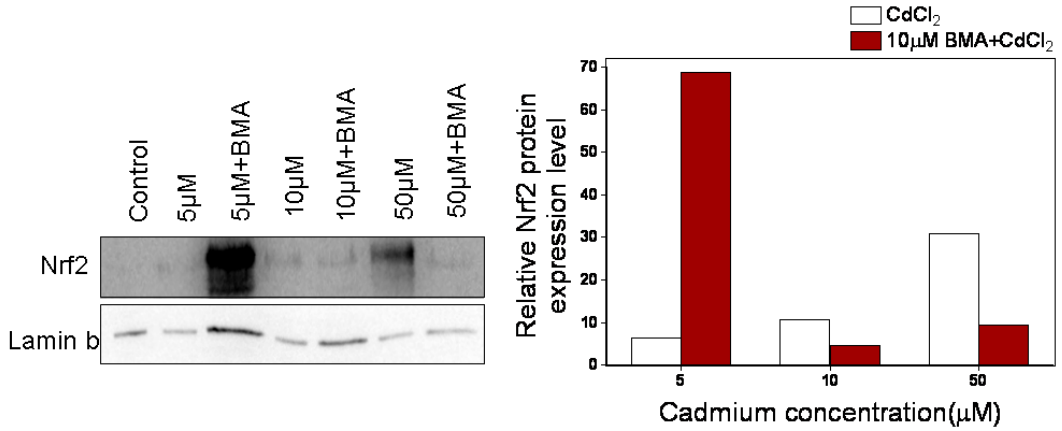

HEK 293 cells were pre-treated with 10μM BMA for 1hour followed by treatment with 5, 10 and 50μM $CdCl_2$ for 24hr in both the BMA pre-treated and unpretreated cells. (A) Cytosolic and (B) Nuclear fractions were prepared by differential centrifugation and Western blot analyses were carried out using Nrf2 specific antibody as described in Materials and Methods. Lamin b was used as an internal control for the normalisation and loading of nuclear fraction and GAPDH was used for the normalisation and loading of cytosolic fraction on 10% SDS-PAGE gel. The protein concentrations of the loaded samples were determined by Bradford method and approximately 12μg of samples were loaded. Protein bands were quantified by image J relative to untreated control. Relative Nrf2 expression was represented as histogram.

5.3.7. Effects of $CdCl_2$ on PKCδ, p-PKCδ and PKCα protein expression.

PKCs have been implicated in Nrf2 translocation in response to stress. Therefore, in order to ascertain the involvement of PKCα and PKCδ in eliciting Nrf2-ARE mediated protective response in Cd exposed cells, cells were exposed to 5, 10 and 50μM $CdCl_2$ for 24hr and the expression of individual PKCs was evaluated using Western blots. The results revealed a 2.49 and 2.59-fold increase in PKCδ expression levels at 10 and 50μM $CdCl_2$ exposure respectively in HepG2 cells (Fig.5.12A). A corresponding increase of 3.67, 13 and 10.67-fold were obtained in the phosphorylated form of PKCδ (p-PKCδ) expression after exposure to 5, 10 and 50μM $CdCl_2$ respectively in HepG2 cells (Fig.5.12A). The results also show a 7.73 and 9.27-fold increased PKCα expression at 10 and 50μM $CdCl_2$ respectively in HepG2 cells (Fig.5.12B). There were 12, 8 and 11-fold increased in p-PKCδ expression after exposure to 5, 10 and 50μM $CdCl_2$ in HEK 293 cells (Fig.5.13A). There was a 2.0-fold increased in PKCα expressions at 10 and 50μM $CdCl_2$ in HEK 293 cells (Fig.5.13B). These results seem to suggest that PKCδ and PKCα may be activated in Cd exposed HepG2 and HEK 293 cell lines.

Figure5.12. Effects of $CdCl_2$ exposure on PKCδ, p-PKCδ and PKCα expressions in HepG2 cells

A.

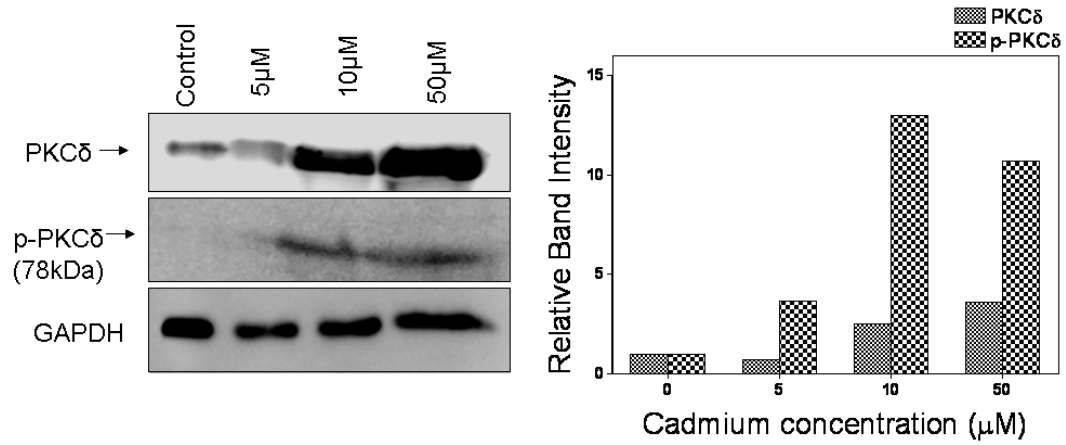

B.

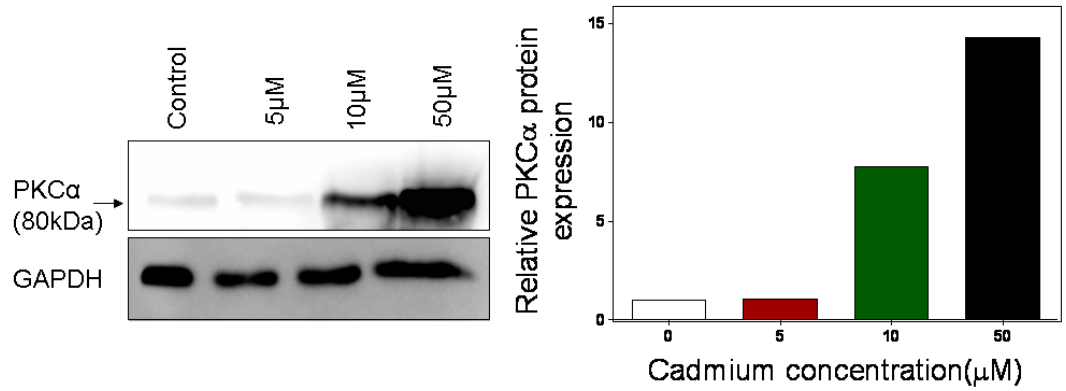

HepG2 cells were treated with 5, 10 and 50μM $CdCl_2$ for 24hr and (A) PKCδ and p-PKCδ and (B) PKCα expression levels were determined in the whole cell extracts by western blot using specific PKCδ, p-PKCδ and PKCα antibodies. GAPDH was used as an internal control for normalisation and loading of samples on 10% SDS-PAGE gel. The protein concentrations of the loaded samples were determined by Bradford method and approximately 9μg of samples were loaded. Protein bands were quantified by image J and compared relative to untreated control. Relative PKCδ, p-PKCδ and PKCα protein expressions were represented as histogram.

Figure5.13. Effects of $CdCl_2$ exposure on PKCδ, p-PKCδ and PKCα expressions in HEK 293 cells

A.

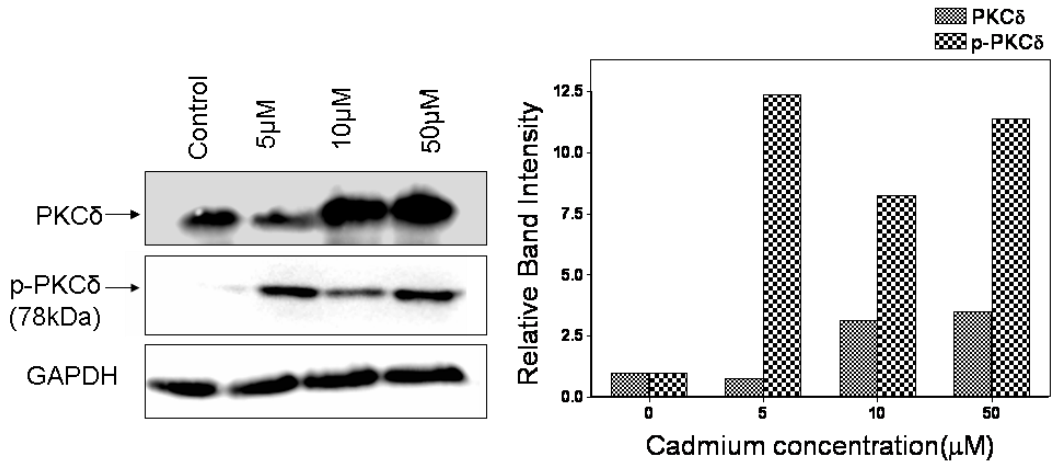

B.

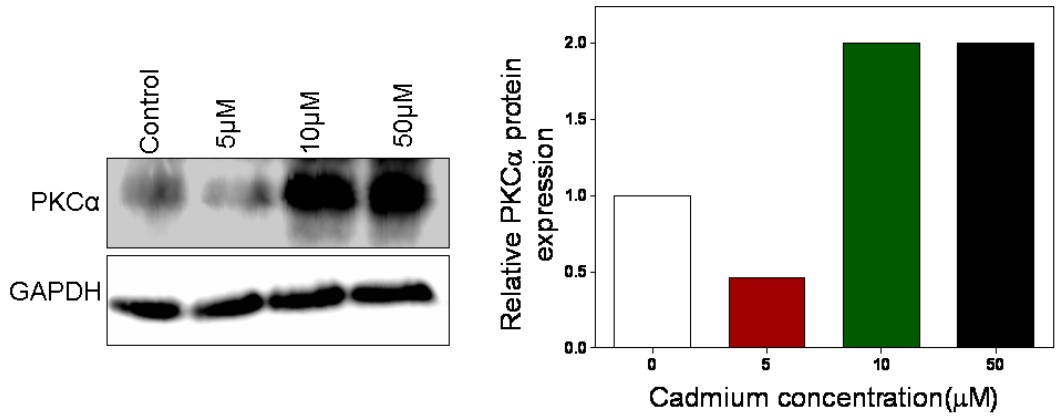

HEK 293 cells were treated with 5, 10 and 50μM $CdCl_2$ for 24hr and (A) PKCδ and p-PKCδ and (B) PKCα expression levels were determined in the whole cell extracts by western blot using specific PKCδ, p-PKCδ and PKCα antibodies. GAPDH was used as an internal control for normalisation and loading of samples on 10% SDS-PAGE gel. The protein concentrations of the loaded samples were determined by Bradford method and approximately 9μg of samples were loaded. Protein bands were quantified by image J and compared relative to untreated control. Relative PKCδ, p-PKCδ and PKCα protein expressions were represented as histogram.

5.3.8. Effects of PKCδ inhibitor (rottlerin) on GSTA1 mRNA expression in 1321N1 cells after $CdCl_2$ exposure

In order to evaluate the effect of PKCδ on the GSTA1 gene transcription after $CdCl_2$ exposure, 1321N1 cells were pre-treated with 10μM Rottlerin prior to 24hr exposure to 5 and 10μM $CdCl_2$. The results show 3.85 and 1.92-fold decrease in GSTA1 mRNA levels at 5 and 10μM $CdCl_2$ respectively in the presence of rottlerin when compared with its absence (Fig. 5.14). These results show that PKCδ may play a role in the expression of GSTA1 genes in 1321N1 cells exposed to $CdCl_2$.

5.3.9. Effects of PKCδ inhibitor (rottlerin) on NQO1 mRNA expression in 1321N1 cells after $CdCl_2$ exposure

NQO1 is one of the cytoprotective enzyme regulated by the Nrf2-Keap1 pathway. Therefore, in order to define the involvement of PKCδ in the expression of this protein, 1321N1 cells were exposed to 10μM Rottlerin prior to 24hr exposure to 5 and 10μM $CdCl_2$. The results show a 3.68 and 8.77-fold decreased in NQO1 mRNA levels at 5 and 10μM $CdCl_2$ respectively in the presence of rottlerin when compared with its absence (Fig.5.15). These results show that PKCδ may be involve in NQO1 gene expression in 1321N1 cells exposed to $CdCl_2$.

Figure 5.14. Effects of PKCδ inhibitor (rottlerin) on GSTA1 mRNA levels in 1321N1 cells after exposure to $CdCl_2$

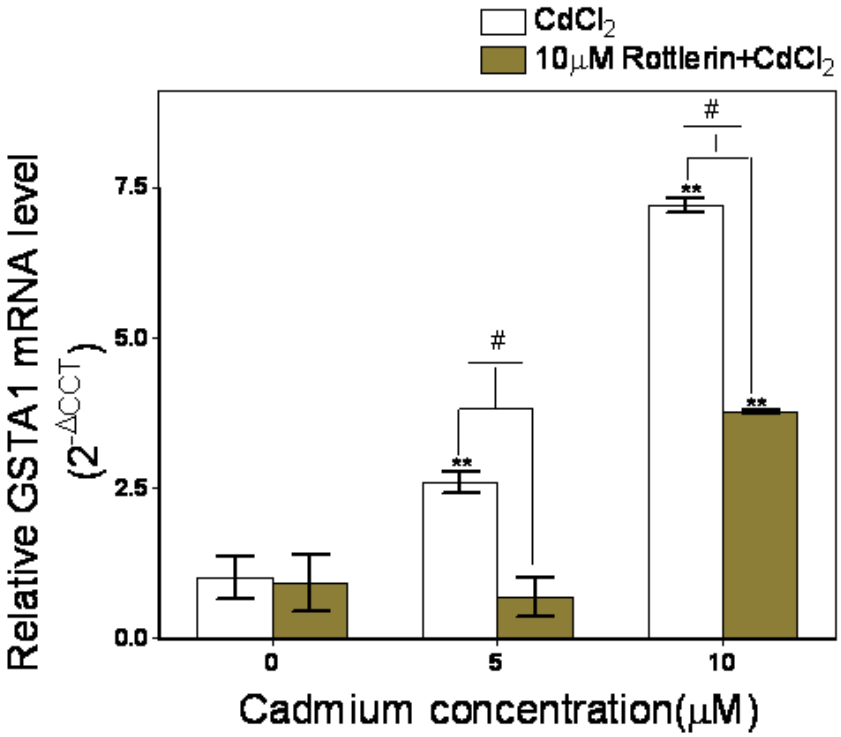

1321N1 cells were pre-treated with 10μM Rottlerin for 1hour before 24hr exposure to 5 and 10μM $CdCl_2$. Total RNA was isolated and qRT- PCR was carried out as described in Materials and Methods. GSTA1 mRNA was normalised to GAPDH mRNA and expressed relative to untreated control. Relative GSTA1 mRNA expression levels were calculated by the delta-delta Ct ($2^{-\Delta\Delta CT}$) method. Data represent the mean value (n=3 individual assay done in triplicate) relative to control ±SD. Asterisks indicate significant compared with untreated control (***p<0.005 **p<0.01 *p<0.05) using one-way ANOVA with Dunnett's post test; Comparison between pre-treated and unpre-treated groups was performed using the unpaired student t-test (#p<0.05).

Figure5.15. Effects of PKCδ inhibitor (rottlerin) on NQO1 mRNA levels in 1321N1 cells after exposure to $CdCl_2$

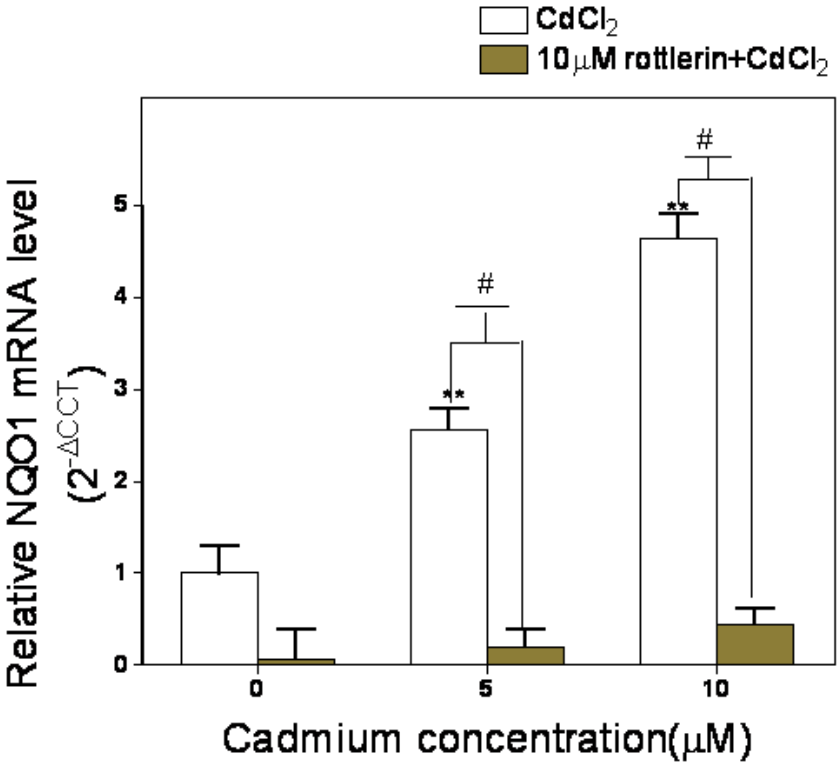

1321N1 cells were pre-treated with 10μM Rottlerin for 1hour before 24hr exposure to 5 and 10μM $CdCl_2$. Total RNA was isolated and qRT- PCR was carried out as described in Materials and Methods. NQO1 mRNA was normalised to GAPDH mRNA and expressed relative to untreated control. Relative NQO1 mRNA expression levels were calculated by the delta-delta Ct ($2^{-\Delta\Delta CT}$) method. Data represent the mean value (n=3 individual assay done in triplicate) relative to control ±SD. Asterisks indicate significant compared with untreated control (***$p<0.005$ **$p<0.01$ *$p<0.05$) using one-way ANOVA with Dunnett's post test; Comparison between pre-treated and unpre-treated groups was performed using the unpaired student t-test (#$p<0.05$).

5.3.10. Effects of PKCδ inhibitor, rottlerin, on Nrf2 protein translocation in 1321N1 cells after Cd exposure

In order to evaluate the effects of PKCδ on Nrf2 translocation from the cytosol into the nucleus, 1321N1 cells was treated with 10μM rottlerin for 1hour before 24hr exposure to 5 and 10μM $CdCl_2$. The results show a 1.54 and 4.1-fold decrease in cytosolic Nrf2 levels at 5 and 10μM $CdCl_2$ in the absence of rottlerin when compared with its absence (Fig.5.16A). A corresponding increase of 7 and 5-fold in nuclear Nrf2 was observed in absence of rottlerin when compared with its presence (Fig.5.16B). These results show that PKCδ may be involved in mediating Nrf2 translocation from the cytosol into the nucleus and may therefore play an important role in the regulation of cytoprotective enzymes levels.

Fig.5.16.Effects of PKCδ inhibitor, rottlerin, on Nrf2 protein expression in the cytosolic and nuclear fractions of 1321N1 cells after Cd exposure

A.

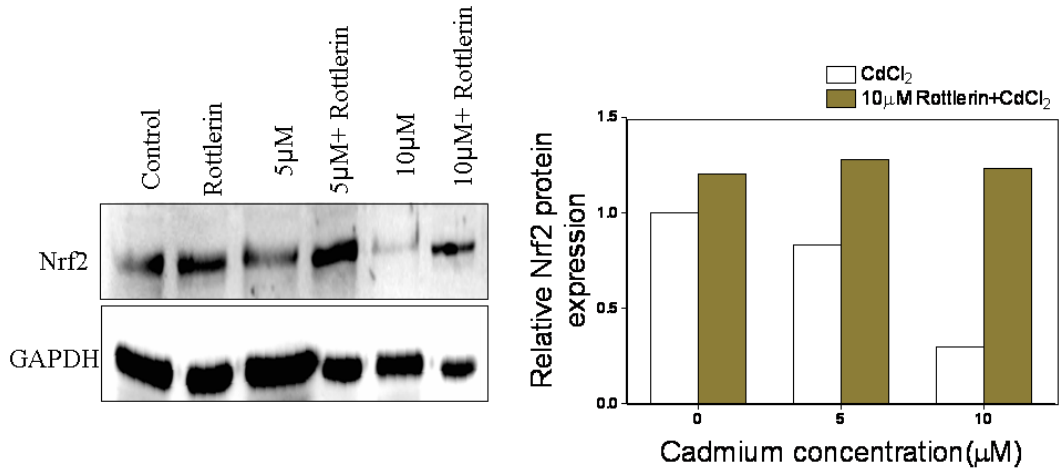

B.

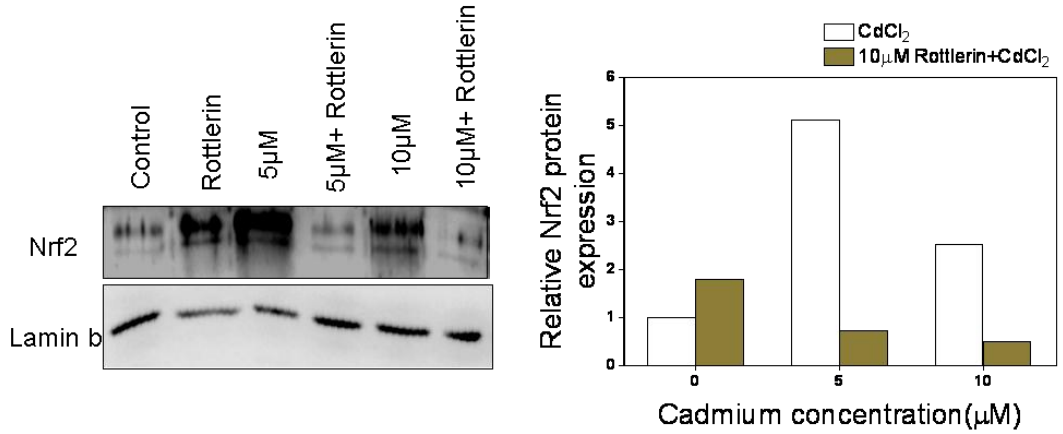

1321N1 cells were pre-treated with 10μM rottlerin for 1hour followed by treatment with 5, 10 and 50μM $CdCl_2$ for 24hr in both the rottlerin pre-treated and unpretreated cells. (A) Cytosolic and (B) Nuclear fractions were prepared by differential centrifugation and Western blot analyses were carried out using Nrf2 specific antibody as described in Materials and Methods. Lamin b was used as an internal control for the normalisation and loading of nuclear fraction and GAPDH was used for the normalisation and loading of cytosolic fraction on 10% SDS-PAGE gel. The protein concentrations of the loaded samples were determined by Bradford method and approximately 12μg of samples were loaded. Protein bands were quantified by image J relative to untreated control. Relative Nrf2 expression was represented as histogram.

5.3.11. Effects of PKCs and ERK1/2 inhibitors on cell viability in the presence of $CdCl_2$

In order to determine the role of PKC and ERK1/2 in mediating the adaptive response to Cd toxicity, cells were pre-treated with 10μM of BMA (a non-specific PKC inhibitor), Safingol (PKCα specific inhibitor), Rottlerin (PKCδ specific inhibitor) and PD98059 (ERK1/2 specific inhibitor) for 1 hour prior to $CdCl_2$ exposure for 24hr. The results show that there was a significant decrease in HepG2 cell viability in the presence and absence of each of the inhibitors when compared with control (Fig.5.17A). However, there was no significant difference in HepG2 cell viability between the cells pre-treated with any of the inhibitors and the cells treated with $CdCl_2$ alone, except at 5μM $CdCl_2$ in the presence of BMA (Fig.5.17A). The data show that the presence of BMA in HepG2 cells impaired cell survival more than any of the other inhibitors with 1.79, 1.91 and 2.35-fold decrease in cell viability in the presence of 5, 10 and 25μM $CdCl_2$ when compared with HepG2 cells that had not been exposed to inhibitor (Fig.5.17A). In 1321N1 cells, the presence of BMA significantly decreased cell viability when compared with control (Fig5.17B). Also when compared with cells exposed to $CdCl_2$ only, the presence of BMA significantly decreased 1321N1 cell viability by 1.7, 1.78 and 2.23-fold at 5, 10 and 50μM $CdCl_2$. A significant decrease in 1321N1 cell viability were also observed in rottlerin pre-treated cells at 25μM (1.62-fold) and 50μM (1.43-fold) when compared with cells treated with $CdCl_2$ only (Fig.5.17B). The results also show that with the exception of safingol, all the inhibitors decreased HEK 293 cell viability when compared with cells exposed to $CdCl_2$ only (Fig.5.17C). However the presence of rottlerin significantly decreased cell survival at 5 and 25μM $CdCl_2$ by 1.7 and 1.64-fold respectively when compared to the absence of the inhibitor (Fig.5.17C).These

data seem to suggest the involvement of PKC and possibly PKCδ in cell survival of 1321N1 and HEK 293 cells exposed to $CdCl_2$.

Figure 5.17. Effects of broad spectrum PKC inhibitor, bisindolylmaleimide (VIII) acetate (BMA), PKCα inhibitor (safingol), PKCδ inhibitor (rottlerin) and ERK1/2 inhibitor (PD98059) on cell viability after exposure to $CdCl_2$

A

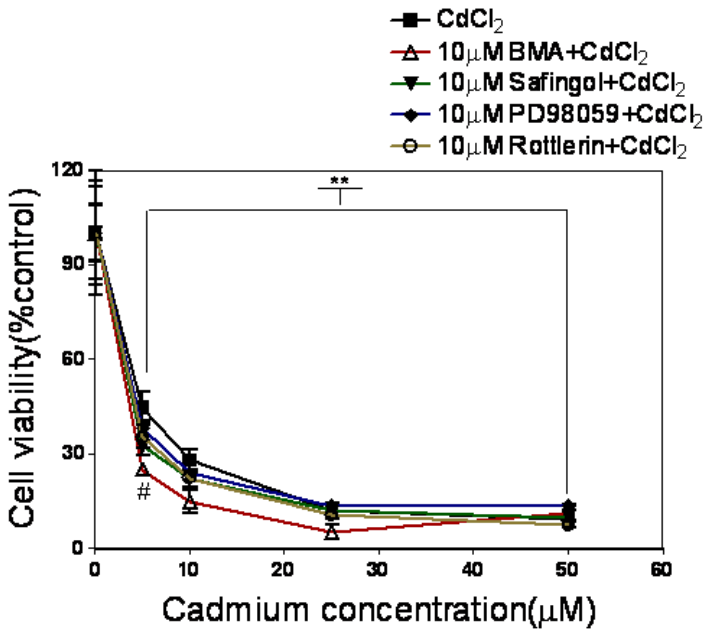

B

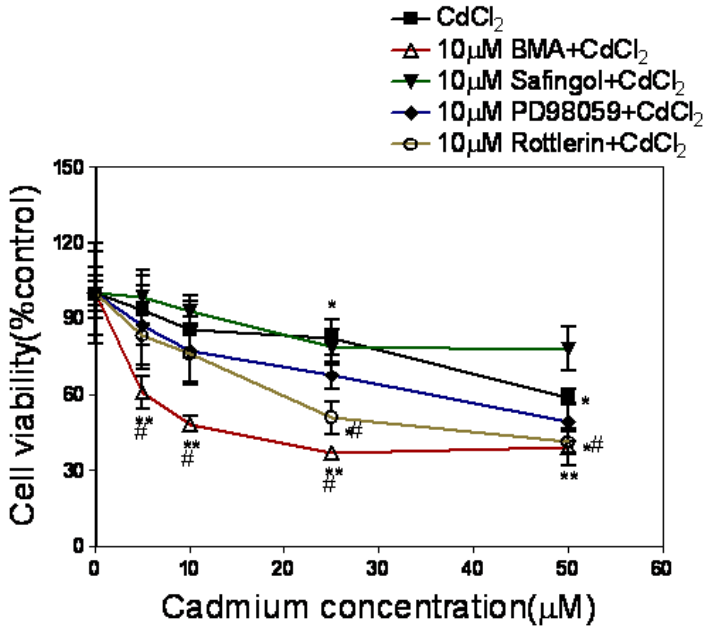

C.

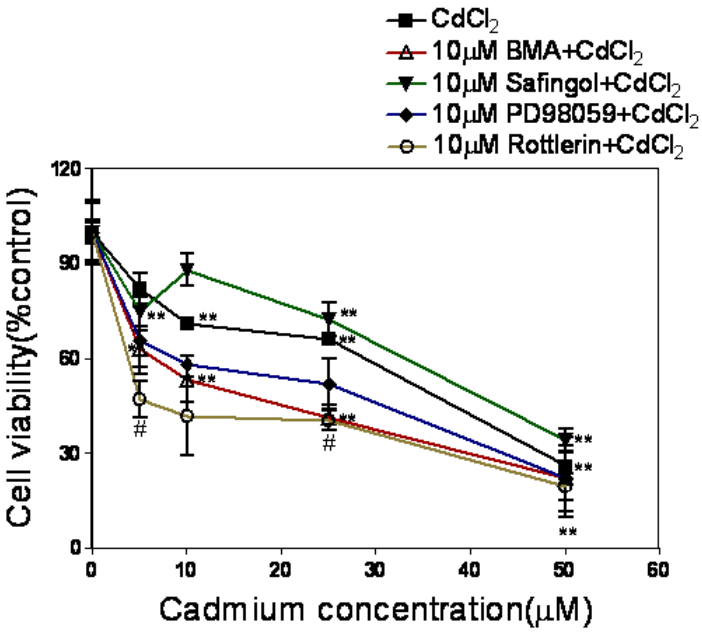

(A) HepG2, (B) 1321N1 and (C) HEK 293cells were pre-treated with 10μM of each inhibitor for 1hr before exposure to 5, 10, 25 and 50μM $CdCl_2$ for 24hr. Cell viability was then assessed by MTT assay as described in Materials and Methods. Data represent the mean value (n=6 individual assay done in triplicate) relative to control ±SD. Asterisks indicate significant compared with untreated control (***$p<0.005$ **$p<0.01$ *$p<0.05$) using one-way ANOVA with Dunnett's post test; Significant compared with Cd alone at the respective concentration using unpaired student's t-test (#$p<0.05$).

5.4. Discussion

Cd exposure leads to induction of Nrf2-dependent enzymes

The work described in this Chapter aims to examine the role of the Nrf2 protein in regulating cytoprotective genes in response to Cd exposure. The role of PKC in activating the translocation of Nrf2 from the cytosol into the nucleus was also examined. One mechanism, by which cells cope with stress imposed by toxicants and xenobiotics, is through the induction of protective enzymes that neutralize and remove the stress. Previous studies have shown Nrf2 to regulate the expression of phase II and antioxidant enzymes such as GSTA1, NQO1, HO1, **γ**-GCSc and SOD1 (Kensler *et al*., 2007). The present study shows that exposure of HepG2, 1321N1 and HEK 293 cells to increased concentrations (5 to 50μM) of $CdCl_2$ for 24hr resulted in an increased expression of NQO1, HO1 and **γ**-GCSc in all the three cell lines (Fig. 5.1). These results show that the three cell lines respond to stress (Cd) by inducing the expression of the antioxidant enzymes in a process known as an adaptive response. Adaptive response is the ability of cells to resist the damaging effect of xenobiotics at low dose of exposure in order to resist the effect of subsequent high dose (Crawford and Davies, 1994). Although, Cd at 50μM enhances cytoprotective enzymes expression, these inductions seem not sufficient to prevent the damaging effects of Cd as observed in increase LDH and MDA (Chapter 3) and necrotic cell death (Chapter4). The interplay of a number of factors involved in 50μM Cd exposure may contribute to the observed cell death due to their overwhelming effect on the induced protective enzymes.

Cd-induced Nrf2 translocation mediates protective enzymes expression

In order to verify the involvement of Nrf2 in the expression of these protective enzymes, Nrf2 protein levels were determined in the cytosol and nucleus after Cd exposure. Nrf2 protein is kept in the cytosol in an unstressed condition by binding to suppressor Keap1 protein to form a complex (Itoh *et al*., 1999). In the presence of stress such as in exposure to heavy metal, Nrf2 is released from the complex and thus migrates into the nucleus where its binds to the antioxidant response element (ARE) present at the promoter end of the responsive genes such as the antioxidant genes leading to transcriptional induction of these genes (Harvey *et al*., 2009). From this present study, exposure of HepG2, 1321N1 and HEK 293 cells to 5, 10 and 50μM $CdCl_2$ showed a decrease in cytosolic Nrf2 levels and a corresponding increased in the nuclear Nrf2 (Fig. 5.2, 5.3 & 5.4). Hence the observed induction in the cytoprotective enzymes in the three cell lines following Cd exposure may be as a result of the translocation of Nrf2 from the cytosol into the nucleus .To further confirm this, the levels of cytosolic Keap1 protein were found to increase in all three cell lines indicating the release of Nrf2 from the Nrf2-Keap1 complex prior to Nrf2 migration into the nucleus. Also observed in this study were increases in the mRNA levels of the cytoprotective genes, GSTA1 and NQO1, in 1321N1 and HEK 193 cells (Fig.5.7& 5.8) especially at sub-toxic (5 and 10μM) $CdCl_2$ and corresponding increases in Nrf2 mRNA (Fig.5.5) which further confirmed the involvement of Nrf2 in the up-regulation of these cytoprotective genes in Cd induced stress.

Mechanism of Cd-induced Nrf2-dependent protective enzymes

Although the involvement of Nrf2 in regulating cytoprotective genes transcription is well established, the mechanism by which it does this is still controversial. One proposed mechanism by which Nrf2 is liberated from Keap1 is by phosphorylation of Nrf2 Ser 40 by PKC and this has been demonstrated in HepG2 cells exposed to tBHQ (Huang *et al*. 2002). In this study we attempted to elucidate the role of protein kinase C and mitogen-activated protein kinase (ERK1/2) in the activation and subsequent translocation of Nrf2 from its Keap1 repressor in the cytosol to the nucleus following $CdCl_2$ exposure. The impaired cell survival observed in the three cell lines in the presence of PKC broad spectrum inhibitor (bisindolylmaleimide VII acetate, BMA) after Cd exposure (Fig.5.17) show that the cells became more susceptible to the effect of Cd than in the absence of the inhibitor and this indicates that PKC may be involved in mediating adaptive response of these Cd exposed cells. To confirm the link between the observed increase in cell death in the presence of BMA and Nrf2 translocation, Nrf2 levels were examined in the cytosolic and nuclear fractions of BMA pre-treated cells and the unpretreated cells. The observed accumulated levels of Nrf2 in the cytosols of the three cell lines after BMA pre-treatment and the corresponding decreased in nuclear levels (Fig.5.9, 5.10 & 5.11) is an indication of impaired translocation of Nrf2 into the nucleus, a process that is important in the cell's response to stress, and this may be responsible for the increased susceptibility to Cd insult observed in the viability study (Fig.5.17).

It has also been reported in certain studies that extracellular signal-regulated kinases control the phosphorylation and activation of Nrf2 (Zhang *et al*., 2006). However, the presence of ERK1/2 inhibitor (PD98059) does not significantly impair cell survival in any of the cell lines (Fig.5.17). These results show that PKC and not ERK1/2 may be involved in the cytoprotective response of these cell lines to Cd exposure.

Cd alters PKC*α*, PKCδ and p-PKCδ expressions

The involvement of PKC in Nrf2 mediated response to Cd exposure was further confirmed in HepG2 cells which revealed increases in expression of both PKC*α* and PKCδ after Cd exposure (Fig.5.12). Phosphorylation of PKC at multiple serines/threonines is a requirement for PKC activity in response to stress (Newton, 2003). The increase observed in phosphorylated PKCδ level after Cd exposure in HepG2 cells correlates with increased PKCδ protein levels (Fig.5.12A). This shows that PKCδ activation was stimulated by Cd and this may account for the observed Nrf2 translocation and activation. Increased PKCδ, p-PKCδ and PKC*α* protein expression was also observed in HEK 293 cells (Fig.5.13) which further confirmed the viability studies that PKCδ may be involved in protective response of this cell line to Cd exposure.

PKCδ mediates Nrf2 release from Keap1

Atypical PKCs were reported to be responsible for the phosphorylation of Nrf2 in human fibroblast WI-38 cells in response to phorone and 4-hydroxy-2, 3-nonenal (Numazawa *et al*., 2003). Therefore, to identify the PKC isoenzyme involved in mediating cytoprotection in cells exposed to Cd, cell viability was examined in HepG2, 1321N1 and HEK 293 cells pre-treated

with a PKCα specific inhibitor (L- threo-dihydrosphingosine, safingol) and a PKCδ specific inhibitor (rottlerin) (Fig.5.17). The presence of rottlerin enhanced Cd toxicity and this is seen in the significantly decreased cells viability observed in 1321N1 and HEK 293 cells in the presence of rottlerin when compared with cells exposed to $CdCl_2$ alone (Fig.5.17B&C). The decrease in GSTA1 (Fig.5.14) and NQO1 (Fig.5.15) gene transcription observed in the presence of rottlerin further confirmed the viability study and indicates that PKCδ may be one of the PKC isoforms involved in the release of Nrf2 from Keap1 repressor into the nucleus for the consequent transcription of the cytoprotective genes in an event of Cd exposure in the three cell lines under-study. This was confirmed in 1321N1 cells by the decreased Nrf2 protein expression in the nucleus and corresponding increase in the cytosol in the presence of rottlerin when compared with its absence (Fig.5.16). The results obtained from this present study were in agreement with earlier work that shows that disruption of PKCδ in osteoblasts resulted in reduced Nrf2 accumulation after sodium arsenate treatment (Li *et al*., 2004).

In addition, compounds that induced the antioxidant responsive element (ARE) or electrophile responsive element (EpRE) are reported to have the ability to react with thiol/disulfide groups (Prochaska *et al*., 1985). Cd is known to scavenge for the thiol group as one mechanism of its toxicity and this makes it a possible candidate for modifying the reactive cysteine on the Keap1 resulting in the release of Nrf2. Therefore, the observed translocation of Nrf2 from cytosol into the nucleus may be as a result of a direct effect of Cd acting on the reactive cysteine on Keap1 resulting in the subsequent released of Nrf2 leading to the expression of the antioxidant genes in the

adaptive response of the three cell lines. However, this direct effect needs further clarification.

In summary, this present work shows that Nrf2 mediates the adaptive response of HepG2, 1321N1 and HEK 293 cells exposed to Cd. This mediation involves the release of Nrf2 from the Keap1 repressor in a process that may involve PKC probably PKCδ. However, the direct involvement of Cd^{2+} in the activation of the Nrf2-Keap1 pathway needs further investigation.

CHAPTER 6

The Chemopreventive Effects of Diallydisulfide and Garlic Extracts against Cadmium-induced Toxicity

Chapter 6

6.0. The Chemopreventive Effects of Diallydisulfide and Garlic Extracts against Cadmium-induced Toxicity

6.1. Introduction

The use of chemopreventive agents has been exploited in the therapy against the toxic effect of many chemicals including heavy metals. Many plants, vegetables and synthetic compounds have also been screened in order to ascertain their potential in the prevention and cure of a range of chronic diseases and conditions (WCRF and AICR, 1997). One of those exploited extensively is garlic. Garlic (*Allium sativum*) has been used since ancient times as a cure for a range of conditions and diseases (Block, 1985). Garlic is said to possess antibacterial, antifungal, antithrombotic, antihypertensive, anticarcinogenic and antioxidant properties (Wei and Lau, 1998).

Epidemiological studies have consistently shown a relationship between intake of high quantities of garlic and a reduced incidence of cancer in most tissues especially in the stomach and colon (Fleischauer and Arab 2001). Garlic contains both water- and lipid-soluble organosulphur compounds (OSC) which have been reported to be responsible for its therapeutic properties (Block, 1985). It was also found that extraction of garlic and then storage for a long period of time (10-20months) "ages" the garlic, resulting in an enhanced antioxidant power within the Aged Garlic Extract (AGE). The major water soluble organosulfur compounds in AGE are S-allylcysteine (SAC) and S-allylmercaptocysteine (SAMC) both of which have strong antioxidant activity (Wei and Lau, 1998). In addition, AGE contains lipid soluble OSC and these include dially sulphide (DAS), triallyl sulphide,

diallyl disulphide (DADS) and dially polysulfides (Awazu and Horie, 1997). The organosulfur compounds (OSCs) in garlic and AGE have been suggested to exert their chemopreventive effect by influencing the drug metabolising enzymes and this effect is closely related to their structures (Yang *et al*., 2001). Previous work has shown that DADS and DATS have positive effects on gutathione S-transferase (GST) (Hatono *et al*., 1996), glutathione reductase (Wu *et al*., 2001) and quinone reductase (NQO1) (Singh *et al*., 1998). Garlic extracts have also been shown to increase superoxide dismutase (Geng and Lau, 1997), glutathione peroxidase (Wei and Lau, 1998) and catalase activities (Wei and Lau 1998) in cultured vascular cells.

Of all the OSCs in garlic, SAC has been identified as the only reliable marker in human for studies that involve garlic intake since it is easily detectable and increases quantitatively in blood following oral intake of garlic capsules (Amagase, 2006). On the other hand, the oil soluble organosulfur compounds in garlic such as allicin, sulfides, ajoene and vinyldithiins are not detectable in the blood or urine following garlic consumption and therefore may not likely to be involve in the therapeutic effects of garlic (Amagase et al, 2001; Freeman and Kodera, 1995). Pharmacokinetics studies in many animal models have shown that SAC is easily absorbed from the gastrointestinal tract and readily distributed in plasma, liver and other organs with bioavailability of 98% in rats (Nagae at al., 1994), 103.0% in mice and 87.2% in dogs (Amagase,2006). According to German Kommission E monograph (1988), a daily intake of 1-2 cloves of garlic or 4g of intact garlic was said to be required to provide health benefit.

Many chemopreventive agents exert their action via the induction of detoxifying enzymes, leading to decreased toxicity of many carcinogens, xenobiotics and reactive intermediates by enhancing oxidation, reduction and hydrolysis (Phase I), and conjugation (Phase II) of reactive compounds thereby facilitating their removal from the body system (Kensler, 1997). In addition, enzymes that contribute to restoring redox balance by enhancing glutathione biosynthesis and metabolism are also induced. Enzymes that are induced by chemopreventive agents include aldo-keto reductases, quinone reductase, glutathione S-transferases, and glutathione reductase. One of the mechanisms of action of these chemopreventive compounds has been reported to be mediated via the action of Nrf2.

Having established in the previous chapter the involvement of Nrf2 in mediating the adaptive response of cells to sublethal cadmium exposure, this present study tries to examine the effect of different garlic preparations in the protection against cadmium toxicity and to define the role of Nrf2 in this protection.

6.2. Materials and Methods

The methods are as described in Chapter 2

6.2.1. Cell Culture

HepG2, 1321N1 and HEK 293 Cells were cultured as previously described in section 2.2.1.

6.2.2. Sample preparation for enzyme assay

Samples are prepared by freeze-thaw as previously described in section 2.2.3

6.2.3. Garlic extracts preparation

Garlic bulbs were obtained from Ondo-state, Nigeria. Aqueous extracts of garlic (GA) were prepared by soaking crushed garlic in distilled water and then filtering with whatman paper. Concentrated extracts were obtained by placing the aqueous extracts in a rotary evaporator at 25^{o}C. Aged Garlic Extracts (AGE) was prepared by soaking the crushed garlic in distilled water and allows the extraction to occur for 12months. The extracts were solidified in rotary evaporator at 25^{o}C. DADS were prepared in 0.1% DMSO.

6.2.4. Cell treatment and assays

Cells were pre-treated with either 100 μg/ml AGE or 100 μg/ml GA or 100 μM DADS for 24hr. After the incubation, cells were washed in PBS and then exposed to different concentrations of $CdCl_2$ for 24hr. MTT, LDH leakage, lipid peroxidation, ROS, GSH, and Calpain activity assays and western blots were carried out as previously described in Chapter 2 and 4.

6.2.5. MTT assay for inhibitors study

Cells were seeded in 96 well plates at a density of 10^3cells/ml. The cells were allowed to reach 80% confluent before the administration of either 1mM aminotriazole (catalase inhibitor) or 1mM Mercaptosuccinate (Glutathione peroxidase inhibitor) for 30min. After the incubation period, the media were removed and cell monolayer was washed with PBS. The cells were then treated with either 100 μg/ml AGE or 100 μg/ml GA or 100 μM DADS for 24hr and the media were removed after the incubation and cells were then washed with PBS before 24hr exposure to different concentrations of $CdCl_2$ (0-50μM). MTT assay was performed according to the method described in section 2.2.4. Cells viability was expressed as percentage of control.

6.3. Results

6.3.1. Effect of garlic extracts and diallydisulfide (DADS) on cell viability after $CdCl_2$ exposure

To determine the effect of garlic extracts (GA and AGE) and DADS on Cd-induced toxicity, cells were pretreated with either 100 μg/ml AGE or 100 μg/ml aqueous garlic extract (GA) or 100μM DADS for 24hr before exposure to 5, 10, 25 and 50 μM $CdCl_2$ for 24hr. Cell viability was then determined using the MTT assay. The results show increased cell viability in HepG2 cells pretreated with AGE, GA and DADS compared to cells exposed to $CdCl_2$ alone (Fig.6.1A). However, the differences were not significant except at 5 μM $CdCl_2$ in DADS pretreated cells. In 1321N1 cells, there were significant increases in cell viability in AGE pretreated cells at all $CdCl_2$ concentrations used, but significant differences were obtained only at 10 and 25 μM $CdCl_2$ following DADS pretreatment (Fig.6.1B). There were significant increases in cell viability in AGE pretreated HEK 293 cells at 10 and 25μM $CdCl_2$, when compared with unpretreated cells (Fig.6.1C). However, the presence of GA and DADS does not enhance cell viability in HEK 293 cells after $CdCl_2$ exposure.

6.3.2. Effects of garlic extracts and diallydisulide (DADS) on Lactate dehydrogenase (LDH) leakage after $CdCl_2$ exposure

In order to further assess the protective effect of AGE, GA and DADS against $CdCl_2$ cytotoxicity, the LDH assay was used as a measure of cell membrane damage in cells pre-treated with AGE (100 μg/ml), GA (100 μg/ml) and DADS (100 μM) for 24hr before exposure to 5, 10 and 50μM $CdCl_2$ for 24hr. Increased LDH leakage was observed in the absence of AGE, GA and DADS pre-treatment in HepG2 cells (Fig.6.2A). GA pretreatment showed the

greatest reduction in Cd-induced LDH leakage following treatment with 10 μM $CdCl_2$ (167-fold decrease) and DADS pretreatment showed the least reduction in LDH leakage at 10μM $CdCl_2$ (6.4-fold decrease) (Fig.6.2A). There were significant reductions in LDH leakage in the AGE, GA and DADS pre-treated 1321N1 cells when compared to cells that were not pretreated cells at all $CdCl_2$ concentrations (Fig.6.2B). The decrease was highest (10.6-fold) in AGE pre-treated 1321N1 cells exposed to 50μM $CdCl_2$ and lowest (1.86-fold) in AGE pre-treated 1321N1 cells exposed to 10μM $CdCl_2$. The results show that the presence of AGE, GA and DADS resulted in a reduction in LDH leakage in HEK 293 cells when compared with cells exposed to $CdCl_2$ only (Fig.6.2C). However, these differences were not significant in AGE and DADS pre-treated HEK 293 cells exposed to 5μM $CdCl_2$ or in GA treated cells exposed to 10 μM $CdCl_2$.

Figure 6.1.Effects of AGE, GA and DADS on cell viability in the presence of $CdCl_2$

A.

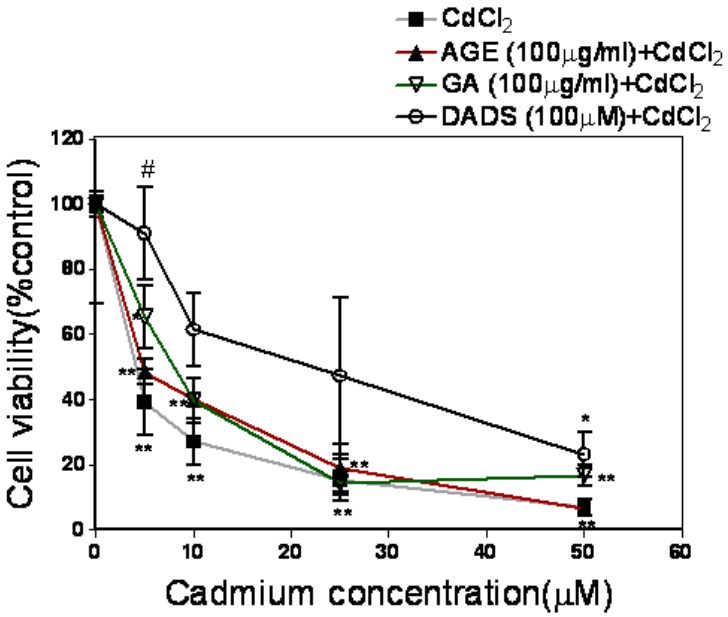

B.

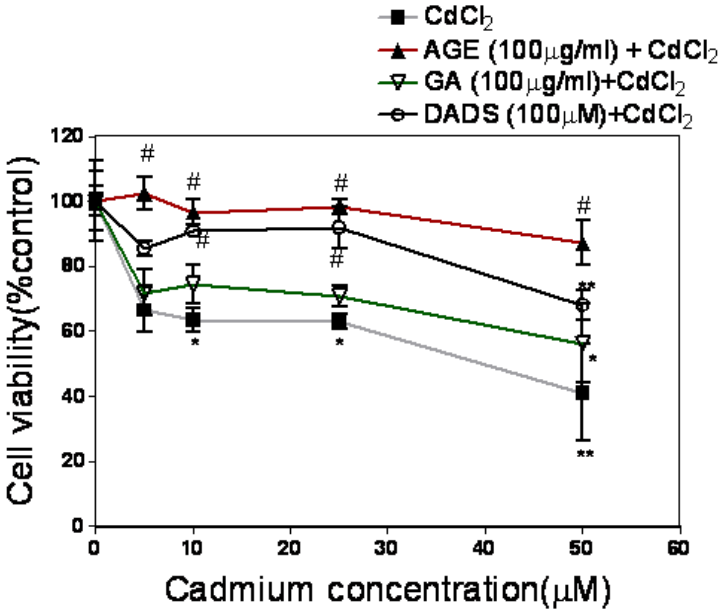

C.

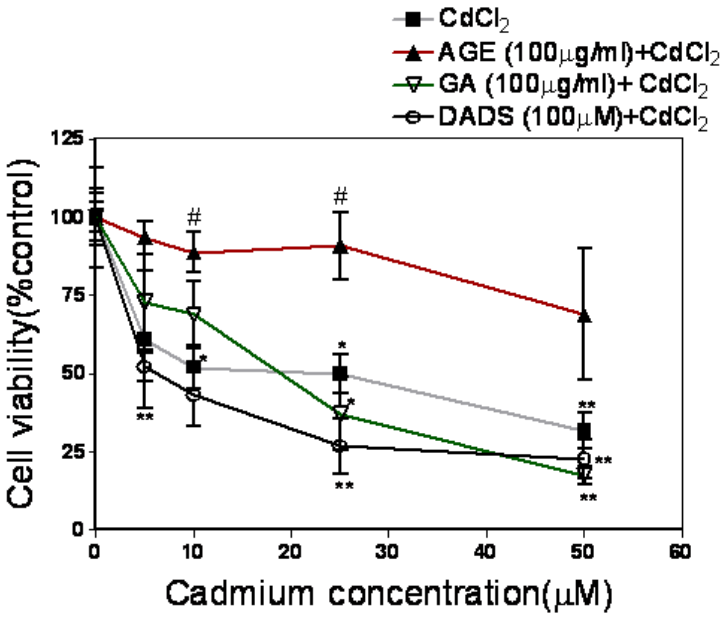

(A) HepG2, (B) 1321N1 and (C) HEK 293 cells were pre-treated with 100μg/ml AGE and GA and 100μM DADS for 24hr before exposure to 5, 10, 25 and 50μM $CdCl_2$ for 24hr. Cell viability was determined as described in Materials and Methods; Data represent the mean value (n=6 of individual experiments done in triplicate) of percentage of control ±SD. Asterisks indicate significant compared with untreated control (***$p<0.005$ **$p<0.01$ *$p<0.05$) using one-way ANOVA with Dunnett's post test. # ($p<0.05$) represents significant difference between pre-treated group and unpretreated group (unpaired student's t-test).

Figure6.2. Effects of AGE, GA and DADS on LDH leakage in the presence of $CdCl_2$

A.

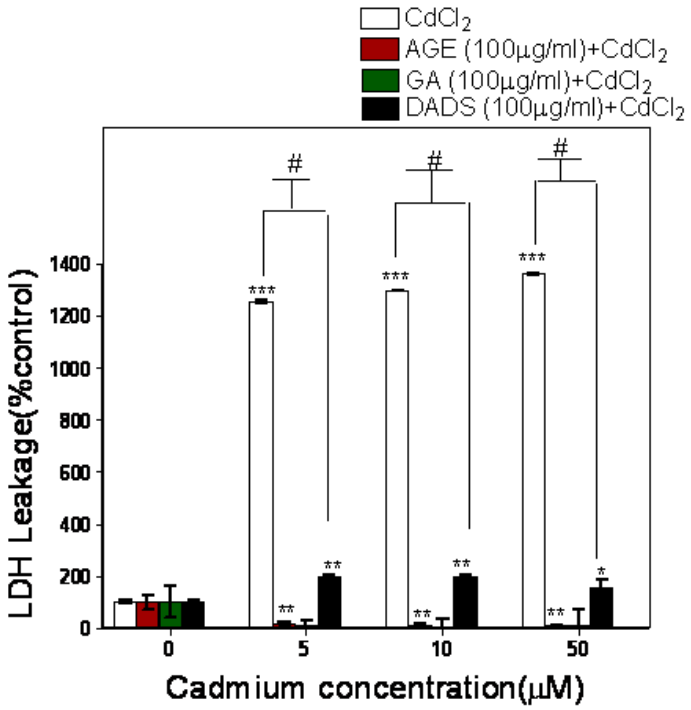

B.

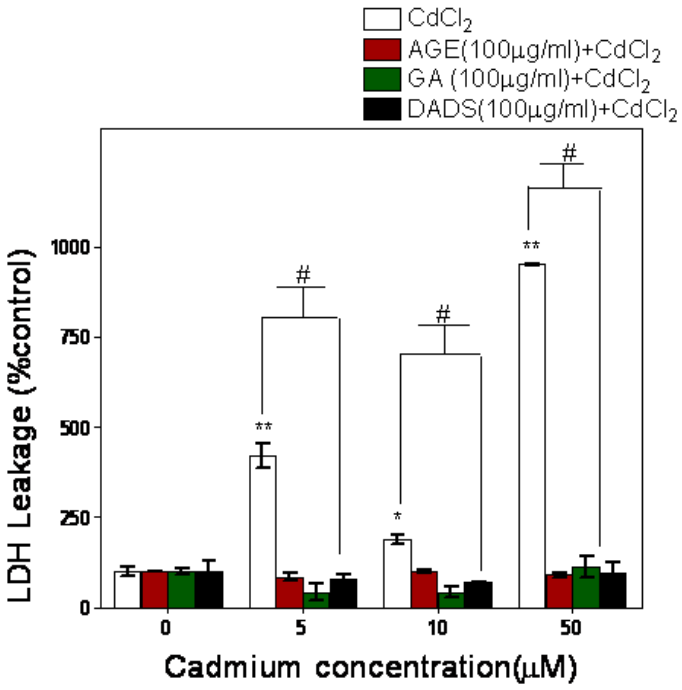

C.

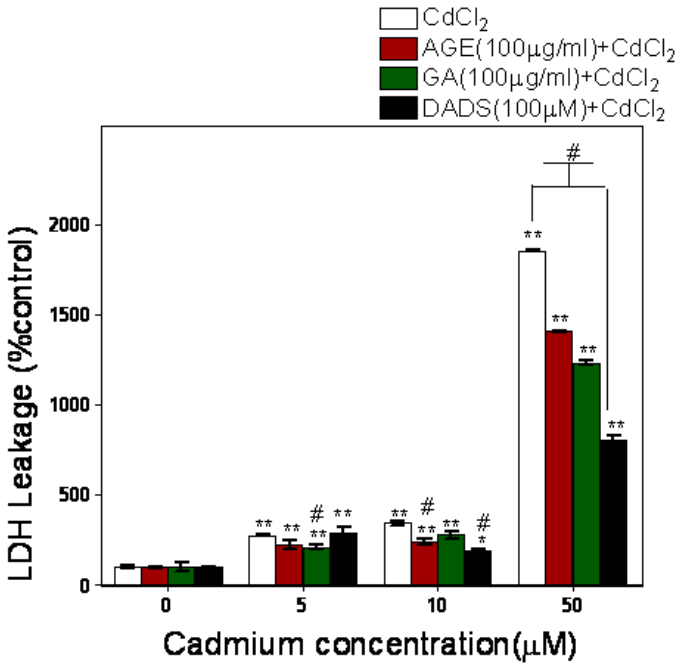

(A) HepG2, (B) 1321N1 and (C) HEK 293 cells were pretreated with 100µg/ml AGE and GA and 100µM DADS for 24hr before exposure to 5, 10, 25 and 50µM $CdCl_2$ for 24hr. Cell cytotoxicity was determined by the LDH leakage as described in Materials and Methods; Data represent the mean value (n=6 of individual experiments done in triplicate) of percentage of control ±SD Asterisks indicate significant compared with untreated control (***p<0.005 **p<0.01 *p<0.05) using one-way ANOVA with Dunnett's post test. # (p<0.05) represents significant difference between pre-treated group and unpretreated group (unpaired student's t-test).

6.3.3 Effects of garlic extracts and diallydisulide (DADS) on lipid peroxidation after $CdCl_2$ exposure

In order to evaluate the protective effect of GA, AGE and DADS on membrane lipid damage induced by $CdCl_2$, malondialdehyde levels were determined by the thiorbarbituric acid reactive substance (TBARS) method in cells pretreated with either 100 μg/ml AGE or 100 μg/ml GA or 100 μM DADS for 24hr prior to 24hr exposure to 5, 10 and 50 μM $CdCl_2$. The results show that there was a significant reduction in malondialdehyde levels in extracts and in DADS pretreated HepG2 cells compared with cells exposed to $CdCl_2$ alone (Fig.6.3A). The highest decrease (10.61-fold) in malondialdehyde (MDA) levels in HepG2 cells was observed in GA pretreated cells exposed to 5μM $CdCl_2$ and the lowest effect (1.84-fold) was observed in DADS pretreated cells exposed to 10μM $CdCl_2$ (Fig.6.3A). There were also significant reductions in MDA levels in AGE, GA and DADS pretreated 1321N1 cells when compared with the unpretreated cells exposed to $CdCl_2$ (Fig.6.3B).The highest reduction was observed (6.81-fold) in AGE pretreated 1321N1 cells exposed to 50 μM $CdCl_2$ while the lowest reduction (1.16-fold) was observed in DADS pretreated cells exposed to 50μM $CdCl_2$ (Fig.6.3B). In HEK 293 cells, there were no significant reductions in MDA levels after exposure to 5 μM $CdCl_2$ in the absence and presence of AGE, GA and DADS (Fig.6.3C). However, MDA levels significantly reduced in AGE, GA and DADS pretreated HEK 293 cells exposed to 10 and 50 μM $CdCl_2$ compared to the unpretreated cells (Fig.6.3C). The highest reduction (4.53-fold) in MDA levels in HEK 293 cells was observed in cells pretreated with GA at 5μM $CdCl_2$ exposure while the lowest reduction (1.32-fold) was observed in DADS pretreated cells exposed to 5μM $CdCl_2$ (Fig.6.3C). These results seem to suggest that DADS is less effective in protecting 1321N1 and HEK 293 cells

from $CdCl_2$-induced lipid peroxidation when compared with AGE and GA especially at 50 μM.

6.3.4. Effects of garlic extracts and diallydisulfide (DADS) on reactive oxygen species (ROS) levels after $CdCl_2$ exposure

To assess the role of ROS on $CdCl_2$ induced toxicity and to evaluate the effect of 24hr pretreatment with either 100 μg/ml AGE or 100 μg/ml GA or 100μM DADS on ROS production in cells exposed to 5, 10 and 50 μM $CdCl_2$ for 24hr, ROS levels were determined using dihydrofluorescein diacetate (DHFDA). The results show that the different concentrations of $CdCl_2$ used in this work produced significant increased in ROS level in HepG2 cells (Fig.6.4A). The presence of AGE, GA and DADS resulted in significantly decreased in ROS levels at 5, 10 and 50 μM $CdCl_2$ when compared with unpretreated HepG2 cells exposed to $CdCl_2$ (Fig.6.4A). The highest decrease (2.16-fold) in ROS was obtained in AGE pre-treated HepG2 cells exposed to 50 μM $CdCl_2$ (Fig.6.4A) while the lowest decrease (1.69-fold) in ROS levels was obtained in GA pre-treated HepG2 cells exposed to 10μM $CdCl_2$ (Fig6.4A). Only DADS caused a significant decrease (1.41-fold) in ROS levels in HepG2 cells after exposure to 5 μM $CdCl_2$ (Fig.6.4A). However, there were significant increased in ROS levels in 100μg/ml GA pretreated HepG2 cells at 10 and 50 μM $CdCl_2$ exposure when compared with control (Fig.6.4A). The increase in ROS levels observed in AGE, GA and DADS pretreated 1321N1 cells was not significant when compared to the cells exposed to $CdCl_2$ alone (Fig.6.4B). The results also show that 5, 10 and 50 μM $CdCl_2$ do not enhance ROS production in 1321N1 cells. No significant changes in ROS levels were observed in HEK 293 cells both in the presence and absence of pretreatment (Fig.6.4C). These results show that $CdCl_2$ toxicity in 1321N1 and HEK 293 cell lines does not

involve elevated ROS production and the presence of AGE, GA and DADS has no effect on ROS levels in these two cell lines in the presence of $CdCl_2$. However, the presence of AGE, GA and DADS are efficient in preventing ROS production in HepG2 cells with DADS and AGE been more efficient than GA.

Figure6.3. Effects of AGE, GA and DADS on lipid peroxidation in the presence of $CdCl_2$

A.

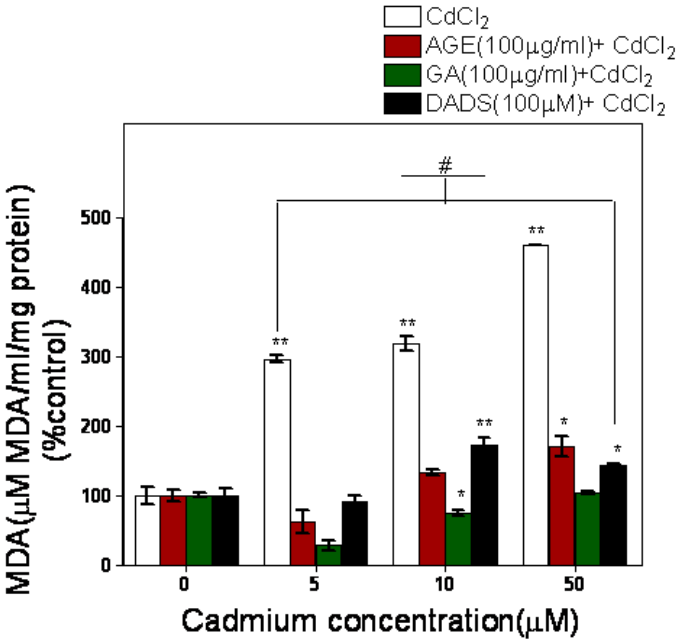

B.

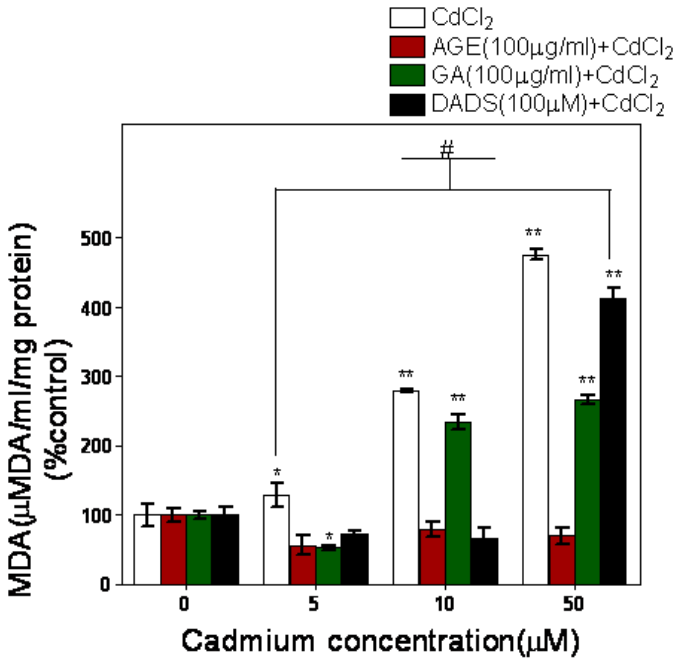

C.

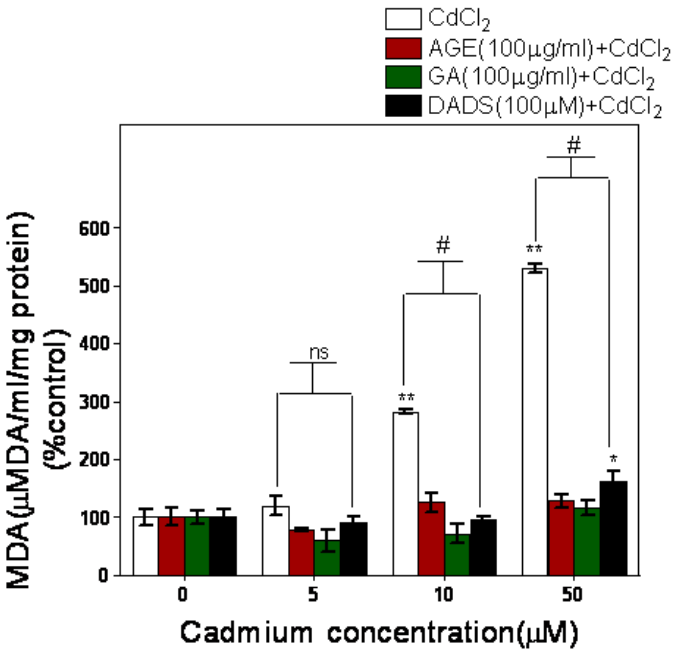

(A) HepG2, (B) 1321N1 and (C) HEK 293 cells were pretreated with 100µg/ml AGE and GA and 100µM DADS for 24hr before exposure to 5, 10, 25 and 50µM $CdCl_2$ for 24hr. Lipid peroxidation was determined by the TBARS assay as described in Materials and Methods; Data represent the mean value (n=6 of individual experiments done in triplicate) of percentage of control ±SD. Asterisks indicate significant compared with untreated control (***$p<0.005$ **$p<0.01$ *$p<0.05$) using one-way ANOVA with Dunnett's post test. # ($p<0.05$) represents significant difference between pre-treated group and unpretreated group and ns represents non-significant between pre-treated and unpretreated groups (unpaired student's t-test).

Figure6.4. Effects of AGE, GA and DADS on reactive oxygen species production in the presence of $CdCl_2$

A.

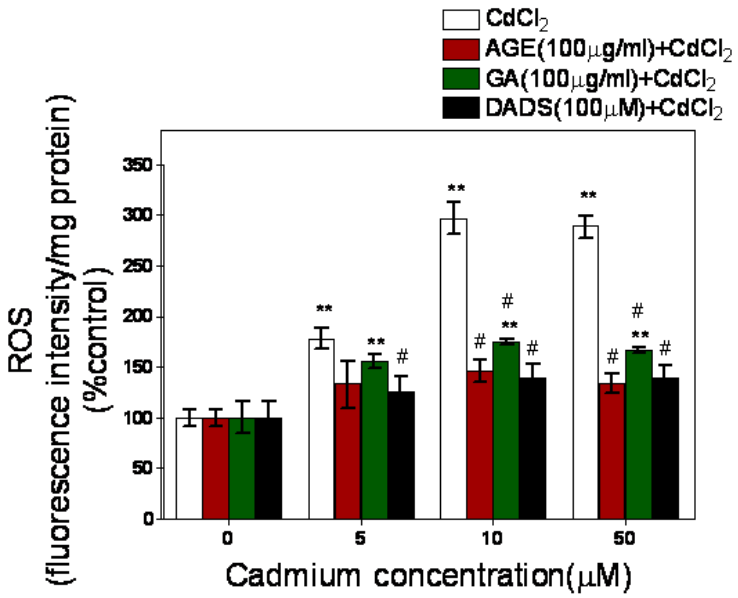

B.

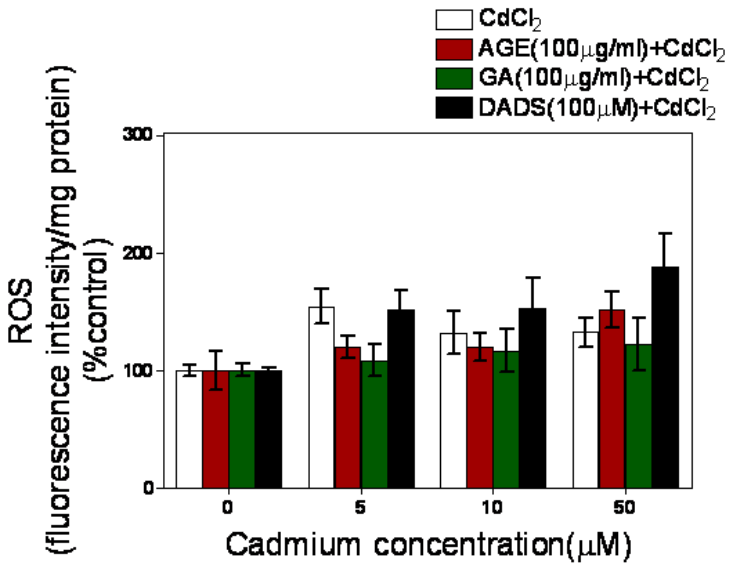

C.

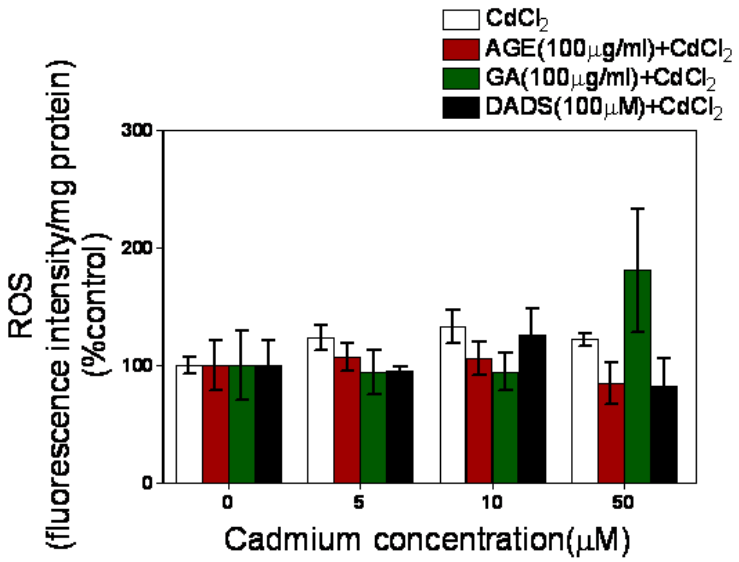

(A) HepG2, (B) 1321N1 and (C) HEK 293 cells were pretreated with 100μg/ml AGE and GA and 100μM DADS for 24hr before exposure to 5, 10, 25 and 50μM $CdCl_2$ for 24hr. ROS was determined as described in Materials and Methods; Data represent the mean value (n=6 of individual experiments done in triplicate) of percentage of control ±SD. Asterisks indicate significant compared with untreated control (***p<0.005 **p<0.01 *p<0.05) using one-way ANOVA with Dunnett's post test. # (p<0.05) represents significant difference between pre-treated group and unpretreated group and ns represents non-significant between pre-treated and unpretreated groups (unpaired student's t-test).

6.3.5. Effects of garlic extracts and diallydisulfide (DADS) on GSH levels after $CdCl_2$ exposure

To determine the effect of AGE, GA and DADS pretreatment on total GSH levels after $CdCl_2$ exposure, cells were pretreated with either 100μg/ml AGE or 100 μg/ml GA or 100μM DADS for 24hr followed by 24hr exposure to 5, 10 and 50μM $CdCl_2$. GSH levels were then determined using Ellman reagent. The results show increased GSH levels in all the pretreated HepG2 cells when compared with HepG2 cells exposed to $CdCl_2$ alone (Fig.6.5A). The highest increase (6.22-fold) was obtained in AGE pretreated HepG2 cells exposed to 10μM $CdCl_2$ and the lowest increase (2.2-fold) was obtained in GA pretreated HepG2 cells exposed to 5 μM $CdCl_2$ (Fig.6.5A). Pre-treatment of 1321N1 cells with 100 μg/ml AGE resulted in significantly decreased GSH levels when compared with cells treated with 5 and 10μM $CdCl_2$ alone (Fig.6.5B). The presence of GA and DADS resulted in increased GSH levels at 10 and 50μM $CdCl_2$ with the highest increase (6.79-fold) observed in 1321N1 cells pretreated with GA at 50μM $CdCl_2$ and the lowest increase (1.31-fold) observed in 1321N1 cells pretreated with DADS at 10μM $CdCl_2$ (Fig.6.5B). There were significant differences in GSH levels between the AGE pretreated HEK 293 cells and cells exposed to $CdCl_2$ alone at 5 and 50μM $CdCl_2$ and GA pretreated HEK 293 cells and cells exposed to 10 and 50μM $CdCl_2$ (Fig.6.5C). The highest increase (2.68-fold) in GSH level in HEK 293 cells was obtained in AGE pretreated cells at 50μM $CdCl_2$ and the lowest increase (1.42-fold) was obtained in GA pretreated HEK 293 cells at 10μM $CdCl_2$ (Fig.6.5C). These results seem to suggest that the total GSH levels in HepG2 cells are the most elevated in response to AGE, GA and DADS when compared with the other two cell lines.

Figure6.5. Effects of AGE, GA and DADS on GSH levels in the presence of $CdCl_2$

A.

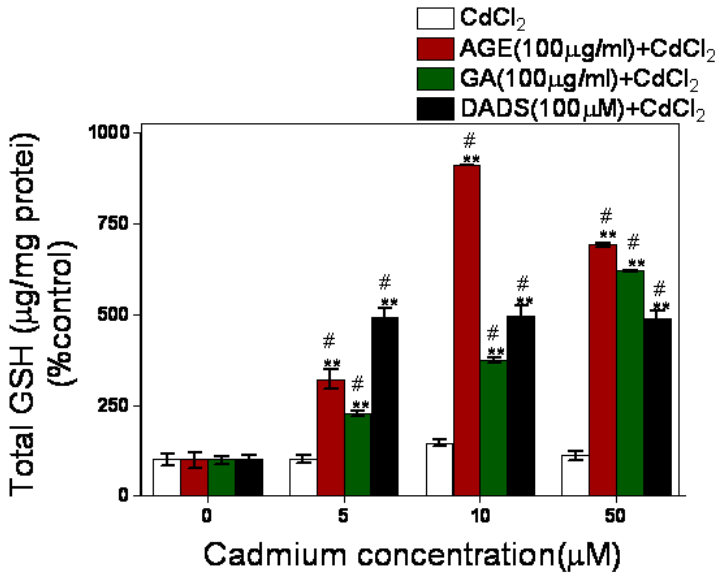

B.

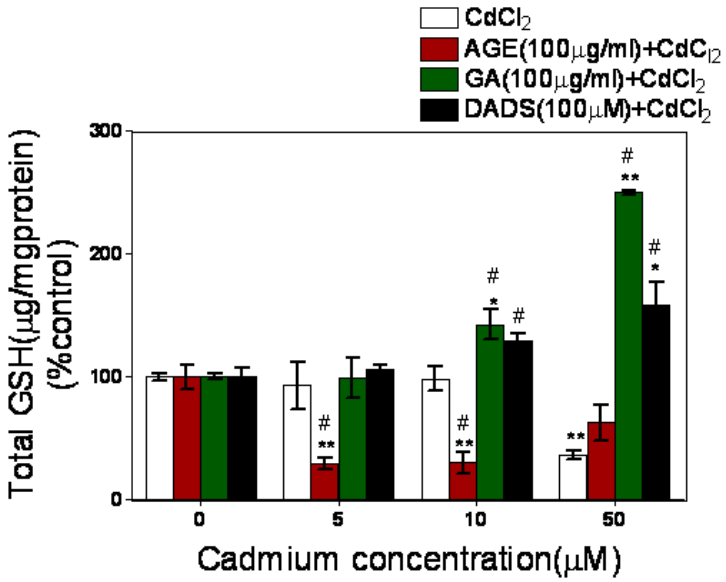

C.

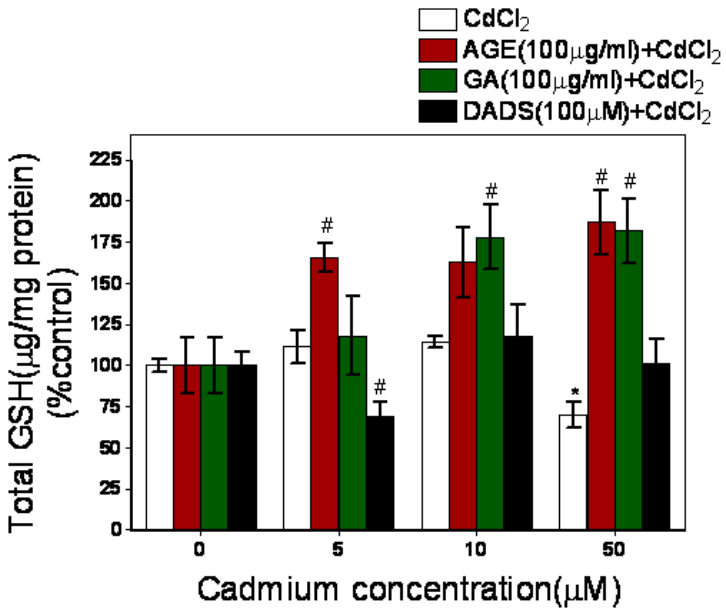

(A)HepG2, (B) 1321N1 and (C) HEK 293 cells were pretreated with 100μg/ml AGE and GA and 100μM DADS for 24hr before exposure to 5, 10, 25 and 50μM $CdCl_2$ for 24hr. GSH levels was determined as described in Materials and Methods; Data represent the mean value (n=6 of individual experiments done in triplicate) of percentage of control ±SD. Asterisks indicate significant compared with untreated control (***p<0.005 **p<0.01 *p<0.05) using one-way ANOVA with Dunnett's post test. # (p<0.05) represents significant difference between pre-treated group and unpretreated group and ns represents non-significant between pre-treated and unpretreated groups (unpaired student's t-test).

6.3.6. Effects of DADS on Nrf2 and NQO1 expression in 1321N1 cells exposed to $CdCl_2$

To assess whether the presence of garlic extracts and DADS has any effect on the expression levels of Nrf2 and NQO1 protein in 1321N1 cells following $CdCl_2$ treatment, cells were pretreated with either 100 μg/ml AGE or 100 μg/ml GA or 100μM DADS for 24hr prior to treatment with 5 μM $CdCl_2$ for 24hr and western blot analysis was performed using Nrf2 and NQO1 specific antibody. There was a 3.79-fold significant increase in Nrf2 expression in presence of DADS in 1321N1 cells when compared with the control (Fig.6.6A). There was also a 1.32-fold significant increase in Nrf2 protein expression in the DADS pre-treated 1321N1 cells when compared with cells exposed to 5μM Cd without pre-treatment (6.6A). The presence of DADS (3.79-fold) alone, 5μM $CdCl_2$ (1.80-fold) and DADS (2.38-fold) pre-treated cells significantly increased Nrf2 expression when compared with control (Fig.6.6A)The results also show a 3.33, 8.83 and 6.67-fold significant increased in NQO1 expression in the presence of DADS treated, 5μM and DADS pre-treated 1321N1 cells when compared to control respectively (Fig.6.6B). But there was no significant difference in NQO1 expression between DADS pre-treated cells and cells exposed to 5μM without pre-treatment. These set of data seems to suggest that the presence of DADS enhances the induction of Nrf2 protein in the absence and presence of 5 μM $CdCl_2$ and this may be important in protecting 1321N1 cells in Cd exposed cells.

6.3.7. Effects of DADS on Nrf2 and NQO1 expression in HEK 293 cells exposed to $CdCl_2$

In order to determine the effects of DADS on Nrf2 and NQO1 proteins expression in HEK 293 cells in the presence and absence of Cd, cells were

exposed to 100 μM DADS for 24hr followed by 24hr treatment with 5 μM $CdCl_2$. Western blot was performed on the cell extracts using Nrf2 and NQO1 specific antibodies. The results show 1.5, 2.17 and 6.46-fold significant increases in Nrf2 protein expression levels in the presence of DADS treatment, 5 μM $CdCl_2$ and in DADS pre-treated HEK 293 cells exposed to 5 μM $CdCl_2$ respectively when compared with control cells (Fig.6.7A). There was also a significant increase of 2.98-fold in Nrf2 expression in DADS pre-treated cells when compared with cells exposed to 5μM $CdCl_2$ without pre-treatment (Fig.6.7A). The results also show that the presence of DADS treatment alone, 5 μM $CdCl_2$ and DADS pre-treated cells exposed to 5 μM $CdCl_2$ significantly increased NQO1 protein expression by 3.33, 8.83 and 6.67-fold respectively when compared with control (Fig.6.7B). However there was no significant difference in NQO1 expression between DADS pre-treated cells and cells exposed to 5 μM $CdCl_2$ alone (Fig.6.7B). These results show that Nrf2 and NQO1 induction was enhanced by the presence of DADS and that the induction of Nrf2 may be important in the protective effects of DADS in HEK 293 cells exposed to Cd.

Figure6.6. Effects of DADS on the expression of Nrf2 and NQO1 in 1321N1 cells after $CdCl_2$ exposure

A.

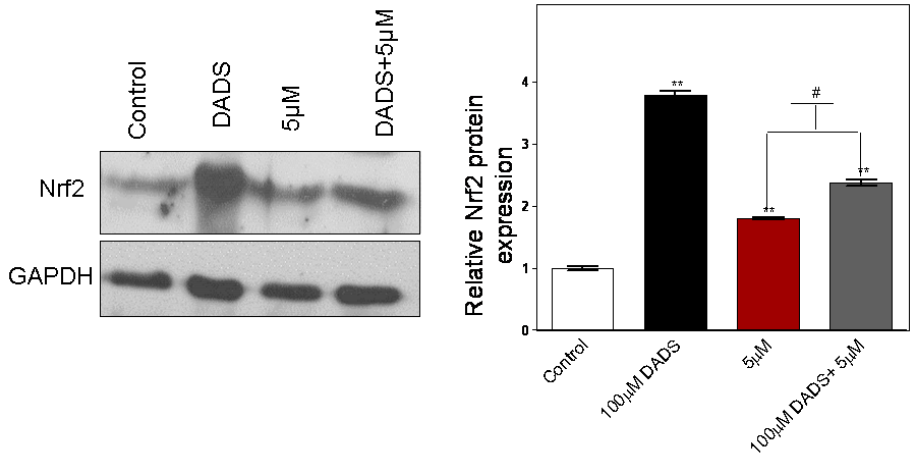

B.

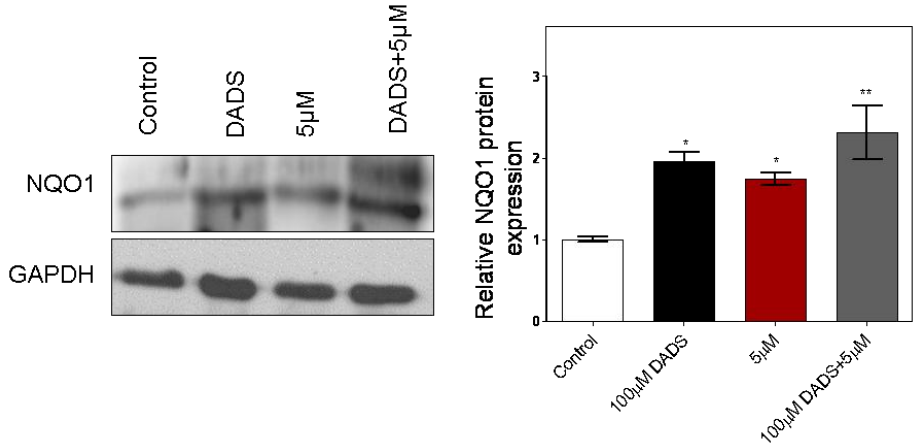

1321N1 cells were pretreated with 100μM DADS for 24hr and then exposed to 5 μM $CdCl_2$ for 24hr. After the incubation, cell extracts were prepared and 10μg of proteins were loaded on SDS-PAGE. Western blot was performed using (A) Nrf2 and (B) NQO1 specific antibodies as described in materials and Methods. Protein loading was normalised with GAPDH antibody. Intensity of the bands was evaluated with image J analysis software and relative protein expressions were compared to control. Data represent the mean value (n=3 of individual experiments done in triplicate) of percentage of control ±SD. Asterisks indicate significant compared with untreated control (***$p<0.005$ **$p<0.01$ *$p<0.05$) using one-way ANOVA with Dunnett's post test. # ($p<0.05$) represents significant difference between pre-treated group and unpretreated group (unpaired student's t-test).

Figure6.7. Effects of DADS on the expression of Nrf2 and NQO1 in HEK 293 cells after $CdCl_2$ exposure

A.

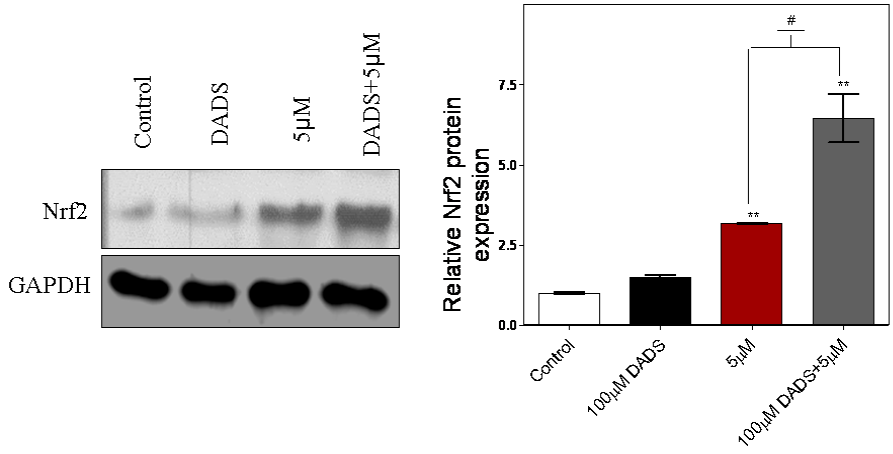

B.

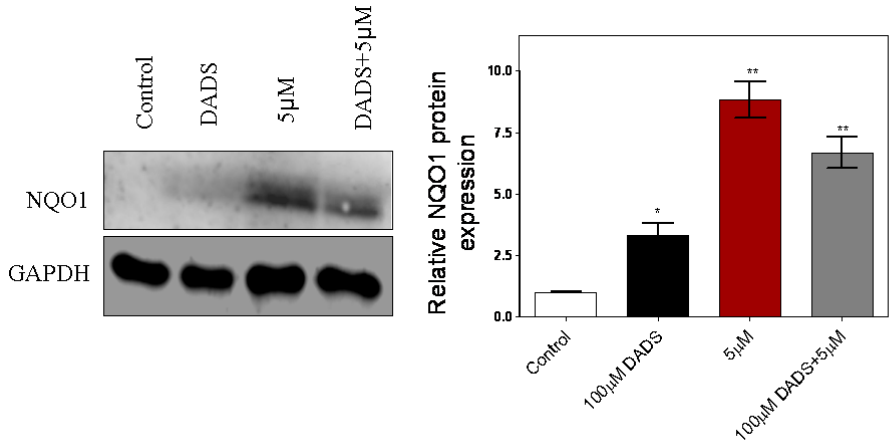

HEK 293 cells were pretreated with 100μM DADS for 24hr and then exposed to 5 μM $CdCl_2$ for 24hr. After the incubation, cell extracts were prepared and 10μg of proteins were loaded on SDS-PAGE. Western blot was performed using (A) Nrf2 and (B) NQO1 specific antibodies as described in materials and Methods. Protein loading was normalised with GAPDH antibody. Intensity of the bands was evaluated with image J analysis software and relative protein expressions were compared to control. Data represent the mean value (n=3 of individual experiments done in triplicate) of percentage of control ±SD. Asterisks indicate significant compared with untreated control (***$p<0.005$ **$p<0.01$ *$p<0.05$) using one-way ANOVA with Dunnett's post test. # ($p<0.05$) represents significant difference between pre-treated group and unpretreated group (unpaired student's t-test).

6.3.8. Effects of AGE on Nrf2 and NQO1 expressions in 1321N1 cells exposed to $CdCl_2$

AGE garlic extracts is said to have enhanced antioxidant property due to the aging of garlic extracts that converts some volatile antioxidant compounds in garlic to a more stable and potent compounds. Therefore, in order to assess the protective effects of AGE in Cd exposed 1321N1 cells, the cells were exposed to 100 μg/ml AGE for 24hr and then treated with 5 μM $CdCl_2$ for 24hr. Levels of Nrf2 and NQO1 protein expression were then determined in the whole cell extracts by western blot using Nrf2 and NQO1 specific antibodies. The results show significant increases of 6.21 and 6.6-fold in Nrf2 expression in cells exposed to 5 μM $CdCl_2$ alone and cells treated with 100 μg/ml AGE plus 5 μM $CdCl_2$ respectively when compared with control (Fig.6.8A). There was no significant difference in Nrf2 protein expression in AGE plus 5 μM $CdCl_2$ treated cells when compared with cells exposed to Cd alone (Fig.6.8A). However, the increase (5.67-fold) in Nrf2 expression in the presence of AGE alone was significantly different from control cells (Fig.6.8A). Significant increases of 8 and 5-fold in NQO1 protein expression were also observed in 1321N1 cells exposed to 5 μM $CdCl_2$ and AGE plus $CdCl_2$ treated cells respectively (Fig.6.8B). A significant increase (1.6-fold) in NQO1 expression was observed in cells exposed to 5 μM $CdCl_2$ alone when compared to cells exposed to AGE plus 5μM $CdCl_2$ (Fig.6.8.B). These data suggest that AGE does not enhance Nrf2 and NQO1 expression in the presence of 5 μM $CdCl_2$ but its presence in cells can boost Nrf2 expression in the absence of $CdCl_2$.

6.3.9. Effects of AGE on Nrf2 and NQO1 expression in HEK 293 cells exposed to $CdCl_2$

The effects of AGE pre-treatment on Nrf2 and NQO1 expressions was investigated in HEK 293 cells in order to define the role of Nrf2 in the protective effects of AGE. The cells were pre-treated with 100 μg/ml AGE for 24hr followed by 24hr exposure to 5 μM $CdCl_2$. The results of the western blot show significant increases in Nrf2 expression in cells exposed to 100 μg/ml AGE (9.7-fold), 5 μM $CdCl_2$ (32.3-fold) and 100 μg/ml AGE pre-treatment before exposure to 5 μM $CdCl_2$ (19.6-fold) when compared with control (Fig.6.9A). There was also a significant difference in Nrf2 expression between AGE pre-treated cells and cells exposed to 5 μM $CdCl_2$ alone (Fig.6.9A). The presence of 5 μM $CdCl_2$ and AGE pre-treatment significantly increased NQO1 expressions by 6.6 and 8.3-fold respectively when compared with control (Fig.6.9B). However, there was no significant difference in NQO1 expression between AGE treatment and control and between exposure to 5 μM $CdCl_2$ and in AGE pre-treated cells exposed to 5 μM $CdCl_2$ (Fig.6.9B). These sets of data suggest that AGE enhanced induction of Nrf2 and this induction leads to enhanced transcription of NQO1 genes in cells exposed to 5 μM $CdCl_2$ but not in the absence of $CdCl_2$

Figure6.8. Effects of AGE on the expression of Nrf2 and NQO1 in 1321N1 cells after $CdCl_2$ exposure

A.

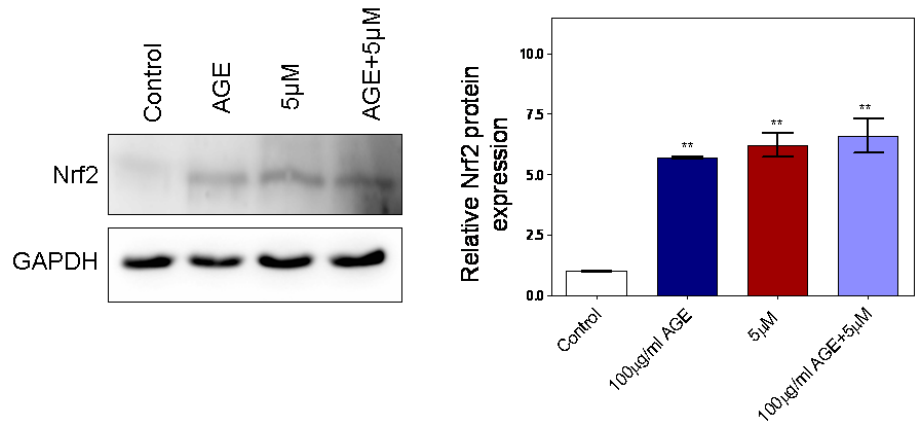

B.

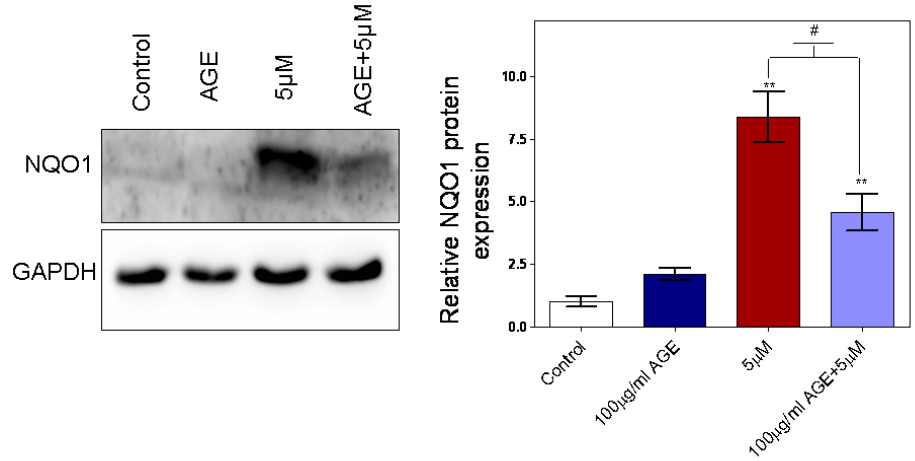

1321N1 cells were pretreated with 100µg/ml AGE for 24hr and then exposed to 5 µM $CdCl_2$ for 24hr. After the incubation, cell extracts were prepared and 10µg of proteins were loaded on SDS-PAGE. Western blot was performed using (A) Nrf2 and (B) NQO1 specific antibodies as described in materials and Methods. Protein loading was normalised with GAPDH antibody. Intensity of the bands was evaluated with image J analysis software and relative protein expressions were compared to control. Data represent the mean value (n=3 of individual experiments done in triplicate) of percentage of control ±SD. Asterisks indicate significant compared with untreated control (***$p<0.005$ **$p<0.01$ *$p<0.05$) using one-way ANOVA with Dunnett's post test. # ($p<0.05$) represents significant difference between pre-treated group and unpretreated group (unpaired student's t-test).

Figure6.9. Effects of AGE on the expression of Nrf2 and NQO1 in HEK 293 cells after $CdCl_2$ exposure

A.

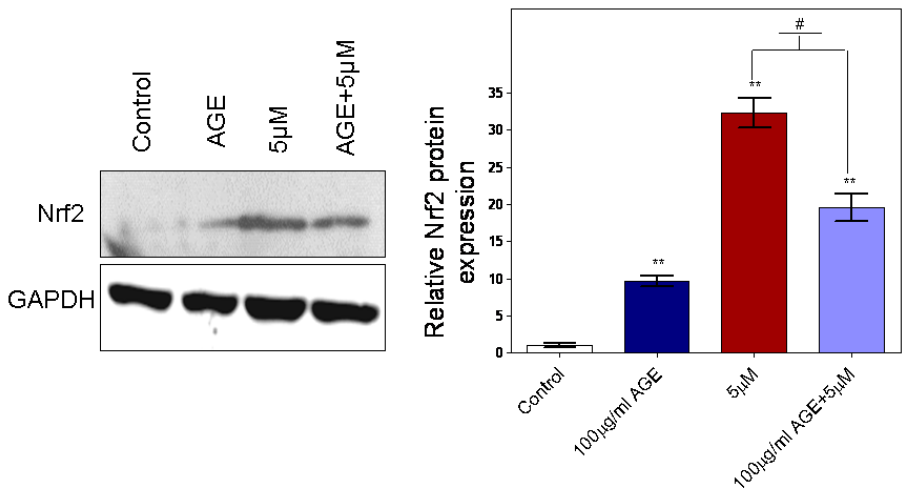

B.

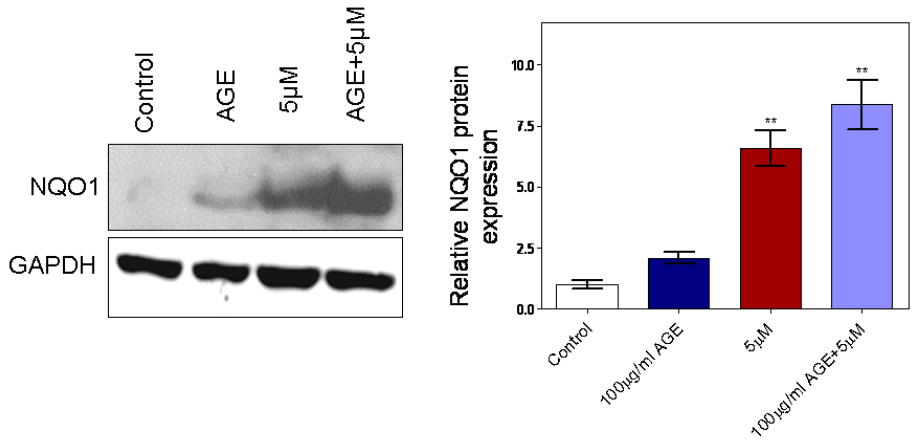

HEK 293 cells were pretreated with 100µg/ml AGE for 24hr and then exposed to 5 µM $CdCl_2$ for 24hr. After the incubation, cell extracts were prepared and 10µg of proteins were loaded on SDS-PAGE. Western blot was performed using (A) Nrf2 and (B) NQO1 specific antibodies as described in materials and Methods. Protein loading was normalised with GAPDH antibody. Intensity of the bands was evaluated with image J analysis software and relative protein expressions were compared to control. Data represent the mean value (n=3 of individual experiments done in triplicate) of percentage of control ±SD. Asterisks indicate significant compared with untreated control (***$p<0.005$ **$p<0.01$ *$p<0.05$) using one-way ANOVA with Dunnett's post test. # ($p<0.05$) represents significant difference between pre-treated group and unpretreated group (unpaired student's t-test).

6.3.10. Effects of GA on Nrf2 expression in 1321N1 cells exposed to $CdCl_2$

In order to determine whether GA treatment prior to exposure to 5 μM $CdCl_2$ has any effect on Nrf2 protein expression, 1321N1 cells were pre-treated with 100 μg/ml GA for 24hr before exposure to 5 μM $CdCl_2$. The results show significant increases of 4.87 and 6.7-fold in Nrf2 expression in the presence of 5 μM $CdCl_2$ and in GA pre-treated cells exposed to 5 μM $CdCl_2$ respectively, when compared with control (Fig.6.10). Increase in Nrf2 expression in GA treated cells was not significantly different compared to the control (Fig.6.10). Similarly, the increase in GA pre-treated cells prior to Cd exposure was not significantly different compared to cells exposed to 5 μM $CdCl_2$ (Fig.6.10).

Figure6.10. Effects of GA on the expression of Nrf2 in 1321N1 cells after $CdCl_2$ exposure

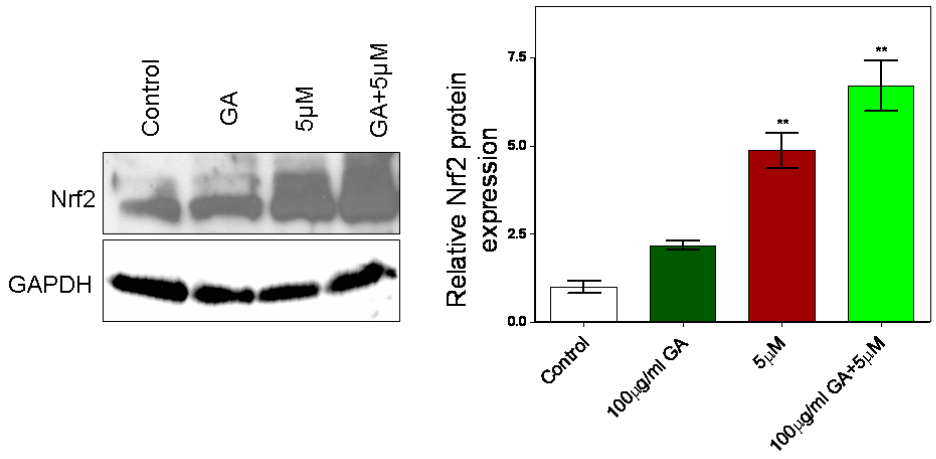

1321N1 cells were pretreated with 100µg/ml GA for 24hr and then exposed to 5 µM $CdCl_2$ for 24hr. After the incubation, cell extracts were prepared and 10µg of proteins were loaded on SDS-PAGE. Western blot was performed using Nrf2 specific antibody as described in materials and Methods. Protein loading was normalised with GAPDH antibody. Intensity of the bands was evaluated with image J analysis software and relative protein expressions were compared to control. Data represent the mean value (n=3 of individual experiments done in triplicate) of percentage of control ±SD. Asterisks indicate significant compared with untreated control (***$p<0.005$ **$p<0.01$ *$p<0.05$) using one-way ANOVA with Dunnett's post test. # ($p<0.05$) represents significant difference between pre-treated group and unpretreated group (unpaired student's t-test).

6.3.11 GA pre-treatment alters calpain activity in presence of $CdCl_2$

In order to elucidate the mechanism involved in the protective effect of GA pre-treatment against $CdCl_2$-induced toxicity, 1321N1 and HEK 293 cells were pre-treated with 100μg/ml GA for 24hr before 24hr exposure to 5μM $CdCl_2$ and calpain activity was determined in the cell extracts. The results show that the presence of GA significantly decreased (2.7-fold) calpain activity in HEK 293 cells when compared with cells exposed to 5μM $CdCl_2$ (Fig.6.11B). However, there was no significant difference in calpain activity between the GA pre-treated 1321N1 cells and the cells exposed to 5μM $CdCl_2$ alone (Fig.6.11A). These results infer that decreased calpain activity may be involved as one mechanism by which GA prevents Cd toxicity in HEK 293 cells but not in 1321N1 cells.

6.3.12. DADS pre-treatment alters calpain activity in cells exposed to $CdCl_2$

To elucidate the mechanism involved in the protective effects of DADS against $CdCl_2$ toxicity, 1321N1 and HEK 293 cells were pre-treated with 100μM DADS for 24hr before 24hr exposure to 5μM $CdCl_2$ and calpain activity was determined in the cell extracts. The results show no significant difference in calpain activity in 1321N1 cells pre-treated with DADS and the cells exposed to 5μM $CdCl_2$ alone (Fig.6.12A). DADS pre-treatment significantly decreased (5.29-fold) calpain activity in HEK 293 cells when compared with cells exposed to 5μM $CdCl_2$ (Fig.6.12B). These results seem to suggest that decreased calpain activity may play a role in the protective effect of DADS against $CdCl_2$ toxicity in HEK 293 cells but not in 1321N1 cells.

6.3.13. AGE pre-treatment alters calpain activity in HEK 293 cells exposed to $CdCl_2$

In order to determine the effects of AGE pre-treatment on calpain activity in HEK 293 cells exposed to 5 μM $CdCl_2$ cells were pre-treated with 100 μg/ml AGE before exposure to 5 μM $CdCl_2$ for 24hr and calpain activity was determined. The results show a 5.5-fold decrease in calpain activity in the presence on AGE when compared with cells exposed to 5 μM $CdCl_2$ (Fig.6.13). This suggests the involvement of decreased calpain activity in the protective mechanism of AGE against Cd toxicity in HEK 293 cells.

Figure6.11. Effects of GA pre-treatment on Calpain activity in the presence of $CdCl_2$

A.

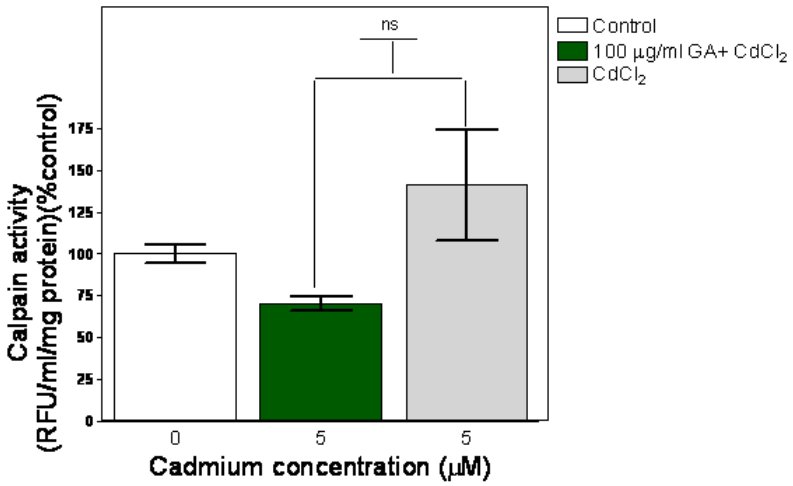

B.

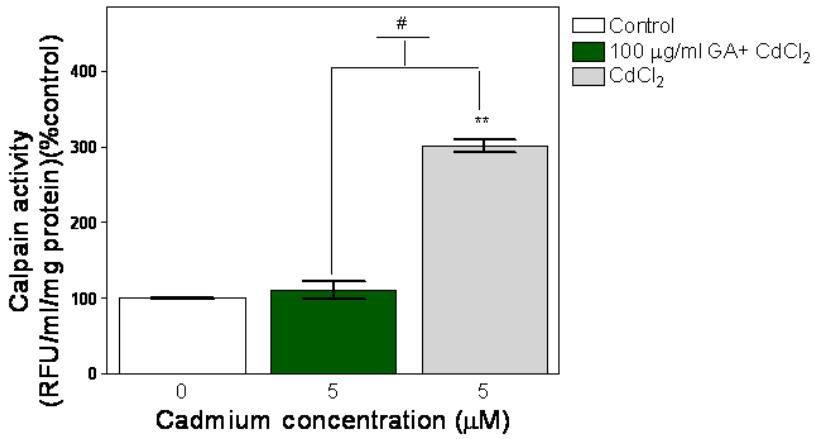

(A) 1321N1 and (B) HEK 293 cells were pre-treated with 100µg/ml GA for 24hr before exposure to 5 µM $CdCl_2$ for 24hr. Calpain activity was determined in the cell extracts as described in Materials and Methods**.** Data represent the mean value (n=3 of individual experiments done in triplicate) of percentage of control ±SD. Asterisks indicate significant compared with untreated control (***p<0.005 **p<0.01 *p<0.05) using one-way ANOVA with Dunnett's post test. # (p<0.05) represents significant difference between pre-treated group and unpretreated group and ns represents non-significant between pre-treated and unpretreated groups (unpaired student's t-test).

Figure6.12. Effects of DADS pre-treatment on Calpain activity in the presence of $CdCl_2$

A.

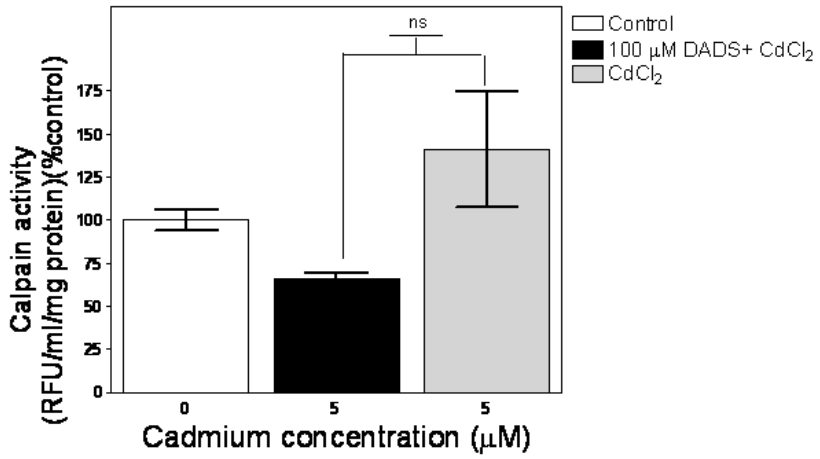

B.

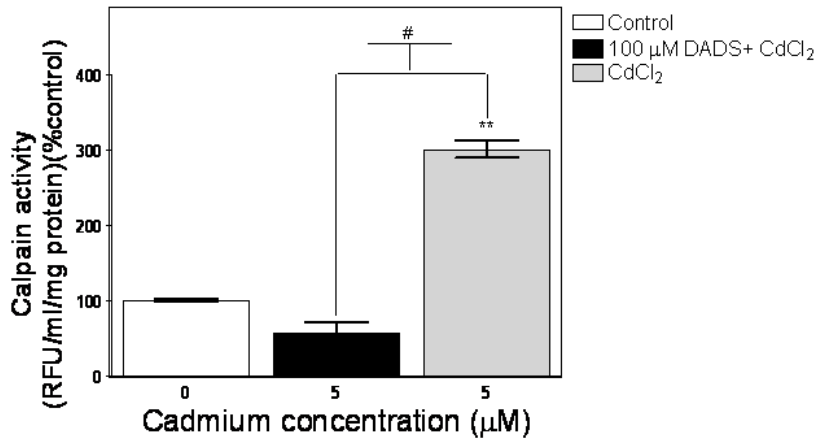

1321N1 and (B) HEK 293 cells were pre-treated with 100µM DADS for 24hr before exposure to 5 µM $CdCl_2$ for 24hr. Calpain activity was determined in the cell extracts as described in Materials and Methods**.** Data represent the mean value (n=3 of individual experiments done in triplicate) of percentage of control ±SD. Asterisks indicate significant compared with untreated control (***p<0.005 **p<0.01 *p<0.05) using one-way ANOVA with Dunnett's post test. # (p<0.05) represents significant difference between pre-treated group and unpretreated group and ns represents non-significant between pre-treated and unpretreated groups (unpaired student's t-test).

Figure6.13. Effects of AGE pre-treatment on Calpain activity in HEK 293 cells in the presence of $CdCl_2$

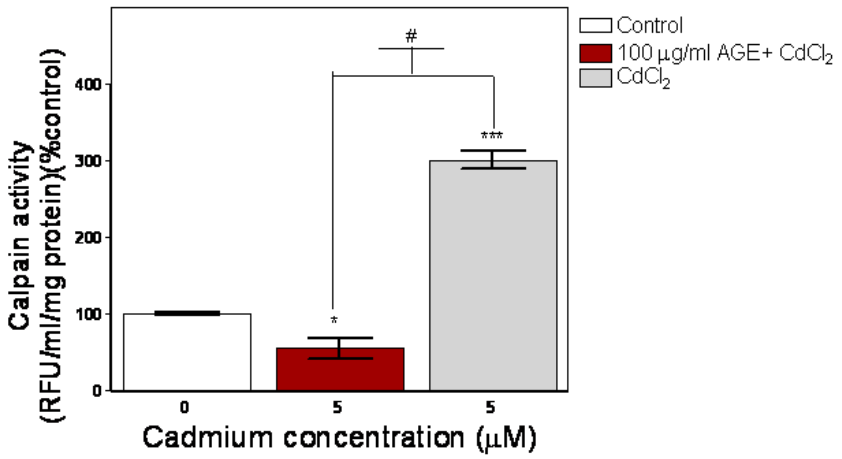

HEK 293 cells were pre-treated with 100µg/ml AGE for 24hr before exposure to 5 µM $CdCl_2$ for 24hr. Calpain activity was determined in the cell extracts as described in Materials and Methods**.** Data represent the mean value (n=3 of individual experiments done in triplicate) of percentage of control ±SD. Asterisks indicate significant compared with untreated control (***p<0.005 **p<0.01 *p<0.05) using one-way ANOVA with Dunnett's post test. # (p<0.05) represents significant difference between pre-treated group and unpretreated group and ns represents non-significant between pre-treated and unpretreated groups (unpaired student's t-test).

6.3.14. Effects of catalase and glutathione peroxidase inhibitors on cell viability in AGE, GA and DADS pre-treated 1321N1 cells exposed to $CdCl_2$

In order to determine the mechanism by which AGE, GA and DADS protect 1321N1 cells from $CdCl_2$ insults, cells were treated with 1 mM aminotriazole (Catalase inhibitor) or 1 mM mercaptosuccinate (Glutathione peroxidase inhibitor) for 30min before 24hr treatment with either100 μg/ml AGE or 100 μg/ml GA or 100μM DADS. The cells were then exposed to 5, 10, 25 and 50 μM $CdCl_2$ for 24hr and cell viability was determined by the MTT assay. The results show that the presence of aminotriazole does not impair cell viability when compared with 1321N1 cells pre-treated with GA (Fig.6.14B).The results also show that the presence of aminotriazole decreased 1321N1 cell viability when compared with the cells pre-treated with DADS (Fig.6.14C). The difference was significant at 10 and 25 μM $CdCl_2$. No significant difference in cell viability between the aminotriazole pre-treated 1321N1 cells and cells exposed to AGE was observed (Fig.6.14A). The presence of mercaptosuccinate does not impair cell survival in both AGE and GA pre-treated cells (Fig.6.15A&B). The results show that the presence of mercaptossuccinate significantly increases cell survival when compared with cells pre-treated with GA without inhibitor (Fig.6.15B). On the other hand, the presence of mercaptosuccinate impairs cell survival when compared with cells pre-treated with DADS without the inhibitor (Fig.6.15C). These decreases were significant at 10 and 25 μM $CdCl_2$.This set of data indicates that enhanced catalase and glutathione peroxidase activities may be important in the protective effects of DADS against Cd toxicity in 1321N1 cells but may not be involved in the protective effects of AGE and GA.

Figure6.14. Effects of aminotriazole on 1321N1 cell viability in the presence of AGE, GA and DADS after $CdCl_2$ exposure

A.

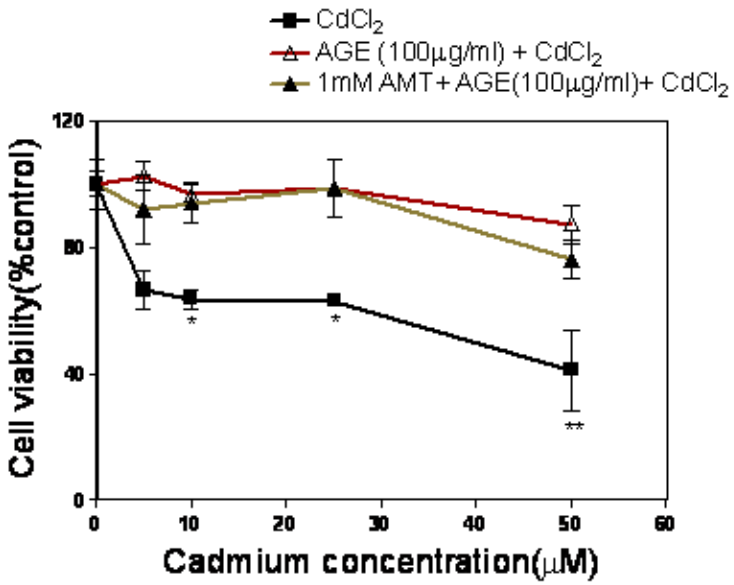

B.

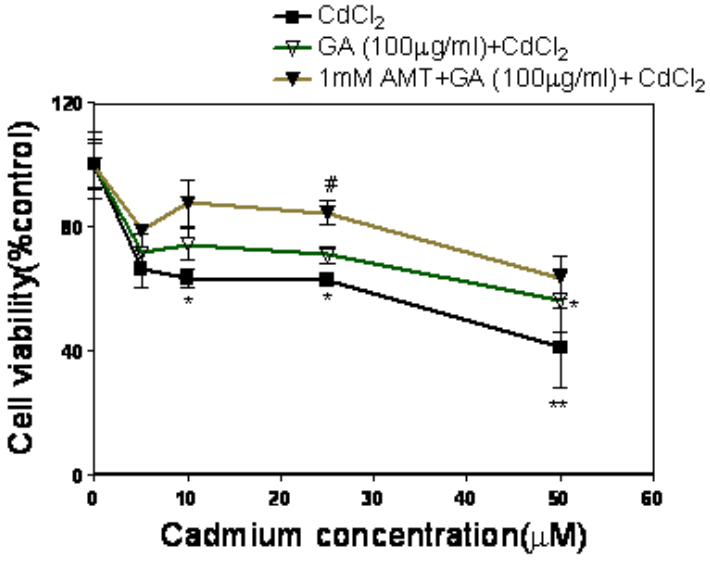

C.

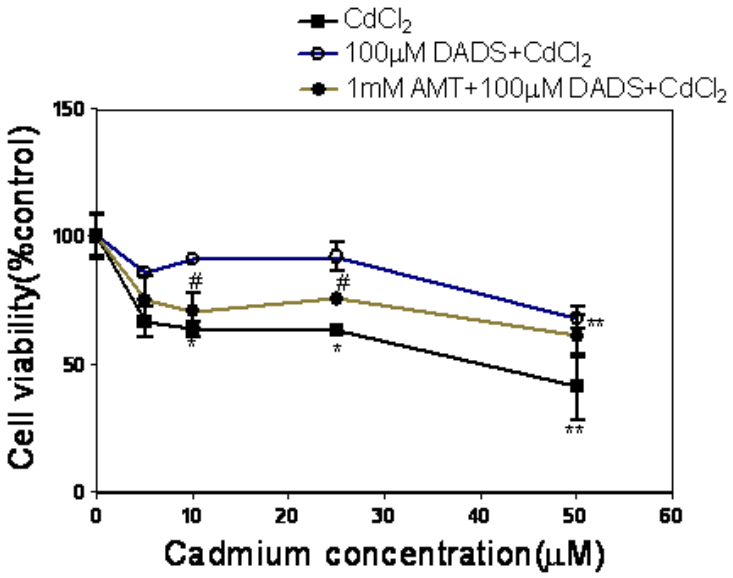

1321N1 cells were pretreated with 1mM aminotriazole (AMT) for 30min before 24hr treatment with either (A)100 μg/ml AGE or (B) 100 μg/ml GA or (C)100 μM DADS. Cells were then exposed to 5, 10, 25 and 50 μM $CdCl_2$ for 24hr and cell viability was determined by the MTT assay as described in Material and Method. Data represent the mean value (n=4 of individual experiments done in triplicate) of percentage of control ±SD. Asterisks indicate significant compared with untreated control (***$p<0.005$ **$p<0.01$ *$p<0.05$) using one-way ANOVA with Dunnett's post test. # ($p<0.05$) represents significant difference between inhibited group and non-inhibited group (unpaired student's t-test).

Figure6.15. Effects of mercaptosuccinate on 1321N1 cell viability in the presence of AGE, GA and DADS after $CdCl_2$ exposure

A.

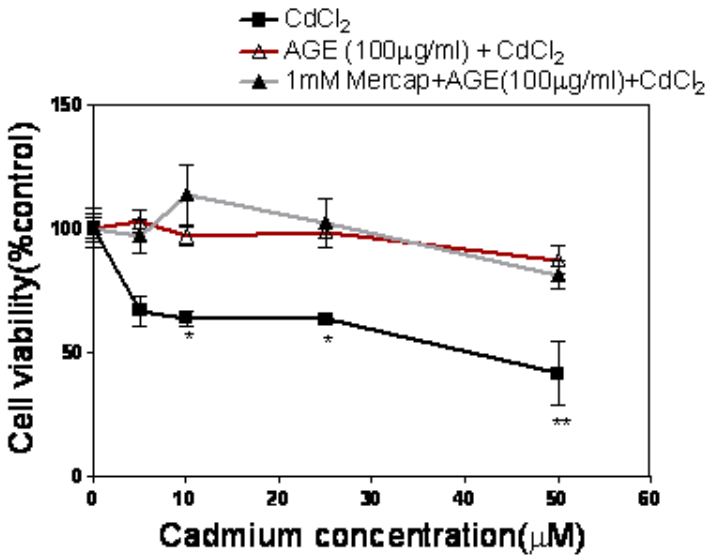

B.

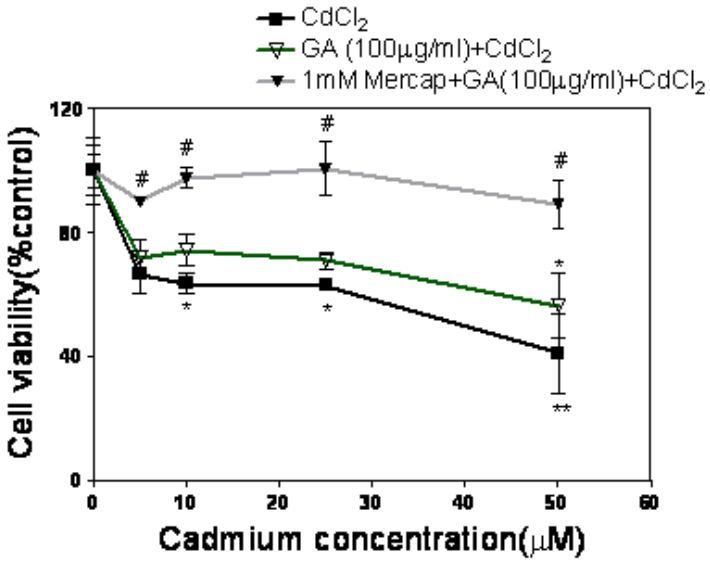

C.

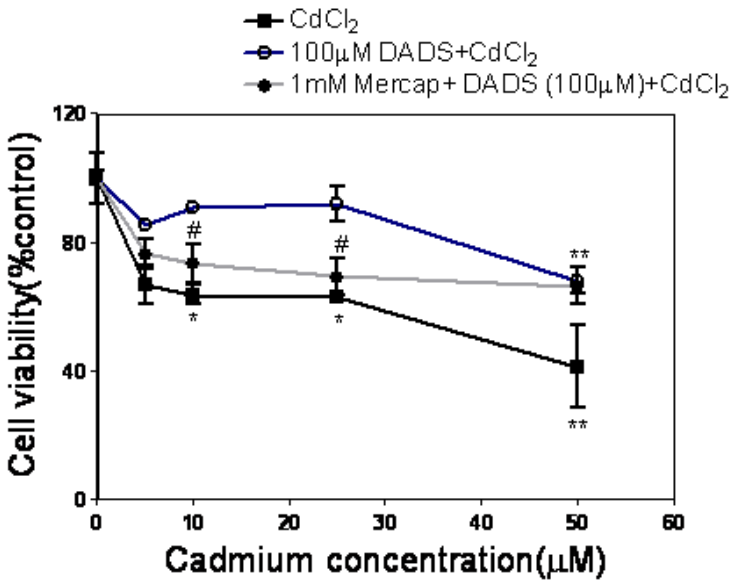

1321N1 cells were pretreated with 1mM mercaptosuccinate (Mercap) for 30min before 24hr treatment with either (A)100 µg/ml AGE or (B) 100 µg/ml GA or (C)100 µM DADS. Cells were then exposed to 5, 10, 25 and 50 µM $CdCl_2$ for 24hr and cell viability was determined by the MTT assay as described in Material and Method. Data represent the mean value (n=4 of individual experiments done in triplicate) of percentage of control ±SD. Asterisks indicate significant compared with untreated control (***$p<0.005$ **$p<0.01$ *$p<0.05$) using one-way ANOVA with Dunnett's post test. # ($p<0.05$) represents significant difference between inhibited group and non-inhibited group (unpaired student's t-test).

6.3.15. Effects of catalase and glutathione peroxidase inhibitors on cell viability in AGE, GA and DADS pre-treated HEK 293 cells exposed to $CdCl_2$

In order to determine the mechanism by which AGE, GA and DADS protect HEK 293 cells from $CdCl_2$ insults, cells were treated with 1mM aminotriazole (Catalase inhibitor) or 1mM Mercaptosuccinate (Glutathione peroxidase inhibitor) for 30min before 24hr treatment with either100 μg/ml AGE or 100 μg/ml GA or 100μM DADS. The cells were then exposed to 5, 10, 25 and 50 μM $CdCl_2$ for 24hr and cell viability was determined by the MTT assay. The results show that the presence of aminotriazole decreased HEK 293 cell viability when compared with AGE pre-treated cells that are not exposed to aminotriazole (Fig.6.16A). On the other hand, aminotriazole does not impair HEK 293 cell viability when compared with cells pre-treated with GA and DADS (Fig.6.16B&C). The presence of mercaptosuccinate significantly enhanced cell survival in DADS pre-treated cells when compared with cells that are not treated with inhibitor (Fig.6.17C). Also significant increases in surviving cells were obtained in the presence of mercaptosuccinate in GA pretreated cells exposed to 25 and 50 μM $CdCl_2$ when compared to cells not treated with inhibitor (Fig.6.17B). The results also show that the presence of mercaptosuccinate does not impair cell survival in AGE pre-treated cells when compared with cells pre-treated with AGE (Fig.6.17A). This set of data indicates that enhanced catalase and glutathione peroxidasee activity may not be involved in the protective effects of AGE, GA and DADS against Cd toxicity in HEK 293 cells.

Figure6.16. Effects of aminotriazole on HEK 293 cell viability in the presence of AGE, GA and DADS after $CdCl_2$ exposure

A.

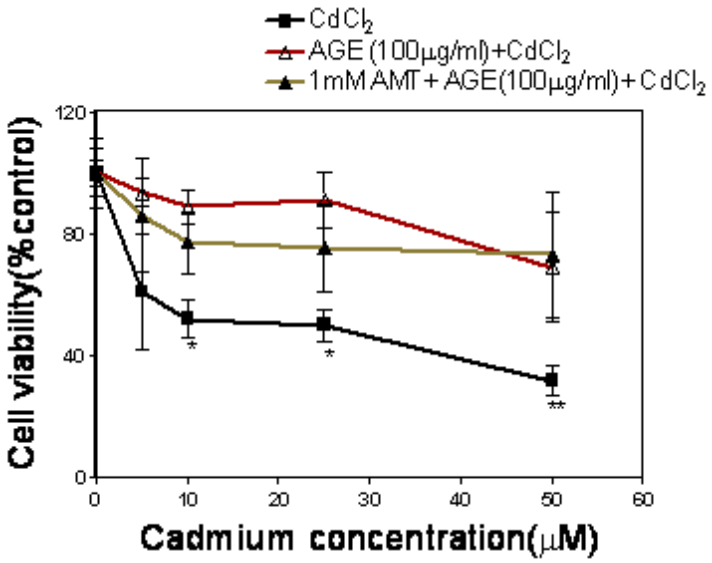

B.

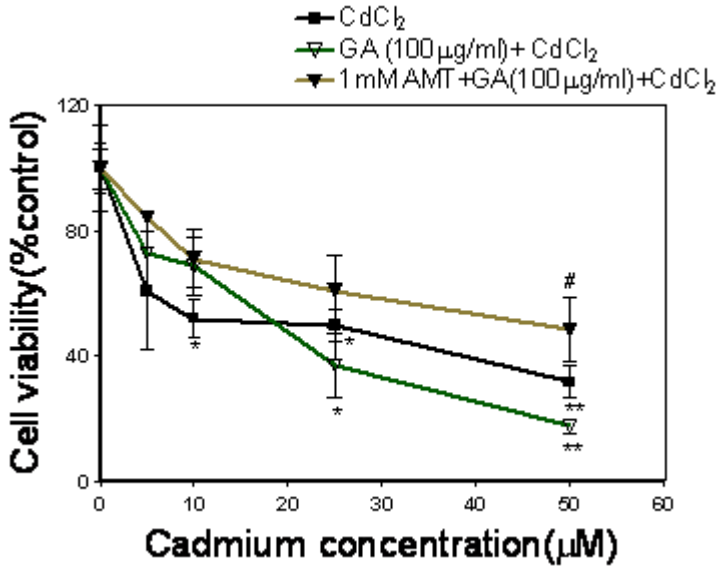

C.

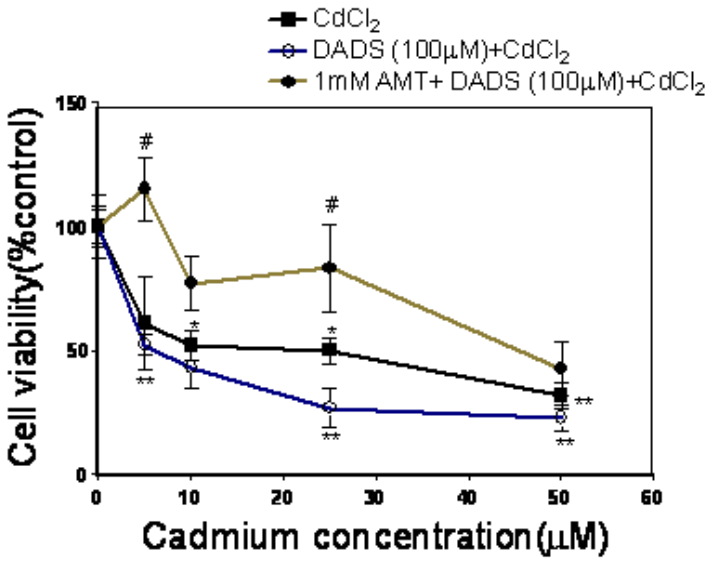

HEK 293 cells were pretreated with 1mM aminotriazole (AMT) for 30min before 24hr treatment with either (A)100 μg/ml AGE or (B) 100 μg/ml GA or (C)100 μM DADS. Cells were then exposed to 5, 10, 25 and 50 μM $CdCl_2$ for 24hr and cell viability was determined by the MTT assay as described in Material and Method. Data represent the mean value (n=4 of individual experiments done in triplicate) of percentage of control ±SD. Asterisks indicate significant compared with untreated control (***$p<0.005$ **$p<0.01$ *$p<0.05$) using one-way ANOVA with Dunnett's post test. # ($p<0.05$) represents significant difference between inhibited group and non-inhibited group (unpaired student's t-test).

Figure6.17. Effects of mercaptosuccinate on HEK 293 cell viability in the presence of AGE, GA and DADS after $CdCl_2$ exposure

A.

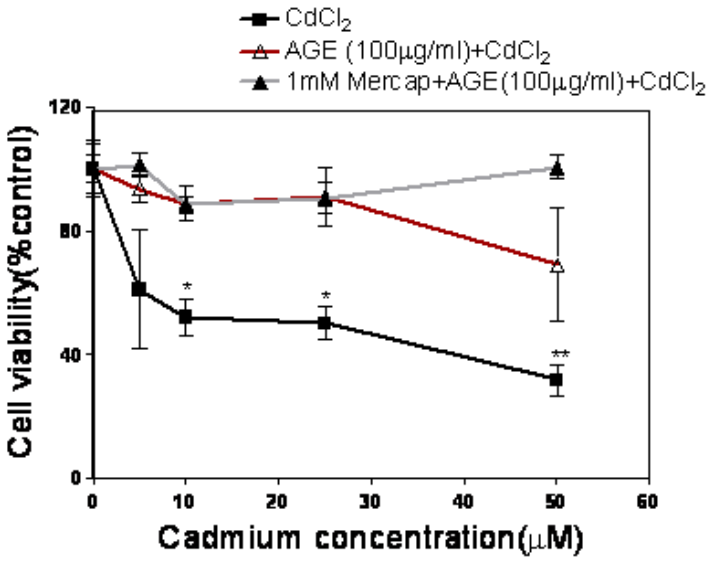

B.

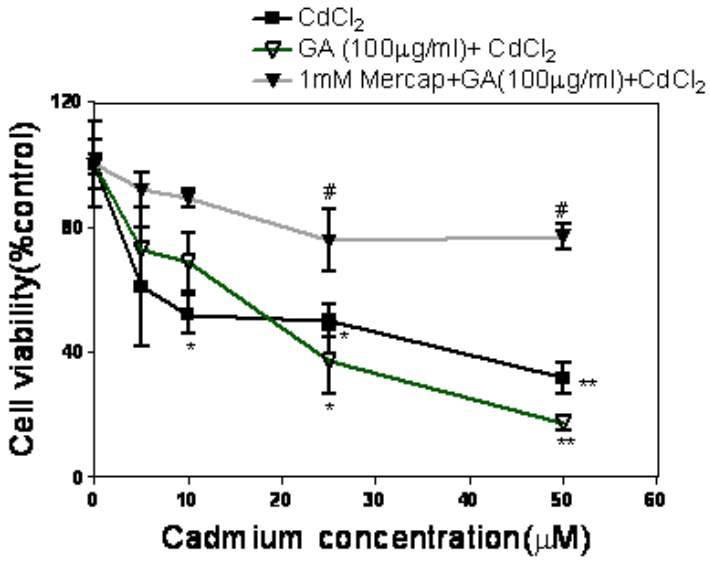

C.

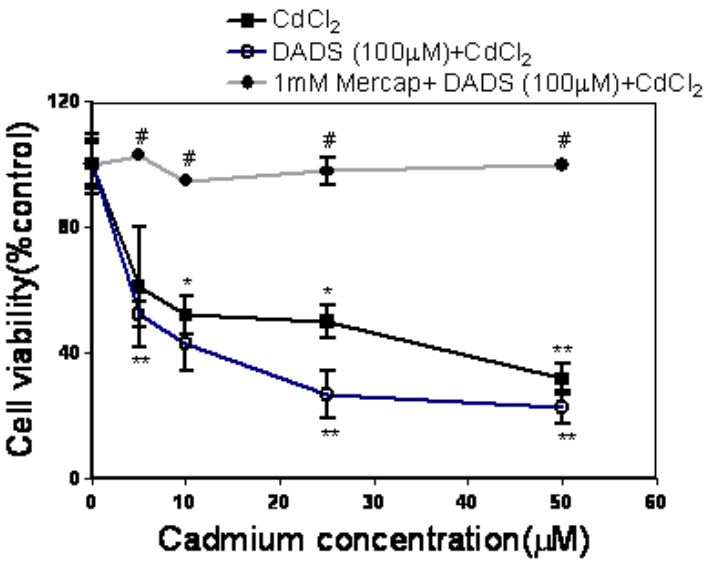

HEK 293 cells were pretreated with 1mM mercaptosuccinate (Mercap) for 30min before 24hr treatment with either (A)100 μg/ml AGE or (B) 100 μg/ml GA or (C)100 μM DADS. Cells were then exposed to 5, 10, 25 and 50 μM $CdCl_2$ for 24hr and cell viability was determined by the MTT assay as described in Material and Method. Data represent the mean value (n=4 of individual experiments done in triplicate) of percentage of control ±SD. Asterisks indicate significant compared with untreated control (***$p<0.005$ **$p<0.01$ *$p<0.05$) using one-way ANOVA with Dunnett's post test. # ($p<0.05$) represents significant difference between inhibited group and non-inhibited group (unpaired student's t-test).

6.4. Discussion

Exposure to cadmium is known to produce a number of health hazards in both experimental animals and humans. Though the body has a number of intrinsic protective machineries, these can be overwhelmed in an event of oxidative stress. Therefore, there is a need to fortify the body defences and this can occur through the intake of exogenous compounds. These exogenous compounds may be able to prevent damage to the cells through a process known as chemoprevention. It has been established that chemopreventive compounds can act by enhancing the removal of carcinogens, electrophiles and other reactive products through the up-regulation of protective enzymes as well as through direct effects. In this present study the efficacy of aged garlic extract (AGE), aqueous garlic extract (GA) and an organosulfur compound in garlic, dially disulfide (DADS) in protecting Cd induced toxicity in cells was examined.

An examination of cell viability showed that AGE enhanced survival of 1321N1 and HEK 293 cells exposed to 10 and 25 μM $CdCl_2$ (Fig.6.1B&C). These result support an earlier report on the study of the effect of AGE and S-allycysteine (SAC), a major compound in AGE, in preventing endothelial cell (bovine pulmonary artery and human umbilical vein) damage caused by oxidized LDL-induced injury (Ide and Lau, 2001). This report showed that both AGE and SAC prevented loss of cell viability in the endothelial cells. From the present study GA seems to be less effective in enhancing cell survival than AGE and DADS. The reduced potency of GA may be due to the nature of the organosulfur compound it contains. GA contains mainly the volatile and less stable allicin which is easily degraded and converted to other compounds. In the LDH experiment, Cd-induced membrane damage

was eliminated by the presence of AGE, GA and DADS at all the concentrations of exposure in HepG2 and 1321N1 cells but they were less effective in HEK 293 depending on Cd concentration (Fig.6.2). The study of Ide and Lau (2001) with the endothelial cells exposed to oxidized LDL also found decreased LDH leakage in the presence of AGE and SAC. In addition, AGE and SAC were found to prevent thiobarbituric acid reactive substance (TBARS) formation and also inhibit reactive oxygen species (ROS) production (Ide and Lau, 2001& 1997). In this present study, AGE, GA and DADS were found to inhibit TBARS formation induced by 5, 10 and 50μM $CdCl_2$ in HepG2 and 1321N1 cells and at 10 and 50μM $CdCl_2$ in HEK 293 cells (Fig.6.3). However, no significant changes were observed in ROS levels in the presence of $CdCl_2$ and in AGE, GA and DADS treated 1321N1 and HEK 293 cells (Fig.6.4). In contrast, AGE, GA and DADS pre-treatment in HepG2 cells significantly decreased ROS production induced by 10 and 50 μM cadmium, and also at 5 μM $CdCl_2$ in the presence of DADS. This infers that the reduced LDH leakage and MDA levels and the enhanced cell survival observed in HepG2 cells after pre-treatment may have been as a result of decreased ROS level.

GSH is an important endogenous antioxidant that directly scavenges for reactive oxygen species (ROS). The presence of sulphur compounds such as the OSCs in garlic serves as a source of available electrons for the removal of electrophiles by conjugation reactions. Therefore, the net effect of the administration of OSCs in garlic is the enhancement of intracellular GSH level (Chichen *et al.*, 2004). In one *in vivo* study using rats as a model, aqueous garlic (GA) extract was shown to protect against decreased GSH levels and increased MDA levels during thermal injury (Sener *et al*., 2003).

Also AGE and SAC were found to prevent GSH depletion in endothelial cells exposed to oxidised LDL (Ide and Lau, 2001). Similarly, an increase in GSH levels was obtained in this study after exposure to 5, 10 and 50 μM $CdCl_2$ in HepG2 cells pre-treated with AGE, GA and DADS but AGE is more efficacious in enhancing GSH levels in HepG2 cells at higher Cd concentrations (Fig.6.5A).1321N1 cells pre-treated with GA and DADS also show a significant elevation in GSH levels (Fig.6.5B). Similarly, significant increases in GSH levels were observed at 50 μM Cd in AGE and GA pre-treated HEK 293 cells (Fig.6.5C). These results show that the elevated GSH levels especially at 50 μM Cd brought about by pre-treatment of 1321N1 with GA and DADS and HEK 293 with AGE and GA may account for the enhanced cell survival in 1321N1 and the reduced toxicity of Cd at this concentration as reflected in the lower LDH leakage and MDA levels in both cell lines. GSH levels were not significantly affected by DADS in HEK 293 cells (Fig.6.5C) which is an indication that the net effect of garlic OSCs on GSH levels in the presence of Cd may be cell-type dependent. It has already been reported that treatment of primary rat hepatocytes with OSC caused a drastic reduction in GSH levels at early hours of treatment (Sheen *et al.*, 1996) which infers that different GSH level responses may occur in a cell at different exposure time and with different chemical compounds.

The "Antioxidant" effects of OSCs were reported to increase with the number of sulphur atoms (Imai *et al.*, 1994). In one study, diallyl tetrasulfide (DTS) was reported to protect rat brain against Cd toxicity by increasing GSH and decreasing TBARS level (Pari and Murugavel, 2007). In this present study, a similar result was observed in the presence of DADS in cells exposed to Cd. DADS prevented an increase in TBARS levels induced by

cadmium in all three cell lines (Fig.6.3) and it also prevented decreased GSH levels induced by cadmium in HepG2 and 1321N1 cells (Fig.6.5A&B).

Nrf2 is a transcription factor whose activity can be modulated by the presence of dietary compounds (Lee and Surh, 2005). One hypothesis for the observed Nrf2 protein elevation in the pre-treated cells is the modification of the Keap1 cysteine residue by garlic OSCs and DADS to form a disulfide and this may play important role in the release of Nrf2 from Keap1 thereby leading to the observed Nrf2 protein elevation in DADS and AGE treated 1321N1 cells (Fig.6.6A&6.8A) and AGE treated HEK 293 cells (Fig.6.9A) when compared to control. Compounds that react with the thiol/disulfide groups have been reported to induce Nrf2-dependent genes via the ARE (Prochaska *et al*., 1985). Cd is known to scavenge for thiol groups and thus may also induce the release of Nrf2 from Keap1 as it is capable of modifying the cysteine residues on the Keap1. This would account for the enhanced Nrf2 protein levels observed in the cell lines in the presence of 5μM Cd which represents a lower dose that can trigger an adaptive response. Through the Nrf2-keap1-ARE pathway this induces the transcription of cytoprotective genes such as NQO1 expression, which is in agreement with the earlier observation in Chapter 5. In this study, we aimed to examine the effects of AGE, GA and DADS pre-treatment on the induction of a protective response to Cd via Nrf2 induction. In essence this would show whether pre-treatment has additive or synergistic or antagonistic effects on Nrf2 induction by Cd. The present study shows that the presence of DADS, AGE and GA increases Nrf2 protein expression in 1321N1 cells following exposure to 5 μM when compared to cells exposed to 5 μM $CdCl_2$ only. Similar results were obtained in HEK 293 cells pre-treated with DADS (Fig.6.7A). These

results show that the presence of these extracts and DADS seems to have an additive effect with 5 μM Cd in boosting the protective response of the cells.

The results of this present study clearly show that Nrf2 may play a role in AGE, GA and DADS-induced phase II and antioxidant enzymes expressions. It has earlier been shown that dially disulfide (DADS), dially sulphide (DAS) and dially trisulfide (DATS) upregulate NAD (P) H: quinone oxidoreductase 1 (NQO1) and heme oxygenase1 (HO1) expression in human hepatoma HepG2 cells via ARE activation, as a consequence of Nrf2 induction (Chi Chen *et al*., 2004). In this present study, 1321N1 cells pre-treated with DADS and HEK 293 cells pre-treated with AGE before Cd exposure show an increase in NQO1 expression in the cell lines. These increases correspond with the increase observed in Nrf2 expression which further supports the involvement of Nrf2 in the protective action of AGE, GA and DADS against Cd toxicity.

It was reported in one study using protein kinase inhibitors that DADS induced ARE activity in HepG2 cells via a calcium-dependent signalling pathway (Chen *et al*., 2004). In the present study, the presence of AGE, GA and DADS were found to significantly reduce calpain activity in the presence of 5 μM $CdCl_2$ in HEK 293 cells when compared with the absence of pre-treatment. Calpain is a Ca^{2+}-activated protease which has been implicated in apoptosis. In Chapter 4, calpain was reported to be involved in HEK 293 cell death as a result of intracellular Ca^{2+} elevation via PLC-IP_3 pathway. The decrease in LDH leakage and MDA levels and the enhanced cell survival observed at 5 μM $CdCl_2$ following AGE and GA pre-treatment in HEK 293 cells may be due to the observed decrease in calpain activity

(Fig.6.11B&6.13B). The mechanism involved needs further clarification. However, alteration in calpain activity seems not to be crucial to 1321N1 protection by the extracts.

To further gain insight as to the mechanisms involved in the protective influence of AGE, GA and DADS against Cd toxicity, this present work explored the use of specific enzyme inhibitors. The significant decrease in cell survival observed in the presence of catalase and glutathione peroxidase inhibitors in 1321N1 cells pre-treated with DADS at 10 and 25 μM implicates that enhanced catalase and glutathione peroxidase activities may play a role in DADS mediated protection of 1321N1 against Cd toxicity.

In summary, the data obtained from this study show that AGE, GA and DADS have beneficial actions against cadmium induced toxicity in HepG2, 1321N1 and HEK 293 cells and these include inhibition of membrane damage, reduction in lipid peroxidation and reactive oxygen production. These protective effects are likely to be mediated at least in part by the enhanced induction of the cytoprotective enzymes through the release and activation of Nrf2 in 1321N1 and HEK 293 cells and also through the inhibition of calpain activity in HEK 293 cells. However, these mechanisms need further clarification.

CHAPTER 7

Changes in Proteins Expressions in Response to Cadmium Toxicity

Chapter 7

7.0. Changes in Protein Expression in Response to Cadmium Toxicity

7.1 Introduction

In previous Chapters, the effect of Cd on cell lines was investigated. In Chapter 4, we have shown that cadmium –induced intracellular Ca^{2+} elevation in HEK 293 cells and it also causes elevation in ATP production in HepG2, 1321N1 and HEK 293 cells after 24hr exposure. In many cases, Cd causes significant changes in the expression of various proteins and mRNA molecules within the cell (Chapter 5). These changes have the potential of being used as markers of Cd exposure, if a clear and specific link can be demonstrated.

Several techniques have been developed for monitoring protein expression. 2-D electrophoresis is an analysis technique first introduced by O'Farrell (1975) and it is used for the comprehensive analysis of protein mixtures from different cells, tissues and biological samples in order to establish their protein profiling. The technique separates proteins based on their isoelectric points (pI) in the first dimension step, followed by the second dimension step in which the proteins are separated on the basis of their molecular weight (MW) in an SDS-PAGE. Each spot of the separated proteins corresponds to a single protein of different molecular mass (MW) and isoelectric point (pI) and can be identified and quantified. This technique can also detect post- and co-translationally modified proteins which can not normally be predicted from their genomic sequences.

In this Chapter, in order to gain further insight into the changes in the proteome induced by Cd, 2D-gel electrophoresis was performed on the cell extracts after Cd exposure and proteins spots were compared using Phoretix™2D analysis software. Comparisons were made between treated and untreated cells and spots were identified by mass spectroscopy using peptide-mass fingerprinting and database searching.

7.2. Materials and Methods

7.2.1. Cell culture

HepG2, 1321N1 and HEK 293 Cells were cultured as previously described in Section 2.2.1.The cells were allowed to grow to 90% confluent in tissue culture flasks and then treated with 5, 10 and 50 μM $CdCl_2$ for 24hr.

7.2.2. Cell Sample Preparation for 2-D Gel Electrophoresis

Chemical and Reagent

Lysis Solution (L)

Lysis Solution contained 13.5g Urea; 0.5 ml Triton X-100; 0.5 ml 2-Mercaptoethanol; 0.5 ml Pharmalyte 3-10; 75 mg Dithiothreitol (DTT) (added just before use); 35 mg Phenylmethylsulfonyl fluoride (PMSF) (added freshly on the day of the experiment) and made up to 25 ml with ultra high quality water. The solution was stored as 1 ml aliquots in Eppendorf tubes at -20°C.

Sample Solution (S)

Sample Solution contained 13.5g Urea; 0.13 ml Triton X-100; 0.5 ml 2-Mercaptoethanol; 0.5 ml Pharmalyte 3-10; 75 mg Dithiothreitol (DTT) (added freshly just before use); 35 mg Phenylmethylsulfonyl fluoride (PMSF) (added freshly before use) and made up to 25 ml with ultra high quality water. A few grains of bromophenol blue were added to the solution and the solution was stored as 1 ml aliquots in Eppendorf tubes at -20°C.

Sample Preparation Procedure

The control (untreated) and $CdCl_2$ treated cells were washed twice with ice cold Phosphate Buffer Saline (PBS) and scraped with the rubber policeman

into a 1 ml Eppendorf tube. The cells were centrifuged at 3000 x *g* for 1min and the pellets obtained were washed again in ice-cold PBS and recentrifuged at the same speed and time. The resultant pellets were then stored at -80°C before use. The pellets were resuspended in 200 µl Lysis Solution (L) and mixed by vortexing. The resulting cells lysates were then centrifuged at 10,000 x *g* for 5 min. The clear supernatant containing the cell extracts was then transferred into a fresh Eppendorf tube and stored at -80°C. Protein contents of the extracts were determined by Bradford method and the cell extract was diluted in Sample Solution (S) to give a loading concentration of about 240 µg in a loading volume of 100 µl.

7.2.3. Rehydration of Immobiline DryStrips (pH 3-10)

Materials

180mm long Immobiline ™ IPG gel strips (pH 3-10) were obtained from Amersham Pharmacia Biotech (Sweden) and stored at -20°C.
Immobiline DryStrip Reswelling Tray with twelve reservoirs or channels.
DryStrip cover fluid.

Rehydrating Solution

This solution contains 12.0g Urea; 0.13 ml Triton X-100; 0.13 ml Pharmalyte 3-10; 50 mg DTT and made up to 25 ml with distilled water.

Procedures

The plastic cover of the immobiline™ IPG DryStrips was peeled off from the acidic (+) end and then placed in such a way that the surface of the gel is downward into the channel of the reswelling tray which already contains 340 µl rehydrating solution. The strip was placed in such way that the acidic end

was placed against the slope end of the channel. Care was taken to avoid bubble formation under the strip. The channel was then overlayed with 2 ml of DryStrip cover fluid to prevent evaporation of the rehydrating solution and urea crystallization and the lid of the reswelling tray was replaced. The Strip was allowed to rehydrate overnight or at least 10hours at room temperature.

7.2.4. Running First Dimension: Isoelectric Focussing (IEF)

Ettan IPGphor IEF system from Amersham Biosciences, UK was used in the first dimension isoelectric focusing for the separation of protein according to their isoelectric point (pI) on the rehydrated IPG strips. The IEF electrophoresis unit was connected to the Multi Temp TM III Thermostatic circulator set at 20^{o}C and 3 ml of DryStrip Cover Fluid was pipetted into the strip channels of the electrode plate. The rehydrated Immobiline™ IPG DryStrips were removed from the reswelling tray and placed gel side up into the strip channel of the electrode plate with the acidic (+) ends toward the anode avoiding bubble formation. Care was taken to ensure that the strips were aligned in the electrode plate. IEF Electrode wicks were soaked in distilled water, blotted dry briefly and placed over both ends of the IPG strips. The electrodes were carefully lowered on top of the moist paper wicks at both ends of the strip to provide electrical contact. The sample cups were then placed on top of the IPG strips near the anodic end of the electrode with the cup touching the gel surface ensuring good contact to prevent leakage from the cups. 110 ml of DryStrip Cover Fluid was poured into the electrode plate to completely cover the cups. 100 μl (240 μg protein) of sample mixture was loaded into the sample cup and the electrophoresis unit was covered with the lid. The electrodes were then connected to the source of power and

the first dimension separation was carried out according to the following programme:

Phase	Voltage mode	Voltage (V)	Time (hr:min)	Volt-hours(KVh)
1	Step and Hold	300	3:00	0.9
2	Gradient	1000	6:00	3.9
3	Gradient	8000	3:00	13.5
4	Step and Hold	8000	9:30	9.7
	Total		21.30	28.0

7.2.5. IPG Strip Equilibration

SDS Equilibration Buffer

This contains 6.7 ml Tris (1.5M,pH8.8); 72.07g Urea; 69 ml Glycerol (87%v/v); 4.0g SDS; a trace amount of Bromophenol blue; made up to 200 ml with distilled water. This solution was stored at -20^{o}C.

Equilibration solution I

This contains 1 %(w/v) DTT prepared freshly in SDS equilibration buffer.

Equilibration solution II

This contains 2.5% (w/v) iodoacetamide prepared freshly in SDS equilibration buffer.

Procedures

Each of the IPG strips from the first dimension process were soaked in approximately 10 ml equilibration solution I for about 15min and afterward soaked in 10 ml of equilibration solution II.

7.2.6. Running Second Dimension: SDS-PAGE

Gel caster assembly

Gel plates were cleaned thoroughly with ethanol and then inserted into the gel caster in such away that a thin space was left between the gel plate sets. The gel caster was laid lying flat to ease assembly. After the assembly of the plates, the other side of the gel caster was placed on top and the sides of the caster clamped together and the screw at the bottom was tightened to prevent leakage.

10% Acrylamide Gel Solution (450 ml)

The 10% Acrylamide Gel Solution were prepared using the following mixture:

	Volume (ml)
30% Acrylamide/bisacrylamide solution	150
Tris (1.5M; pH 8.8)	113
Distilled water	178
10% (w/v) SDS	4.5
10% (w/v) Ammonium persulfate	4.5
10% TEMED	0.77

450 ml of the 10% acrylamide solution were poured into the gel caster almost to the top leaving a 5mm gap at the top. 1 ml of saturated isobutanol was poured on top of each gel and then left to set. After setting, the gel caster assembly was dismantled, and the top of each gel (25.5 x 20.5 cm, 1mm thick) was rinsed with distilled water. This was then allowed to drain briefly and the gel plates were laid flat with the shorter glass plate uppermost. The equilibrated IPG Strip was then laid on top of each gel in such a way that it just touched the gel with the IPG Strip gel side up and avoiding air bubble formation between the gel and the IPG Strip. The gel plates were then stood in an upright position and the IPG Strips was sealed with about 500 µl low melting agarose solution (0.5%).

Electrophoresis system for second dimension

10 x SDS electrophoresis buffer (30.28 g Tris base; 144 g Glycine; 10 g SDS; made up to 1 litre with distilled water).

Procedures

The electrophoresis system (EttanDaltSix ; Amersham Biosciences, UK) was used for the second dimension separation of the proteins on the equilibrated IPG strip from the first dimension separation. The gel plate containing the IPG strip was inserted into the EttanDaltSix electrophoresis unit and the unit was filled with SDS electrophoresis buffer (as shown below) and connected to the Multitemp cooler system at 20^{o}C. Separation of the protein was then carried out in two steps of 5W / gel for 30min followed by 17W / gel for 4h.

Anode (lower chamber)	Volume (L)
1X SDS electrophoresis buffer	4.3

Cathode (upper chamber)	Volume (L)
2X SDS electrophoresis buffer	0.8

7.2.7. Staining the gel

The gel was removed from the plate after electrophoresis and placed gently into a plastic tray. The fixing of the gel was done by adding the fixing solution to the gel and leaving it for 60min. The gel was then stained overnight with the staining solution after which the gel was transferred into the neutralisation solution for 1-3min and then washed with 25% (v/v) methanol for 2hr. The gel was further stained by first soaking it in stabilising solution for at least one day and then repeating the staining procedures. The gel can remain in the staining or stabilising solution over the weekend without affecting the results. Repeating the staining protocol for 3-5times enhanced the clarity and sensitivity of the spot.

Solutions

Fixing solution

The fixing solution contains 5 ml of o-Phosphoric acid (85%, v/v), 100 ml of methanol, made up to 500 ml with distilled water.

Stock staining solution A

The solution contains 9.5 ml of o-Phosphoric acid (85%, v/v), 40g ammonium sulphates (10%, w/v), made up to 400 ml with distilled water.

Stock staining solution B

2.5g of coomassie brilliant blue G250 (5% w/v), made up to 50 ml with distilled water.

Staining solution

10 ml of stock staining solution B was mixed with 400 ml of stock solution A and 100 ml of methanol added. This solution was prepared freshly each time.

Neutralisation solution

This solution contains 6g of Tris-base (0.1M) dissolved in 500 ml distilled water and the pH was adjusted to 6.5 with o-Phosphoric acid.

Washing solution

This solution contains 125 ml methanol made up to 500 ml with distilled water.

Stabilising solution

This solution contains 100g of ammonium sulphate made up to 500 ml with distilled water.

7.2.8. Imaging the gel

After repeated staining, the gel was then photographed using the Fujifilm LAS-3000 Imaging system and the image was stored as 16-bit greyscale TIFF images.

7.2.9. Image analysis using Phoretix™2D analysis software

Phoretix™ 2D analysis software (Nonlinear dynamics ltd, UK) was used for analysing the protein spots on the 2D-gel. First, images were closely aligned to match the protein spots from different gels by automatic alignment vectors and manually using the Phoretix software. Reference gel was then created from the control gel and the other gels were aligned carefully to match the protein spots on the reference image. The gel images were then inspected for individual spot outlines and background correction was applied using the Phoretix software. The unwanted areas of the gel were excluded and spot analysis was performed automatically. The expression tables and histograms of each spot relative to the reference spot were automatically generated

7.2.10. Picking, digesting and identification of protein

Data from the Phoretix™ 2D analysis software was used as guide for picking spots of interest using a manual one touch spot picker (Web Scientific, UK). The picked spots were kept in Eppendorf tubes at -80^{o}C for further processing. MALDI-TOF Tandem mass spectroscopy (TOF MS/MS) analysis of the digested spots were done at the Sir Henry Wellcome Functional Genomic facility at Glasgow University, UK

7.3 Results

7.3.1. Protein separation by 2-D electrophoresis from HepG2, 1321N1 and HEK 293 cell lines after $CdCl_2$ exposure

In order to determine the influence of 5, 10 and 50 μM $CdCl_2$ on the proteomic profile of HepG2, 1321N1 and HEK 293 cell lines after 24 hr exposure, 2D-gel electrophoresis was carried out on the whole cell extracts using Immobiline ™ IPG gel strips (pH 3-10) (based on isoelectric point, pI) for the first dimensional separation, and SDS-PAGE electrophoresis (based on molecular weight) for the second dimensional separation. The gels were then stained with colloidal coomassie blue for easy visualization of the protein spots and the spots were analysed with the Phoretix 2D software and identified using MALDI-TOF mass spectroscopy. Fig.7.1, 7.2 and 7.3 are the 2-D electrophoresis patterns of the proteomic profiles in HepG2, 1321N1 and HEK 293 cells after 24hr exposure to 5, 10 and 50 μM $CdCl_2$. Table.7.1 reveals the total number of protein spots that were present in each of the cell lines. Table 7.2 reveals the total number of proteins that are induced and repressed by at least 2-fold in the each of the three cell lines after Cd exposure. Table 7.3 identifies some of the proteins that are induced by Cd exposure in the three cell lines.

Figure7.1. 2-dimensional gel electrophoresis of HepG2 cells after 24hr treatment with $CdCl_2$.

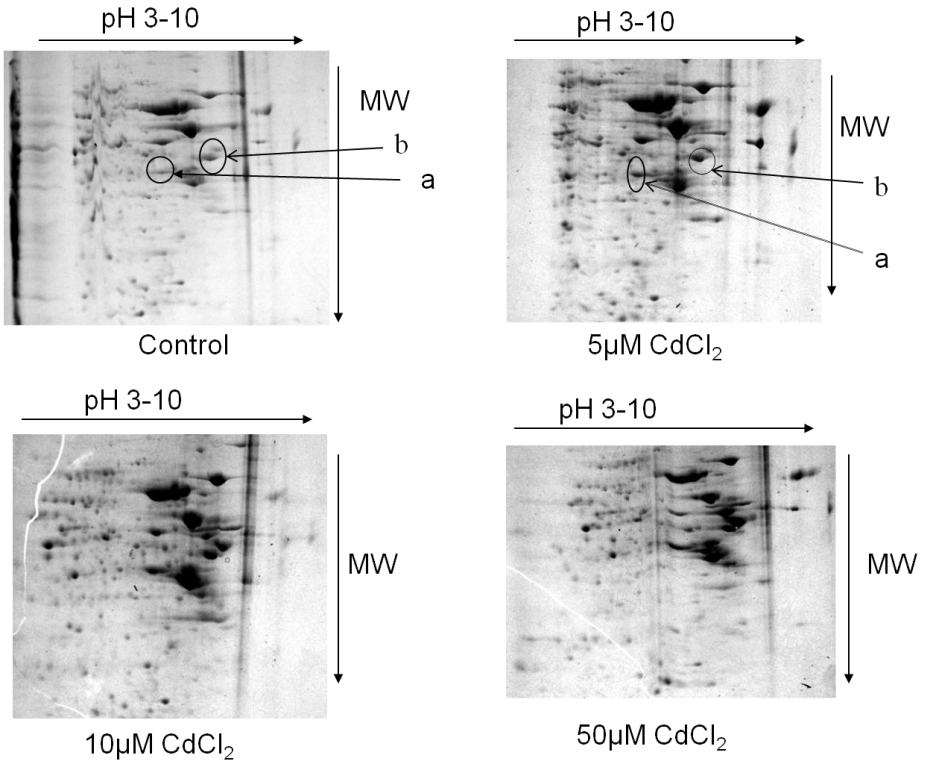

HepG2 cells were exposed to 5, 10 and 50 μM $CdCl_2$ for 24hr and cells samples were separated on based on isoelectric point on a rehydrated immobiline™ IPG DryStrips (pH 3-10).The second dimensional separation was performed based on Molecular weight in a SDS-PAGE electrophoresis. Analysis of spot was performed on phoretix software using a reference gel produced from control gel. Mass spectroscopy analysis was carried out on the spots

Figure.7.2. 2-dimensional gel electrophoresis of 1321N1 cells after 24hr treatment with $CdCl_2$.

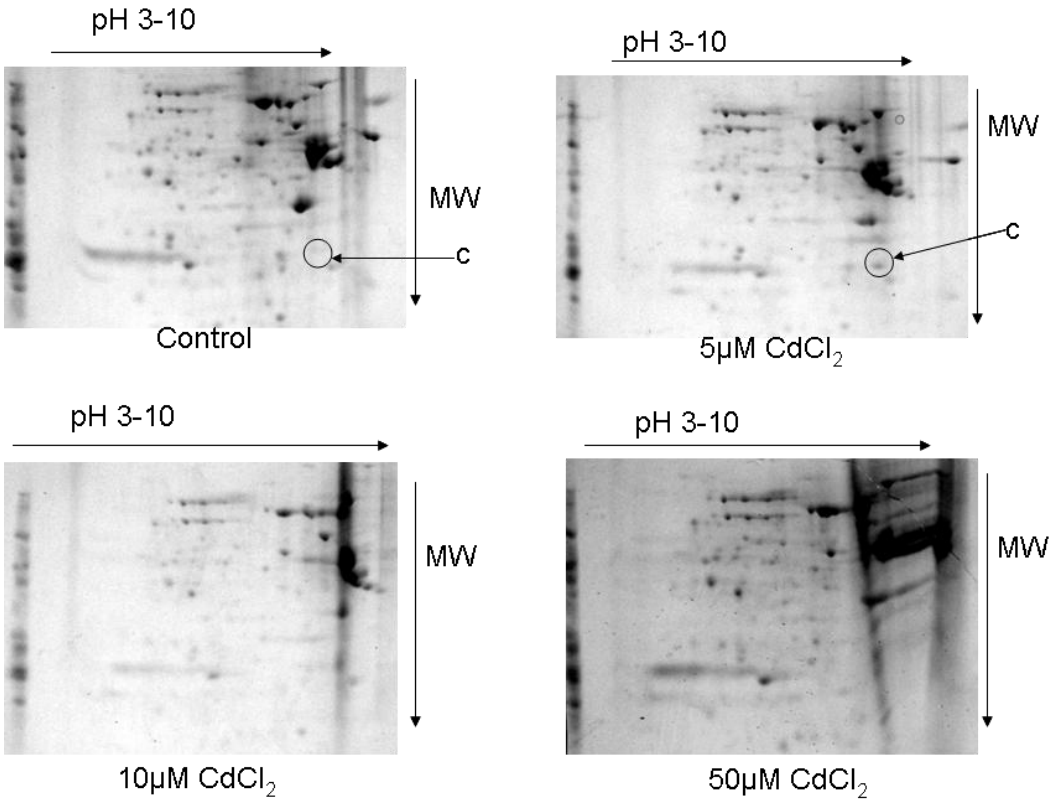

1321N1 cells were exposed to 5, 10 and 50 µM $CdCl_2$ for 24hr and cells samples were separated on based on isoelectric point on a rehydrated immobiline™ IPG DryStrips (pH 3-10).The second dimensional separation was performed based on Molecular weight in a SDS-PAGE electrophoresis. Analyses of spots were performed on phoretix 2-D software using a reference gel produced from control gel. Mass spectroscopy analysis was carried out on the spots.

Figure7.3. 2-dimensional gel electrophoresis of HEK 293 cells after 24hr treatment with $CdCl_2$.

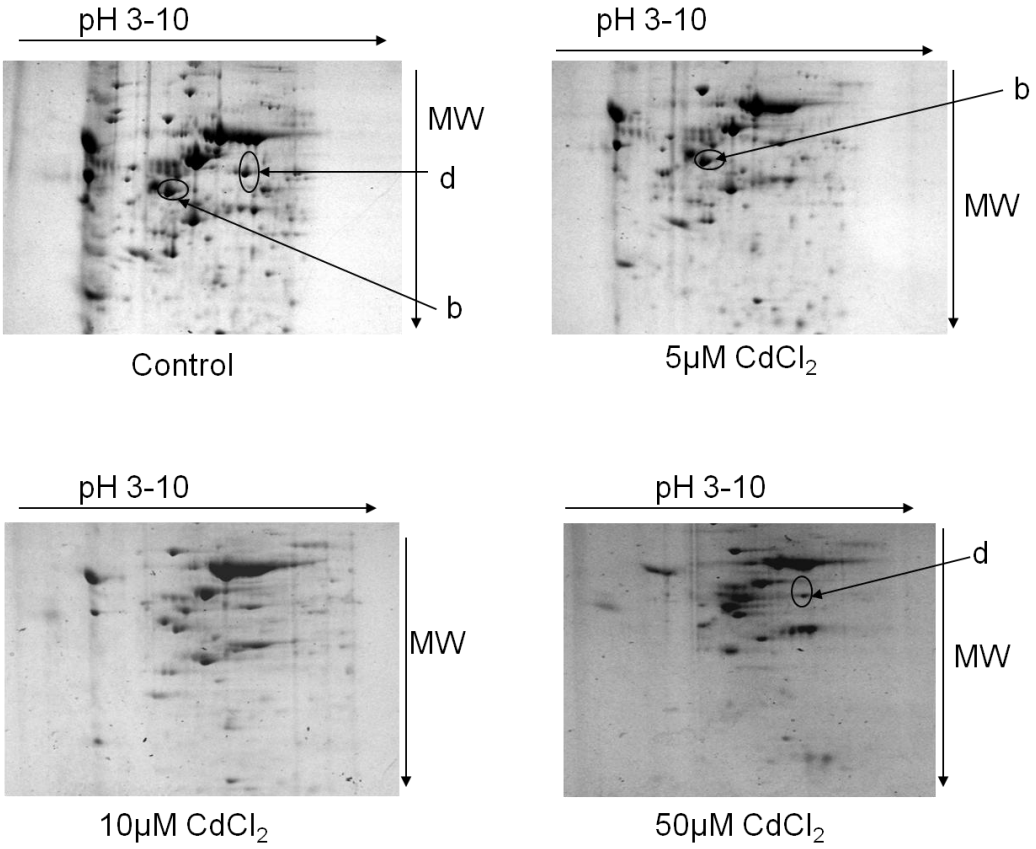

HEK 293 cells were exposed to 5, 10 and 50 μM $CdCl_2$ for 24hr and cells samples were separated on based on isoelectric point on a rehydrated immobiline™ IPG DryStrips (pH 3-10).The second dimensional separation was performed based on Molecular weight in a SDS-PAGE electrophoresis. Analyses of spots were performed on phoretix software using a reference gel produced from control gel. Mass spectroscopy analysis was carried out on the spots.

Table. 7.1. Total number of protein spots present in HepG2, 1321N1 and HEK 293 cell lines by 2-D electrophoresis after $CdCl_2$ exposure

Cells	Spots
HepG2	157
1321N1	368
HEK 293	188

Table.7.2. Number of induced and repressed protein in HepG2, 1321N1 and HEK 293 cell lines by 2-D electrophoresis after $CdCl_2$ exposure

	5 μM	10 μM	50 μM
HepG2	14 (I) 13 (R)	7 (I) 6 (R)	6 (I) 12 (R)
1321N1	10 (I) 22 (R)	7(I) 18 (R)	16 (I) 18 (R)
HEK 293	5 (I) 10 (R)	9 (I) 7 (R)	4 (I) 11 (R)

I= Induced; R= Repressed

Table 7.3. Identification of Proteins from Cd treated HepG2, 1321N1 and HEK 293 cells compared with untreated cells

Cell	Spot	Protein name	NCBI Database accession number	*Mw (kDa)	**Isoelectric point (pI)	Protein expression ***fold change compared with control
HepG2	A	Calreticulin	gi/475790	46.47	4.29	+2.2-fold
HepG2	B	ATP synthase,β subunit	gi/321893	57	5.00	+2.54-fold
HEK 293	B	ATP synthase, β subunit	gi/321893	57	5.00	+2.95-fold
1321N1	C	Cprotein	gi/306875	31.96	5.10	+1.82-fold
HEK 293	D	ALB protein	gi/74267962	66.47	5.67	+1.7-fold

*mass (Mw) and **isoelectric point (pI) were determined from 2d-electrophoresis, ***relative fold change in normalized volume of protein spots compared with control

7.3.2. $CdCl_2$-induced Calreticulin Proteins Expression in HepG2 cells after 24hrs Exposure to 5 μM $CdCl_2$

From the 2-D electrophoresis protein profiles, the result showed a 2.2-fold increase (Fig.7.4) in the level of Spot a. protein at 5 μM $CdCl_2$ exposure when compared with control. This was identified as Calreticulin. There was a decrease (20-fold) in expression at 50 μM $CdCl_2$ and no expression at 10 μM $CdCl_2$.

7.3.3. $CdCl_2$-induced ATP Synthase, H^+ Transporting, Mitochondrial F1 Complex, Beta Subunit Expression in HepG2 and HEK 293 Cell Lines after 24hrs Exposure to 5 μM $CdCl_2$

From the protein profiles, it was clear that the exposure of HepG2 and HEK 293 cells to 5 μM $CdCl_2$ for 24hr induced the expression of ATP synthase, H+ transporting, mitochondrial F1 complex (β-subunit) in both cell lines. The results of the Phoretix 2-D analysis showed a 2.95-fold increased (Fig.7.5B) in Spot b expression in HEK 293 cells after 5 μM $CdCl_2$ exposure when compared with control but no significant difference in expression was observed at 50 μM $CdCl_2$ and no expression at 10 μM. In HepG2 cells (Fig.7.5A; spot b), a 2.54-fold increased in expression was observed at 5 μM $CdCl_2$ when compared to control and a 5-fold decreased in expression at 50 μM $CdCl_2$. Identification of this spot revealed it to be ATP synthase, H+ transporting, mitochondrial F1 complex beta subunit. These data revealed that ATP synthase induction may play important role in adaptive response to Cd-insults in these two cell lines at low concentration (5 μM).

Figure7.4. Relative expression of Spot a (Calreticulin protein) in HepG2 cells as analysed by phoretix 2-D software after 24hr exposure to $CdCl_2$

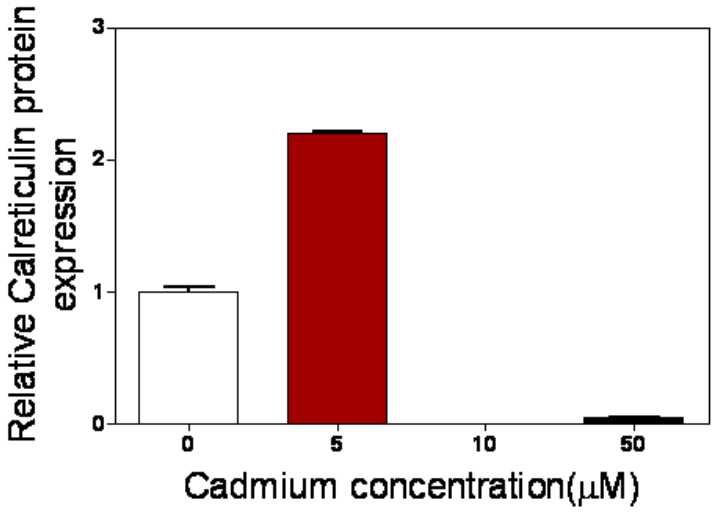

Histogram representative of the relative expression of Calreticulin in HepG2 cells exposed to 5, 10 and 50 μM $CdCl_2$ as analysed by Phoretix™ 2-D software. Calreticulin expression was quantified relative to reference gel produced from control gel. Data represent the mean value (n=3 of individual experiments).

Figure7.5. Relative expression of Spot b (ATP synthase, H+ transporting, mitochondrial F1 complex beta subunit, ATP5B) protein as analysed by phoretix software after 24hr exposure to $CdCl_2$ in HepG2 and HEK 293 cells.

A.

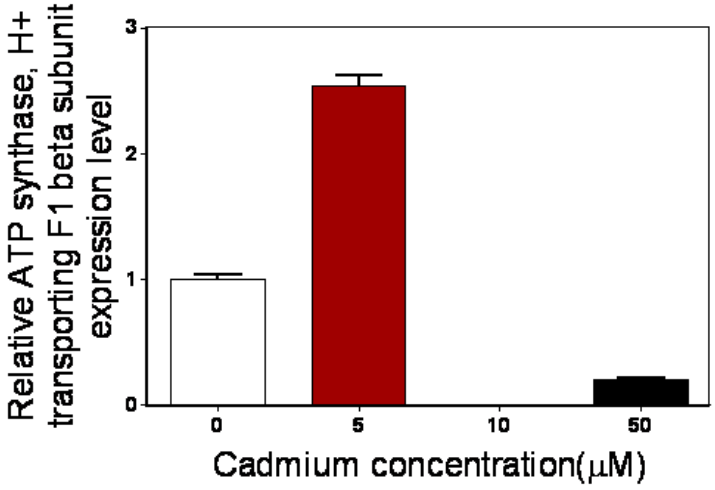

B.

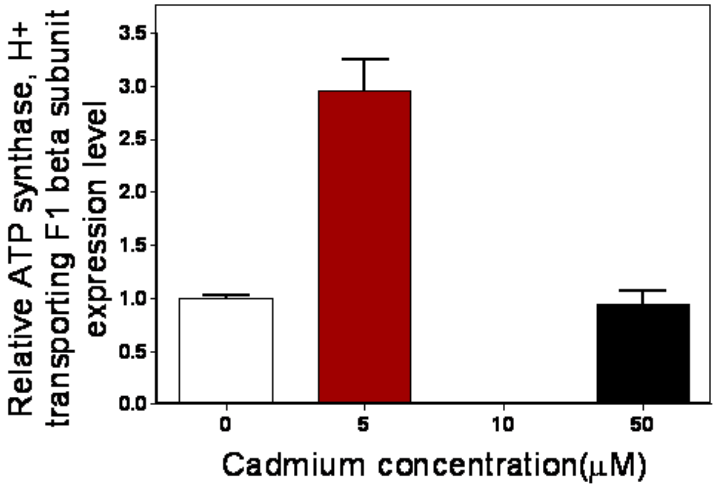

Histogram representative of the relative expression of ATP5B in (A) HepG2 and (B) HEK 293 cells exposed to 5, 10 and 50 μM $CdCl_2$ as analysed by Phoretix™ 2-D software. ATP5B expression was quantified relative to reference gel produced from control gel. Data represent the mean value (n=3 of individual experiments).

7.3.4. $CdCl_2$-induced C-protein Expression in 1321N1 cells after 24hr Exposure to 5 μM $CdCl_2$

From the 2-D electrophoresis protein profiles of 1321N1 cells there was a 1.82-fold increase (Fig.7.6) in C-protein level (spot c) at 5 μM $CdCl_2$ exposure when compared with control. There was no expression at 10 and 50 μM $CdCl_2$.

7.3.5. $CdCl_2$-induced ALB protein Expression in HEK 293 cells after 24hr Exposure to 50 μM $CdCl_2$

From the 2-D electrophoresis protein profiles of HEK 293 cells, it was apparent that exposure of HEK 293 cells to 50 μM $CdCl_2$ resulted in the induction of Spot d (Fig.7.7). Phoretix 2-D analysis show 1.7-fold increased (Fig.7.7) in Spot d when compared with control. Analysis revealed this protein to be albumin (ALB protein).

Figure7.6. Relative expression of Spot c (C- protein) as analysed by phoretix software after 24hr exposure to $CdCl_2$ in 1321N1 cells

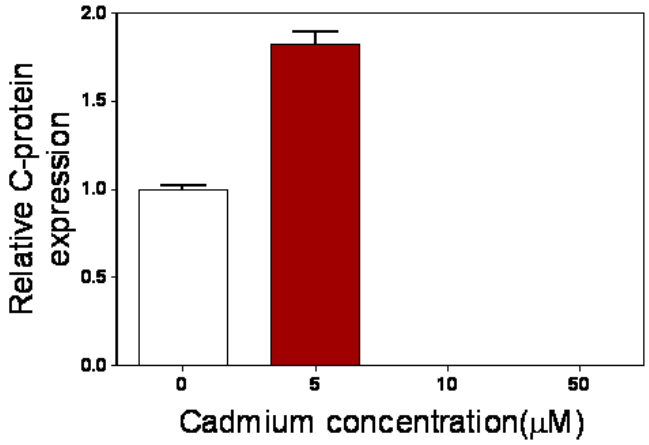

Histogram representative of the relative expression of C-protein in 1321N1 cells exposed to 5, 10 and 50 μM $CdCl_2$ as analysed by Phoretix™ 2-D software. C-protein expression was quantified relative to reference gel produced from control gel. Data represent the mean value (n=3 of individual experiments).

Figure7.7. Relative expression of Spot d (ALB protein) as analysed by phoretix software after 24hr exposure to $CdCl_2$ in HEK 293 cells.

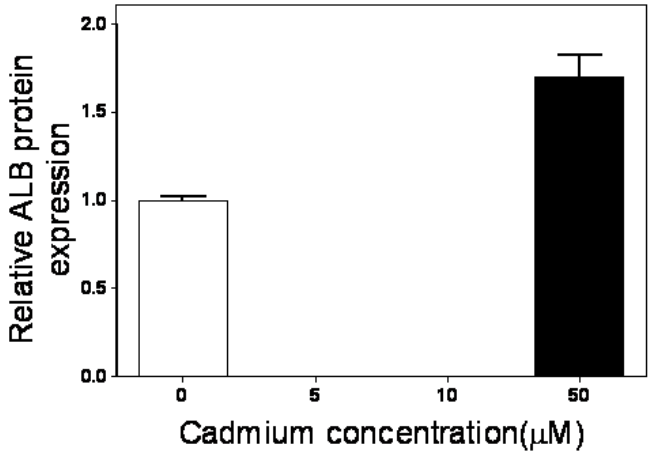

Histogram representative of the relative expression of ALB protein in HEK 293 cells exposed to 5, 10 and 50 μM $CdCl_2$ as analysed by Phoretix™ 2-D software. ALB expression was quantified relative to reference gel produced from control gel. Data represent the mean value (n=3 of individual experiments).

7.3.6. Secondary Validation of ATP5B Protein Expression by Western Blot Analysis

To further elucidate the effect of $CdCl_2$ exposure on ATP5B levels in HepG2, 1321N1 and HEK 293 cell lines, the cells were exposed to 5, 10 and 50 μM $CdCl_2$ for 24hr and western blot was performed on the whole cell extracts using ATP5B specific antibody (Code HPA001520;Sigma Prestige Antibodies). The result reveals a 5, 8 and 12-fold increase in ATP5B protein levels at 5, 10 and 50 μM $CdCl_2$ respectively in HepG2 cells (Fig.7.8A).The results show no significant changes in ATP5B expressions at all the concentrations of $CdCl_2$ in 1321N1 cells (Fig.7.8B). However, an increased (2.43-fold) in ATP5B level was observed at 5 μM $CdCl_2$ in HEK 293 (Fig.7.8C).

Figure7.8. Secondary validation of ATP5B expression by western blot

A.

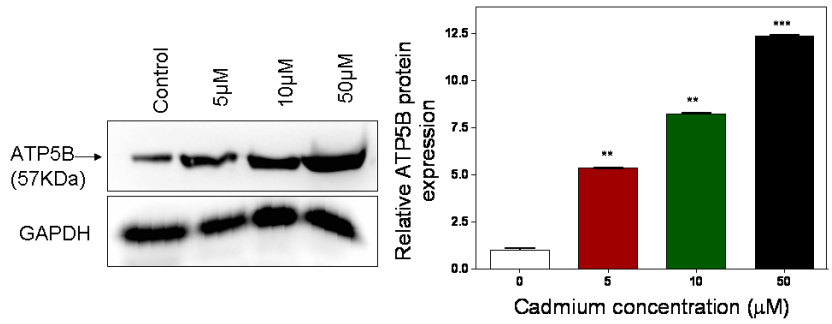

B.

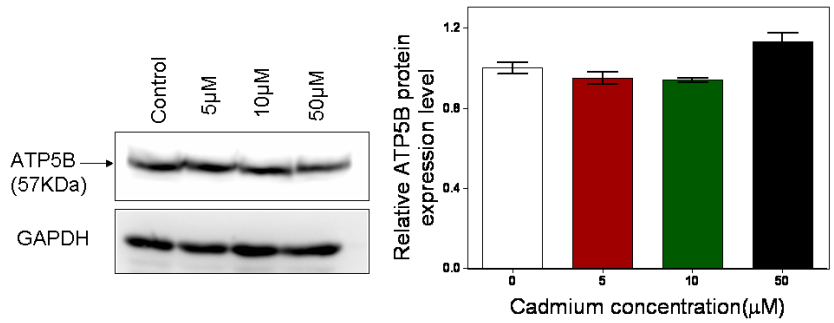

C.

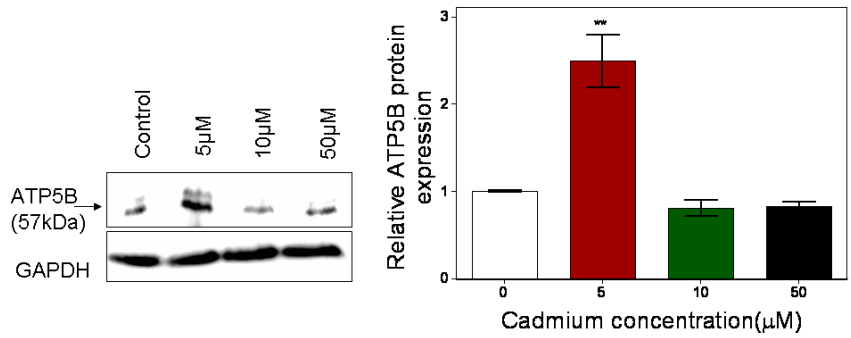

(A) HepG2, (B) 1321N1 and (C) HEK 293 cells were exposed to 5, 10 and 50 µM $CdCl_2$ for 24hr. After the incubation, cell extracts were prepared and 10µg of proteins were loaded on SDS-PAGE. Western blot was performed using ATP5B specific antibody as described in materials and Methods. Protein loading was normalised with GAPDH antibody. Intensity of the bands was evaluated with image J analysis software and relative protein expressions were compared to control. Data represent the mean value (n=3 of individual experiments done in triplicate) of percentage of control ±SD. Asterisks indicate significant compared with untreated control (***$p<0.005$ **$p<0.01$ *$p<0.05$) using one-way ANOVA with Dunnett's post test.

7.4. Discussion

This chapter tries to examine the effect of cadmium on the proteomic profile of exposed HepG2, 1321N1 and HEK 293 cells in order to identify biomarkers for Cd toxicity. About 27, 33 and 18 proteins were found to be elevated by at least 2-fold in HepG2, 1321N1 and HEK 293 cells respectively after exposure to different concentrations (5-50 μM) of $CdCl_2$. Among these induced proteins are ATP synthase H^+ transporting, mitochondrial complex beta subunit precursor in HepG2 and HEK 293 cells and calreticulin, a protein involved in Ca^{2+} homeostasis, in HepG2 cells.

ATP synthase, H^+ transporting, mitochondrial F1 complex, beta subunit(Swiss-Prot P06576) (EC 3.6.3.14) also known as ATP5B, ATPMB, or ATPSB ,is a mitochondrial inner membrane bound ATP synthase (F_1F_0 ATP synthase or complex) with a molecular weight of 57KDa (56,560Da) and isoelectric point of 5.00 with 529 amino acid residues which belongs to ATPase alpha/beta chains family. The ATP synthase consist of two linked structural domains: the soluble extramembraneous catalytic core, F_1, and the membrane spanning proton channel, F_0. The two are linked together by a central stalk and a peripheral stalk. The catalytic core of the ATP synthase consists of 5 different subunits; $alpha_3$, $beta_3$, $Gamma_1$, $delta_1$ and $epsilon_1$,while the membrane proton channel, F_0, has three main subunits; a, b and c.

Function

Mitochondrial ATP synthase catalyses the production of ATP from ADP by using the electrochemical gradient of protons produced across the inner mitochondrial membrane during oxidative phosphorylation.

$ATP + H_2O + H^+ (In) = ADP + phosphate + H^+ (Out)$.

Significance of Results

The induction in ATP synthase observed at 5 μM in HepG2 and HEK 293 cells after 24hr $CdCl_2$ exposure may be as a result of the altered metabolism in these two cell lines. ATP synthase is an enzyme that catalyses ATP synthesis. In chapter 4, increased ATP levels were observed in all the cell lines at 24hr $CdCl_2$ exposure and these increases were consistent with the observed induction in ATP synthase obtained from the proteomic study especially in HEK 293cells at 5 μM $CdCl_2$. Although the results from the phoretix analysis of the 2-D electrophoresis show 2.95-fold increases in ATP synthase (ATP5B) in HEK 293 (Fig.7.5B) cells at 5 μM $CdCl_2$, the secondary validation result from western blot shows less of an induction of 2.43-fold in HEK 293(Fig.7.8C) at the same concentration. This discrepancy may be due to the fact that proteins can be modified at the N and C-terminal ends after translation and 2-D electrophoresis can detect post and co-translational modified proteins which are not detected in the western blot analysis which used specific antibodies. Therefore, it is possible that the modified forms of the ATP5B proteins are apparent in the 2-D electrophoresis results but are not obvious in the western blot.

One reason for the observed induction in ATP synthase may be as a result of the altered Ca^{2+} homeostasis after Cd exposure as observed in Chapter 4. In cells, most of the calcium is bound to macromolecules leaving only about 0.1% Ca^{2+} in free form. This free form of Ca^{2+} is kept at 0.1 μM in the cytosol and this is the form available for performing Ca^{2+}-dependent functions (Kass and Orrenius, 1999). Therefore in order to maintain this low cytosolic

Ca^{2+}level (μM range) in comparison to the high extracellular level (mM range), cells have mechanisms that pump Ca^{2+} out from the intracellular to the extracellular space and also sequester Ca^{2+} into the intracellular stores such as endoplasmic and sarcoplasmic reticulum (Pozzan *et al*., 1994). This Ca^{2+} movement is against the concentration gradient therefore ATP is required. Because the cells tend to maintain intracellular Ca^{2+}level as low as possible, therefore the increased Ca^{2+} levels sparked by Cd exposure especially in HEK 293 cells (Chapter 4) were regulated by the induction in ATP synthase that generates more ATP which is required for the translocation of Ca^{2+} from the cytosol into the extracellular space and into the intracellular store. Therefore ATP synthase induction at 5 μM may be an adaptive response of the cells to Cd insult by helping to maintain low intracellular Ca^{2+}.

Another protein found to be induced in HepG2 cells after 5 μM $CdCl_2$ exposure is calreticulin. Calreticulin (Swiss-Prot P27797) also known as CRP55, Calregulin, CaBP3, HACBP and Calsequestin-like protein is a multifunctional protein that binds Ca^{2+} thereby rendering it inactive. Calreticulin has a MW of 46.47KDa (46466.37Da) and isoelectric point (pI) of 4.29 with 417 amino acid sequence. It is located in the storage compartments associated with the ER, extracellular space and extracellular matrix (White *et al*. 1995). It is also found on the cell surface of T cells (Dupuis *et al*., 1993), cytosol and extracellular matrix and it is associated with the lytic granules in the cytolytic T-lymphocytes. Calreticulin protein can be divided into three domains; the N-terminal globular domain, the proline-rich P-domain (arm like structure) and the C-terminal acidic domain. Both the P and C-domains bind calcium ions with different affinity and capacity. The P-domain binds

one molecule of calcium with high affinity while the acidic C-domain binds multiple calcium ions with low affinity.

Function

Calreticulin is the molecular calcium binding chaperone protein of the endoplasmic reticulum (ER) (Helenius *et al*., 1997) and promotes protein folding (Gething and Sambrook, 1992), oligomeric assembly, cell adhesion (Opas *et al*., 1996), gene expression regulation (Burns *et al*., 1994) and quality control in the ER through the calreticulin/calnexin cycle (Helenius *et al*., 1997). It also serves as a marker of phagocytosis of apoptotic cells and mediates nuclear export by interacting with the DNA-binding domain of NR3C1. Calreticulin plays an important role in maintaining intracellular Ca^{2+} homeostasis (Mery *et al*., 1996) by binding to Ca^{2+}. It binds Ca^{2+} with low affinity, but high capacity, and can be released on a signal. Calreticulin of the ER regulates cellular adhesiveness by upregulating vinculin expression (Opas *et al*., 1996).

Significance of Results

Calreticulin is an ER Ca^{2+}- storing protein (Liu *et al*., 1994) that helps in maintaining Ca^{2+} homeostasis by binding to Ca^{2+} with low affinity and high capacity. This protein acts as a heat shock protein that can be induced in response to changes in Ca^{2+}, Cd^{2+} and other heavy metals. Changes in intracellular Ca^{2+} have been reported to induced calreticulin (Little *et al*., 1994). Apart from this, the presence of Cd induced the generation of abnormal or denatured proteins which can serves as a signal for the induction of heat shock proteins (Parsell, 1994). The induction of calreticulin in HepG2 cells (Fig.7.1, spot a) after 5 μM $CdCl_2$ exposure may be an

adaptive response to Cd-insults and may be responsible for the non-significant changes observed in cytosolic Ca^{2+} level after Cd treatment as seen in chapter 4. Calreticulin located in ER may play important role in sequestering the Ca^{2+} pump into the ER thereby enhancing the buffering capacity of ER in dealing with Ca^{2+} elevation. In addition calcreticulin is known to promote cell adhesion (Opas *et al.* 1996) and can therefore prevent Cd-mediated carcinogenesis. One mechanism by which Cd^{2+} initiates cancer and tumour formation is by disrupting E-Cadherin formation by binding to the Ca^{2+} -binding site of E-Cadherin (Prozialeck and Lamar, 1999). E-Cadherin plays an important role in Ca^{2+}-dependent cell-cell adhesion and has been implicated as a tumour suppressor (Beavon, 2000). The induction of calreticulin may therefore serve as an adaptive response in preventing Cd^{2+}-mediated carcinogenesis by enhancing the mobilisation of Ca^{2+} from the cytosot to the Ca^{2+}- binding site of E-Cadherin . HEK 293 cells did not show any induction in calreticulin (Fig.7.3) and this may be responsible for the significant increase in cytosolic Ca^{2+} observed in this cell line as revealed in chapter 4 despite the induction in ATP synthase (Fig.7.3).

Albumin (ALB) (Swiss-Prot P02768) is a monomeric protein with molecular weight of 66.47kDa (66472.21 Da) and isoelectric point (Ip) of 5.67 with 609 amino acid sequence. It constitutes one-half of the blood serum protein and it is synthesized as preproalbumin in the liver. The preproalbumin is processed by the removal of the N-terminal to form proalbumin which is released from ER. The subsequent cleavage of the proalbumin in the Golgi vesicles results in the production of mature ALB.

Function

Albumin is the main globular unglycosylated plasma protein that has a good binding capacity for water, Ca^{2+}, Na^{+}, fatty acid, hormone, bilirubin and drugs. ALB functions mainly to regulate the colloidal osmotic pressure of the blood. A deficiency in ALB causes familial dysalbuminemic hyperthyroxinema, which is a form of euthyroid hyperthyroxinemia (common among caucassian population) that is due to the increased ALB affinity for T_4. ALB is normally secreted and found mainly in the plasma.

Significance of Results

Albumin is another protein with a good capacity for binding Ca^{2+}. Like calreticulin, the protein component of albumin has been reported to cause an uptake of calcium in rat astrocytes into intracellular stores (Nadal et al., 1996). In one study, increased calcium levels have also been reported to correlate with increased serum albumin in a patient with abnormal serum proteins (Payne *et al*., 1973). Therefore, the observed increased in albumin seen in HEK 293 cells after 50 μM $CdCl_2$ exposure may be an adaptive response of these cells to the elevated Ca^{2+} level that was produced by the presence of Cd Chapter 4. Though, it was reported in one study that administration of 5 mg/kg $CdCl_2$ for 2weeks causes a significant decrease in plasma albumin in rats (El-Demerdashi *et al*., 2004), this present study show that albumin induction after Cd exposure may dependent on dose, species and duration of exposure.

Limitation of biomarkers used in this work

The evaluation of a biomarker accuracy depends on its sensitivity ie ability to detect disease when disease is actually present and its specificity ie ability to

recognise the absence of disease when a disease is actually absent (Ramalhandran et al., 2006). The role of intracellular signalling networks in cellular processes such as proliferation and differentiation in cell-cycle arrest and apoptosis can not be overemphasised. Therefore the elucidation of the mechanisms of disease development and maintenance can be achieved by identifying alterations in intracellular signalling networks which are associated with the disease (Danna and Nolan, 2006). The use of small molecular weight (LMW) signalling molecules will enhance the better understanding of the mechanisms involved in disease generation and where appropriate therapy could be directed. Accumulating evidence has shown that the LMW range of circulating proteome contains abundant source of information that may be able to detect disease at the early stage and elucidate the risk involved (Calvo et al., 2005). The high molecular weight biomarkers used in this work represent end products of one or more pathways and these are less specific and less effective tools in diagnosing a disease.

In summary, the data obtained from the proteomic studies show that depending on cell type, dose and duration of exposure, increased metabolism, alteration in heat shock and Ca^{2+}-regulatory protein expression may be a hallmark in the cells response to Cd toxicity and these could serve as suitable biomarkers for Cd toxicity.

CHAPTER 8

General Discussion

Chapter 8

8.0. General Discussion

8.1 Summary

Previous studies have attempted to elucidate the exact mechanism involved in cadmium toxicity using a range of different cells and animal models. Many of these studies have deduced different mechanisms for Cd toxicity, and these differences were found to depend largely on the Cd compound used, cell type, dose and duration of exposure. However, to date no universally accepted mechanism has been proposed for Cd–induced toxicity.

This present study aimed to determine the possible mechanism(s) that may be involved in Cd toxicity in three human cell lines; human hepatoma (HepG2), human embryonic kidney cells (HEK 293) and human astocytoma cells (1321N1 cells), with the aim of identifying common themes between the cell lines, and areas where therapeutic intervention could be directed. The study also examined the mechanisms involved in the protective response of these cell lines to Cd insults and the identification of possible biomarkers that can be used as a diagnostic tool for Cd toxicity.

8.2 Oxidative Stress and the Role of Nrf2

In agreement with previous studies, the data presented in Chapter 3 shows that Cd toxicity is dose and time dependent as seen in the MTT and LDH assays, with the most pronounced toxic effect occurring at the highest dose of 50 μM Cd at 24hr exposure. Some studies have reported decreased enzyme activities in Cd toxicity (Del Carmen et al., 2002), whereas others have reported increased activities in antioxidant enzymes, especially after chronic exposure (Casalino et al., 1997). In this study, increased enzyme activities

were observed in all the cell lines after 24hr exposure to 50μM $CdCl_2$ which may be as a result of the adaptive response to Cd insult. To further substantiate this hypothesis, the effect of Cd exposure on Nrf2 was examined in both the cytosol and nuclear fractions (Chapter 5). The increase in nuclear Nrf2 with the corresponding decrease in cytosolic levels after Cd exposure attests to the fact that Nrf2 is being translocated from the cytosol into the nucleus. This translocation corresponds with increased expression of protective enzymes such as γGCS, NQO1 and HO1 in all the three cell lines. Nrf2 has been reported to regulate the transcription of genes that contain an ARE in their promoter (Kensler et al., 2007). Most of these genes code for protective enzymes such as antioxidant and phase II enzymes. In addition, it was also reported by Harvey et al (2009) that Nrf2 regulates the GSH redox cycle via the transcriptional regulation of glutathione reductase (GSR), glutathione peroxidase 2 (GPX2), glutathione S-transferase (GST) and γ-glutamylcysteine synthase (γGCSc). This adds credence to observed increase in activities in GST, GPX and GSR observed at 50μM $CdCl_2$ in all the three cell lines after 24hr exposure in this study (Chapter 3). Furthermore, the impaired cell survival observed in HEK 293 cells pretreated with BCNU before exposure to 50μM $CdCl_2$ (Chapter 3) implies the involvement of GSH in the protection against Cd toxicity. GSH is an antioxidant that plays a very crucial role in maintaining the redox status and thus protects cells against reactive oxygen species, either by direct scavenging for free radicals or by acting as cofactor for antioxidant enzymes such as GST, GPX and GSR. In the presence of cadmium, GSH is depleted due to the binding of the metal to the thiol group of GSH (Leverrier et al., 2007) The significant decrease in GSH levels at 50μM $CdCl_2$ in 1321N1 and HEK 293 cells (Chapter 3) may serve as a feedback signal for the translocation of Nrf2 from the cytoplasm into the

nucleus (Chapter 5) with the subsequent induction and hence increased activities observed in the GSH redox cycle enzymes. γGCSc is a rate limiting enzyme in GSH synthesis and therefore plays a crucial role in maintaining the GSH redox status. The observed induction in the expression of γGCSc (Chapter 5) may therefore be in response to GSH depletion via the Nrf2 activation. Superoxide dismutase1 (SOD1) has also been reported to be regulated by Nrf2 transcription factor and therefore the observed increase SOD1 activities at 50μM in HepG2 and HEK 293 cells at 24hr exposure (Chapter 3) correlates with increased Nrf2 activation.SOD1 is an incomplete antioxidant that requires the presence of catalase to convert the hydrogen peroxide to water. The corresponding increase in catalase activities in the HepG2 and HEK cells (Chapter 3) implies the involvement of superoxide anion and hydrogen peroxide in Cd toxicity. This was in agreement with a report that identifies the involvement of superoxide anions and hydrogen peroxide in Cd toxicity (Stohs et al., 2001).

Investigation into the mRNA levels of these Nrf2 transcriptional regulated genes show significant increases in the mRNA levels of all the protective enzymes at 5, 10 and 50μM which correspond with increases in Nrf2 mRNA in HEK 293 cells and 1321N1 cells (Chapter 5). Nrf2 levels and activities are regulated at transcription, degradation, translocation and post-translocational degradation levels. Therefore, mRNA levels of genes regulated by Nrf2 may not correlate with the Nrf2 mRNA level due to the turn-over rate of the Nrf2 protein which determines the transcriptional levels of the Nrf2 dependent genes. This may account for the observed difference in Nrf2 mRNA and the mRNA levels of some of the Nrf2-dependent genes especially at 50μM $CdCl_2$ in 1321N1 cells (Chapter 5). To further clarify the

involvement of Nrf2-Keap1-ARE pathway in mediating the adaptive response of the three cell lines to $CdCl_2$ exposure, Nrf2 translocation from the cytosol to the nucleus was monitored. The results in this work established that there were Nrf2 translocations from the cytosol into the nucleus in all the cell lines corresponding with the released of Keap1 into the cytosol. The involvement of PKC in this translocation was also examined in order to have a better understanding of the mechanisms involved in this translocation. This study shows that the presence of PKC inhibitor impaired cells survival and Nrf2 translocation. This study discovered that PKCδ inhibitor specifically inhibits cells survival and mRNA levels of GSTA1 and NQO1, two Nrf2-dependent regulated genes (Chapter 5).

8.3 Apoptosis and the Role of Calcium

Apoptosis has been reported as one mechanism of Cd toxicity in a number of exposed cells and animal models (Qu et al., 2007). In Chapter 4, there was an increase in the population of apoptotic cells with increased Cd concentrations in all the three cell lines and some of the cells move toward necrosis as the concentration increases. This was further confirmed by the flowcytometry studies. To understand the mechanism (s) involved in the observed apoptosis, the levels of intracellular Ca^{2+} were determined. Cd has been reported to alter the intracellular Ca^{2+} level and this alteration is said to be responsible for the observed cell death in Cd exposed cells (Misra et al., 2002). Ca^{2+} homeostasis must be maintained as Ca^{2+} is a second messenger that can trigger a number of signalling pathways with consequent activation of proteases such as calpain which can eventually leads to apoptosis or necrosis depending on the level of alterations. In order to determine the role of intracellular Ca^{2+} and the involvement of the PLC-IP_3 pathway in Cd

toxicity, U73122, an inhibitor of PLC was used. This present study shows that intracellular Ca^{2+} alteration was pronounced in HEK 293 cells in the absence of the inhibitor but not in the other cell lines (Chapter 4). This observation may be due to the presence of a Ca^{2+}-sensing receptor (CSR) found in proximal tubule of the kidney as well as in parathyroid and gut cells (Tfelt-Hansen and Brown, 2005). Therefore, sensitivity to Cd^{2+}-mediated alteration in intracellular Ca^{2+} depends largely on receptors, channels as well as Ca^{2+} pumps on the cell surface.

To further elucidate the mechanism of Cd induced toxicity in the three cell lines, the role of mitochondrial-cytochrome c dependent pathway in Cd toxicity was examined (Chapter 4). Increased caspase 3 activities, cytosolic cytochrome c levels and mitochondrial Bax protein were found in all the cell lines. These indicate that the mitochondrial-cytochrome c pathway participated in the cell death observed in all the three cell lines.

8.4 Biomarkers for Cd Exposure

This study further examined the effect of Cd on the proteomic structures of the exposed cells in an attempt to develop suitable biomarkers for Cd toxicity. A common feature in the proteomic profile was identified in HepG2 and HEK 293 cells after exposure to 5μM $CdCl_2$ and this was the induction in one of the subunits of ATP synthase. This work showed an increase in ATP levels in all the cell lines after 24hr Cd exposure (Chapter 4) and this correlates with the induction in ATP synthase observed in the 2D electrophoresis study of HepG2 and HEK 293cells. Also calreticulin and ALB protein induction was observed in HepG2 and HEK 293 cells respectively after 5μM $CdCl_2$ treatment. Both proteins are Ca^{2+} -binding proteins and can

help in maintaining the intracellular Ca^{2+} homeostasis. This shows that the capacity of these two cell lines to adapt to cope with Cd-induced toxicity, and the consequent increased intracellular Ca^{2+} required ATP synthase, Calreticulin and ALB proteins induction. The maintenance of intracellular Ca^{2+} requires active transport that uses ATP to pump $Ca^{2+}$from the cytosol into intracellular stores and extracellular space. Also the presence of Ca^{2+} scavenging proteins such as calreticulin that sequesters Ca^{2+} into intracellular stores also help in maintaining the homeostasis state of intracellular Ca^{2+}.Therefore, ATP synthase, calreticulin and ALB induction may be suitable biomarkers for Cd toxicity in these two cell lines.

8.5 Conclusions and Future Work

In conclusion, we are able to show in this work that the mechanisms involved in Cd-induced oxidative stress depend largely on cell type: whereas ROS production may be important in Cd-induced toxicity in HepG2, GSH depletion may be important in 1321N1 and HEK 293 cells. The adaptive response of the cells to Cd toxicity is associated with Nrf2-keap1-ARE pathway. Also, mitochondrial-caspase dependent pathways may play a crucial role in Cd toxicity in all three cell lines. Finally, this present study reveals that alteration in both metabolic process and intracellular Ca^{2+} homoeostasis may be the general hallmarks of Cd toxicity.

Future Work

Identification of G-protein coupled receptor and Ca^{2+} channels

This present work shows that alteration in intracellular Ca^{2+} in HEK 293 cells occur via the PLC-IP_3 pathway. The question now is what type of G-protein metal coupled receptor is involved in this alteration and what is the role of

other calcium receptors and channels in this alteration? Therefore, my further work will employ the use of specific inhibitors and mutants of HEK 293 cells to elucidate of the role of these receptors and channels in intracellular Ca^{2+} alteration in HEK 293 cells exposed to Cd.

Complete MS identification of protein from 2D electrophoresis

Because of the limited time, only very few of the total induced proteins were identified by MS. Therefore, in order to have complete protein expression map for each of the cell line after Cd exposure, my further work will try to identify all the remaining induced proteins and thereby create a reference protein profile for Cd in these cell lines.

Study using animal model

Having established in this in vitro study the involvement of the PLC-IP_3 pathway in cadmium induced Ca^{2+} alteration in HEK 293 cells, and the mitochondrial-cytochrome c pathway in Cd toxicity in all the cell lines used in this work, the question now is, do these two pathways play a role in Cd-induced toxicity in liver and kidney of exposed rats?. It therefore becomes imperative to examine the role of these pathways in Cd toxicity in an animal model because the physiological environment and in vivo animal model is not represented in the in vitro study.

Effects of Nrf2 silencing in Cd exposed cells and animal model

Though this present work has shown the translocation of Nrf2 from the cytosol to the nucleus and the induction of Nrf2-dependent cytoprotective genes in the three cell lines after Cd exposure, the effects of Nrf2 silencing in the survival of these cell lines and in animal model after Cd exposure need

further clarification in order to define the role of Nrf2 in protection after Cd exposure. Therefore, my further work will focus on the use of Nrf2-siRNA to silence Nrf2 in cells and Nrf2 knockout mice to further evaluate the role of Nrf2 in Cd exposed cells and animals.

Protective mechanisms of garlic against Cd toxicity

This present study shows that garlic extracts have protective effect against Cd toxicity; however, the exact mechanisms by which they do this needs further clarification. Therefore, my future work will employ the use of Nrf2 silenced cells and knockout mice to identify the role of Nrf2 in the protective effects of garlic against Cd toxicity.

9.0. References

Achanzar, W. E., Achanzar, K. B., Lewis J. G., Webber, M. W., Waalkes, M. P., 2000. Cadmium induces c-myc p53, and c-jun expression in normal human prostate epithelial cells as a prelude to apoptosis. Toxicol. Appl. Pharmacol. 164, 291-300.

Aden, D. P., Fogel, A., Plotkin, S., Damjanov, I. and Knowles, B. B., 1979. Controlled synthesis of HBsAg in a differentiated human liver carcinoma-derived cell line. Nature 282, 615-6.

Aebi, H., 1973. In Methods of Enzymatic Analysis, Bergmeyer, H. U., ed., Verlag Chemie (Weinheim). 673- 684.

Aiba, I., Hossain, A. and Kuo, M. T., 2008. Elevated GSH level increases cadmium resistance through down-regulation of Sp1-dependent expression of the cadmium transporter ZIP8. Mol Pharmacol. 74, 823-33.

Alam, J., Killeen, E., Gong, P., Naquin, R., Hu, B., Stewart, D., Ingelfinger, J. R., Nath, K. A., 2003. Heme activates the heme oxygenase-1 gene in renal epithelial cells by stabilizing Nrf2. Am. J. Physiol. 284, 743-752.

Alam, J., Camhi, S., Choi, A. M., 1995. Identification of a second region upstream of the mouse heme oxygenase-1 gene that functions as a basal level and inducer-dependent transcription enhancer. J. Biol Chem. 270, 11977-11984.

Alnemri, E. S., Livingston, D. J., Nicholson, D. W., Salvesen, G., Thornberry, N. A., Wong, W. W., Yuan, J., 1996. Human ICE/CED-3 protease nomenclature. Cell 87, 171.

Amagase, H., 1998. Intake of garlic and its components: Nutritional and Health Benefits of Garlic as a Supplement Conference, Newport Beach, CA, p4 (abstract).

Amagase, H., 2006. Significance of Garlic and its Constituents in Cancer and Cardiovascular Disease. J. Nutr. 136, 716-725.

Amagase, H., Petesch, B. L., Matsuura, H., Kasuga, S., Itakura, Y., 2001. Intake of garlic and its bioactive compounds. J. Nutr. 131, 955-962.

Anwar, A. A., Li, F. Y. L., Leake, D. S., Ishii, T., Mann, G. E., Siow, R. C. M., 2005. Induction of heme oxygenase 1 by moderately oxidized low-density lipoproteins in human vascular smooth muscle cells: role of mitogen-activated protein kinases and Nrf2. Free Radic. Biol. Med. 39, 227-236.

Archanzer, W. E., Webber, M. M., Waalkes, M. P., 2002. Altered apoptotic gene expression and acquired apoptotic resistance in cadmium-transformed human prostate epithelial cells. Prostate 52, 236-244.

Andrews, N. C., Erdjument-Bromage, H., Davidson, M. B., Tempst, P., Orikin, S. H., 1993. Erythroid transcription factor NF-F2 is a haematopoietic-specific basic-leucine zipper protein. Nature 339, 722-727.

ATSDR, 1997. Top 20 Hazardous Substances. ATSDR/EPA Priority List for 1997. Agency for Toxic Substances and Disease Registry, Atlanta, GA.

ATSDR., 1999. Toxicological Profile for Cadmium (Final Report). NTIS Accession No. PB99-166621. Atlanta, GA: Agency for Toxic Substances and Disease Registry. 434pp.

ATSDR., 2005. Agency for Toxic Substance and Disease Registry, US. Toxicological Profile for Cadmium. Department of Health and Human Services, Public Health Service, Centers for Disease Control, Atlanta, GA, USA.

Awazu, S., Horie, T., 1997. Antioxidants in garlic II. Protection of heart mitochondria by garlic extract and dially polysulfide from the doxorubicin-induced lipid peroxidation. In: Nutraceuticals: Designer Foods III Garlic, Soy and Licorice (Lanchance, P P., ed). 131-138. Food & Nutrition Press, Trumbull, C. T

Bagchi, D., Vuchetich, P. J., Bagchi, M., Hassoun, E. A., Tran, M. X., Tang, L., Stohs, S. J., 1997. Induction of oxidative stress by chronic administration of sodium dichromate and cadmium chloride to rats. Free Radic. Biol. Med. 22, 471-478.

Beavon, I. R., 2000. The E-cadherin-catenin complex in tumour metasis: structure, function and regulation. Eur. J. Cancer. 36, 1607-1620.

Belyaeva, E. A., Dymkowska, D., Wieckowski, M. R., Wojtczak L., 2008. Mitochondria as an important target in heavy metal toxicity in rat hepatoma AS-30D cells. Toxicol. Appl. Pharmacol. 231, 34-42.

Bernard, A., Lauwerys, R., 1986. Cadmium in human population. Experentia. 50: (Supplement) 114-123.

Berridge, M. J., Lipp, P., Bootman, M. D., 2000. The versatility and universality of calcium signalling. Nat. Rev. Mol. Cell Biol. 1, 11-21.

Beyersmann D., Hechtenberg, S., 1997. Cadmium, gene regulation and cellular signalling in mammalian cells. Toxicol. Appl. Pharmacol. 144, 247-261.

Beyer,T. A., Teupser, D., Keller, U., Blugnon, P., Hildt, E., Thiery, J., Khan, Y. W., Werner, S., 2008. Impaired liver regeneration in Nrf2 knockout mice: role of ROS-mediated insulin/IGF-1 resistance. The EMBO Journal. 27, 212-223.

Block, E., 1985. The chemistry of garlic and onion. Sci. Am. 252, 114-119.

Bloom, D. A., Jaiswal, A. K., 2003. Phosphorylation of Nrf2 at Ser(40) by protein kinase C in response to antioxidants leads to the release of Nrf2 from INrf2, but is not required for Nrf2 stabilization/accumulation in the nucleus and transcriptional activation of antioxidant response element-mediated NAD(P)H:quinone oxidoreductase-1 gene expression. J. Biol. Chem. 278, 44675-44682.

Boise, L. H., Thompson, C. B., 1997. BCL-XL can inhibit apoptosis in cells that have undergone Fas-induced protease activation. Proc. Natl. Acad. Sci. USA. 94, 3759-3764.

Bonkovsky, H. L., Elbirt, K. K., 2002. Heme oxygenase: its regulation and role. In oxidative stress and aging (Cutter, R. G., and Rodriquez, H., eds) pp 690-706. World Scientific, River Edge. NJ.USA.

Borek, C., 2001. Antioxidant Health effect of Aged Garlic Extract. Am. Soc. Nutr. Sci. 131, 1010-1015.

Bradford, M. M. (1976). A rapid and sensitive method for the quantitation of microgram quantities of protein utilizing the principle of protein-dye binding. Anal Biochem 72, 248-254.

Braun, S., Hanselmann, C., Gassmann, M. G., auf dem Keller, U., Born-Berclaz, C., Chan, K., 2002. Nrf2 transcription factor, a novel target of keratinocyte growth factor action which regulates gene expression and inflammation in the healing skin wound. Mol Cell Biol. 2002, 5492-5505.

Bruner, G., Murphy, S., 1993. Purinergic P2Y receptors on astrocytes are directly coupled to phospholipase A2. Glia. 7, 219-224.

Buckley, B. J., Marshall, Z. M., Whorton, A. R., 2003. Nitric oxide stimulates Nrf2 nuclear translocation in vascular endothelium. Biochem. Biophys. Res. Commun. 307, 973-979.

Burns, K., Duggan, B., Atkinson, A. E., Famulski, K. S., Nemer, M., Bleackley, R. C. Michalak, M., 1994. Modulation of gene expression by calreticulin binding to the glucocorticoid receptor. Nature. 367, 476-480.

Calvo, K. R., Liotta, L. A., Petricoon, E. F., 2005. Clinical Proteomics: From Biomarker Discovery and Cell Signaling Profiles to Individualized Personal Therapy. Bioscience Reports 25, 107-125.

Carlberg, I. and Mannervik, B. (1977). Purification by affinity chromatography of yeast glutathione reductase, the enzyme responsible for the NADPH-dependent reduction of the mixed disulfide of coenzyme A and glutathione. Biochim Biophys Acta 484, 268-74.

Casalino, E., Calzaretti, G., Landriscina, M., Sblano, C., Fabiano, A., Landriscina, C., 2007. The Nrf2 transcription factor contributes to the induction of alpha-class GST isoenzymes in the liver of acute cadmium or manganese intoxicated rats: comparison with the toxic effect on NAD(P)F:quinone reductase. Toxicol. 237, 24-34.

Casalino, E., Sblano, C., Landriscuna, C., 1997. Enzyme activity alteration by cadmium administration to rats: the possibility of iron involvement in lipid peroxidation. Arch. Biochem. Biophys. 346, 171-179.

Caterina, J. J., Donze, D., Sun, C. W., Ciavatta, D.J., Townes, T. M., 1994. Cloning and functional characterization of LCR-F1: a Bzip transcription factor that activates erythroid-specific, human globin expression. Nucleic Acids Res. 22, 2383-2391.

Chao, S. H., Suzuki, J. R., Zysk, J. R., Cheung, W. Y., 1984. Activation of calmodulin by various metal cations as a function of ionic radius. Mol. Pharmacol. 26, 75-82.

Chao, J. I., Yang, J. L., 2001. Opposite roles of ERK and p38 mitogen-activated protein kinases in cadmium-induced genotoxicity and mitotic arrest. Chem. Res. Toxicol. 14, 1193-1202.

Chen, C., Pung, D., Leong, V., Hebbar, V., Shen, G., Nair, S., Li, W., -N, A., Kong, T., 2004. Induction of detoxifying enzymes by garlic organosulfur compounds through transcription factor NRF2: Effect of chemical structure and stress signals. Free Radic. Biol Med. 37, 1578-1590.

Chichen., Pung, D., Leong, V., Hebbar, V., Guoxiang, S., Nasir, S., Wenge, L., Kong, A.N., 2004. Induction of detoxifying enzymes by garlic organosulfur compounds through transcription factor NRF2: Effect of chemical structure and stress signals.Free Radic.Bio.Med. 37, 1578-1590.

Cho, H. Y., Jedlicks, A. E., Reddy, S. P.M., Kensler, T. W., Yamamuto, M., Zhang, L. Y., 2002. Role of Nrf2 in protection against hyperoxic lung injury in mice. Am J Respir Cell Mol Biol, 26, 175-182.

Chuang, S. M., Wang, I. C., Hwua, Y. S., Yang, J. L., 2003. Short-term depletion of catalase suppresses cadmium-elicited c-Jun N- terminal kinase activation and apoptosis: role of protein phosphatases. Carcinogenesis 24, 7-15.

Clapham, D. E., 2007. Calcium signalling. Cell 131, 1047-1058.

Clark, R. B., Su, Y. F., Ortmann, R., Cubeddu, L., Johnson, G. L. and Perkins, J. P. (1975). Factors influencing the effect of hormones on the accumulation of cyclic AMP in cultured human astrocytoma cells. Metabolism 24, 343-58.

Cohen, G. M., 1997. The executioners of apoptosis. Biochem. J. 326, 1-16

Copple, I. M., Goldring, C. E., Kitteringham, N. R., Park, B. K., 2008. The Nrf2-Keap1 defence pathway: role in protection against drug-induced toxicity. Toxicol. 246, 24-33.

Crawford. D. R., Davies, K. J. A., 1994. Adaptive Response and Oxidative stress. Environ Health Perspective. 102, 25-28.

Croall, D. E., DeMartino, G. N., 1991. Calcium-activated neutral protease (calpain) system: Structure, function, and regulation. Physiol Rev. 71, 813-847.

Cullinam, S. B., Zhang, D., Hannik, M., Arvisais, E., Kaufman, R. J., Diehl, J. A., 2003. Nrf2 is a direct PERK substrate and effector of PERK-dependent cell survival. Mol. Cell. Biol. 23, 7198-7209.

Dalton, T. P., He, L., Wang, B., Miller, M. L., Jin, L., Stringer, K. F., Chang, X., Baxter, C. S., Nebert, D. W., 2005. Identification of mouse SLC39A8 as the tranporter responsible for cadmium-induced toxicity in the testis. Proc. Natl. Acad. Sci. U. S. A. 102, 3401-3406.

Danna, E. A., Nolan, G., 2006. Transcending the biomarker mindset: deciphering disease mechanisms at the single cell level. Cur. Opinion in Chem. Biol. 10, 20-27.

Decker, T., Lohmann-Mtthes, M. L., 1988. A quick and simple method for the quantitation of lactate dehydrogenase release in measurements of cellular cytotoxicity and tumor necrosis factor (TNF) activity. J. Immunol. Methods. 15, 61-69.

Del Carmen, E. M., Souza, V. Bucio, L., Hernandez, E., Damian-Matsumura, P., Zaga, V., Gtierrez-Ruiz, M. C., 2002. Cadmium induces alpha (1), collagen (I) and metallothionein II gene and alters the antioxidant system in rat hepatic stellate cells. Toxicol.170, 63-73.

Dempsey, E. C., Newton, A. C., Mochly-Rosen, D., 2000. Protein kinase C isozymes and the regulation of diverse cell responses. Am. J.Physiol. Lung Cell Mol. Physiol. 279, L429- L438.

Dhakshinamoorthy, S., Jain, A. K., Bloom, D. A., Jaiswal, A. K., 2005. Bach1 competes with Nrf2 leading to negative regulation of the antioxidant response element (ARE)-mediated NAD (P) H: quinone oxidoreductase 1 gene expression and induction in response to antioxidants. J. Biol. Chem. 280, 16891-16900.

Dinkova-Kostova, A. T., Holtzclaw, W. D., Cole, R. N., Itoh, K., Wakabayashi, N., Katoh, Y., Yamamoto, M., Talalay, P., 2002. Direct evidence that sulfhydryl groups of Keap1 are the sensors regulating induction of

phase 2 enzymes that protect against carcinogens and oxidants. Proc. Natl. Acad. Sci. USA 99, 11908-11913.

Djukic-Cosic, D., Curcic Jovanovic, M., Plamenac Bulat, Z., Ninkovic, M., Malicevic, Z., Matovic, V., 2008. Relation between lipid peroxidation and iron concentration in mouse liver after acute and subacute cadmium intoxication. J. Trace Elem. Med. Biol. 22, 66-72.

Dorta, D. J., Leite S., DeMarco, K. C., Prado, L. M., Rodrigues, T. Mingatto, F. E., Uyemura, S. A., Santos, A. C., Curti, C., 2003. Aproposed sequence of events for cadmium-induced mitochondrial impairment. J. Inorg. Biochem. 97, 251-257.

Douglas, K. T., 1987. Mechanism of action of glutathione-dependent enzymes. Adv. Enzymol. Relat. Areas Mol. Biol. 59, 103-167.

Dudley, R. E., Klaassen, C. D., 1984. Changes in hepatic glutathione concentration modify cadmium-induced hepatotoxicity. Toxicol. Appl. Pharmacol. 72, 530-538.

Dupuis, M., Schaerer, E., Krause, K. H., Tschopp, J., 1993. The calcium binding protein calreticulin is a major constituent of lytic granules in cytolytic T lymphocytes. J. Exp Med. 177, 1-7.

Durnam, D. M. and Palmiter, R. D. (1981). Transcriptional regulation of the mouse metallothionein-I gene by heavy metals. J Biol Chem 256, 5712-6.

Dutil E. M., Toker, A., Newton, A. C., 1998., Regulation of conventional protein kinase C isozymes by phosphoinositide-dependent kinase 1 (PDK-1). Curr. Biol. 8, 1366-1375.

El-Demerdash, F. M., Yousef, M. I., Kedwany, F. S., Baghdadi, H. H., 2004. Cadmium-induced changes in lipid peroxidation, blood haematology, biochemical parameters and semen quality of male rats: protective role of vitamin E and β-carotene. Food Chem. Toxicol. 42, 1563-1571.

Ellis, E. M. (2007). Reactive carbonyls and oxidative stress: Potential for therapeutic intervention. Pharmacol Ther 115, 13-24.

Esterbauer, H., Cheeseman, K., Dianzani, M., Poli, G. and Slater, T. (1982). Separation and characterization of the aldehydic products of lipid-peroxidation stimulated by ADP-Fe^{2+} in rat-liver microsomes. Biochem. J. 208, 129-140.

Faureau, L. V., Pickett, C.B., 1991. Transcriptional regulation of the rat NAD(P)H:quinine reductase gene. Identification of regulatory elements controlling basal level expression and inducible expression by planar aromatic compounds and phenolic antioxidants. J. Biol Chem. 266, 4556-4561.

Faurskov, B., Bjerregaard, H. F., 2002. Evidence for cadmium mobilization of intracellular calcium through a divalent cation receptor in renal distal epithelial A6 cells. Pflugers. Arch. Eur J. Physiol. 445, 40-50.

Fleischauer A. T., Arab, L., 2001. Garlic and Cancer: a critical review of the epidemiologic literature. J. Nutr. 131, 1032-1040.

Fotakis, G., Cemeli, E., Anderson, D., Timbrell, J. A., 2005. Cadmium chloride- induced DNA and lysosomal damage in a hepatoma cell line.Toxicol. In Vitro. 19, 481-489.

Fotakis, G. and Timbrell, J. A. (2006). In vitro cytotoxicity assays: comparison of LDH, neutral red, MTT and protein assay in hepatoma cell lines following exposure to cadmium chloride. Toxicol Lett 160, 171-7.

Freeman, F., Kodera, Y., 1995. Garlic chemistry: stability of S-(2-propenyl) 2-propane-1-sulfinothioate (allicin) in blood, solvents and simulated physiological fluids. J. Agric. Food Chem. 43, 2332-2338.

Friberg, L., 1979. Cadmium in shipham. Lancet. I, 845-847.

Friberg, L., Elinder, C. G., 1983. Cadmium and compounds. In: Parmeggiani, L., ed. Encyclopedia of occupational health and safety, Geneva, International Labour Organisation Publications, pp. 356-357.

Friberg, L., Elinder, C. G., Kjellstrom, T., Nordberg, G. F. (eds.). 1986. Cadmium and Health: A toxicological and Epidemiological Appraisal. CRC Press, Boca Raton, FL.

Friberg, L., Piscator, M., Nordberg, G. F., Kjellstrom, T. 1974. Cadmium in the environment, 2nd ed., Cleveland, CRC. Press.

Friling, R. S., Bensimon, A., Tichauer, Y., Daniel, V., 1990. Xenobiotic-inducible expression of murine glutathione S-transferase Ya subunit gene is controlled by an electrophile-responsive element. Proc. Natl. Acad. Sci. USA. 87, 6258-6262.

Furukawa, M., Xiong., Y., 2005. BTB protein Keap1 targets antioxidant transcription factor Nrf2 for ubiquitination by the culin 3-Rocl ligase. Mol. Cell Biol. 25, 162-171.

Gabbiani, G., Baic, D. and Deziel, C. (1967). Toxicity of cadmium for the central nervous system. Exp Neurol 18, 154-60.

Galan, A., Troyano, A., Viloboa, E. N., Fernandez, C., DeBlas, E., Aller, P., 2001.Modulation of the stress response during apoptosis and necrosis induction in cadmium-treated U-937 human promocytic cells. Biochim. Biophysic. Acta, 1538, 3846.

Geng, Z., Lau, B. H. S., 1997. Aged garlic modulates glutathione redox cycle and superoxide dismutase activity in vascular endothelial cells. Phyto. Res. 11, 54-56.

Germain, E., Auger, J., Ginies, C., Siess, M. H., Teyssier, C., 2002. In vivo metabolism of diallyl disulfide in the rat: identification of two new metabolites. Xenobiotica. 32, 1127-1138. (abstract).

German Kommission E monograph., 1988. Bundeganzeiger Nr. 122 vom 06.07. 1988; Monographie: Allii Sativi bulbus (Knoblauchrwiebel).

Gething, M. J., Sambrook, J., 1992. Protein folding in the cell. Nature. 355, 33-45.

Ghosh, N., Bhattacharya, S., 1992. Thyrotoxicity of chlorides of cadmium and mercury in rabbit. Biomed. Environ. Sci. 5, 236-240.

Graham, F. L., Smiley, J., Russell, W. C. and Nairn, R. (1977). Characteristics of a human cell line transformed by DNA from human adenovirus type 5. J Gen Virol 36, 59-74.

Habig, W.H., Pabst, M.J., Jakoby, W.B., 1974. Glutathione transferas: a first enzymatic step in mercapturic acid and foration. J. Biol. Chem. 249, 7130-7139.

Habeebu, S. S., Liu, J., Klaassen C. D., 1998. Cadmium-induced apoptosis in mouse liver. Toxicol. Appl. Pharmacol. 149, 203-209.

Hakeem, R., Hakeem, A., Duncan G. S., Henderson, J. T., Woo, M., Soengas, M. S., Elia, A., de la Pompa J. L., Kagi D., Khoo, W., Potter, J., Yoshida R., Kaufman, S. A., Lowe, S. W., Penninger, J. M., Mak, T. W., 1998. Differential requirement for caspase 9 in apoptotic pathways in vivo. Cell 94, 339-352.

Halliwell, B., Gutteridge, J. M. C., 2007. Free Radicals in Biology and Medicine, 4th ed. Oxford University Press.

Hardingham, G. E., Chawla, S., Johnson, C. M., Bading, H., 1997. Distinct functions of nuclear and cytoplasmic calcium in the control of gene expression. Nature 385, 260-265.

Harstad, E. B. Klaassen, C. D., 2002. Gadolinium chloride pre-treatment prevents cadmium chloride-induced liver damage in both wild-type and MT-null nice. Toxicol. Appl. Pharmacol. 180, 178-185.

Hart, B. A., Lee, C. H., Shukla, G. S., Osier, A., Eneman, J. D., Chiu, J. F., 1999. Characterization of cadmium-induced apoptosis in rat lung epithelial cells: evidence for the participation of oxidant stress. Toxicol. 133, 43-58.

Hartwig, A., 1994. Role of DNA repair inhibition in lead- and Cadmim-induced genotoxicity: a review. Environ. Health Perspect. 102. 45-50.

Hartwig, A., Schwerdtle, T. 2002. Interactions by carcinogenic metals compounds with DNA repair processes: toxicological implications. Toxicol. Lett.127, 47-54.

Harvey, C. J., Thimmulappa, R. K., Singh, A., Blake, D. J., Ling, G., Wakabayashi, N., Fujii, J., Myers, A., Biswal, S., 2009. Nrf2-regulated glutathione recycling independent of biosynthesis is crical for cell survival during oxidative stress. Free Radic Biol Med. 46, 443-453.

Hassoun, A.E., Stoh, J. S. 1996. Cadmium production of Super oxide anion and nitric oxide, DNA single strand breaks and lactate dehydrogenase leakage in J774.1 Cell cultures. Toxicol. 112, 219-226.

Hatono, S., Jimenez, A., Wargovich, M. J., 1996. Chemopreventive effect of S-allylcysteine and its relationship to the detoxification enzyme glutathione S-transferase. Carcinogenesis. 17, 1041-1044.

Hayes, J. D., 1983. Rat liver glutathione S-transferase. A study of the structure of the basic YbYb-containing enzyes. Biochem. J. 213, 625-633.

Hayes, J. D., Flanagan, J. U. and Jowsey, I. R. (2005). Glutathione transferases. Annu Rev Pharmacol Toxicol 45, 51-88.

He, X., Chen, M. G., Ma, Q., 2008. Activation of Nrf2 in defense against cadmium-induced oxidative stress. Chem. Res. Toxicol. 21, 1375-1383.

He, X., Lin, G. X., Chen, M. G., Zhang, J. X., Ma Q., 2007. Protection against chromium (VI)-induced oxidative stress and apoptosis by Nrf2. Recruiting Nrf2 into the nucleus and disrupting the nuclear Nrf2/Keap1 association. Toxicol. Sci. 98, 298-309.

Helenius, A., Trombetta, E. S., Hebert, D. N., Simons, J. F., 1997. Calnexin, calreticulin and the folding of glycoproteins. Trends Cell Biol. 7, 193-200.

Hempel, S. L., Buettner, G. R., O'Malley, Y. Q., Wessels, D. A., Flaherty, D. M., 1999. Dihydrofluorescein diacetate is superior for detecting intracellular oxidants: comparison with 2',7'-dichlorodihydrofluorescein diacetate, 5(and 6)-carboxy-2',7'-dichlorodihydrofluorescein diacetate, and dihydrorhodamine 123. Free Radic Biol Med. 27, 146-59.

Henkart, P. A., 1996. ICE family proteases-mediators of all apoptotic cell-death? Immunity.4, 195-201.

Huang, C. S., Chang, L. S., Anderson, M. E., Meister, A., 1993. Catalytic and regulatory properties of the heavy subunit of rat kidney gamma-glutamylcysteine synthase. J. Biol. Chem. 268, 19675-19680.

Huang, H. C., Nguyen, T., Pickett, C. B., 2000. Regulation of the antioxidant response element by protein kinase C-mediated phosphorylation of NF-E2-related factor 2. Proc Natl Acad Sci USA. 97, 12475-12480.

Huang, E. H., Nguyen, T., Pickett, C. B., 2002. Phosphorylation of Nrf2 at ser-40 by protein kinase C regulates antioxidant response element-mediated transcription. J. Biol. Chem. 277, 42769-42774.

IARC., 1993. Beryllium, Cadmium, Mercury and Exposures in the Glass Manufacturing Industry. IARC Monographs on the Evaluation of Carcinogenic Risk of Chemicals to Humans, vol.2. Lyon France: International Agency for Research on Cancer. 444pp.

Ide N., Lau, B., 1997. Garlic compounds protect vascular endothelial cells from oxidized low density lipoprotein-induced injury. J. Pharm. Pharmacol. 49, 908-911.

Ide, N., Lau, B. H., 2001. Garlic Compounds Minimise Intracellular Oxidative Stress and Inhibit Nuclear Factor-KB Activation. J. Nutr. 131, 1020-1026.

Igarashi, K., Kataoka, K., Nishizawa, M., Yamamoto, M., 1994. Regulation of transcription of erythroid factor NF-E2 p45 with small Maf proteins. Nature 367, 568-572.

Igarashi, K., Hoshino, H., Muto, A., Suwabe, N., Nishikawa, S., Nakauchi, H., 1998. Multivalent DNA binding complex generated by small Maf and Bach 1 as a possible biochemical basis for β-globin locus control region complex. J. Biol Chem. 273, 11783-11790.

Imai, J., Ide, N., Nagae, S., Moriguchi, T., Matsuura, H., Itakura, Y., 1994. Antioxidant and radical scavenging effects of aged garlic extract and its constituents. Planta Med. 60, 417-420.

Irano, P., Santovito, G., Piccini, E., Albergoni, V., 2001. Oxidative burst and metallothionein as a scavenger in macrophages. Immunol. Cell Biol. 79, 251-254.

Ishii, T., Itoh, K., Takahashi, S., Sato, H., Yanagawa, T., Katoh, Y., Bannai, S., Yamamoto, M., 2000. Transcription factor Nrf2 coordinately regulates a group of oxidative stress-inducible genes in macrophages. J. Biol. Chem. 275, 16023-16029.

Ishii, T., Itoh, K., Ruiz, E., Leake, D. S., Unoki, H., Yamamoto, M., Mann, G. E. 2004. Role of Nrf2 in the regulation of CD36 and stress protein expression

in murine macrophages: activation by oxidatively modified LDL and 4-hydroxynonenal. Circ. Res. 94, 609-616.

Itoh, K., Chiba, T., Takahashi, S., Ishii, T., Igarashi, K., Katoh, Y., 1997. An Nrf2/small Maf heterodimer mediates the induction of phase II detoxifying enzyme genes through antioxidant response elements. Biochem Biophys Res Commun. 236, 313-322.

Itoh, K., Igarashi, K., Hayashi, N., Nishirawa, M., Yamamoto, M., 1995. Cloning and characterization of a novel erythroid cell-derived CNC family transcription factor heterodimerizing with the small maf family proteins. Mol. Cell Biol. 15, 4184-4193.

Itoh, K., Tong, K. I., Yamamoto, M., 2004. Molecular mechanism activating Nrf2-Keap1 pathway in regulation of adaptive response to electrophiles. Free Radic. Biol. Med. 36, 1208-1213.

Itoh, K., Wakabayashi, N., Katoh, Y., Ishii, T., Igarashi, K., Engel, J. D., Yamamoto, M., 1999. Keap1 represses nuclear activation of antioxidant responsive element by Nrf2 through binding to the amino terminal Neh2 domain. Gene Dev. 13, 76-86.

Itoh, K., Wakabayashi, N., Katoh, Y., Ishii, T., O'Connor, T., Yamamoto, M., 2003. Keap1 regulates both cytoplasmic nuclear shuttling and degradation of Nrf2 in response to electrophiles. Genes Cells. 8, 379-391.

Imai, J., Ide, N., Nagae, S., Moriguchi, T., Matsuura, H., Itakura, Y., 1994. Antioxidant and radical scavenging effects of aged garlic extract and its constituents. Planta Med. 60, 417-420.

Iwata, N., Inazu, N., Satoh, T., 1990. The purification and properties of aldose reductase from rat ovary. Arch. Biochem. Biophys. 282, 70-77.

Jain, A. K., Jaiswal, A. K., 2007. GSK-3beta acts upstream of Fyn kinase in regulation of nuclear export and degradation of NF-E2 related factor 2. J. Biol. Chem. 282, 16502-16510.

Jain, A. K., Mahajan, S., Jaiswal, A. K., 2008. Phosphorylation and dephosphorylation of tyrosine 141 regulate stability and degradation of INrf2: a novel mechanism in Nrf2 activation. J. Biol. Chem. 283, 17712-17720.

Jaiswal, A. K., 2004. Nrf2 signaling in coordinated activation of antioxidant gene expression. Free Radic. Biol Med. 36, 1199-1207.

Jin, Y. and Penning, T. M. (2007). Aldo-keto reductases and bioactivation/detoxication. Annu Rev Pharmacol Toxicol 47, 263-92.

Jollow, D.J., Mitchell, J.R., Gillette, J.R., 1974. Bromobenzene induced liver necrosis: Protective role of glutathione and evidence for 3,4-bromobenzene oxide as the hepatotoxic metabolite. Pharmacol. 11, 151-169.

Joseph, P., Jaiswal, A.K., 1994. NAD(P)H:quinone oxidoreductase 1 (DT diaphorase) specifically prevents the formation of benzo(a)pyrene quinone-DNA adducts generated by cytochrome P4501A1 and P450 reductase. Proc. Natl. Acad. Sci. USA. 91, 8413-8417.

Juin, P., Pelletier, M., Oliver, L., Tremblais, K., Gregoire, M., Meflah, K., Vallette, F. M., 1998. Induction of a caspase-3 like activity by calcium in normal cytosolic extracts triggers nuclear apoptosis in a cell-free system. J. Biol Chem. 273, 17559-17564.

Kamiyama, T., Miyakawa, H., Li. J. P., Akiba, T. Liu, J. H., Liu, J. Marumo, F., Sato C., 1995. Effects of one-year cadmium exposure on livers and kidneys and their relation to glutathione levels. Res. Commun. Mol. Pathol. Pharmacol. 88, 177-186.

Kang, K. W., Lee, S. J., Kim. S. G., 2005. Molecular mechanism of Nrf2 activation by oxidative stress. Antiox. Red. Signal. 7, 1664-1673.

Kaplowitz, N., Aw, T. Y., Ooktens, M., 1985. The regulation of hepatic GSH. Annu. Rev. Pharmacol. Toxicol. 25, 714-744.

Kass GEN, Eriksson JE, Weis M, Orrenuis S & Chow SC. 1996; Chromatin condensation during apoptosis requires ATP. *Biochem. J.* 318, 749–752.

Kass, G. E. N., Orrenius, S. 1999. Calcium Signaling and Cytotoxicity. Environ. Health Perspect. 107, 25-34.

Kashiwagi, K., Shirai Y., Kuriyama, M., Sakai, N., Saito, N., 2002. Importance of C1B domain for lipid messenger-induced targeting of protein kinase C. J. Biol. Chem. 277, 18037-18045.

Kensler, T. W., 1997. Chemoprevention by inducers of carcinogen detoxification enzymes. Environmental Health Perspectives. 105, 965-970.

Kensler, T. W., Wakabayashi, N., Biswal, S., 2007. Cell survival responses to environmental stresses via the Keap1-Nrf2-ARE pathway. Annu. Rev. Pharmacol Toxicol. 47, 89-116.

Keum, Y. S., Han, Y. H., Liew, C., Kim, J. H., Xu, C., Yuan, X., Shakarjian, M. P., Chong, S., Kong, A. N., 2006. Induction of Heme oxygenase-1 (HO-1) and NAD(P)H:QuinoneOxidoreductase 1 (NQO1) by a phenolic Antioxidant, Butylated Hydroxyanisole (BHA) and its Metabolite, tert-Butylhydroquinone (tBHQ) in primary-cultured Human and Rat hepatocytes. Pharm. Res. 23, 2586-2594.

Kishimoto, A., Mikawa, K., Hashimotos, K., Yasuda, I., Tanaka, S., Tominaga, M. T., Kuroda, T., Nishizuka, Y., 1989. Limited proteolysis of protein kinase C subspecies by calcium-dependent neutral protease (calpain). J. Biol Chem. 264, 4088-4092.

Knasmuller, S., Mersch-Sundermann, V., Kevekordes, S., Darroudi, F., Hubber, W. W., Hoelzl, C., Bichler, J., Mayer, B. J., 2004. Use of human-derived liver cell lines for the detection of environmental and dietary genotoxicants: current state of knowledge. Toxicol. 198, 315-328.

Knasmuller, S., Parzefall, W., Sanyal R., Ecker, S., Schwab, C., Uhl, M., Mersch-Sundermann, V., Williamson, G., Hietsch, G., Langer, T., Darroudi, F., Natarajan, A. T., 1998. Use of metabolically competent human hepatoma cells of the detection of mutagens and antimutagens. Ind. J. Human Gen. 4, 157-180.

Kobayashi, A., Ito E., Toki, T., Kogame, K., Takahashi, S., Igarashi, K., Hayashi, N., Yamamoto, M., 1999. Molecular cloning and functional characterization of a new cap'n'collar family transcription factor Nrf3. J. Biol. Chem. 274, 6443-6452.

Kobayashi, M., Itoh, K., Suzuki, T., Osanai, H., Nishikawa K., Katoh, Y., Takagi, Y., Yamamoto, M., 2002. Identification of the interactive interface and phylogenic conservation of the Nrf2-Keap1 system. Genes Cells 7, 807-820.

Kobayashi, A., Kang, M. I., Okawa, H., Ohtsuji, M., Zenke, Y., Chiba, T., Igarashi, K., Yamamoto, M., 2004. Oxidative stress sensor Keap1 functions as

an adaptor for Cul3-based E3 ligase to regulate proteasomal degradation of Nrf2. Mol. Cell. Biol. 24, 7130-7139.

Kobayashi, M., Yamamoto, M., 2006. Nrf2-Keap1 regulation of cellular defense mechanisms against electrophiles and reactive oxygen species. Advan. Enzyme Regul. 46, 113-140.

Kobayashi, M., Yamamoto, M., 2005. Molecular mechanisms activating the Nrf2 Keap1 pathway of antioxidant gene regulation. Antioxid. Redox Signal. 7, 385-394.

Kondoh, M., Araragi, S., Sato, K., Higashimoto, M., Takiguchi, M., Sato, M., 2002. Cadmium induces apoptosis partly via caspase-9 activation in HL-60 cells. Toxicol. 170, 111-117.

Koizumi, N., Murata, K., Hayashi, C., Nishio, H. and Goji, J. (2008). High cadmium accumulation among humans and primates: comparison across various mammalian species--a study from Japan. Biol Trace Elem Res 121, 205-214.

Kubbutat, M. H. G., Vousden, K. H., 1997. Proteolytic cleavage of human p53 by calpain: A potential regulator of protein stability. Mol. Cell Biol. 17, 460-468.

Lag, M., Westly, S., Lerstad, T., Bjornsrud,C., Refsnes, M., Schwarze,P. E., 2002. Cadmium-induced apoptosis of primary epithelial lung cells: involvement of Bax and p53, but not of oxidative stress. *Cell. Biol. Toxicol.* 18, 29–42.

Lambrecht, R. W., Fernandez, M., Shan, Y., Bonkorsky, H., 2005. Heme oxygenase and carbon monoxide in cirrhosis and portal hypertension. In Ascites and Renal Dysfunction in Liver Disease, Pathogenesis, Diagnosis and Treatment (Gine P., Anroyo, V., Rodes, J and Schrier, R. W., eds) pp125-136. Blackwell Science, London.

Lawson, L. D., 1996. The composition and chemistry of garlic cloves and processed garlic. In: H.P. Koch and L. D. Lawson, Editors, Garlic. The Science and Therapeutic Application of Allium sativum L. and Related Species (second ed.), Williams and Wilkins, Baltimore, MD.p.37-107.

Lawson, L. D., 1998. Garlic: a review of its medicinal effects and indicated active compounds. In: L. D. Lawson and R. Bauer, Editors, Phytomedicines of Europe: Chemistry and Biological Activity, American Chemical Society, Washington, DC. Pp 51-79.

Leach, F.R., 1981.ATP Determination with Firefly Luciferase. J. Appl.Biochem. 3, 473-517.

Lee, J. S., Surh, Y.J., 2005. Nrf2 as a novel molecular target for chemoprevention. Cancer Lett. 224, 171-184.

Lee, W. K., Abouhamed, M., Thevenod, F., 2006. Caspase-dependent and –independent pathways for cadmium-induced apoptosis in cultured kidney proximal tubule cells. Am J Physiol Renal Physiol. 291, 823-832.

Lee, W. K., Torchalski, B., Thevenod, F., 2007. Cadmium-induced ceramide formation triggers calpain-dependent apoptosis in cultured kidney proximal tubule cells. Am. J. Physiol. Cell Physiol. 293, C839-C847.

Le Good, J. A., Ziegler, W. H., Parekh, D. B., Alessi, D. R., Cohen, P., Parker, P. J., 1998. Protein kinase C isotypes controlled by phosphoinositide 3-kinase through the protein kinase PDK1. Science. 281, 2042-2045.

Leist, M., Jaattela, M., 2001. Triggering of apoptosis by cathepsins. Cell Death Differ 8, 324-326.

Leist M, Single B, Castoldi AF, Kuhnle S & Nicotera P. 1997; Intracellular adenosine triphosphate (ATP) concentration: a switch in the decision between apoptosis and necrosis. J. Exp. Med. 185, 1481−1486.

Leverrier, P., Montigny, C., Garrigos, M., Champeil, P., 2007. Metal binding to ligands: cadmium complexes with glutathione revisited. Anal. Biochem. 371, 215-228.

Levonen, A. L., Landar, A., Ramachandran, A., Ceaser, E. K., Dickinson, D.A., Zanoni, G., Morrow, J. D., Darley-Usmar, V. M., 2004. Cellular mechanisms of redox cell signalling: Role of cysteine modification in controlling antioxidant defences in response to electrophilic lipid oxidation products. Biochem. J. 378, 373-382.

Li, B.,Wang, X., Rasheed, N., Hu, Y., Boast, S., Ishii, T., Nakayama, K., 2004. Distinct roles of c-Ab1 and Atm in oxidative stress response are mediated by protein kinase C δ. Genes Dev. 18, 1824-1837.

Li, M., Kondo, T., Zhao, Q. L., Li, F. J., Tanabe, K., Arai, Y., Zhous, Z. C., Kasuya, Z. M., 2000. Apoptosis induced by cadmium in human lymphoma U937 cell through Ca2+-calpain and caspase-mitochondria-dependent pathways. J. Biol. Chem. 275, 39702-39709.

Li, W. P., Chan, W. Y., Lai, H. W., Yew, D. T., 1997. Terminal dUTP nick end labelling (TUNEL) positive cells in the different regions of the brain in normal aging and Alzheimer patients. J. Mol. Neurosci. 8, 75-82.

Li, Y., Jaiswal, A. K., 1992. Regulation of human NAD(P)H:quinine oxidoreductase gene. Role of API binding site contained within human antioxidant response element. J. Biol Chem. 267, 15097-15104.

Lincoln, B. C., Healey, J. F., Bonkovsky, H. L., 1988. Regulation of hepatic haem metabolism. Disparate mechanisms of induction of haem oxygenase by drugs and metals. Biochem. J. 250, 189-196.

Little, E., Ramakrishnan, M., Roy, B., Gazit, G., Lee, A. S., 1994. The glucose-regulated proteins (GRP78 and GRP94): functions, gene regulation, and applications. Crit Rev Eukaryotic Gene Expr. 4, 1-18.

Liu, F., Jan, K. Y., 2000. DNA damage in arsenite- and cadmium-treated bovine aortic endothelial cells. Free Radic. Biol. Med. 28, 55-63.

Liu, J., Kershaw, W. C., Klaassen, C. D., 1990. Rat primary hepatocyte cultures are a good model for examining metallothionein-induced tolerance to cadmium toxicity. In vitro Cell Dev. Biol. 26, 75-79.

Liu, J., Qu, W., Kadiiska, M. B., 2009. Role of oxidative stress in cadmium toxicity and carcinogenesis. Toxicol. Appl. Pharmacol.238, 209-214.

Liu, N. Fine, R. E., Simons, E., Johnson, R. J., 1994. Decreasing calreticulin expression lowers the Ca^{2+} response to bradykinin and increases sensitivity to ionomycin in NG-108-15 cells. J. Biol. Chem. 269, 28635-28639.

Liu, Y., Graham, C., Li, A., Fisher, R. J., Shaw, S., 2002. Phosphorylation of the protein kiase C-theta activation loop and hydrophobic motif regulates its

kinase activity, but only activation loop phosphorylation is critical to in vivo nuclear-factor-kappaB induction. Biochem. J. 361, 255-265.

Manca, D., Richard, A.C., Van Tra, H., Chevalier, G., 1994. Relation between lipid peroxidation and inflammation in the pulmonary toxicity of cadmium. Arch. Toxicol. 68, 364-369.

Mannervik, B., Jensson, H., 1982. Binary combinations of four protein subunit with different catalytic specificities explain the relationship between six basic glutathione S-transferase in rat liver cytosol. J. Biol. Chem. 257, 9909-9912.

Mao, W. P., Ye, J. L., Guan, Z. B., Zhao, J. M., Zhang, C., Zhang, N. N., Jiang, P. and Tian, T. (2007). Cadmium induces apoptosis in human embryonic kidney (HEK) 293 cells by caspase-dependent and -independent pathways acting on mitochondria. Toxicol In Vitro 21, 343-54.

Markovich, J., Borras, C., Ortega, A., Sastre, J., Vina, J., Pallardo, F. V., 2007. Glutathione is Recruited into the Nucleus in Early Phases of Cell Proliferation. J. Biol. Chem. 282, 20416-20424.

Martelli, A., Rousselet, E., Dycke, C., Bouron, A., Moulis, J-M., 2006. Cadmium toxicity in animal cells by interference with essential metals. Biochimie.88, 1807-1814.

Mathew, F. S., 1985. The structure, function and evolution of cytochromes. Prog. Biophys. Mol. Biol. 45, 1-56.

Maines, M. D., 1988. Hemeoxygenase: function, multiplicity, regulatory mechanisms, and clinical applications. FASEB J. 2, 2557-2568.

McCoubrey, W. K. J., Huang, T. J., Maines, M. D., 1997. Isolation and characterization of a cDNA from the rat brain that encodes hemoprotein heme oxygenase-3. Eur J Biochem. 247, 725-732.

McMahon, M., Itoh, K., Yamamoto, M., Chanas S. A. Hendenson, C. J., McLellan, L., Wolf, C. R., Cavin, C. Hayes, J. D., 2001. The cap'n' collar basic leucine zipper transcription factor Nrf2 (NF-E2 p45-related factor2) controls both constitutive and inducible expression of intestinal detoxification and glutathione biosynthesis enzymes. Cancer Res. 61, 3299-3307.

McMahon, M., Itoh, K., Yamamoto, M., Hayes, J. D., 2003. Keap1-dependent proteasomal degradation of transcription factor Nrf2 contributes to the negative regulation of antioxidant response element-driven gene expression. J. Biol Chem. 278, 21592-21600.

McCarthy, K. D., Salm, A. K., 1991. Pharmacologically- distinct subsets of asroglia can be identified by their calcium response to neuroligands. Neurosci. 41, 325-333.

Meister, A., Anderson, M. E., 1983. Glutathione. Annu. Rev. Biochem. 52, 711-760.

Merrill, J.C., Morton, J.J.P., Soileau, S.D., 2001. Metals: Cadmium In: Hayos. A.W. (Ed), Principles and Methods of Toxicology. Taylor and Francis, London, pp 665-667.

Mery, L., Mesaeli, N., Michalak, M., Opas, M., Lew, D. P., Krause, K. H., 1996. Overexpression of calreticulin increases intracellular Ca^{2+}- storage and decrease store-dependent Ca^{2+} influx. J. Biol. Chem. 271, 9332-9339.

Miguel, B. G., Rodriquez, M. E., Aller, P., Martinez, A. M., Meta, F., 2004. Regulation of cadmium-induced apoptosis by PKCδ in U937 human promonocytic cells. Biochim Biophys. Acta. 1743, 215-222.

Miller, E. C., 1978. Some current properties on chemical carcinogenic N-nitroso compounds by ascorbic acid and other compounds. In: J. H Burchenal and H. F.Oettgen (eds.). Cancer achievements. Challenges and Prospects for the 1980's, pp557-588. New York: Grune and Stratton.

Mirvish, S. S., 1981. Inhibition of the formation of carcinogenic N-nitroso compounds (eds.), Cancer Achievements, Challenges and Prospects for the 1980's, pp557-588. New York: Grune and Stratton.

Misra, U.K., Grandi, G., Akabani, G., Pizzo, S.V., 2002. Cadmium-induced DNA synthesis and cell proliferation in macrophages: the role of intracellular calcium and signal transduction mechanisms. Cell Signal. 14, 327-340.

Mohler, J., Vani, K., Leung, S., Epstein, A., 1991. Segmentally restricted, cephalic expression of a leucine zipper gene during Drosophila embryogenesis. Mech Dev. 34, 3-9.

Moi, P., Chan, K., Asunis, I., Cao, A., Kan, Y. W., 1994. Isolation of NF-E2 related factor 2 (Nrf2), a NF-E2 like basic leucine zipper transcriptional activator that binds to the tandem NF-E2/API repeat of β-globin locus control region. Proc. Natl. Acad. Sci. USA. 91, 9926-9930.

Moriguchi, T., Salto, H., Nishiyama, N., 1997. Anti-aging effect of aged garlic extract in the inbred brain atrophy mouse model. Clin. Exp. Pharmacol. Physiol. 24, 235-242.

Mossmann, T., 1983. Rapid colorimetric assay for cellular growth and survival: application to proliferation and cytotoxicity assays. J.Immunol. Meth.65, 55-63.

Mulcahy, R. T., Gipp, J. J., 1995. Identification of a putative antioxidant response element in the 5'-flanking region of the human γ-glutamylcysteine synthase heavy subunit gene. Biochem Biophys Res Commun. 209, 227-233.

Mulcahy,R. T., Wartman, M. A., Bailey, H. H., Gipp, J. J., 1997. Constitutive and beta-naphthoflavone-induced expression of the human gamma-glutamylcysteine synthase heavy subunit gene is regulated by a distal antioxidant response element/TRE sequence. J. Biol. Chem. 272, 7445-7454.

Muto, A., Hoshino, H., Madisen, L., Yanai, N., Obinata, M., Karasuyama, H., Hayashi, N., Nakauchi, H., Yamamoto, M., Groudine, M., Igarashi, K., 1998. EMBO J. 17, 5734-5743.

Nadal, A., Fuentes, E., McNaughton, P. A., 1996. Albumin stimulates uptake of calcium into subcellular stores in rat cortical astrocytes. J. Physiol. 492, 737-750.

Nagae, S., Ushijima, M., Hatono, S., Imai, J., Kasuga, S., Matsuura, H., Itakura, Y., Higashi, Y., 1994., Pharmacokinetics of the garlic compound S-allylCysteine. Planta. Med. 60, 214-217.

Nakaso, K., Yano, H., Fukuhara, Y., Takeshima, T., Wada-Isoe, K., Nakashima, K., 2003. P13K is a key molecule in the Nrf2-mediated regulation of antioxidative proteins by hemin in human neuroblastoma cells. FEBS Lett. 546, 181-184.

Newton, A. C., 2003. Regulation of the ABC kinases by phosphorylation: Protein kinase C as a paradigm. Biochem. J. 370, 361-371.

Ney, P. A., Andrews, N. C., Jane, S. M., Safer, B., Purucker, M. E., Weremowicz, S., Morton, C. C., Goff, S. C., Orkin, S. H., Nienhuis, A. W., 1993. Purification of the human NF-E2 complex: cDNA cloning of the hematopoietic cell-specific subunit and evidence for an associated partner. Mol. Cell. Biol. 13, 5604-5612.

Nguyen, T., Sherratt, P. J., Pickett, C., 2003. Regulatory mechanisms controlling gene expression mediated by the anti-oxidant response element. Annu. Rev. Pharmacol. Toxicol. 43, 233-260.

Nguyen, T., Sherratt, P. J., Huang, H. C., Yang, C. S., Pickett, C. B., 2003. Increased protein stability as a mechanism that enhances Nrf2-mediated transcriptional activation of the antioxidant response element. Degradation of Nrf2 by the 26 S proteasome. J. Biol Chem. 278, 4536-4541.

Nishizuka, Y., 1995. Protein kinase C and lipid signalling for sustained cellular responses. FASEB J. 9, 484-496.

Nishizuka, Y., 1988. The molecular heterogeneity of protein kinase C and its implications for cellular regulation. Nature. 334, 661-665.

Niture, S. K., Kaspar, J. W., Shen, J., Jaiswal, A. K., 2009. Nrf2 signaling and cell survival. Toxicol. Appl. Pharmacol, doi: 10.1016/j.taap.2009.06.09.

Norgen, N. R., 2005. "Physiological and Pathological aspects of GSH metabolism". Acta Paediatr. 94. 132-137.

Nriagu, J.O., Pacyna. J.M., 1988. Quantitative assessment of worldwide contamination of air, water and soils by trace metals. Nature. 333, 134-139.

Numarazawa, S., Ishikawa, M., Yoshida, A. Tanaka, S., Yoshida, T., 2003. Atypical protein kinase C mediates activation of NF-E2-related factor 2 in a response to oxidative stress. Am. J. Physiol. Cell Physiol. 285, C334-C342.

Nunez, G., Benedict, M, A., Hu, Y., Inohara, N., 1998. Caspases : the proteases of the apoptotic pathway. Oncogene.17, 3237-3245.

Nzengue, Y., Steiman, R., Garrel, C., Lefebvre, E. and Guiraud, P. (2008). Oxidative stress and DNA damage induced by cadmium in the human

keratinocyte HaCaT cell line: role of glutathione in the resistance to cadmium. Toxicol. 243, 193-206.

O'Brien, P., Salacinski, H. J., 1998. Evidence that the reactions of cadmium in the presence of metallothionein can produce hydroxyl radicals. Arch. Toxicol. 72, 690-700.

Ochi, T., Takahashi, K., Ohsawa, M., 1987. Indirect evidence for the induction of a pro-oxidant state by cadmium chloride in cultured mammalian cells and a possible mechanism for the induction. Mutat. Res. 180, 257-266.

O'Farrell, P. H., 1975. High resolution two-dimensional electrophoresis of proteins. J. Biol. Chem. 250, 4007-4021.

Oh, S., Lim, S., 2006.A rapid and transient ROS generation by Cadmium triggers apoptosis via Caspase-dependent pathway in HepG2 cells and this is inhibited through N-acetyl cysteine-mediated catalase regulation. Toxicol. Appl. Pharmacol, 212, 212-223.

Ohmori S., Sakai, N., Shirai, Y., 2000. Importance of protein kinase C targeting for the phosphorylation of its substrate, myristoylated alanine-rich C-kinase substrate. J. Biol. Chem. 275, 26449-26457.

Okuda, A., Imagawa, M., Meada, Y., Sakai, M., Muramatsu, M., 1989. Strutural and functional analysis of an enhancer GPE1 having a phorbol 12-O-tetradeconoate 13-acetate responsive element-like sequence found in the rat glutathione transferase P. Gene 264, 16919-16926.

Oltvai, Z. N., Milliman, C. L., Korsmeyer, S. J., 1993. Bcl-2 Heterodimerizes in vivo with a Conserved Homology Bax, That Accelerates Programmed Cell Death. Cell 74, 609-619.

Opas, M., Szewczenko-Pawlikowski, M., Jass, G. K., Masaeli, N., Michalak, M., 1996. Calreticulin modulates cell adhesivness via regulation of vinculin expression. J Cell Biol. 135, 1913-1923.

Orrenius, S., Nicotera, P., 1994.The calcium ion and cell death. J. Neural Transm Suppl. 43, 1-11.

Oyake, T., Itoh, K., Motohashi, H., Hayashi, N., Hoshino, H., Nishizawa, M., 1996. Bach proteins belong to a novel family of BTB-basic leucine zipper transcription factors that interacts with MafK and regulate transcription through the NF-E2 site. Mol. Cell Biol.16, 6083-6095.

Page, A. L., Bingham, F. T., Chang, A. C., 1981. Cadmium. In: Lepp, N. W., ed. Effect of heavy metal pollution on plants, London, Applied Science, Vol. 1, pp. 77-109.

Pan, G., Humke, E., Dixit, V. M., 1998. Activation of caspases triggered by cytochrome c in vitro. FEBS Lett. 426, 151-154.

Pari, L., Murugavel, P., 2007. Diallyl tetrasulfide improves cadmium induced alterations of acetylcholinesterase, ATPases and oxidative stress in brain of rats. Toxicol. 234, 44-50.

Parsell, D. L. S., 1994. In: Morimoto, R. I., Tissieres, A., Georgopoulos, C. (Eds.), The Biology of Heat Shock Proteins and Molecular Chaperones. CSHL Press, New York, pp. 457-494

Pathak, N., Khandelwal, S., 2006. Oxidative stress and apoptotic changes in murine splenocytes exposed to cadmium. Toxicol. 220, 26-36.

Payne, R. B., Little, A. J., Williams, R. B., Milner,J. R., 1973. Interpretation of serum calcium in patients with abnormal serum proteins. Br. Med. J. 4, 643-646.

Pearce, B., Murphy, J., Morrow, C., Dandona, P., 1989. ATP-evoked Ca^{2+} mobilisation and prostanoid release from astrocytes: P2-purinergic receptors linked to phosphoinositide hydrolysis. J. Neurochem. 52, 971-977.

Philchenkov, A., 2004. Caspases and cancer: mechanisms of inactivation and new treatment modalities. Exp. Oncol. 26, 82-97.

Pozzan, T., Rizzuto, R., Volpe, P., Meldolesi, J., 1994. Molecular and cellular physiology of intracellular calcium stores. Physiol Rev 74, 595-636.

Prestera, T., Holtzclaw, W. D., Zhang, Y., Talalay, P., 1993. Chemical and molecular regulation of enzymes that detoxify carcinogens. Proc. Natl. Acad. Sci. USA. 90, 2965-2969.

Prestera, T., Talalay, P., Alam, J., Ahn, Y. I., Lee, P. J., Choi, A. M., 1995. Parallel induction of heme oxygenase-1 and chemoprotective phase 2 enzymes by electrophiles and antioxidants: regulation by upstream antioxidant-response element (ARE).Mol. Med. 1, 827-837.

Prochaska, H. J., De Long, M. J., Talalay, P., 1985. On the mechanisms of induction of cancer-protective enzymes: a unifying proposal. Proc. Natl. Acad. Sci. USA. 82, 8232-8236.

Prozialeck W. C., Lamar, P. C., 1999. Interaction of cadmium (Cd^{2+}) with a 13-residue polypeptide analog of a putative calcium –binding motif of E-cadherin. Biochim. Biophyys. Acta. 1451, 93-100.

Purdom-Dickinson, S., Lin,Y., Dedek, M., Johnson, J., Chen, Q., 2007. Induction of antioxidant and detoxification response by oxidants in cardiomyocytes: evidence from gene expression profiling and activation of the Nrf2 transcription factor. J. Mol Cell Cardiol. 42, 159-176.

Qu, W., Diwan, B. A., Reece, J. M., Bortner, C. D., Pi, J., Liu, J., Waalkes, M. P., 2005. Cadmium-induced malignant transformation in rat liver cells: role of aberrant oncogene expression and minimal role of oxidative stress. Int. J. Cancer 114, 346-355.

Qu, W., Ke, H., Pi, J., Broderick, D., French, J. E., Webber, M. M., Waalkes, M. P., 2007. Acquisition of apoptotic resistance in cadmium-transformed human prostate epithelial cells: Bcl-2 overexpression blocks the activation of JNK signal transduction pathway. Environ. Health Perspect. 115, 1094-1100.

Ramirez, D. C., Gimenez, M. S., 2003. Induction of redox changes, inducible nitric oxide synthase and cyclooxygenase-2 by chronic cadmium exposure in mouse peritoneal macrophages. Toxicol. Lett. 145, 121-132.

Ramalhandrans, S., Vasan, M. D., 2006. Biomarkers of Cardiovascular Disease. Circ. 113, 2335-2362.

Reinhart, T., Perason, W. R., 1993. The structure of two murine class-mu glutathione transferase genes co-ordinately induced by butylated hydroxyanisole. Arach Biochem Biophys.303, 383-393.

Redondo, M. Garcia, J., Rodrigo, T., Villar, E., Gonzalez, C., Morell, M., 2003. Expression of bax and p53 proteins in the tumorigenesis and progression of breast carcinomas. Tumor Biol. 24, 23-31.

Richter C, Schweizer M, Cossarizza A & Franceschi C. 1996; Control of apoptosis by the cellular ATP level. FEBS Lett. 378, 107–110.

Risso-de Faverney, C., Devaux, A., Lafaurie, M., Girrard, P.J., Bailly, B., Rahmani, R., 2001. Cadmium induces apoptosis and genotoxicity in rainbow trout hepatocytes through generation of reactive oxygen species. Aquatic Toxicol. 53, 62-76.

Robertson, J. D., Orrenius, S., 2000. Molecular mechanisms of apoptosis induced by cytotoxic chemicals. Crit. Rev. Toxicol. 30, 609-627.

Rushmore, T. H., King, R. G., Paulson, K. E., Pickett, C. B., 1990. Regulation of glutathione S-transferase Ya subunit gene expression: identification of a unique xenobiotic-responsive element controlling inducible expression by planar aromatic compounds. Proc Natl Acad Sci USA. 87, 3826-3830.

Rushmore, T. H., Morton, M. R., Pickett C. B., 1991. The antioxidant responsive element. J. Biol. Chem. 266, 11632-11639.

Rushmore, T. H., Pickett, C. B., 1990. Transcriptional regulation of the rat glutathione S-transferase Ya subunit gene characterization of a xenobiotic-responsive element controlling inducible expression by phenolic antioxidants. J. Biol Chem. 265, 14648-14653.

Sakurai, A., Nishimoto, M., Himeno, S., Imura, N., Tsujimoto, M., Kunimoto, M., Hara, S., 2004. Transcriptional regulation of thioredoxin reductase 1 expression by cadmium in vascular endothelial cells: Role of NF-E2 related factor. J. Cell. Physiol. 203, 529-537.

Sauer, J. M., Waalkes, M. P., Hooser, S. B., Kuester, R. K., McQueen, C. A., Sipe, I. G., 1997. Suppression of Kupffer cell function prevents cadmium induced hepatocellular necrosis in the male Sprague-Dawley rat. Toxicol. 121, 155-164.

Scheibmeir, H. D., Christensen, K., Whitaker,S. H., Jegaethesan, J., Clancy, R., Pierce, J. D., 2005. A review of free radicals and antioxidants for critical care nurses. Intens. Crit. Care Nursing 21, 24-28.

Selimi. F., Campana, A., Weitzman, J., Vogel, M. W., Mariani J., 2000. Bax and p53 are differentially involved in the regulation of caspase-3 expression and activation during neurodegeneration in Lurcher mice. Comptes Rendus del' Academie des Sciences. 323, 967-973.

Sener, G., Satyroglu, H., Sehirli, A. O., Kacmaz, A., 2003. Protective effect of aqueous garlic extract against oxidative organ damage in a rat model of thermal injury. Life Sci. 73, 81-91.

Sekhar, K. R., Soltaninassah, S. R., Borrelli, M. J., Xu, Z. Q., Meredith, M. J., Domann, F. E., Freeman, M. L., 2000. Inhibition of the 26S proteasome induces expression of GLCLC, the catalytic subunit for gamma-glutamylcysteine synthase. Biochem. Biophys. Res. Commun. 270, 311-317.

Shaikh, Z. A., Vu T. T., Zaman, K., 1999. Oxidative stress as a mechanism of chronic-induced hepatotoxicity and renal toxicity and protection by antioxidants. Toxicol. Appl. Pharmacol. 154, 256-263.

Shan, Y., Pepe, J., Lu, T. H., Elbirt, K. K Lambrecht, R. W. Bonkovsky, H. L., 2000. Induction of the heme oxygenase-1 gene by metalloporphyrins. Arch. Biochem. Biophys. 380, 219-227.

Shan Y., Lambrecht, R. W, Donohue, S. E., 2006. Role of Bach1 and Nrf2 in up-regulation of the heme oxygenase-1 gene by cobalt protoporphyrin. FASEB J. 20, 2258-2267.

Sheehan, D. Meade, G., Foley, V. M., Dowd, C. A., 2001. Structure, function and evolution of glutathione transferases: implications for classification of non-mammalian members of an ancient enzyme superfamily. Biochem. J. 360, 1-16.

Sheen, L. Y., Lii, C. K., Sheu, S. F., Meng, R. H., Tsai, S. J., 1996. Effect of the active principle of garlic-dially sulphide-on cell viability, detoxification capability and the antioxidant system of primary rat hepatocytes. Food Chem. Toxicol. 34, 971-978.

Shen, H. M., Dong, S.Y., Ong, C.N., 2001. Critical role of calcium overloading in cadmium induced apoptosis in mouse thymocytes. Toxicol. Appl. Pharmacol. 171, 12-19.

Shih, C.M., Ko, W.C., Wu, J.S., Wei, Y.H., Wang, L.F., Chang, E.E., Lo, T.Y., Cheng, H.H., Chen, C.T., 2003. Mediating of caspase-independent apoptosis by cadmium through the mitochondria-ROS pathway in MRC-5 fibroblasts. J. Cell. Biochem. 91, 384-397.

Singh, M. T., McCoy, M. T., Tice, R. R., Schneider, E. L., 1988. A simple technique for quantification of low levels of DNA damage in individual cells. Exp. Cell Res. 17, 184-191.

Singh, S. V., Pan, S. S., Srivastava, S. K., Xia, H., Hu, X., Zaren, H. A., Orchard, J. L., 1998. Differential induction of NAD(P): quinone oxidoreductase by anti-carcinogenic orgaosulfides from garlic. Biochem. Biophys. Res. Commun. 244, 917-920.

Sittig, M., ed. 1985. Handbook of toxic and hazardous chemicals and carcinogens, Park Ridge, Noyes Publication, pp. 169-173.

Smith, J. B., Dwyer, S.D., Smith, L., 1989. Cadmium evokes inositol phosphate formation and calcium mobilization. J. Biol Chem. 264, 7115-7118.

Somji, S., Zhou, X. D., Garrett, S. H., Sens, M. A., Sens, D. A., 2006.Urothelial cells malignantly transformed by exposure to cadmium (Cd(+2)) and arsenate (As(+3)) have increased resistant to Cd(+2) and As(+3)-induced cell death. Toxicol. Sci. 94, 293-301.

Sorimachi, H., Saido, T. C., Suzuki K., 1994. New era of calpain research: Discovery of tissue-specific calpains. FEBS Lett. 341, 1-5.

Squier, M. K.T., Cohen, J. J. 1997. Calpain, an upstream regulator of thymocyte apoptosis. J. Immunol. 158, 3690-3697.

Squier, M. K., Miller, A. C., Malkinson, A. M., Cohen, J. J., 1994. Calpain activation in apoptosis. J. Cell Physiol. 159, 229-237.

Srivastava, K. K., Cable, E. E., Donohue, S. E. Bonkovsky, H. L., 1993. Molecular basis for heme-dependent induction of heme oxygenase in primary cultures of chick embryo hepatocytes. Demonstration of acquired refractoriness to heme. Eur. J. Biochem. 213, 909-917.

Stohs, S. J., Bagchi, D., Hassoun, E., Bagchi, M., 2001. Oxidative mechanisms in the toxicity of chromium and cadmium ions. J. Environ. Pathol. Toxicol. Oncol. 20, 77-78

Stokinger, H. E., 1981. The metals. In: Clayton, G. D & Clayton, F. E., eds. Patty's Industrial Hygiene and Toxicology, volume 2A Toxicology, New York, John Wiley & Sons Inc., pp1563-1583.

Suzuki, T., Takagi, Y., Osanai, H., Li, L., Takeuchi, M., Katoh, Y., Kobayashi, M., Yamamoto, M., 2005. Pi-class glutathione S-transferase genes are regulated by Nrf2 through an evolutionarily conserved regulatory element in Zebrafish. Biochem. J. 388, 65-73.

Synder, G. H., Cennerazzo, M. J., Karalis, A. J., Field, D., 1981. Electrostatic influence of local cysteine environments on disulfide exchange kinetics. Biochem. 20, 6509-6519.

Talalay, P., De Long, M. J., Prochaska, H. J., 1988. Identification of a common chemical signal regulating the induction of enzymes that protect against chemical carcinogenesis. Proc. Natl. Acad. Sci. USA 85, 8261-8265.

Talalay, P., Dinkova-Kostova, A. T., Holtzclaw, W. D., 2003. Importance of phase 2 gene regulation in protection against electrophile and reactive oxygen toxicity and carcinogenesis. Adv. Enzyme Regul. 43, 121-134.

Tanimoto, A., Hamada, T., Koide, O. 1993. Cell death and regeneration of renal proximal tubular cells in rats with subchronic cadmium intoxication. Toxicol. Pathol. 21, 341-352.

Tatrai, E., Kovacikova, Z., Hudak, A., Adamis, Z., Ungvary, G., 2001. Comparative in vitro toxicity of cadmium and lead on redox cycling in type II pneumocytes. J. Appl. Toxicol. 21, 479-483.

Thevenod, F., 2009. Cadmium and cellular signalling cascade: To be or not to be? Toxicol. Appl. Pharmacol.238, 221-239.

Thijssen, S., Cuypers, A., Maringwa, J., Smeets, K., Horemans, N., Lambrichts, L., Van Kerkhove, E., 2007. Low cadmium exposure triggers a biphasic oxidative stress response in mice kidneys. Toxicol. 236, 29-41.

Thornberry, N. A., 1997. The caspase family of cysteine proteases. Br Med Bull 53, 478-490.

Thornberry, N. A., Lazebnik, Y., 1998. Caspases: Enemies within. Science 281, 1312-1316.

Tinel, A., Tschopp, J., 2004. The PIDDosome, a protein complex implicated in activation of caspase-2 in response to genotoxic stress. Science 304, 843-846.

Troy, C. M., Rabacchi, S. A., Friedman, W. J., Frappier, T. F., Brown, K., Shelanski, M. L., 2000. Caspase-2 mediates neuronal cell death induced by beta-amyloid. J. Neurosci. 20, 1386-1392.

Tsuchida, S., Sato, K., 1992. Glutathione Transferases and Cancer. Crit. Rev. biochem. Mol. Biol. 27, 337-384.

Tsujimoto, Y., 1997. Apoptosis and necrosis: intracellular ATP levels as a determinant for cell death modes. Cell death Differ. 4, 429-434.

Tenhunen, R., Marver, H. S., Schmid, R., 1969. Microsomal heme oxygenase. J. Biol. Chem. 244, 6388-6394.

Tfelt-Hansen, J., Brown, E. M., 2005. The calcium-sensing receptor in normal physiology and pathophysiology: a review. Crit. Rev. Clin. Lab. Sci. 42, 35-70.

Thompson C. B., 1995. Apoptosis in the pathogenesis and treatment of diseases. Science. 5203, 1456-1462.

Thomson, M., Ali, M., 2003. Garlic (Allium sativum): a review of its potential use as an anti-cancer agent. Curr. Cancer Drug Targets. 3, 67-81.

Van Assche, F. J., 1998. " A stepwise model to quantify the relative contribution of different environmental sources to human cadmium exposure, " Paper to be presented at NiCad'98, Prague, Czech Republic, Sept. 21-22.

Vanags, D. M., Pom-Ares, M. I., Coppola, S., Burgess, D. H., Orrenius, S., 1996.Protease involvement in fodrin cleavage and phospatidylserine exposure in apoptosis. J. Biol. Chem.271, 31075-31085.

Vargas, M. R., Pehar, M., Cassina, P., Martinez-Palma, L., Thompson, J. A., Beckman, J. S., Barbeito, L., 2005. Fibroblast growth factor-1 induces heme oxygenase-1 via nuclear factor erythroid 2-related factor 2 (Nrf2) in spinal cord astrocytes: consequences for motor neuron survival. J. Biol. Chem. 280, 25571-25579.

Venugopal, R., Jaiswal, A. K., 1996. Nrf1 and Nrf2 positively and c-Fos and Fra I negatively regulate the human antioxidant response element-mediated expression of NAD(P)H:quinine oxidoreductase 1 gene. Proc. Natl Acad Sci. USA. 93, 14960-14965.

Venugopal, R., Jaiswal, A.K., 1998. Nrf2 and Nrf1 in association with Jun proteins regulate antioxidant response element-mediated expression and coordinated induction of genes encoding detoxifying enzymes. Oncogene. 17, 3145-3156.

Waalkes, M. P., 2000. Cadmium carcinogenesis in review. J. Inorg. Biochem. 79, 241-244.

Waalkes, M. P., 2003. Cadmium carcinogenesis. Mutat. Res. 533, 107-120.

Waalkes, M. P., Rehm, S., 1994. Cadmium and prostate cancer. J. Toxicol. Environ. Health. 43, 251-269.

Waisberg, M., Joseph, P., Hale, B., Beyersmann, D., 2003. Molecular and cellular mechanisms of cadmium carcinogenesis. Toxicol. 192, 95-117.

Wakabayashi, N., Dinkova-Kostova, A. T., Holtzclaw, W. D., Kang, M. I., Kobayashi, A., Yamamoto, M., Kensler, T. W., Talalay, P., 2004. Protection against electrophile and oxidant stress by induction of the phase 2 response: fate of cysteines of the Keap1 sensor modified by inducers. Proc. Natl. Acad. Sci. USA 101, 2040-2045.

Wang, K. K., 2000. Calpain and caspase: can you tell the differences? Trends Neurosci. 23, 20-26.

Wang, Y., Fang, J., Leonard, S. S., Rao, K. M., 2004. Cadmium inhibits the electron transfer chain and induces reactive oxygen species. Free Radic. Biol. Med. 36, 1434-1443.

Wang, X., Sun, Z., Chen, W., Eblin, K. E., Gandolfi, A. J., Zhang, D, D., 2007. Nrf2 protects human bladder urothelial cells from arsenite and monomethylarsonous acid toxicity. Toxicol. Appl Pharmacol. 225, 206-213.

Wang, Z., Templeton, D. M., 1998. Induction of c-fos proto-oncogene in mesangial cells by cadmium. J. Biol. Chem. 273, 73-79.

Watjen, W., Cox, M., Biagioli, M., Beyersmann, D., 2001. Cadmium-induced apoptosis in C6 glioma cells: mediation by caspase 9-activation. Biometals 15, 15-25.

Watjen, W., Haase, H., Biagioli, M., Beyersmann, D., 2002. Induction of apoptosis in mammalian cells by cadmium and zinc. Environ.Health Perspect. 110, 865-867.

Watkin, R. D., Nawrot, T., Potts, R. J., Hart, B. A., 2003. Mechanisms regulating the cadmium-mediated suppression of Sp1 transcription factor activity in alveolar epithelial cells. Toxicol. 184, 157-178.

Wattenberg, L. W., 1985. Chemoprevention of cancer. Cancer Res. 45, 1-6.

WCRF and AICR. , 1997. Vegetables and fruits. In: World Cancer Research Fund and American Institute for Cancer Research (Eds), Food, Nutrition and the Prevention of Cancer: A global Perspective, American Institute for Cancer Research, Washington, DC. 436-446.

Wei, Z., Lau, B. H. S., Lau., 1998. Garlic inhibits free radical generation and augments antioxidant enzyme activity in vascular endothelial cells. Nutr. Res. 18, 61-70.

Weis, M., Kass, G. E. N., Orrenius, S., 1994. Further characterization of the events involved in mitochondrial Ca2+ release and pore formation by prooxidants. Biochem Pharmacol. 47, 2147-2156.

Wendel, A., 1980. in "Enzymatic Basis of Detoxification" Vol. 1, Academic Press (New York, NY), 333-353.

White, T. K., Zhu, Q., Tanzer, M. L., 1995. Cell surface calreticulin is a putative mannoside lectin which triggers mouse melanoma cell spreading. J Biol Chem. 270, 15926-15929.

WHO., 1992. Cadmium.Environmental Health Criteria. 134. World health organisation.

Wild, A. C., Moinova, H. R., Mulcahy, R. T., 1999. Regulation of gamma-glutamylcysteine synthase subunit gene expression by the transcription factor Nrf2. J Biol Chem. 274, 33627-33636.

Williams, G. T. and Morimoto, R. I. (1990). Maximal stress-induced transcription from the human HSP70 promoter requires interactions with the basal promoter elements independent of rotational alignment. Mol Cell Biol 10, 3125-36.

Windholz, M., Budavari, S., Stroumtsis, L. Y., Fertig, M. N., ed. 1976., The Merck Index, Rahway, New Jersey, Merck & Co., Inc.

Wolf, B. B., Goldstein, J. C., Stennicke, H. R., Beeve, H., Amarantc-cndes, G. P., Salvcsen, G. S., Green, D. R., 1999. Calpain functions in a caspase-independent manner to promote apoptosis-like events during platelets activation. Blood. 94, 1683-1692.

Wolter, K. G., Hsu, Y., Smith, C. L., Mechyshtan, A., Xi, X., Youle, R. J., 1997. Movement of BAX from cytosol to mitochondrial during Apoptosis. J. Cell Biol. 139, 1281-1292.

Wood, D. E., Thomas, A., Deri L. A., Berman, Y., Beavis, R. C., Reed, J. C., Newcomb, E. W., 1998. Bax cleavage is mediated by calpain during drug-induced apoptosis. Oncogene 17, 1069-1078.

Wu, C.C Sheen, L. Y., Chen, H. W., Tsai, S. J., Lii, C. K., 2001. Effects of organosulfur compounds from garlic oil on the antioxidation system in rat liver and red blood cells. Food Chem. Toxicol. 39, 563-569.

Xu, C., Johnson, J. E., Singh, P. K., Jones, M. M., Yan, H., Carter, C. E., 1996. In vivo studies of cadmium-induced apoptosis in testicular tissue of the rat and its modulation by a chelating agent. Toxicol.107, 1-8.

Xu, G., Zhou, G., Jin, T., Zhou, T., Hammarstrom, S., Bergh, A., Nordberg, G., 1999. Apoptosis and p53 gene expression in male reproductive tissues of cadmium exposed rats. Biometals.12, 131-139.

Yamagami, K., Nishimura, S., Sorimachi, M., 1998. Cd^{2+} and Co^{2+} at micromolar concentrations mobilize intracellular Ca^{2+} via the generation of inositol 1, 4, 5- triphosphate in bovine chromaffin cells. Brain Res. 798, 316.

Yamano, T., DeCicco, L. A., Rikans, L. E., 2000. Attenuation of cadmium-induced liver injury in senescent male fischer 344 rats: role of Kupffer cells and inflammatory cytokines. Toxicol. Appl. Pharmacol. 162 68-75.

Yang, C. S., Chhabra, S. K., Hong, J. Y., Smith, T. J., 2001. Mechanisms of inhibition of chemical toxicity and carcinogenesis by diallyl sulphide (DAS) and its metabolites. Chem Res. Toxicol. 4, 642-647.

Yang, C. S., Tzou, B. C., Liu, Y. P., Tsai, M. J., Shyue, S. K. and Tzeng, S. F. (2008). Inhibition of cadmium-induced oxidative injury in rat primary astrocytes by the addition of antioxidants and the reduction of intracellular calcium. J Cell Biochem 103, 825-834.

Yang, J., Liu, X., Bhalla, K., Kim, C. N., Brado, A. M., Cai, J., Peng, T. L., Jones, D. P. Wang, X., 1997. Prevention of apoptosis by Bcl-2: release of cytochrome C from mitochondrial blocked. Science. 275, 1126-1132.

Yang, P. M., Chen, H. C., Tsai, J. S. and Lin, L. Y. (2007a). Cadmium induces Ca^{2+}-dependent necrotic cell death through calpain-triggered mitochondrial depolarization and reactive oxygen species-mediated inhibition of nuclear factor-kappaB activity. Chem Res Toxicol 20, 406-15.

Yang, Z., Yang, S., Qian, S. Y., Hong, J. S., Kadiiska, M. B., Tennant, R. W., Waalkes, M. P. and Liu, J. (2007b). Cadmium-induced toxicity in rat primary mid-brain neuroglia cultures: role of oxidative stress from microglia. Toxicol Sci 98, 488-94.

Yoshida, C., Tokumasu, F., Hohmura, K. I., Bungert, J., Hayashi, N., Nagasawa, T., Engel, J. D., Yamamoto, M., Takeyasu, K., Igarashi, K., 1999. Long range interaction of cis-DNA elements mediated by architectural transcription factor Bach1. Genes Cells 4, 643-655.

Yu, R., Mandlekar, S., Weber, M. J., Der, C. J., Wu, J., Tony-Kong, A. N., 1999. Role of mitogen-activated protein kinase pathway in the induction of phaseII detoxifying enzymes by chemicals. J. Biol. Chem. 274, 27545-27552.

Zamaraeva, M. V., Sabirov,R. Z., Maeno, E., Ando-Akatsuka, Y., Bessonova, S. V., Okada, Y., 2005. Cells death with increased cytosolic ATP during apoptosis: a bioluminescence study with intracellular luciferase. Cell death and differentiation. 12, 1390-1397.

Zhang, D. D., 2006. Mechanistic studies of the Nrf2-Keap1 signaling pathway. Drug Metab Rev. 38, 769-789.

Zhang, D. D., Hannink, M., 2003. Distinct cysteine residues in Keap1 are required for Keap1-dependent ubiquitination of Nrf2 and for stabilization of Nrf2 by chemopreventive agents and oxidative stress. Mol Cell Biol. 23, 8137-8151.

Zhang, A., Wu, Y., Lai, H. W. L., Yew, D. T., 2004. Apoptosis. A brief review. Neuroembryology. 3, 47-59.

Zipper, L. M., Mulcahy, R. T., 2002. The Keap1 BTB/POZ dimerization function is required to sequester Nrf2 in cytoplasm. J. Biol. Chem. 277, 36544-36552.

Appendix

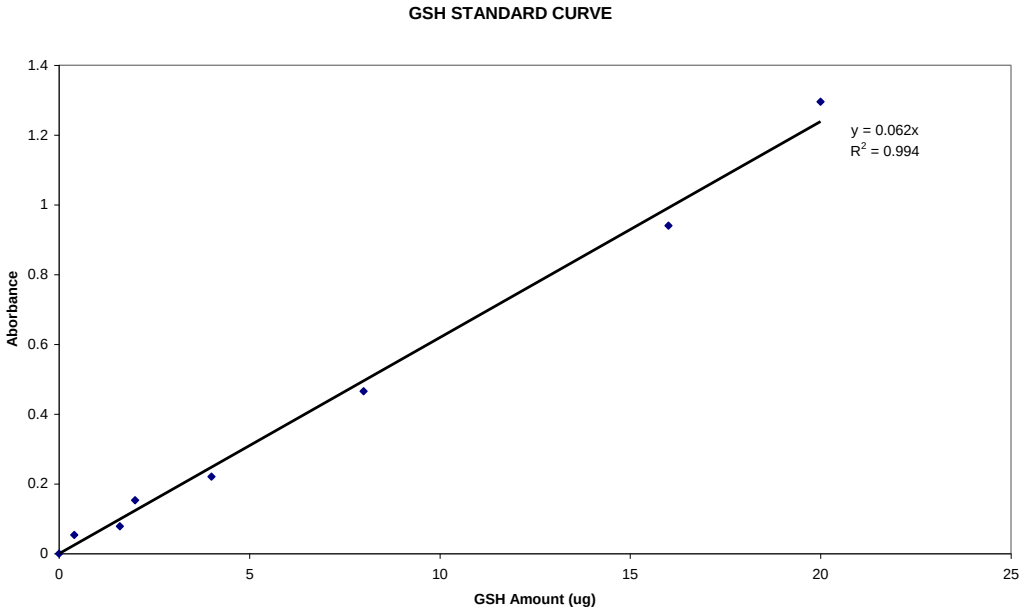
GSH STANDARD CURVE
y = 0.062x
R2 = 0.994
Aborbance
GSH Amount (ug)
0
0.2
0.4
0.6
0.8
1
1.2
1.4
0
5
10
15
20
25

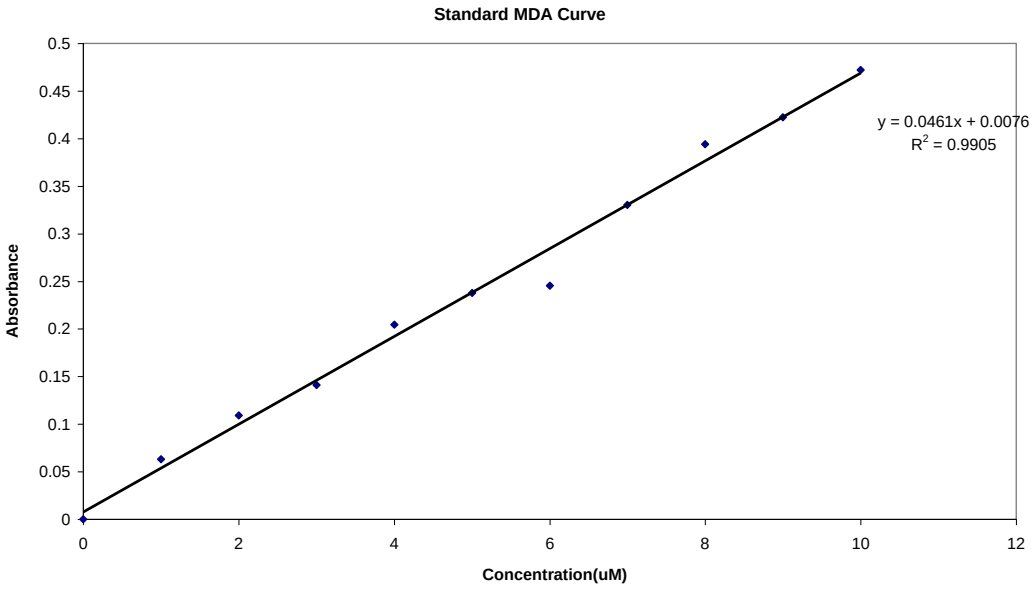
Standard MDA Curve
y = 0.0461x + 0.0076
R2 = 0.9905
Absorbance
Concentration(uM)
0
0.05
0.1
0.15
0.2
0.25
0.3
0.35
0.4
0.45
0.5
0
2
4
6
8
10
12

ATP STANDARD

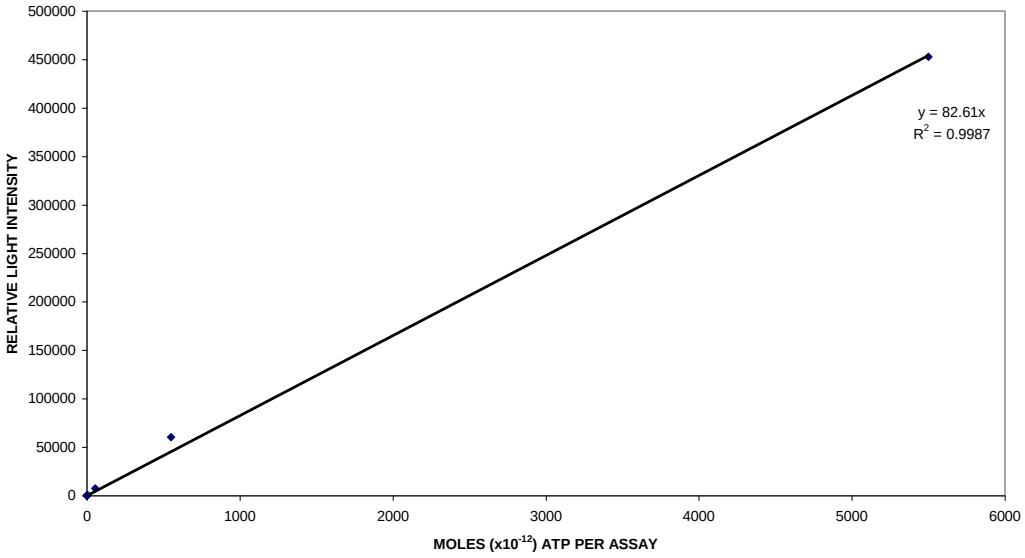

CASPASE STANDARD CURVE

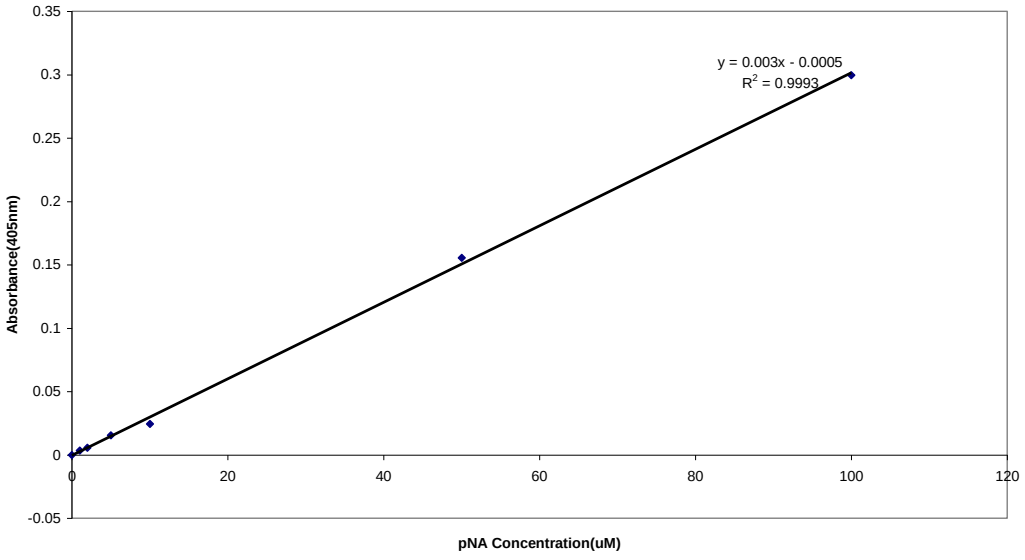

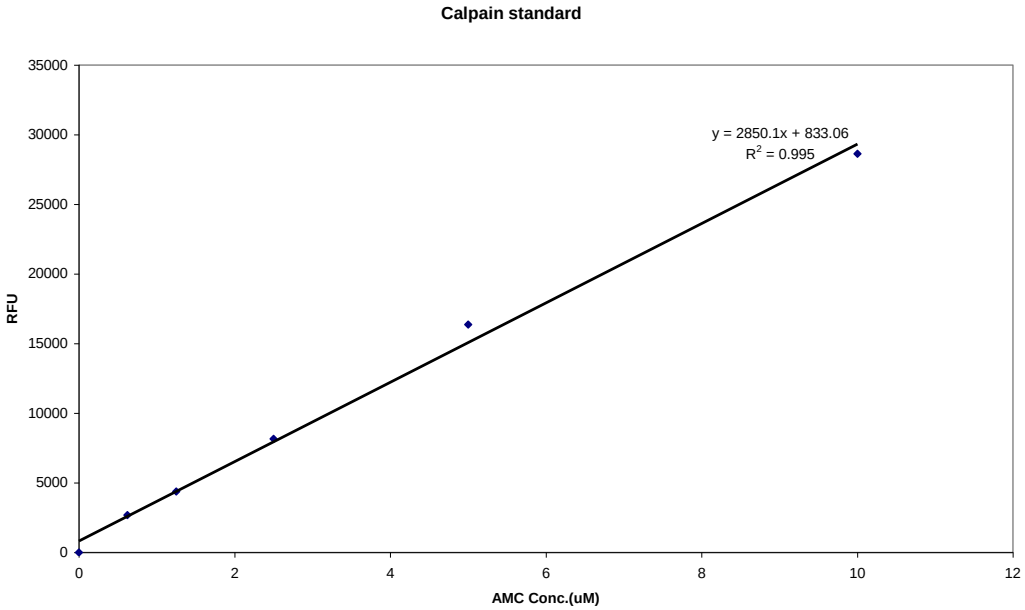
Calpain standard
y = 2850.1x + 833.06
R2 = 0.995
RFU
AMC Conc.(uM)
35000
30000
25000
20000
15000
10000
5000
0
0
2
4
6
8
10
12

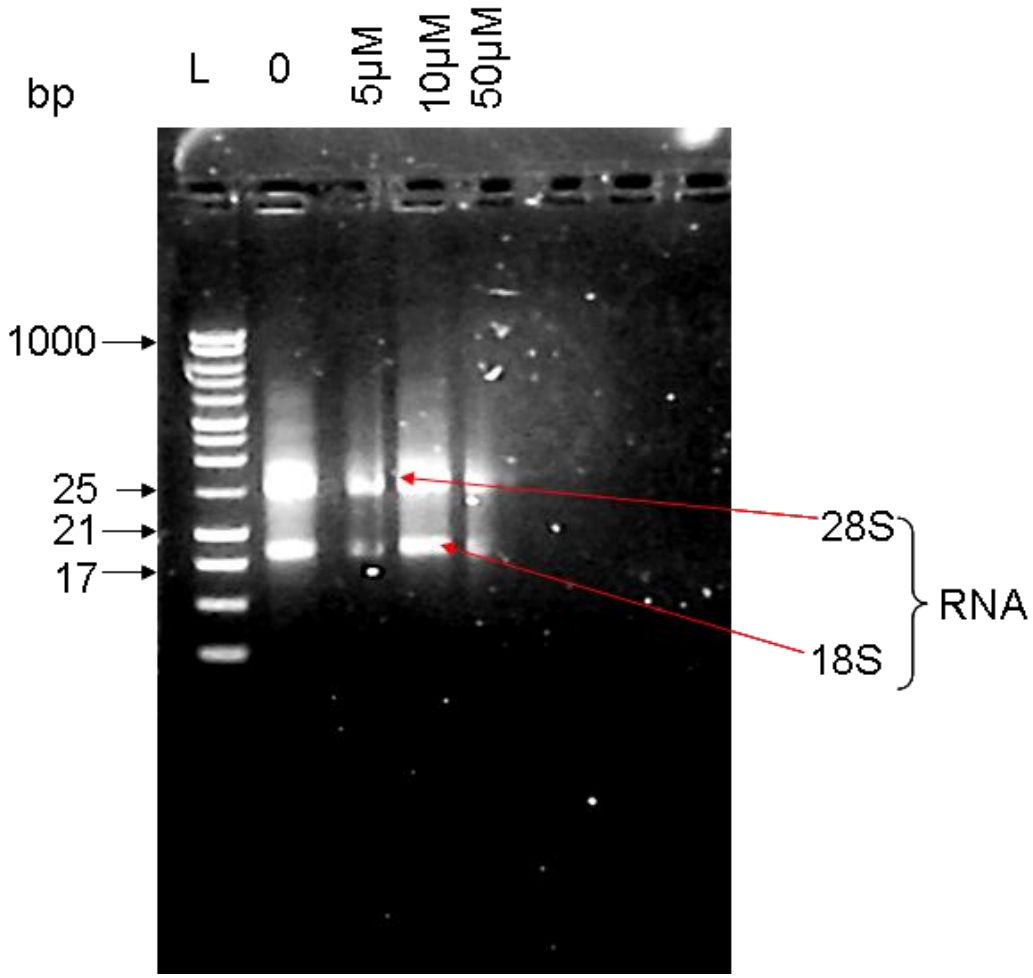

1% TAE agarose gel electrophoresis of RNA isolated from 1321N1 cells after CdCl2 treatment. L, DNA ladder; bp, base pair

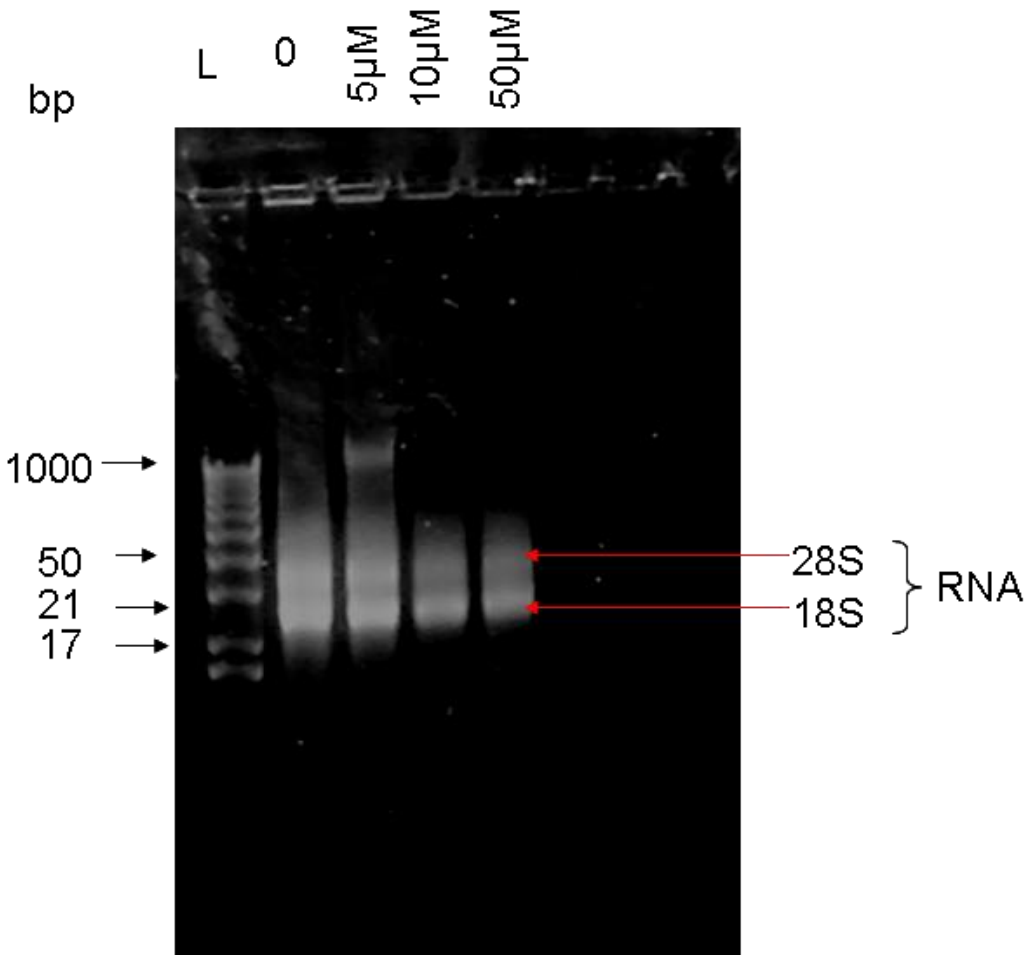

1% TAE agarose gel electrophoresis of RNA isolated from HEK 293 cells after CdCl2 treatment. L, DNA ladder; bp, base pair

Melting Curve of GAPDH genes in 1321N1 cells after 24hrs exposure to $CdCl_2$.

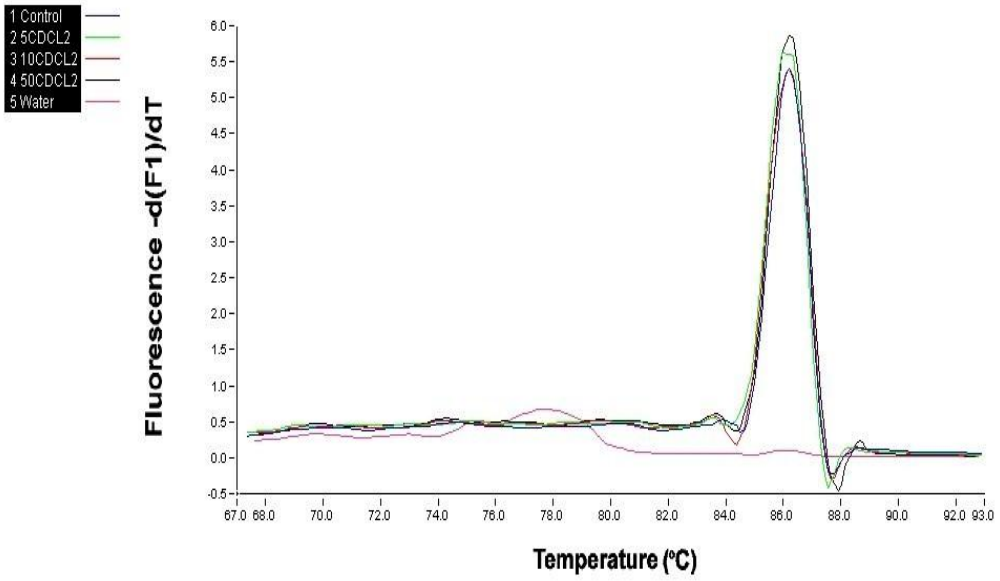

Amplification Curve of GAPDH genes in 1321N1 cells after 24hrs exposure to $CdCl_2$

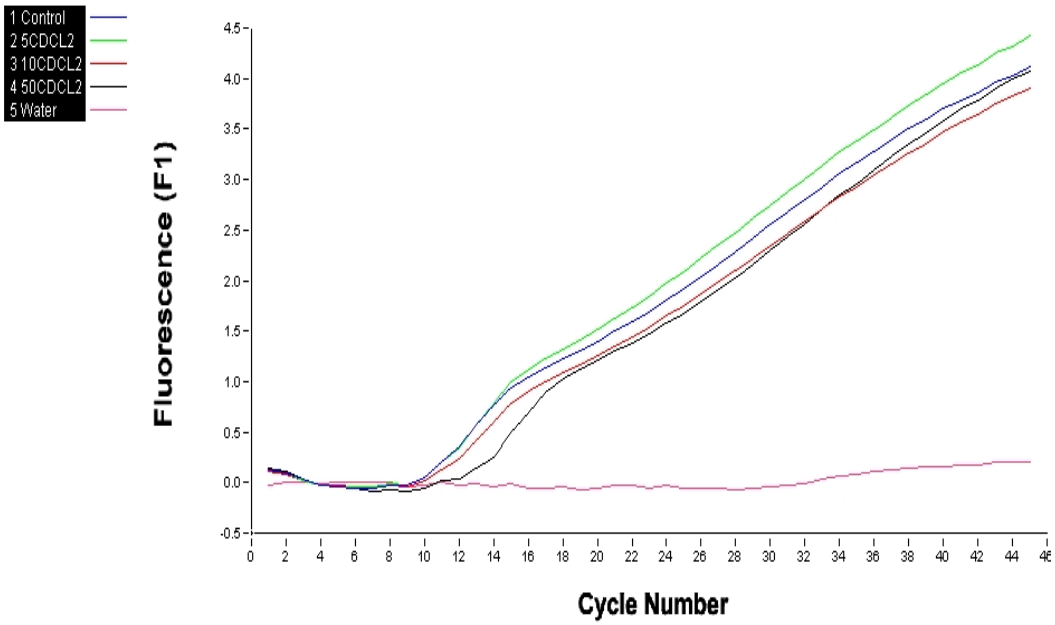

Melting Curve of GAPDH genes in HEK 293 cells after 24hrs exposure to $CdCl_2$.

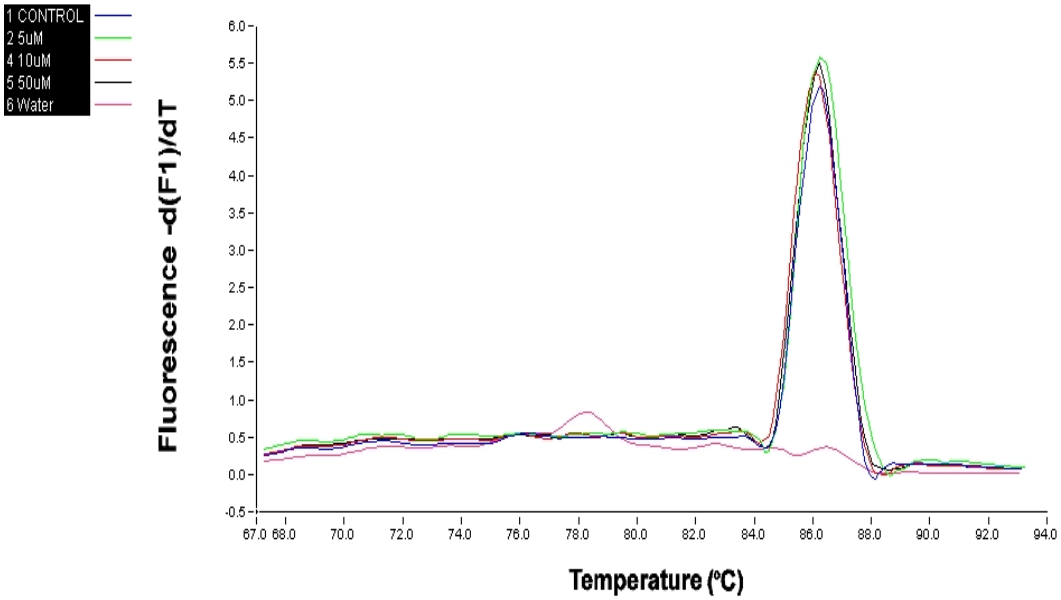

Amplification Curve of GAPDH genes in HEK 293 cells after 24hrs exposure to $CdCl_2$.